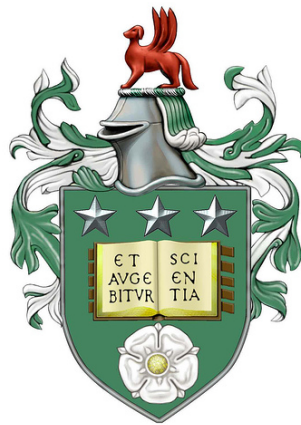


Colour Characterisation of LCD Display Systems



Marjan Vazirian

School of Design
The University of Leeds

This thesis is submitted for the degree of
Doctor of Philosophy

March 2018

I would like to dedicate this thesis to my beloved husband

Ali Hadavi

&

my loving parents

for their endless love, support and encouragement. . .

Declaration

I hereby declare that except where specific reference is made to the work of others, the contents of this thesis are original and have not been submitted in whole or in part for consideration for any other degree or qualification in this, or any other university. This thesis is my own work and contains nothing which is the outcome of work done in collaboration with others, except as specified in the text and Acknowledgements. ©2016 The University of Leeds

Marjan Vazirian
March 2018

Acknowledgements

I am very grateful for all time spent during my PhD course at the University of Leeds. Firstly, I would like to express my sincere gratitude to my advisor Prof. Stephen Westland for the continuous support of my PhD study and related research, for his patience, motivation, and immense knowledge. His guidance helped me in all the time of research and writing of this thesis. I could not have imagined having a better advisor and mentor for my PhD study. Besides my advisor, I would like to thank my second supervisor, Dr Vien Cheung and the rest of my thesis committee: Prof. Ronnier Luo, Dr Huw Owens, Dr. Jim Nobbs and Professor Stephen Russell for their insightful comments and encouragement, but also for the hard question which incited me to widen my research from various perspectives. I would like to acknowledge Dr Peter Rhodes who gave access to the laboratory and research facilities as well as for theoretical colour science course. I am especially grateful for the time spending with Professor Michael Hann, preparing illustrative materials for his books during my PhD study.

My sincere thanks also go to our school manager Mr Azim Abadi for precious support and help during my study. He always was ready to spend his time to support and advice.

Words cannot express how grateful I am to my parent-in-law, grandparents and my parents. I sincerely appreciated all emotional and supports which I received from my sisters; Mahsa, Aalam, Mahro and Nazi and my brothers Mohammad and Mohsen. I would also like to thank all of my friends; Maryam, Chaoran, Kholoud, Valentina, Shima and Abbas who supported me during my PhD course and encourage me to strive towards my goal.

Above all, I would like to give the deepest appreciation to my beloved husband, Dr Ali Hadavi, who spent sleepless nights with and was always my support, faith and encouragement throughout my studies.

Abstract

The main purpose of this research is to study the colour characterisation of digital display systems. Three distinct models for characterisation (GOG, PLCC and PLVC) are evaluated and compared and for two of these models (GOG and PLCC) two different sets of linearisation samples (either colour-ramps or grey-ramp samples) are used to perform the linearisation. To evaluate these models colorimetric measurements are made for 20 different display devices and colour characterisation performance is reported as the main measure. Characterisation performance is calculated using several sets of samples including the widely used Macbeth ColorChecker chart and two new charts called Chart4 and Matlab60 (one of which was based on a method previously published by Cheung and Westland [24] and another was based on a new method).

A key aspect of this work is that all 256 levels of intensity were measured for the colour-ramps and for the grey-ramp linearisation samples for each of the 20 displays to allow subsampling of these data to explore the effect of the number of linearisation samples on characterisation performance. When the number of linearisation samples used was small (less than 10) the GOG model sometimes resulted in the smallest characterisation colour differences. However, for the PLCC and PLVC models performance tended to increase with the number of linearisation samples and both of these models outperformed GOG with more than 10 linearisation samples. For the PLCC model, better performance was usually obtained using the grey-ramp linearisation samples rather than using the colour-ramps linearisation samples. It was possible, for each of the 20 displays, to reach average ΔE_{ab}^* values that are less than 1.5 ($\Delta E_{ab}^* < 1.5$, 90%) or $\Delta E_{ab}^* < 1.0$ (75%); however, the model that yields the best performance is difficult to ascertain in advance (a good strategy would be to evaluate all five models and select the one that performs best for the characterisation of any particular display). However, in the majority of cases, lowest colour differences (ΔE_{ab}^*) were obtained using the PLCC model and all 256 of the

grey-ramp samples for linearisation. This work has compared the performance of five different models using a large number of displays and has allowed a number of recommendations to be made about display characterisation. Although the majority of the work in this thesis was based on stationary displays the effect of motion on characterisation performance was also explored. This is important since moving images are now commonplace in many applications. The results showed that a moving background has a small, but statistically significant, effect on the colour of patches.

Table of contents

List of figures	xvii
List of tables	xxiii
1 Introduction	1
1.1 Motivation	1
1.2 Aims and scope	2
1.3 Thesis structure	2
1.4 Summary of contribution to work	3
2 Literature Survey	5
2.1 Introduction	5
2.2 CIE System	5
2.2.1 Colorimetry	5
2.2.2 Light Source and CIE standard illuminants	6
2.2.3 Correlated Colour Temperature	6
2.2.4 CIE Standard Illuminant and light sources	6
2.2.5 Colour matching function	7
2.2.5.1 Two sets of colour matching functions	11
2.2.6 Chromaticity diagram	12
2.2.7 Uniform colour space	13

2.2.8	CIE Colour Space	14
2.3	Colour appearance	19
2.3.1	Visual area in the observing field	19
2.3.1.1	The colour element stimulus considered	20
2.3.1.2	The proximal field	21
2.3.1.3	The background	21
2.3.1.4	Surround	21
2.3.1.5	Adapting field	22
2.3.2	Colour appearance attributes	22
2.3.3	Colour appearance phenomena	23
2.3.4	Colour appearance model	25
2.3.4.1	The <i>CIECAM97s</i> and <i>CIECAM02</i>	25
2.4	RGB colour system	26
2.4.1	additive colour mixing	26
2.4.2	Trichromatic colour reproduction	26
2.4.3	RGB Colour space	27
2.4.3.1	sRGB	30
2.4.3.2	Adobe (1998) RGB	31
2.4.4	White Point	31
2.5	Colour management	33
2.5.1	Colour management procedure	35
2.5.2	ICC profiles	36
2.5.2.1	Type of profiles and their uses	37
2.6	Display technologies	37
2.6.1	CRT	37
2.6.2	Basic principle and structure of LCD	38
2.6.3	LED display	40

2.6.3.1	OLED	40
2.6.4	PDP	41
2.7	Device characterisation	44
2.7.1	Device independent colour reproduction	46
2.7.2	GOG model	47
2.7.2.1	Gamma	47
2.7.3	Device-independent transformation	49
2.7.4	PLCC	50
2.7.5	3D-Look-Up-Table	51
2.7.6	Review of previous studies of the display characterisation . .	52
2.8	Summary relevant to the current research	53
3	Overview of Experimental Work	55
3.1	Introduction	55
3.2	Research Questions	55
3.3	Colour-Measurement Equipment	57
3.3.1	Repeatability of Konica Minolta CS-2000 device	60
3.4	Implementation Details	63
3.4.1	General Approach	63
3.4.2	Characterisation Process	64
3.4.3	Result analysis	66
4	Methodology	69
4.1	Introduction	69
4.2	Different types of samples	69
4.2.1	Linearisation samples	70
4.2.1.1	Grey-ramp	70
4.2.1.2	Colour-ramps	71

4.2.2	Test samples	71
4.2.2.1	Macbeth ColorChecker chart	72
4.2.2.2	Chart4	72
4.2.2.3	Chart2	74
4.2.2.4	Matlab60	74
4.3	Experimental Settings	76
4.4	Summary	77
5	Display Characterisation	79
5.1	Introduction	79
5.2	Colour measurements	80
5.3	White point and Grey-scale tracking	80
5.4	Colour tracking (Chromaticity changes of primaries)	82
5.5	Colour Gamut	83
5.6	Spatial Uniformity	84
5.7	Channel Independence	86
5.8	Spatial Independence	87
5.9	Non-Linearity of Response	87
5.10	Linearisation	89
5.10.1	Effect of using a various number of samples on data linearisation	92
5.11	Characterisation Performance	101
5.12	Summary and Conclusion	111
6	Display Characterisation Meta-Analysis	115
6.1	Introduction	115
6.2	Colour measurements	115
6.3	White-point evaluation	116
6.4	Channel and Spatial Independence	119

6.5	Colour Gamut	122
6.6	Contrast ratio	123
6.7	Linearisation	123
6.8	Characterisation Performance	124
6.9	Statistical analysis	138
6.10	Effect of using different number of samples (Sub sampling).	140
6.11	Chromaticity Constancy	146
6.12	Conclusions	149
7	Testing the PLVC model	151
7.1	Introduction	151
7.2	The PLVC model	151
7.3	Experimental work	153
7.4	Performance of the PLVC model	154
7.5	The effect of using different models	157
7.6	Conclusion	170
8	Effect of background colour on monitor characterisation	173
8.1	Introduction	173
8.2	Experiment I	174
8.2.1	Experimental setting	174
8.2.2	Results	175
8.3	Experiment II	179
8.3.1	Experimental setup	179
8.3.2	Results	181
8.4	Summary and conclusion	190
9	Conclusion and future work	191

9.1	Conclusion	191
9.2	Future works	195
	References	197

List of figures

2.1	Different Illuminant	7
2.2	The <i>RGB</i> colour matching functions	8
2.3	The CIE 1964 colour matching functions for the 10° standard observer and the imaginary XYZ primaries.	10
2.4	Comparison between the CIE 1931 and 1964 colorimetric observer	11
2.5	CIE 1931 chromaticity diagram.	12
2.6	<i>x, y</i> chromaticity coordinates in a rectangular coordinate system.	13
2.7	The CIE 1976 UCS chromaticity diagram.	14
2.8	CIELAB L^* , a^* and b^* coordinates.	17
2.9	Schematic diagram of the observing field according to Hunt (1998).	20
2.10	<i>RGB</i> colour space.	27
2.11	Gamut of colours using the Rec. 709 primaries.	29
2.12	HP Dream colour LP2480z sRGB 3D gamut shows on <i>xy</i> chromaticity diagram.	30
2.13	sRGB gamut.	31
2.14	Comparing sRGB and Adobe (1998) RGB.	32
2.15	Gamut of the Rec 2020 and Rec 709 with the white point.	32
2.16	Matching colour with profile profiling.	34
2.17	CRT structure	38
2.18	LCD structure	39

2.19	Structure of OLED	41
2.20	Flexible OLED	42
2.21	PDP structure	42
2.22	Display specifications	43
2.23	System diagram for input and output components of a colorimetric colour reproduction system	47
3.1	Experimental setup using the Konica Minolta CS-2000	59
3.2	Konica Minolta CS-2000	59
3.3	Minolta CS-2000-screen specification	60
3.4	Minolta CS-2000 specification	61
3.5	Konica Minolta CS-2000 measurements over the time	62
3.6	XYZ to RGB	63
3.7	RGB to XYZ	64
3.8	Display A Histograma	67
5.1	Chromaticities of white point (green circle) and grey levels (black crosses) for display A without black correction.	81
5.2	Chromaticities of white point (black circle) and grey levels (black crosses) for display A after black correction.	82
5.3	Colour and greyscale tracking and chromaticities of white point (green circle) before (left) and after (right) black correction in $u'v'$ -diagram.	83
5.4	Colour gamut of display A (black line) and chromaticities of white point (green circle) in comparison with the $sRGB$ (red line and red square) plotted in $u'v'$ -diagram.	84
5.5	Position of white measurements.	85
5.6	Spatial uniformity colour difference (ΔE_{ab}^*) between the centre and the different position of the display.	86
5.7	The tone-reproduction curves (TRC) for the three channels.	88

5.8	The tone-reproduction curves (TRC) for the three channels.	89
5.9	The data fitted with GOG and PLCC.	91
5.10	The effect of linearisation using both GOG and PLCC method. . . .	92
5.11	The r^2 values for four different methods using the various training data sets.	94
5.12	The effect of choosing 6 linearisation samples ($N = 6$) by using either the GOG or PLCC method (with the grey samples being used). 95	
5.13	The effect of choosing 10 linearisation samples ($N = 10$) by using either the GOG or PLCC method (with the grey samples being used). 96	
5.14	The effect of choosing 18 linearisation samples ($N = 18$) by using either the GOG or PLCC method (with the grey samples being used). 97	
5.15	The effect of choosing 34 linearisation samples ($N = 34$) by using either the GOG or PLCC method (with the grey samples being used). 98	
5.16	The effect of choosing 66 linearisation samples ($N = 66$) by using either the GOG or PLCC method (with the grey samples being used). 99	
5.17	The effect of choosing 129 linearisation samples ($N = 129$) by using either the GOG or PLCC method (with the grey samples being used). 100	
5.18	Max ΔE_{ab}^* over Median ΔE_{ab}^*	103
5.19	Characterisation performances of the GOG (blue symbols) and PLCC (red symbols) models using the grey-ramp linearisation samples for the three different set of samples (Chart4, Macbeth and Matlab60). .	105
5.20	Characterisation performances of the GOG (blue symbols) and PLCC (red symbols) models using the colour-ramps linearisation samples for the three different set of samples (Chart4, Macbeth and Matlab60). 106	
5.21	Characterisation performances (ΔE_{ab}^*) of the GOG and PLCC models using the grey-ramp linearisation samples with 256 linearisation samples for all different set of samples (Chart4, Macbeth and Matlab60) over the Lightness and Chroma of display A.	107

5.22	Characterisation performances (ΔE_{ab}^*) of the GOG and PLCC models using the colour-ramps linearisation samples with 256 linearisation samples for all different set of samples (Chart4, Macbeth and Matlab60) over the Lightness and Chroma of display A.	108
5.23	Characterisation performances (ΔE_{ab}^*) of the GOG and PLCC models using the grey-ramps linearisation samples with 6 linearisation samples for all different set of samples (Chart4, Macbeth and Matlab60) over the Lightness and Chroma of display A.	109
5.24	Characterisation performances (ΔE_{ab}^*) of the GOG and PLCC models using the colour-ramps linearisation samples with 6 linearisation samples for all different set of samples (Chart4, Macbeth and Matlab60) over the Lightness and Chroma of display A.	110
6.1	Whitepoint Evaluation of displays.	117
6.2	Spatial Independence test.	119
6.3	Spatial Dependence test.	120
6.4	<i>sRGB</i> colour gamut (green line triangle) and all display gamuts (black line triangle) in CIE 1976 $u'v'$ chromaticity diagram. D_{65} (green square) and each display white-point (black square) is illustrated.	122
6.5	TRC of A-D displays.	130
6.6	TRC of E-H display.	131
6.7	TRC of I-L display.	132
6.8	TRC of M-P display.	133
6.9	TRC of Q-T display.	134
6.10	Characterisation result using grey-ramp linearisation samples for all display devices and all samples (N=256).	135
6.11	Characterisation result using colour-ramp linearisation samples for all display devices and all samples (N=256).	136
6.12	Characterisation result using both linearisation samples and both models for all display devices and all samples (N=256).	137

6.13	Characterisation result using grey-ramp linearisation samples testing GOG and PLCC for A-J display devices using different linearisation samples ($N = 256, 129, 66, 34, 18, 10, 6$).	141
6.14	Characterisation result using grey-ramp linearisation samples testing GOG and PLCC for K-T display devices using different linearisation samples ($N = 256, 129, 66, 34, 18, 10, 6$).	142
6.15	Characterisation result using colour-ramp linearisation samples testing GOG and PLCC for A-J display devices using different linearisation samples ($N = 256, 129, 66, 34, 18, 10, 6$).	144
6.16	Characterisation result using colour-ramp linearisation samples testing GOG and PLCC for K-T display devices using different linearisation samples ($N = 256, 129, 66, 34, 18, 10, 6$).	145
6.17	The chromaticity graph for display A – T.	147
6.18	The chromaticity graph for display A – T.	148
7.1	The median ΔE_{ab}^* for the Macbeth chart (averaged over 20 displays) as a function of N (the number of linearisation samples).	156
7.2	The median ΔE_{ab}^* using all sets of samples (Chart4, Macbeth and Matlab60) as a function of N (the number of linearisation samples).	156
7.3	The average ΔE_{ab}^* for the Macbeth sample set for display A – J as a function of N (the number of linearisation samples).	161
7.4	The average ΔE_{ab}^* for the Macbeth sample set for display K – T as a function of N (the number of linearisation samples).	162
7.5	Visualisation of errors using three different models (GOG, PLCC and PLVC) for all three testing sample sets on the a^*b^* diagram for displays A – F.	163
7.6	Visualisation of errors using three different models (GOG, PLCC and PLVC) for all three testing sample sets on the a^*b^* diagram for displays G – L.	164
7.7	Visualisation of errors using three different models (GOG, PLCC and PLVC) for all three testing sample sets on the a^*b^* diagram for displays M – R.	165

7.8	Visualisation of errors using three different models (GOG, PLCC and PLVC) for all three testing sample sets on the a^*b^* diagram for displays S and T	166
7.9	Visualisation of errors using three different models (GOG, PLCC and PLVC) for all three testing sample sets on the C^*L^* diagram for displays $A - F$	167
7.10	Visualisation of errors using three different models (GOG, PLCC and PLVC) for all three testing sample sets on the C^*L^* diagram for displays $G - L$	168
7.11	Visualisation of errors using three different models (GOG, PLCC and PLVC) for all three testing sample sets on the C^*L^* diagram for displays $M - R$	169
7.12	Visualisation of errors using three different models (GOG, PLCC and PLVC) for all three testing sample sets on the C^*L^* diagram for displays S and T	170
8.1	The colour stimuli	175
8.2	Difference between Mondrian and Movie Y value plotted against Mondrian Y value for each colour stimulus (HP display).	184
8.3	Difference between Mondrian and Movie Y value plotted against Mondrian Y value for each colour stimulus (EIZO display).	185
8.4	Difference between Mondrian and Movie Y value plotted against Mondrian Y value for each colour stimulus (NEC display).	186
8.5	CIE chromaticity coordinates for Mondrian (black circle symbols) and Movie (white triangle symbols) conditions respectively as well as the white point of HP display (red circle).	187
8.6	CIE chromaticity coordinates for Mondrian (black circle symbols) and Movie (white triangle symbols) conditions respectively as well as the white point of EIZO display (red circle).	188
8.7	CIE chromaticity coordinates for Mondrian (black circle symbols) and Movie (white triangle symbols) conditions respectively as well as the white point of NEC display (red circle).	189

List of tables

2.1	The CIE 1931 chromaticity coordinates of the SMPTE-C, Rec. 601 and Rec. 709 primaries.	28
3.1	Repeatability measurement of the Konica Minolta CS-2000 tele-spectroradiometer.	62
3.2	The set of thresholds we used to assess the quality of a colour characterisation model depending on the purpose.	68
4.1	RGB values of grey-ramp samples.	70
4.2	RGB values of colour-ramps samples.	71
4.3	RGB values of Macbeth ColorChecker samples.	72
4.4	RGB values of the Chart4 and Chart2 samples.	73
4.5	The <i>RGB</i> values of the Matlab60 sample set.	75
4.6	Age, Luminance of black level (cd/m^2), the chromaticity of white point, gamut size and contrast ratio specification of each display. . .	76
5.1	Spatial uniformity of display A.	85
5.2	Channel Independency test for display A.	86
5.3	Spatial Independence of the display A.	87
5.4	r^2 linearisation values (display A) for the methods when all 256 levels are used in the training using either grey or colour ramps.	90
5.5	The r^2 values for using each of four methods with various training sets of data.	93

5.6	CIELAB colour differences (ΔE_{ab}^*) for each set of the linearisation samples in the Macbeth ColorChecker sample set.	102
5.7	CIELAB colour differences (ΔE_{ab}^*) of different statistic parametric for each set of the linearisation samples in the Macbeth ColorChecker sample set using grey-ramp linearisation samples.	102
5.8	The Overall results of median ΔE_{ab}^* units for display A using the grey-ramp linearisation samples and three different set of samples (Chart4, Macbeth and Matlab60).	104
5.9	The Overall results of median ΔE_{ab}^* units for display A using the Colour-ramp linearisation samples and three different set of samples (Chart4, Macbeth and Matlab60).	104
6.1	Whitepoint evaluation of display devices.	118
6.2	Channel and Spatial Independence in all display devices (the spatial independence was measured as the colour difference between a white patch with a white and black background; channel independence - or additivity - is the colour difference between the white and the additive sum of the three primaries).	120
6.3	Spatial dependency in all display devices (in this table the colour differences are between grey patches measured with a red, green or blue background).	121
6.4	Contrast ratio of 20 displays.	123
6.5	The average r^2 values for all displays using all ($N = 256$) samples.	124
6.6	Median ΔE_{ab}^* values for 20 displays using the grey-ramp and colour-ramps linearisation samples and three different test sets for all linearisation samples ($N = 256$).	126
6.7	Median ΔE_{ab}^* values for 20 displays using the grey-ramp and colour-ramps linearisation samples and three different test sets for 129 linearisation samples ($N = 129$).	126
6.8	Median ΔE_{ab}^* values for 20 displays using the grey-ramp and colour-ramps linearisation samples and three different test sets for 66 linearisation samples ($N = 66$).	127

6.9	Median ΔE_{ab}^* values for 20 displays using the grey-ramp and colour-ramps linearisation samples and three different test sets for 34 linearisation samples ($N = 34$).	127
6.10	Median ΔE_{ab}^* values for 20 displays using the grey and colour-ramp linearisation samples and five different test sets for 18 linearisation samples ($N = 18$).	128
6.11	Median ΔE_{ab}^* values for 20 displays using the grey-ramp and colour-ramps linearisation samples and three different test sets for 10 linearisation samples ($N = 10$).	128
6.12	Median ΔE_{ab}^* values for 20 displays using the grey-ramp and colour-ramps linearisation samples and three different test sets for 6 linearisation samples ($N = 6$).	129
6.13	Statistical t.test for GOG vs PLCC linearisation samples for all displays using Macbeth set of samples.	138
6.14	Statistical t.test for Grey vs Colour linearisation samples for all displays using Macbeth set of samples.	139
6.15	The median ΔE_{ab}^* values for a various number of linearisation samples using grey-ramp linearisation samples for all displays testing Macbeth set of samples.	140
6.16	The median ΔE_{ab}^* values for various number of linearisation samples using colour-ramps linearisation samples for all displays testing Macbeth set of samples.	143
7.1	Median ΔE_{ab}^* values for all displays testing all sets of samples for $N=256, 129, 66, 34, 18, 10$ and 6 sub-sampling using PLVC model.	155
7.2	The effect of using different sub-sampling sets (N) on the median ΔE_{ab}^* values of using different sets of samples (Chart4, Macbeth and Matlab60) for all displays using PLVC model (the lowest value in each row is highlighted).	157
7.3	The median ΔE_{ab}^* results for the Macbeth sample set for the five models (two GOG models, two PLCC models and PLVC) for $N=256, 129, 66$ and 34 sub-sampling data sets.	159

7.4	The median ΔE_{ab}^* results for the Macbeth sample set for the five models (two GOG models, two PLCC models and PLVC) for $N=18$, 10 and 6 sub-sampling data sets.	160
8.1	Colour samples of fourteen stimuli.	175
8.2	<i>CIEXYZ</i> measurements of the stimuli and <i>CIELAB</i> values of the grey background condition.	176
8.3	<i>CIEXYZ</i> measurements of the stimuli and <i>CIELAB</i> values of the Mondrian background condition.	177
8.4	<i>CIEXYZ</i> measurements of the stimuli and <i>CIELAB</i> values of the black background condition.	177
8.5	<i>CIEXYZ</i> measurements of the stimuli and <i>CIELAB</i> values of the white background condition.	178
8.6	<i>CIEXYZ</i> measurements of the stimuli and <i>CIELAB</i> values of the moving Mondrian background condition.	178
8.7	Colour differences between Mondrian- and movie-condition backgrounds and the grey-condition backgrounds as well as the black-condition and white-condition background.	179
8.8	Colour samples of 20 stimuli.	180
8.9	<i>XYZ</i> values for measuring the Mondrian condition of 20 stimuli.	181
8.10	<i>XYZ</i> values for measuring the Mondrian with moving condition of 20 stimuli.	182
8.11	<i>CIELAB</i> (ΔE_{ab}^*) colour differences between the two conditions (solid Mondrian vs. Moving Mondrian).	183

Chapter 1

Introduction

1.1 Motivation

Colour management is ubiquitous in the modern world. Whenever someone uses a computer, watches television, goes to the cinema, uses a digital camera or looks at their mobile phone they are, without realising it, using colour management. Of course, there are different levels of colour management. There is the everyday colour management which is invisible to users but which is nevertheless critical (and this is driven by the International Colour Consortium ICC). There is also, at the other end of the spectrum, advanced colour management that is used in high-end research laboratories and which relies upon user expertise and specialised equipment. The former simply ensure that reds, for example, always appear red no matter whether they are viewed on a screen or printed in hard copy and is far from perfect in terms of colour fidelity, but adequate for the average user. On the other hand, colour management in research laboratories is more expensive (in every sense) but far more accurate. There are, of course, interactions and connections between the work of the ICC system (which now forms part of both Microsoft and Apple operating systems) and the high-end colour management that is referred to as colour characterisation. It is with the high-end colour characterisation that this research work is concerned.

1.2 Aims and scope

This research focuses on the colour characterisation of display devices and is not concerned with the capture of digital images (characterisation of cameras and scanners) nor their hard-copy output (characterisation of printers). At this point, we can define display colour characterisation with methods to allow the display of specific colours (by specific colours we normally mean colours identified by their CIE colour coordinates). A number of characterisation methods exist but three of these (referred to as the GOG, PLCC and the PLVC models) are particularly widely used. The main purpose of this research is to investigate the impact of using different types of characterisation models (GOG, PLCC and PLVC) using different sample sets and different linearisation samples for display characterisation as well as the effect of having a various number of linearisation samples available. Colour is a complex concept, therefore it requires more knowledge than just the colour area to cover all of the parts. To have a general understanding of this area, the CIE system; colour specification, measured or reproduction, colour management, colour display systems; the different technology of the display, colour characterisation, different methods of display characterisation, define the different test samples, critical reviews will be appropriate.

1.3 Thesis structure

This research is based on a number of different questions (see Chapter 3). In order to prepare for this research, a literature review has been carried out for the key ideas and concepts that will underpin the research.

Chapter 3 presents the framework and considers more about the main research question of this thesis. The evaluation of colour measurement equipment is considered. The general approach to the evaluation of the performance of characterisation models is also considered. Two characterisation models (GOG and PLCC) are described.

In Chapter 4 the different sets of samples which have been used in the experimental work are introduced. The different display devices and their specifications and settings are also described.

The main part of this thesis considers the challenging issue of using different methods of device characterisation as well as the effect of using a various number of linearisation samples. The work is described in Chapters 5 and 6. Chapter 5 looks a single display in detail and the rationale for this chapter is to introduce and demonstrate the methods and analyses that will be used in Chapter 6 where these methods are applied to a population of 20 different displays. Chapter 7 introduces the PLVC characterisation models, implements the model, and evaluates it in comparison to the earlier results from the GOG and PLCC models.

Chapter 8 is about the effect of using the different background on the colour of central calibration patches. The main concern in this chapter is about the new so-called moving Mondrian background which has been tested and results have been compared with using the different static backgrounds.

Chapter 9 is a summary of the findings from Chapters 5-8, which explains the results of the experimental work, and suggests some future work.

1.4 Summary of contribution to work

The principal findings from this study are:

- A meta-analysis of display characterisation finds strong evidence that the PLCC model (interpolation) is more accurate than the parametric GOG model.
- A meta-analysis of display characterisation finds strong evidence that use of grey-ramp linearisation samples should be preferred to colour-ramps linearisation samples to characterise the non-linear response of the displays.

In addition, it was found that:

- A large database of previous studies of display characterisation is accumulated in this study.
- The current research verifies and extends the display characterisation of various display technologies.
- A method for generating samples for a characterisation chart is put forward.

The following publications were produced in the course of this thesis:

Vazirian M, Westland S and Cheung V, 2013. Effect of background colour on monitor characterisation. Proceedings of AIC Conference, Newcastle (UK) [167].

Vazirian M, Cheung V and Westland S, 2013. Display characterisation for moving images. Proceedings of the IS&T/SID's Twenty first Colour and Imaging Conference, Albuquerque (USA) [166].

Chapter 2

Literature Survey

2.1 Introduction

In this chapter, the relevant study of colour science to the work is summarised. The practice of CIE colorimetry is introduced in this chapter including observations of colour perception, the CIE recommendations on standard illuminants, standard colorimetric observers, uniform colour spaces, colour difference formulae and colour-appearance models. Furthermore, the different display technologies as well as, the different methods of characterisation, are explained.

2.2 CIE System

2.2.1 Colorimetry

The science of specifying colour is termed colorimetry. A standard method for specifying a colour stimulus was developed by the Commission International de l'Eclairage or international committee on Illumination (CIE). The CIE system defined standard illuminants and standard observers to specify the colour of an object under standardised conditions. There are many excellent textbooks of colour science which demonstrate the importance of this topic to manufacturing industry and outline the history and development of the CIE system [181, 71, 119, 145, 74].

Two versions of the standard system were defined by the CIE, which are known as the CIE 1931 and CIE 1964 systems respectively; the difference is mainly the size of the stimuli (CIE 1931 is for 2-degree stimuli whereas CIE 1964 is for 10-degree stimuli).

2.2.2 Light Source and CIE standard illuminants

Physical emitters of radiation such as candles, lamps or sunlight are light sources that are characterised numerically by the spectral power distribution (SPD) curve. The SPD is the level of energy at each wavelength that is given in terms of radiant power and is often referred to as relative spectral power distribution. A light source may also be more simply (and less completely) specified in terms of colour temperature. The CIE distinguishes between illuminants, which are defined in terms of SPDs, and sources which are characterised as physically realisable producers of radiant power. There may not be a corresponding light source for a specific illuminant [154].

2.2.3 Correlated Colour Temperature

Correlated colour temperature (CCT) can describe the colour of a light source by associating its chromaticity with a corresponding point on the Planckian or blackbody locus. The SPD of a blackbody radiator can be specified by absolute temperature (K). The CCT of an illuminant is defined as the temperature of a blackbody radiator having the nearest chromaticity associated with the given spectral distribution in the CIE 1960 $u - v$ diagram [28, 108].

2.2.4 CIE Standard Illuminant and light sources

A standard illuminant is a series of spectral power distributions recommended by the CIE for use as standard light sources for measuring colours [145, 146]. The SPD is given in terms of radiant power and referred to as relative spectral power distribution. CIE illuminant A corresponds to a blackbody radiator functioning at a colour temperature of 2856K [108]. Illuminants B and C are corresponding sources which can be created using illuminant A source with additional filters.

As illuminant A simulates blackbody radiators in the range from 1600K to 3000K, it reproduces the tungsten filament lamp. Illuminant B simulates noon sunlight at a temperature of 4800K. Illuminant C is approximate daylight (composed of a mixture of light from the sun and the sky) with a temperature of 6774K. Since the colour of sunlight varies with solar altitude and with weather condition daylight, it is variable in its SPD (Fig. 2.1). There are several CIE standard illuminants which represent various daylight conditions through the day. The most important of these are D55 (used for balanced daylight film), D65 (daylight illuminant in colorimetry, represent indoor daylight) and D75 (cold indoor daylight used for critical inspection of yellowish colours) at colour temperatures of 5500k, 6500k and 7500k respectively.

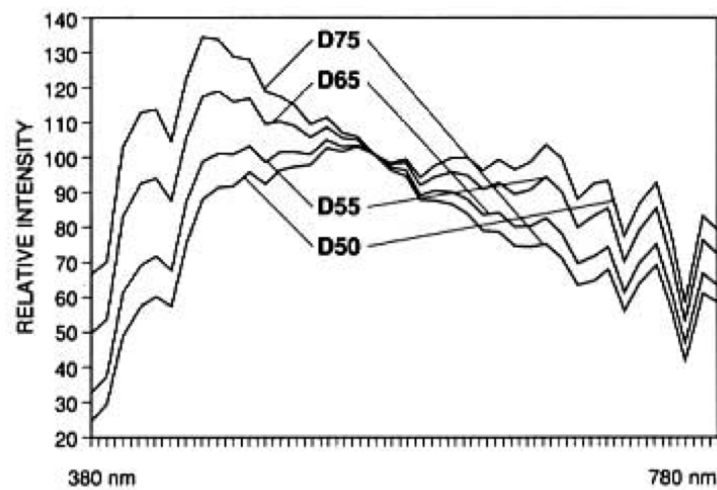


Fig. 2.1 Relative SPD of the CIE standard illuminants D50, D55, D65, D75 [45].

2.2.5 Colour matching function

The CIE colour matching functions were based on a series of experimental results performed in the late 1920s by Wright [178] and Guild [61]. The concept of this system is based on the assumption that any coloured light can be matched by an additive mixture, three monochromatic or broadband primaries. Thus, three primary lights (typically Red, Green and Blue) are required to visually match a stimulus [81] (see Equation 2.1).

$$C \equiv R[R] + G[G] + B[B] \quad (2.1)$$

In Equation 2.1, C represents the colour that is matched by R units of $[R]$, G units of $[G]$ and B units of $[B]$ primaries. The $[R]$, $[G]$ and $[B]$ refer to the particular set of primaries and RGB indicates the amounts (tristimulus values) of each primary in the match. The colour-matching functions or curves are normally visualised as a plot of the tristimulus values against wavelength (Fig. 2.2). The original CIE system was based on primaries at the wavelengths $700nm$, $546nm$, and $435.8nm$. Since some stimuli were too saturated to be matched by these primaries a negative amount of the $[R]$ primary was sometimes required.

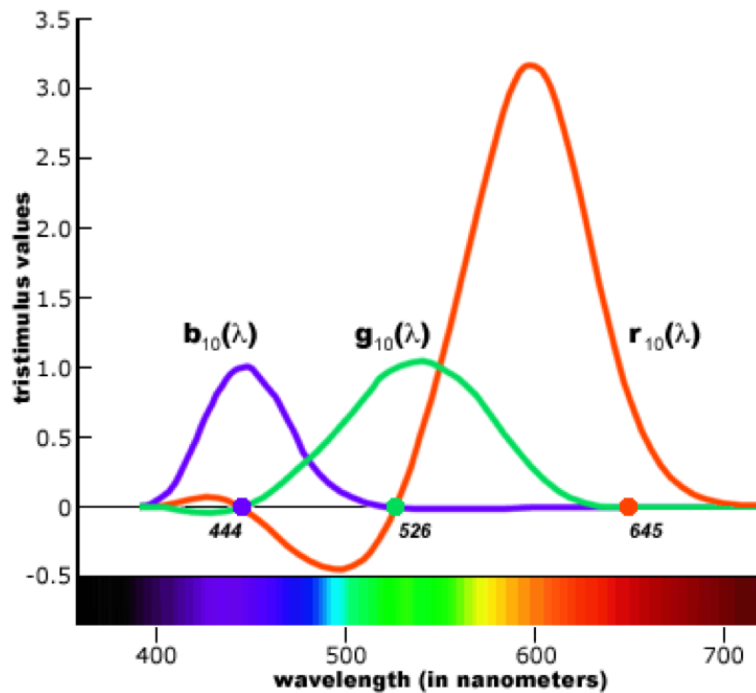


Fig. 2.2 The RGB colour matching functions [105].

The generalised equations for calculating the tristimulus value of a stimulus with spectral power distribution $\phi(\lambda)$ are given by Equations 2.2- 2.4:

$$R = \int_{\lambda} \phi(\lambda) \bar{r}(\lambda) d(\lambda) \quad (2.2)$$

$$G = \int_{\lambda} \phi(\lambda) \bar{g}(\lambda) d(\lambda) \quad (2.3)$$

$$B = \int_{\lambda} \phi(\lambda) \bar{b}(\lambda) d(\lambda) \quad (2.4)$$

where $\bar{r}(\lambda)$, $\bar{g}(\lambda)$, $\bar{b}(\lambda)$ are the colour matching functions.

The summation is taken over a suitable wavelength range in the visible part of the spectrum from $360nm$ to $780nm$ [77] at, usually, intervals of 1, 5 and $10nm$. Performing proper colour matching is difficult with a negative light, therefore the original RGB colour matching functions were transformed to achieve all positive curves by a 3×3 matrix linear transformation and led to the curves we are familiar with today (XYZ).

The main reasons that the CIE transform the RGB primaries to XYZ primaries are, firstly, to eliminate the negative values in colour matching function by choosing two of the imaginary primaries X and Z such that they produce no luminance response; secondly, to force the colour matching functions to equal the CIE 1924 photopic luminous efficiency function $v(\lambda)$.

As shown in Fig. 2.3 these three curves (x, y, z) are known as the CIE 1931 standard colorimetric observer. In 1964, CIE defined the supplementary using a standard colorimetric observer colour matching functions, 10° , stimulus as illustrated in Fig. 2.4.

The 1931 and 1964 standard colorimetric observers are also known as CIE 2° and 10° observers, respectively. The generalised equation for calculating the tristimulus value of a stimulus with weighted spectral power distribution can be calculated as

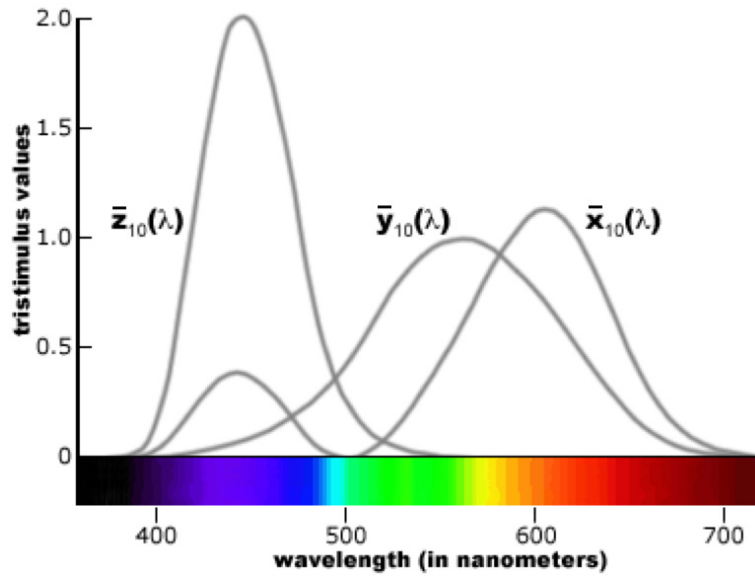


Fig. 2.3 The CIE 1964 colour matching functions for the 10° standard observer and the imaginary XYZ primaries [104].

following Equations 2.5- 2.8:

$$X = k \sum_{\lambda} S(\lambda)R(\lambda)\bar{x}(\lambda)\Delta\lambda \quad (2.5)$$

$$Y = k \sum_{\lambda} S(\lambda)R(\lambda)\bar{y}(\lambda)\Delta\lambda \quad (2.6)$$

$$Z = k \sum_{\lambda} S(\lambda)R(\lambda)\bar{z}(\lambda)\Delta\lambda \quad (2.7)$$

where k is a normalising constant, and $\bar{x}(\lambda)$, $\bar{y}(\lambda)$ and $\bar{z}(\lambda)$ are CIE colour matching functions (CMF) [28].

$$k = \frac{100}{\sum_{\lambda} S(\lambda)\bar{y}(\lambda)\Delta\lambda} \quad (2.8)$$

$S(\lambda)$ is the relative spectral power distribution (SPD) of a CIE standard illuminant source; $R(\lambda)$ is the objects spectral reflectance factor. $\bar{x}(\lambda)$, $\bar{y}(\lambda)$ and $\bar{z}(\lambda)$ are the CIE standard observer at wavelength λ and $\Delta\lambda$ is the measurement wavelength interval and k is a scaling constant.

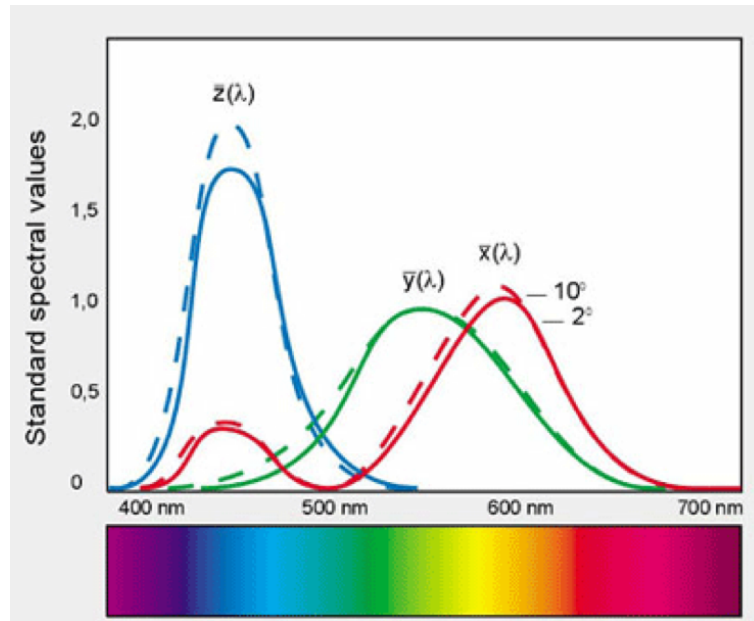


Fig. 2.4 Comparison between the CIE 1931 and 1964 colorimetric observer [26].

2.2.5.1 Two sets of colour matching functions

CIE established two sets of colour matching functions:

1. CIE 1931 standard colorimetric observer:

This was determined from experiments using a visual field that subtended 2-degree; therefore the stimuli were imaged on to the retina completely within the fovea. One disadvantage of the CIE 1931 chart is the fact that if two colours are equidistant from a third reference colour on the chart, it does not represent the colour differences between the two pairs as being perceivable. This is a well-known problem in the xy diagram, i.e. non-uniformity for perceived colour differences [102]. The distance of each vector is perceptually the same according to a CIE 1931, 2-degree standard observer; however, the line lengths largely vary.

2. CIE 1964 standard colorimetric observer:

In 1964 the CIE recommended an alternative set of standard colour matching function denoted by $\bar{x}_{10}(\lambda)$, $\bar{y}_{10}(\lambda)$ and $\bar{z}_{10}(\lambda)$ for use whenever more accurate correlation with visual colour matching in a visual field greater than 4-degree is designed.

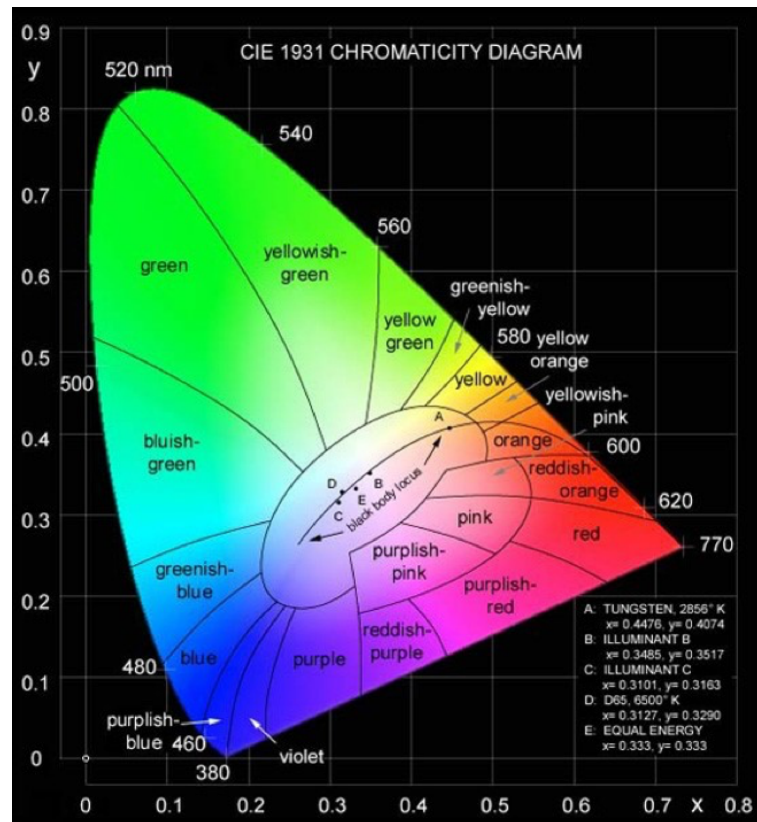


Fig. 2.5 CIE 1931 chromaticity diagram [27].

2.2.6 Chromaticity diagram

Chromaticity diagrams were developed to provide a convenient two-dimensional representation of colours. CIE tristimulus values of XYZ are transformed to chromaticity coordinates as given by Equations 2.9- 2.11 through a normalisation that removes luminance information.

$$x = \frac{X}{X + Y + Z} \quad (2.9)$$

$$y = \frac{Y}{X + Y + Z} \quad (2.10)$$

$$z = \frac{Z}{X + Y + Z} \quad (2.11)$$

where $x + y + z = 1$. Two coordinates out of three, usually x and y , are used to describe chromaticity. Fig. 2.6 plots the x, y chromaticity coordinates in a rectan-

gular coordinate system, giving the x, y chromaticity diagram of the XYZ colour specification system.

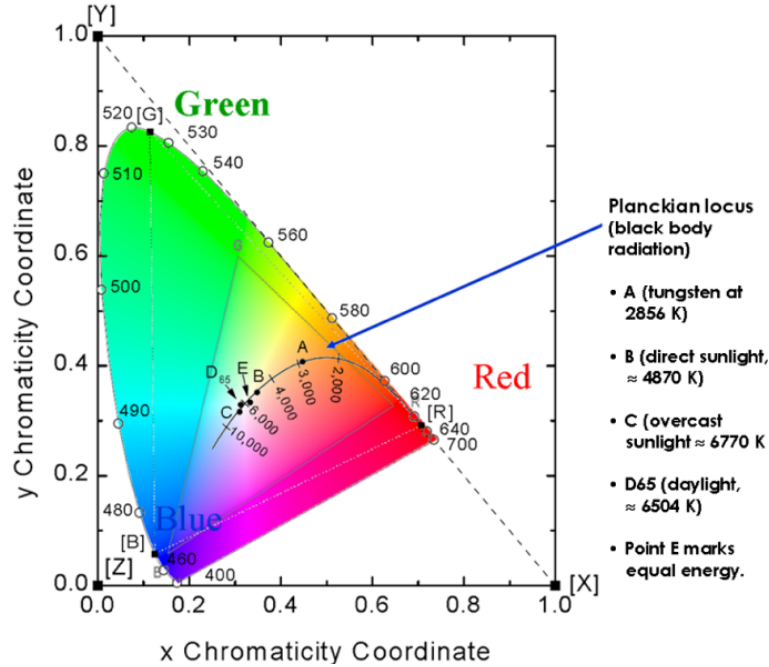


Fig. 2.6 x, y chromaticity coordinates in a rectangular coordinate system [182].

In this figure (Fig. 2.6), E shows the chromaticity of an equal-energy spectrum. This curved line (boundary) is known as the spectrum locus as shows the chromaticity of the spectral colour. Furthermore, the RGB primaries used to define the CIE 1931 RGB trichromatic system are specified by the triangle; $700nm$ for R , $546.1nm$ for G and $435.8nm$ for B .

2.2.7 Uniform colour space

In 1976, CIE introduced new chromaticity coordinates u' and v' (Equations 2.12-2.13) to achieve a more perceptually uniform chromaticity diagram.

$$u' = \frac{4X}{X + 15Y + 3Z} \quad (2.12)$$

$$v' = \frac{9Y}{X + 15Y + 3Z} \quad (2.13)$$

The CIE 1976 uniform colour scale diagram or the CIE 1976 UCS diagram is shown in Fig. 2.7.

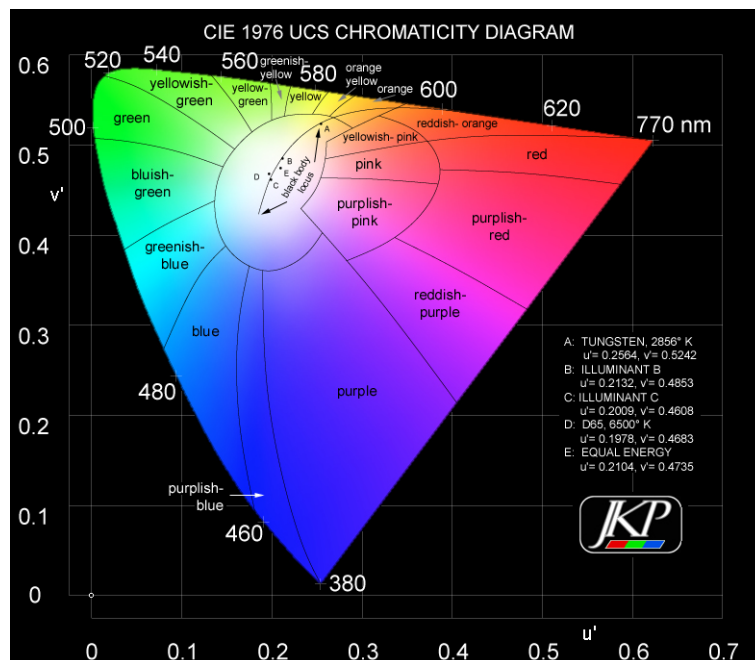


Fig. 2.7 The CIE 1976 UCS chromaticity diagram [32]

2.2.8 CIE Colour Space

A colour stimulus can be described using these three attributes; brightness or lightness, colourfulness, chroma or saturation, and hue. In order to predict lightness, chroma and hue, two uniform colour spaces were recommended by the CIE in 1976: $CIEL^*a^*b^*$ or *CIELAB* and $CIEL^*u^*v^*$ or *CIELUV*. These spaces extend tristimulus colorimetry to three-dimensional spaces with dimensions that approximately correlate with the perceived lightness, chroma and hue of a stimulus. The development, principle and practical uses of the CIE system have been described in a number of good texts [83, 49, 74].

CIELAB is needed to measure the colour differences between different reflective samples in the industry such as printing, inks, paper, textile, dyes and coatings. It is based on the opponent principle that a sample cannot be red and green at the same time and it cannot be blue and yellow at the same time.

L^* indicates the lightness of a sample ($L^* = 0$ black and $L^* = 100$ indicates white).

a^* indicates the redness-greenness of a sample. $+a^*$ indicating red and $-a^*$ indicating green.

b^* indicates the yellowness-blueness of a sample. $+b^*$ indicating yellow and $-b^*$ indicating blue.

CIELAB is expressed by the following orthogonal coordinates:

$$L^* = 116f(Y/Y_n) - 16 \quad (2.14)$$

$$a^* = 500[f(X/X_n) - f(Y/Y_n)] \quad (2.15)$$

$$b^* = 200[f(Y/Y_n) - f(Z/Z_n)] \quad (2.16)$$

where $I = Y/Y_n$ and $f(I) = I^{1/3}$ for $I > (24/116)^{1/3}$
and $f(I) = (841/108)I + 16/116$ for $I \leq (24/116)^{1/3}$

where X, Y, Z represent the tristimulus values of the sample under consideration, and X_n, Y_n, Z_n represent the tristimulus value of a perfect diffuser under the same illuminant. These adopted signals are then subject to a compressive nonlinearity represented by a cube root function in the *CIELAB* equations. This nonlinearity is designed to model the compressive response typically found between physical energy measurements and perceptual responses.

$$C_{ab}^* = [(a^*)^2 + (b^*)^2]^{1/2} \quad (2.17)$$

$$h_{ab}^* = \arctan(b^*/a^*) \quad (2.18)$$

The C_{ab}^* defined in Equation 2.17 represents as the correlated of chroma. In Equation 2.18, the h_{ab} is defined the numerical of the hue angle.

The *CIELUV* colour space is derived from the CIE 1964 $U^*V^*W^*$ which was first proposed by Wyszecki [180] and was adopted by the CIE in 1964. *CIELUV* is expressed by the following orthogonal coordinates.

$$L^* = 116f(Y/Y_n) - 16 \quad (2.19)$$

$$u^* = 13L^*(u' - u'_n) \quad (2.20)$$

$$v^* = 13L^*(v' - v'_n) \quad (2.21)$$

if $I = Y/Y_n$ and $I > 0.008856$, then $f(I) = I^{1/3}$

if $I \leq 0.008856$, then $f(I) = 7.787(I) + 16/116$

$$C_{uv}^* = [(u^*)^2 + (v^*)^2]^{1/2} \quad (2.22)$$

$$h_{uv}^* = \arctan(v^*/u^*) \quad (2.23)$$

$$S_{uv}^* = C_{uv}^*/L^* \quad (2.24)$$

In the CIE 1967 $L^*u^*v^*$ space, the quantity derived from C_{uv}^* and L^* can be used as a saturation. As stated in Equation 2.25, by changing the luminance factor in a series of object-colour stimuli of chromaticity constancy, S_{uv}^* remains constant with corresponding changes in C_{uv}^* .

$$S_{uv}^* = 13[(u' - u'_n)^2 + (v' - v'_n)^2]^{1/2} \quad (2.25)$$

Euclidean distance in *CIELAB* colour space can be used to approximately represent the perceived magnitude of colour differences between object colour stimuli. Two equivalent equations describing *CIELAB* colour differences are given in Equations 2.26- 2.27, although, it was found that perceptual uniformity of colour difference is not consistent, in particular with respect to hue [99].

$$\Delta E_{ab}^* = [(\Delta L^*)^2 + (\Delta a^*)^2 + (\Delta b^*)^2]^{1/2} \quad (2.26)$$

$$\Delta E_{ab}^* = [(\Delta L^*)^2 + (\Delta C_{ab}^*)^2 + (\Delta H_{ab})^2]^{1/2} \quad (2.27)$$

where

$$\Delta H_{ab}^* = [(\Delta E_{ab}^*)^2 - (\Delta L^*)^2 - (\Delta C_{ab}^*)^2]^{1/2} \quad (2.28)$$

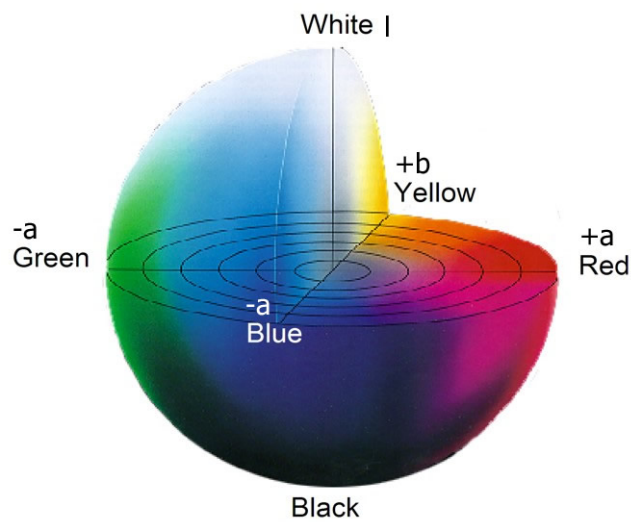


Fig. 2.8 CIELAB L^* , a^* and b^* coordinates [33].

For the hue difference, the indices 1 and 2 refer to any two colour stimuli and ΔH_{ab} is the hue angle difference of the two colour stimuli compared. In Equation 2.27 ΔC_{ab}^{*2} is in the same units of ΔL^* and ΔE^* ; however, ΔH_{ab} is in degrees which is not consistent with the other two variables. To transfer the hue angle difference Δh_{ab} into hue difference ΔH_{ab} (in units commensurate with other variables), Equation 2.28 should be used. According to Equation 2.27 the colour difference ΔE_{ab}^* is obtained from lightness, chroma and hue differences. It can be seen that ΔL^* , ΔC_{ab}^* and ΔH_{ab}^* are included with the same weight; however, there are cases in which a correlation between ΔE_{ab}^* of equation $b^* = 200[f(Y/Y_n) - f(Z/Z_n)]$ with the perceived magnitude of colour difference is improved using different weights for ΔL^* , ΔC_{ab}^* and ΔH_{ab}^* [181, 118].

Hue difference is calculated using the fact that the Euclidean distance in ΔL^* , Δa^* and Δb^* rectangular coordinates is identical to the Euclidean distance in the ro-

tated rectangular coordinates ΔL^* , ΔC_{ab}^* and ΔH_{ab}^* . More different colour difference formulae have been suggested to correct the non-uniformity, e.g., CMC(l:c) [34], BFD(l:c) [98], CIE94 [177] and CIEDE2000. It is necessary to do the software verification for colour-difference computing based on the CIEDE2000 formula which is considerably more sophisticated and computationally involved than the preceding colour-difference equations for CIELAB [28] and the CIE94 [177] colour difference [151]. It has been demonstrated by Luo [99] that the fundamental problems of CIELAB are corrected in CIEDE2000. These corrections contain the lightness weighting function which includes S_L (which predicts the lightness difference), chroma weighting function S_C for normalisation, hue weighting function S_H , R_T for chromatic corrections in the blue region and the $(1 + G)$ factor to correct the achromatic shades. Equation 2.29 shows the CIEDE2000 colour differences formula. The computational process again starts from the coordinates (L^* , a^* and b^*) of the CIELAB.

$$\Delta E_{00} = \sqrt{\left(\frac{\Delta L'}{k_L S_L}\right)^2 + \left(\frac{\Delta C'}{k_C S_C}\right)^2 + \left(\frac{\Delta H'}{k_H S_H}\right)^2 + R_T \left(\frac{\Delta C'}{k_C S_C} \frac{\Delta H'}{k_H S_H}\right)} \quad (2.29)$$

where

$$S_L = 1 + \frac{0.015(\bar{L}' - 50)^2}{\sqrt{(20 + \bar{L}' - 50)^2}}$$

$$S_C = 1 + 0.045\bar{C}'$$

$$S_H = 1 + 0.015\bar{C}'T$$

$$T = 1 - 0.17\cos(\bar{h}' - 30^\circ) + 0.24\cos(2\bar{h}') + 0.32\cos(3\bar{h}' + 6^\circ) - 0.20\cos(4\bar{h}' - 63^\circ)$$

$$R_T = -\sin(2\Delta\Theta)R_C$$

$$\Delta\Theta = 30\exp\left\{-\left[\frac{(\bar{h}' - 275^\circ)}{25}\right]^2\right\}$$

$$R_C = 2\sqrt{\frac{(\bar{C}')^7}{(\bar{C}')^7 + 25^7}}$$

$$L' = L^*$$

$$a' = (1 + G)a^*$$

$$\begin{aligned}
 b' &= b^* \\
 C' &= \sqrt{(a')^2 + (b')^2} \\
 h' &= \tan^{-1}(b'/a')
 \end{aligned}$$

where

$$G = 0.5 \left(1 - \sqrt{\frac{(\bar{C}_{ab}')^7}{(\bar{C}_{ab}')^7 + 25^7}} \right)$$

2.3 Colour appearance

Models of colour vision rely on assumptions provided by the theories of colour perception and so-called colour-appearance models. Generally, colour appearances can be changed by the different illuminant and viewing conditions. Different viewing conditions such as media, light sources, background colours and luminance levels cause changes to the colour appearance of an object [5, 29]. Three relative colour appearance attributes, lightness, chroma and hue can describe colour in *CIELAB* space but under limited viewing conditions. Hence, the aim of a colour appearance model is to predict colour appearance under different light sources and viewing conditions. Various colour appearance phenomena are introduced in the following sections, as well as *CIECAM02*, which is the recent CIE recommended model.

2.3.1 Visual area in the observing field

The appearance of a test stimulus can be influenced by adjacent colours, as well as the environments in which the viewing is taking place. Viewing distance and the size of the target stimulus determine the visual angle. Therefore, the visual angle can be used to define different visual areas in the observing field, such as the area located next to the target stimuli and the area located separately from the target stimulus. Since the eyes are moving continually, it is impossible to separate spatial and temporal effects on the colour appearance of the target stimulus. However, if observers have sufficient time to adapt to the viewing environment and the target

stimulus does not vary in the time domain, temporal effects are generally not encountered in typical colour-appearance applications [49].

Despite the fact that the visual areas in the observing field are almost infinitely variable, attempt has been made by Hunt [74] to define visual areas in the observing field to simplify the visual areas which affect colour appearance as follows. Fig. 2.9 illustrates the visual components.

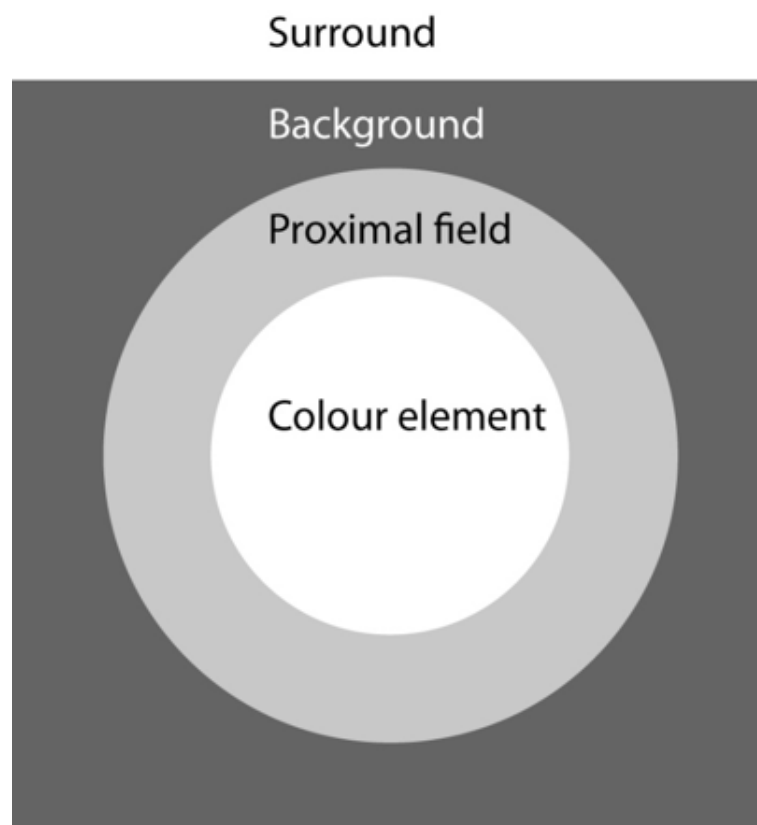


Fig. 2.9 Schematic diagram of the observing field according to Hunt [71].

2.3.1.1 The colour element stimulus considered

Characteristically, a stimulus is taken to be a uniform patch which subtends an arc of around 2 degrees. The explanation for choosing a 2-degree visual angle for defining the stimulus can be found from the nature of the fovea which occupies the central 1.5-degree diameter of the visual field.

2.3.1.2 The proximal field

The immediate environment of the colour element consideration normally extends for about 2-degree from the border of the colour component considered in all or most directions. It is normally specified to be similar to the background in the current standard colour-appearance model *CIECAM02* [31], but is included to facilitate future modelling of simultaneous contrast.

2.3.1.3 The background

The environment of the colour element considered, the background typically extends for about 10 degrees from the edge of the proximal field in all or most directions. When the proximal field is the same colour as the background, the latter is regarded as extending from the edge of the colour element under consideration. The background is usually intended to be a neutral grey with 20% luminance factor. For imaging applications, defining the background is difficult when the angle subtended by a target image is greater than 10 degrees. In this case, the exact specification of the background is dependent on image content and the location of specific objects in the image; however, there is no standard guide for this ambiguous case.

2.3.1.4 Surround

A surround is a field beyond the background. The surround, for practical situations, can be considered to be the entire room in which the viewing is taking place. Real viewing environments; however, include veiling glare, inhomogeneous spatial configuration, and a large variation in surrounding luminance, such that specifying the surround condition precisely is difficult. The colour of a surround is not considered in any colour-appearance model; it is sufficient to know the relative luminance of the surround with respect to the luminance of the colour element considered [49]. Therefore, the surround is expressed as a categorical term, dark, dim or average for practical use of *CIECAM02*.

2.3.1.5 Adapting field

An adapting field is the total surroundings of the colour component under consideration, including the proximal field, the background, the surround and extending to the limit of vision in all directions. The adapting field must be specified by at least its absolute tristimulus values [49]. An alternative and equivalent specification is to have relative tristimulus values and the absolute luminance or illuminance. The absolute luminance of the adapting field is needed to allow colour appearance to be modelled under different degrees of adaptation.

2.3.2 Colour appearance attributes

The fundamental attributes of colour sensation are brightness, hue and colourfulness. The ratio of a surface's brightness and the brightness of the reference white define the lightness sensation [92]. Setting a surface's colourfulness in proportion to the reference brightness yields chroma. Similarly, comparing a surface's colourfulness to its own brightness level provides the saturation sensation.

CIE [74] defines common colour appearance terminologies:

- **Brightness:** Attribute of a visual sensation according to which an area appears to exhibit more or less light.
- **Lightness:** The brightness of an area judged relative to the brightness of a similarly illuminated area that appears to be white or very highly transmitting.
- **Colourfulness:** Attribute of a visual sensation according to which an area appears to exhibit more or less of its hue.
- **Chroma:** The colourfulness of an area judged in proportion to the brightness of a similarly illuminated area that appears to be white or highly transmitting.
- **Saturation:** The colourfulness of an area judged in proportion to its brightness.
- **Hue:** Attribute of a visual sensation according to which an area appears to be similar to one, or to a proportion of two, of the perceived colours, red, yellow, green and blue.

The concepts of colour appearance should be standardised in order to avoid confusion regarding their description, since earlier studies on colour appearance

used these terms in a slightly different manner. This controversial subject was addressed early on, in order to clarify the concepts and terms to describe the chromatic response by which hue is categorised. However, after the concept of 'colourfulness' was suggested by Hunt [69, 128], and it was demonstrated by Pointer to be easily understood by an observer [128, 129], the term 'colourfulness', 'chroma' and 'saturation' became standardised and widely used in the field of colour science.

2.3.3 Colour appearance phenomena

Two stimuli under the specific viewing conditions are considered by the CIE system of colorimetry. Illumination, surround condition, background colour, size, shape, texture and viewing geometry all affect the colour appearance. If any of these constraints are violated, it is likely that the colour match will no longer hold. The various phenomena that break the simple XYZ tristimulus system are called colour appearance phenomena. Changes in luminance, a change in the chromaticity of a light, the background and surrounds and cognitive factors are five attributes of colour appearance phenomena characterisations which some explain in this section. The Hunt and Stevens Effects are two major phenomena related to the change of luminance level [100] which are described here:

- Hunt effect

The Hunt effect [68] can be described as the adaptation effect that light and dark have on colour perception. In other words, the notation that the colourfulness of a given stimulus increases with luminance level. It was found that a colour stimulus of low colorimetric purity, which was viewed in a high level of illumination, could be matched with another colour stimulus of high colorimetric purity. This effect can also be witnessed by taking a colour image and changing the level of illumination under which is viewed. The image object will appear significantly more colourful if the image is moved to a significantly brighter viewing environment.

- Stevens effect

The Stevens effect [158] refers to increase in brightness (or lightness) contrast with increasing luminance, as opposed to the Hunt effect, which focuses on an increase in chromatic contrast (colourfulness) with luminance. Steven's results show that the connection between perceived brightness and considered

luminance tends to follow a power function when observers estimate the magnitude of the brightness of stimuli across various adaptation conditions. They also adjusted the brightness in the matching field until it was perceived to have a similar brightness to each of several areas in an image. The observed relationship follows a power function when plotted on linear coordinates, and becomes a straight line on log-log coordinates. It was demonstrated by the results that the slope of this relationship increases with increasing adapting luminance. The third result was that the rate of departure from the power function at any given level of illumination varies between projected transparency images in a dark surround and printed images in an illuminated surround. In conclusion, the Stevens effect indicates that as the luminance level increases, dark colours will appear darker and light colours will appear lighter.

- Surround effect

The Surround effect describes the phenomenon where the simultaneous contrast is the change in the appearance of a colour through the influence of a contrasting colour in the immediate environment. The smaller colour area can be influenced by the larger surrounding area. Simultaneous contrast usually occurs if the angular subtense of the colour is greater than about 1° .

- Helmholtz-Kohlrausch effect

The Helmholtz-Kohlrausch Effect (brightness increasing with increasing saturation) is an observed variation in lightness between two colours under the same illumination, both having the same Y value but differing in chromaticity in the respect that one is achromatic and the other is chromatic [10]. This is also called heterochromatic brightness matching. In essence, two different colours have the different perceived brightness.

- Bezold - Brücke and Abney effect

The Bezold-Brücke effect (hue changes with luminance) and Abney effect (hue changes with colorimetric purity) are summarised by Pridmore [137]. The Bezold-Brücke effect describes the shifting of the perceived hue, if a given chromaticity is viewed simultaneously as two juxtaposed samples of different luminances (for example, in the ratio 10:1). The Abney effect describes the effect of adding white light or pigment to a full colour, wherein the perceived hue, relative to that of the full colour, usually shifts. The Bezold-Brücke effect

reports that in the case of a change in the luminance of a monochromatic light, hue is shifted. In contrast, the Abney effects report that monochromatic lights at all luminance levels should have the same relative tristimulus values for any given monochromatic light [138].

2.3.4 Colour appearance model

All colorimetric measurements must be made under the same viewing conditions defined by the CIE. However, under different lighting conditions and background, the human visual system perceives the colour of an object in different ways to define a colour appearance model. There is frequently a need to reproduce a particular colour across a wide range of different viewing conditions. Colour appearance models are used to develop a device-independent way of analysing images. For instance, if the output display's illumination conditions are known, one can transfer the internal representation of the image to the correct representation for the output display to display image in the screens, against the colour appearance. Several colour appearance models were proposed since the CIE recommended *CIELAB* in 1976, such as the Hunt model [70], the Nayatani model [116], the *RLAB* model [47, 46], the *LLAB* model [101], the *ATD* models [62, 63], and the *CIECAM97s* model [25]. In this section, *CIELAB* [30] will be reviewed as well as *CIECAM02* which is the recent CIE recommended model.

2.3.4.1 The *CIECAM97s* and *CIECAM02*

CIECAM97s was recommended by the CIE TC 1-34 in 1997; it is the first colour appearance model. In order to improve performance and to simplify the model, a number of revisions to the *CIECAM97s* models were considered. This model, *CIECAM97*, is very similar to the Hunt model but also incorporates the best features from the other existing models including [116], *RLAB*, and *LLAB*. Three major drawbacks in *CIECAM97s* have been illustrated [97]: "overprediction of chroma for near neutral colours, poor prediction of saturation results and large variation of the predicted saturation values for colours having the same chromaticity but different luminance factors." The *CIECAM02* [112] colour appearance model is based on the basic structure of the *CIECAM97* colour appearance model with a few modifications [48, 72]. This model provides all the functionality of *CIECAM97s* and

incorporates several revisions, which results in increased accuracy, performance, and simplification of the structure.

2.4 RGB colour system

2.4.1 additive colour mixing

The additive colour mixing system refers to spotlight emitted directly from a source before an object reflects the light. To produce other colours, various amounts of three primaries (typically red, green and blue) lights are mixed in the additive reproduction process. e.g. additive mixing of red and green light produce the shades of yellow, orange or brown [140]. The additive colour primaries and *RGB* colour model are commonly used by television and other computer and video display devices.

2.4.2 Trichromatic colour reproduction

Human colour vision is trichromatic [115]. It is based on the responses of three classes of cones in the retina; these have broadband spectral sensitivity but maximum sensitivity at different wavelengths. The reproducible gamut of colour in the trichromatic system is not always as large as the gamut of colours in the world, so the gamut is limited. The largest gamut is obtained when the additive primaries are red (*R*), green (*G*) and blue (*B*).

The *RGB* colour cube is, where each of the primaries forms one of the principal axes. As is shown in Fig. 2.10 most *RGB*-based colour spaces can be visualised as a cube, with one corner of black (zero intensity of primaries) and the opposite corner of white (maximum intensity of primaries); the three primaries are red, green and blue, and the secondaries are cyan (blue+ green), magenta (red+ blue) and yellow (green+ blue).

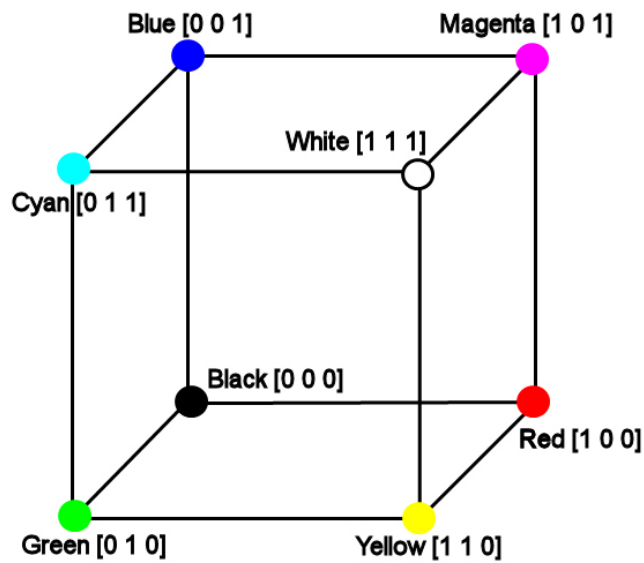


Fig. 2.10 *RGB* colour space [142].

2.4.3 RGB Colour space

A colour model represents colour numerically usually using three or four values. *RGB* (red, green and blue) is the most common colour space used for rendering images in the digital space. Each pixel of colour is formed by a red, green and blue component adding together.

The *RGB* colour model is based on the notion that all visible colours can be created using the primary additive colours; red, green and blue (in practice only a limited gamut can be achieved). In Fig 2.10 white will be created by mixing the maximum amount of all three primaries (red, green and blue), whilst black is generated when each of the red, green and blue channels are absent. In addition, mixing equal amounts of two primaries will create cyan, magenta and yellow.

Image signals are encoded in a colorimetric *RGB* standard in many imaging devices based on the *RGB* primaries and using the additive system [83]. Whilst the *RGB* colour model is ideal for rendering imagery on digital devices, it is less suitable for use in computer vision since the distance between colours do not correspond with the way in which humans perceive colour [139]. CIE colour-matching functions are derived by CIE standard *RGB* primaries.

There are three well-known and most commonly used sets of *RGB* primaries, called SMPTE-C, ITU-R BT. 601 and ITU-R BT. 709-3. Although SMPTE-C and

Table 2.1 The CIE 1931 chromaticity coordinates of the SMPTE-C, Rec. 601 and Rec. 709 primaries.

	SMPTE-C			ITU-R BT. 601			ITU-R BT. 709-3		
	R	G	B	R	G	B	R	G	B
x	0.6300	0.3100	0.1550	0.6400	0.2900	0.1550	0.6400	0.3000	0.1550
y	0.3400	0.5950	0.0700	0.3300	0.6000	0.0600	0.3300	0.6000	0.0600
z	0.0300	0.1050	0.7750	0.0300	0.1100	0.7900	0.0300	0.1000	0.7900

ITU-R BT. 601 have been used by many display systems, ITU-R BT. 709-3 is used as high-definition television develops, and is, therefore, becoming more prevalent. In a chromaticity diagram, the gamut size of *RGB* primaries for each set can be plotted by following Grassman's¹ additivity law [122]. The colour gamut boundaries are indicated by the triangle that connects three primaries in the chromaticity diagram. The ITU-R BT. 709-3 gamut size is slightly larger than for SMPTE-C.

There is no universal acceptance of any *RGB* colour space. Hence, there are many standards depending on consumer demands, professional interest and technological advances. The NTSC which stands for the National Television System Committee specified a set of primaries that were representative of phosphors used in CRTs of that era in the USA [136]. The NTSC primaries were more saturated than those now found in the other modern display devices but as a consequence was not very bright. ITU-R BT. 601 and Rec. 601 is known in the European countries as different sets of primaries established by the European Broadcast Union (EBU). The NTSC primaries were finally replaced by SMPTE-C primaries that are slightly smaller in gamut but can achieve greater brightness. The new sets of primaries were established for high definition television (HDTV) as ITU-R BT. 709-3 or simply Rec. Table 2.1 shows a list of the CIE 1931 chromaticity coordinates of the SMPTE-C, Red. 601 and Rec. 709 primaries.

Fig. 2.11 shows the colour gamut achieved by using the Rec. 709 primaries. The gamut limit triangle shows the maximum extent of display colours, so out-of-gamut colours (which are the colours that lie outside of the triangle) cannot be reproduced by the display. The addition of different luminances, illuminants and other contributing factors mean that the gamut in three-dimensional colour space

¹If a test colour is the combination of two other colours, then in a matching experiment based on mixing primary light colours, an observer's matching value of each primary will be the sum of the matching values for each of the other test colours when viewed separately.

is complex [133]. The colour gamut of any primaries is three-dimensional shaped; consequently, at certain luminance levels within the triangle, many chromaticities would be out of gamut [113]. Fig. 2.12 shows the gamut space for an HP display with no ambient illumination. The addition of a neutral ambient acts to desaturate colours somewhat, the amount depending on the luminance of the source [93].

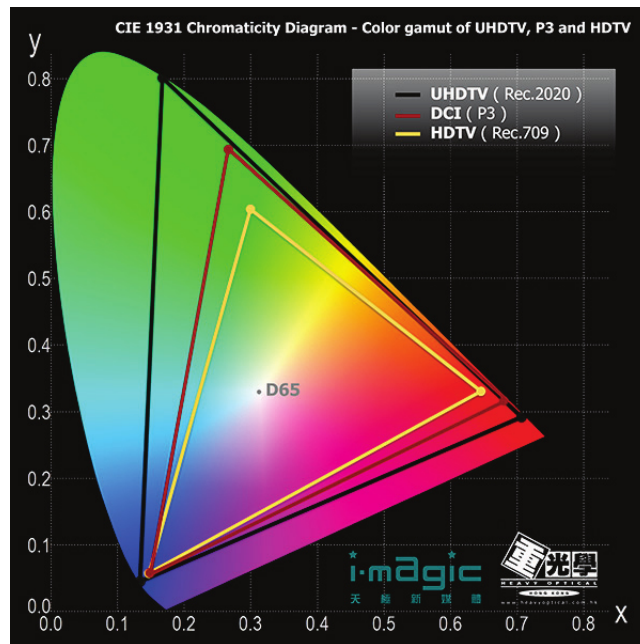


Fig. 2.11 Gamut of colours using the Rec. 709 primaries [141].

By considering the three-dimensional shape of the gamut, the range of colour may be reduced, because the use of more saturated primary colours would in principle allow a greater gamut of reproducible colours. In addition, it is normal to allocate 8 bits per colour channel in the digital *RGB* colour system, resulting in 256 values for each of the primaries (*R*, *G* and *B*). These 8 bit per channel systems (24-bit colour system) can reproduce approximately 16 million colours [130].

The digital steps will be more widely spaced by using the wider *RGB* colour gamut. Therefore, to create high-resolution systems with greater colour bit depth, there will be a high demand for the use of more than 24 bits per pixel [53, 171].

There are different colour spaces within the *RGB* model such as *sRGB* and Adobe *RGB* which can often be selected through the colour setting of each device.

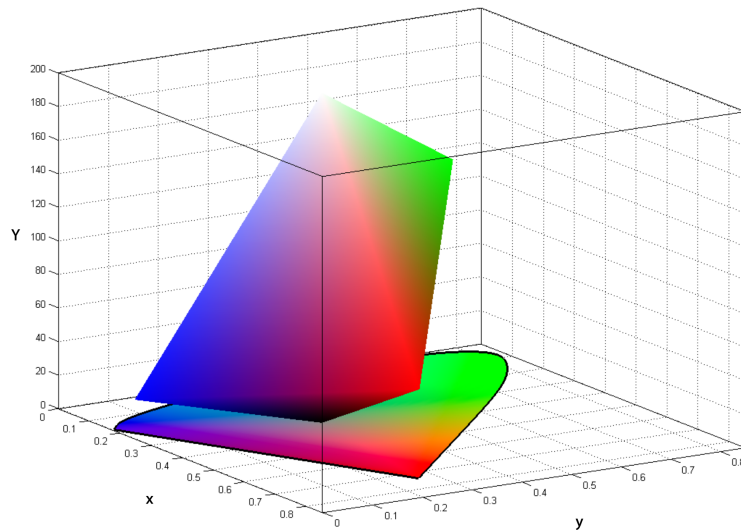


Fig. 2.12 HP Dream colour LP2480z sRGB 3D gamut shows on xy chromaticity diagram.

2.4.3.1 sRGB

In 1996 *sRGB* was introduced as a standard *RGB* colour space by Hewlett-Packard and Microsoft especially for use by HP products, the Microsoft operating system and the Internet [3]. *sRGB* is described by IEC61966-2-1 as a default colour space for multimedia applications [37]. The specification for *sRGB* (IEC61966-2-1) uses BT.709 chromaticity, D65 reference white, a display gamma of 2.2, and linear *RGB* (8 bits per colour) [78]. The chromaticity values of the primaries using Rec. 709 system is the same as the *sRGB* system as it is designed to be compatible with the Rec. 709 standard. *sRGB* values have a normalised range of 0-1, with 8-bit digital *sRGB* values having a range of 0-255 for black-white. In its normative part, the standard defines the relationship between 8-bit *sRGB* values and CIE 1931 XYZ values as measured at the faceplate of the reference display [160]. The definition of a rendered colour space for data interchange in multimedia is the purpose of *sRGB*. *sRGB* 64 is proposed by Microsoft and Hewlett-Packard, which extends the tonal range and coding precision of *sRGB* [155].

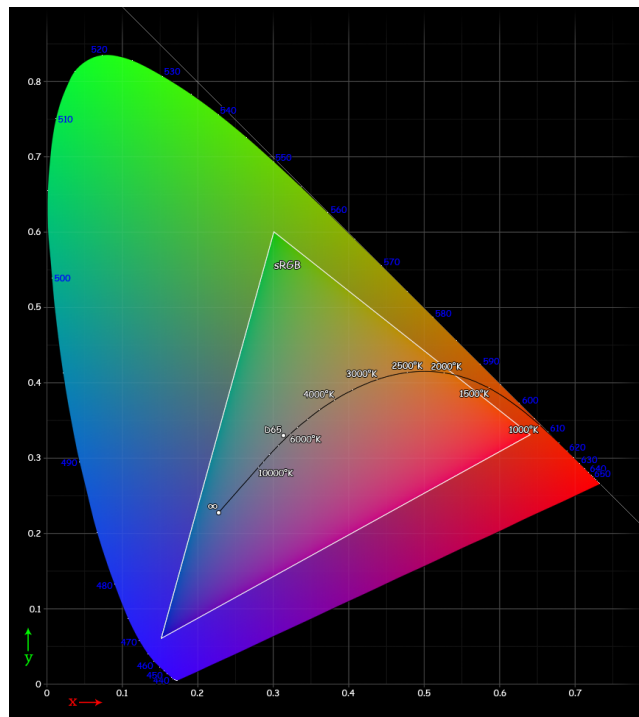


Fig. 2.13 *sRGB* gamut [157].

2.4.3.2 Adobe (1998) RGB

One of the disadvantages of the *sRGB* colour system is that the size of the colour gamut is not sufficient to represent all of the colours that can be reproduced in the printing system, particularly in the blue-green area. Fig. 2.14 illustrates the difference gamut area of the *sRGB* and Adobe *RGB*. In 1998 the Adobe software company established the Adobe *RGB* colour space in order to cover the majority of the achievable colours in CMYK colour printers. In particular, the Adobe *RGB* colour space improves the cyan-green spaces of the *sRGB* colour space.

2.4.4 White Point

Setting up the white point is one of the key factors of display calibration. The combination of red, green and blue lights creates white light while noting that the display devices use the additive colour mixing system. A white point is a calibration setting on a display that determines the colour temperature of the brightest white (reference white or target white), defined by the tristimulus values or chromaticity coordinates [86]. By setting up the white point, all colour temperature appearance

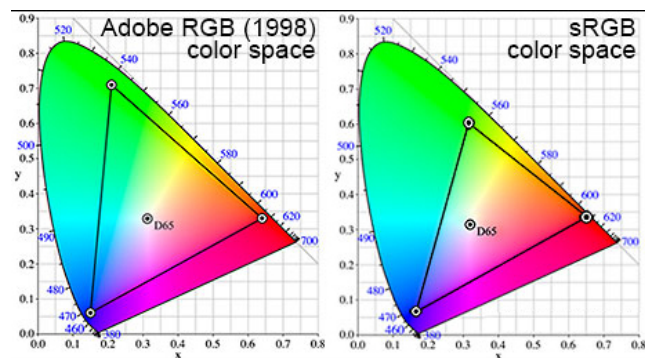


Fig. 2.14 Comparing sRGB and Adobe RGB [156].

in the display will be affected. Colour temperature is expressed in Kelvin, e.g. 6500K. There are more standard illuminants such as D50, D65 to define the colour temperature. Most high-quality LCD displays have a defined "Native" white point which is very close to a colour temperature of 6500K.

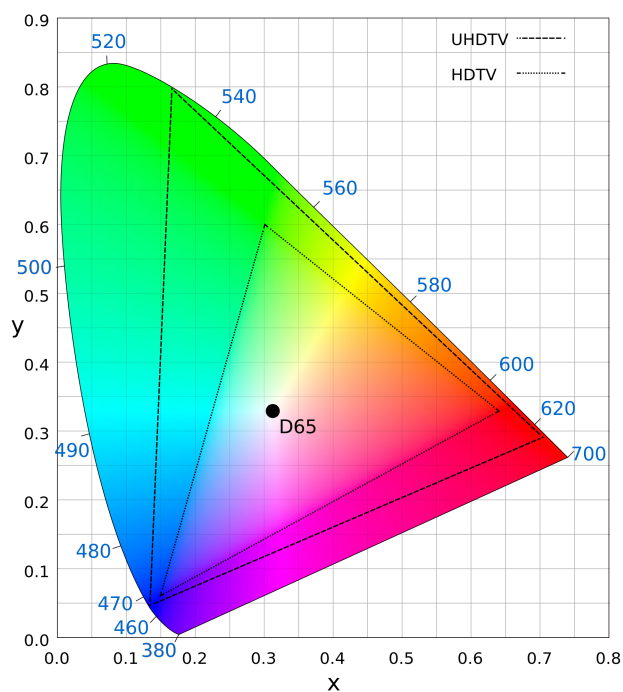


Fig. 2.15 Gamut of the Rec 2020 and Rec 709 with the white point [175].

2.5 Colour management

Managing and controlling colour when it is captured or displayed by a wide variety of devices and technologies (so-called 'Cross-media reproduction') present serious issues, especially for the printing and imaging industries [88]. Accurate colour control is vital for these industries as the same image displayed on different display devices is likely to have a very different colour appearance. Even in a particular device, variations in colour appearance may occur upon changing the settings of the device such as brightness, contrast, gamma, and colour temperature [173]. Further enhancements in multimedia colour reproduction will be accomplished through better algorithms for gamut mapping and colour appearance.

Controlling colour between input and output devices plays an important role in ensuring colour fidelity. There are three distinct clients (end-users, advanced users and high-end) who use colour management systems. The basic colour control of a given device is highly controlled by the majority of manufacturers in order to maintain acceptable colour fidelity. The calibration and characterisation of devices are vital for the second group, which are the professional users of colour such as designers or photographers who want to achieve parity in image representation and colour between input devices (e.g. camera, scanners, etc) and output devices (displays, printing, etc). Finally, high-end users who wish to certify that the colour control of a system works properly. As a result, spectrophotometers and colorimeters are now necessary tools throughout the industry. Colour management systems have been developed to utilise these measurement devices to characterise the colour of input, display and output devices [52, 8]. These hardware and software tools have not yet solved all the problems of colour reproduction, but have made quantification possible, which is essential for controlling quality. Given the fact that each display device is limited to reproducing the range of colours which lie inside of the colour gamut, colour management may not be sufficient to ensure full reproduction of a given colour.

Over the past three or four decades, it has not been possible to provide acceptable colour fidelity between devices from a different manufacturer. This implies that all input and output devices such as scanners, cameras, displays and printers must be from the same producer in order to work properly. High-end clients may use 'closed loop' systems by choosing the manufacturer but not the device technologies [148,

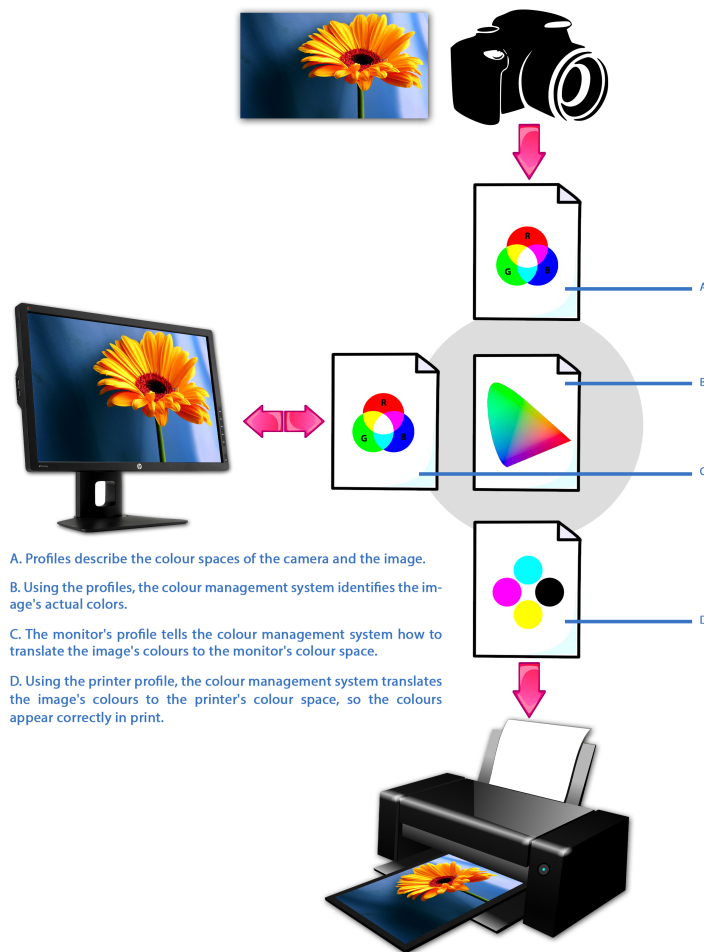


Fig. 2.16 Matching colour with profile [107].

57]. Technological advancement has resulted in a greater diversity of picture sources and printing devices, and the need for inter-manufacturer operability between devices has grown [169]. As a result, there is a requirement for a device profile to translate the colour reproduction conduct of the device into a CIE-based colour space. Hence, open frameworks were set up in accordance with the requirement for a colour management system. The configuration of open frameworks requires an independent, standardised colour management system in order to perform colour transformation between the distinctive device by utilising an independent colour space as an engine [23].

2.5.1 Colour management procedure

A successful colour management system can be obtained by conducting a proper colour transformation, although working in an analogue or digital system can affect this procedure. Subsequently, proper colour transformations configured as calibration, characterisation and colour encoding [150, 55] are required. Device calibration is the process of adjusting the device to maintain the colour fidelity, where the main purpose is to fix the colour response of a device with a known state. Colour calibration is a key procedural element procedure for establishing the colour characterisation of a device. The characterisation procedure bridges the device dependent colour space and device independent colour space representation. Establishing this transformation relation between device independent and device dependent enables colour images prior to colour rendering. Colour encoding can be explained as the appropriate digital colour representation in order to undertake correct colour conversion from one colour space to another in a given workflow [148, 55]. Colour encoding is vital in digital imaging systems as it determines the colour transformations from an input device to an output device. In a digital imaging system, the different types of colour management system require different methods of colour encoding, and consequently, the colour encoding could be applied by an application such as Photoshop and system-level software or a colour management module, such as Adobe CMM.

Providing the means of managing and imparting colour reliably throughout a framework made up of different segments is the objective of any colour management system. Therefore, to achieve these objectives three different procedures must be carried out [103, 59]:

- Calibration and Characterisation of input devices, in order to explain the colorimetric reference space.
- Calibration and Characterisation of output devices, to generate the colour within a gamut.
- Bridge the input device and output device together for processing images with a convenient user interface for setting up and controlling the process.

2.5.2 ICC profiles

Different media, as well as the multiple media, are used in the industry which will often have different reproduction requirements even for the same image depending on the stage in the workflow at which the reproduction is made (within the industry, there is a standard process for colour reproduction. Different media are used in industry, which will often have differing reproduction requirements even for the same image, depending on the stage in the workflow at which the reproduction is made). For example, an image shown on a display may be required to precisely match the colour of the original sources, and it may also be required to be a colour match to a printed reproduction of the original. Therefore, using the appropriate colour reproduction system at each stage of a workflow is the most important decision made by a user.

The International Colour Consortium aimed to define a standard format to be applied within the software and operating systems used in the colour management framework [103], which internationally accepted the CIE system for defining colour matches. Therefore, by using this format, it is possible to ensure that over the process of colour reproduction, colours from an input will match those on output (assuming the output has an adequate colour gamut), for viewing conditions for which the colour is defined [38]. This effort was successful, and many characterisation models can be embedded and used successfully within such a standard file. The assessment of ICC profiles and colour reproduction is a complex issue involving everything from colour science, psychophysics and image analysis to 'preferred' reproduction styles [149]. The reference colour space characterised by ICC is known as the Profile Connection Space (PCS) which defines a translation from a device characterisation to a standard colour interchange space. PCS is either *CIELAB* or *CIEXYZ* (for a 2-degree observer) and a reference illuminant is a 16-bit fractional approximation of *D50* [39]. Fig. 2.16 shows the ICC profiling between different devices. The ICC has defined two colour spaces as intermediate PCS's-*CIELAB* and *CIEXYZ* [168]. A number of colour transformations (in the form of LUT, Matrices, and/or curves) have been characterised by each ICC input (or source) that describes the colour expected from the encoded data of the digital image in an open format. To be clear, the colour expected in a digital image with any set of image values, which are usually device values (such as *sRGB*), is defined by the profile [89]. Using the basic ICC architecture to provide a colour

reproduction system to apply the transformation between input device space to output device space does not cover all needs.

2.5.2.1 Type of profiles and their uses

The device profiles described in the previous section are one of the ICC profile types. The other types of profile, which mainly act on the image data to be processed, are colour space profiles. In this type of profiling, the data can be converted between one colour space to another. The device link profile can combine more than two profiles, which can be produced once and used for numerous sets of data. An abstract profile is one which can apply between device profiles and become one conversion in the resulting device link profile. A named colour profile allows data which is defined in Pantone colours to be converted for viewing or printing [168]. There are associated numeric CIE colour description for each Pantone colour in this profile.

2.6 Display technologies

Although CRTs are now rarely used, LCDs are still prevalent. Other display technologies such as OLEDs and AMOLEDs are becoming increasingly popular for specialised workplace use or other application are also described in this section.

2.6.1 CRT

A cathode ray tube (CRT) is a specialised vacuum tube in which images are produced when an electron beam strikes a phosphorescent surface. The CRT consists of three electron guns which sweep the screen. Each gun is tuned to hit either red, green or blue phosphor dots on the screen, usually aided by a metal shadow mask which prevents (e.g.) the red beam incorrectly stimulating green phosphors. When electrons hit a phosphor, it glows briefly. The greater the number of electrons hitting the phosphor, the brighter it glows. The electron beams complete a full sweep of the screen (a frame) rapidly enough that the phosphors appear to steadily illuminate. The red, green and blue phosphors are arranged in very close spatial proximity, so that at normal viewing distances they appear to be at one

location, for normal viewing distances. This allows their colours to mix additively. Calibration of a CRT displays including brightness and contrast adjustment to preset nominal values [16, 126, 152]. Fig. 2.17 illustrates the structure of a CRTs.

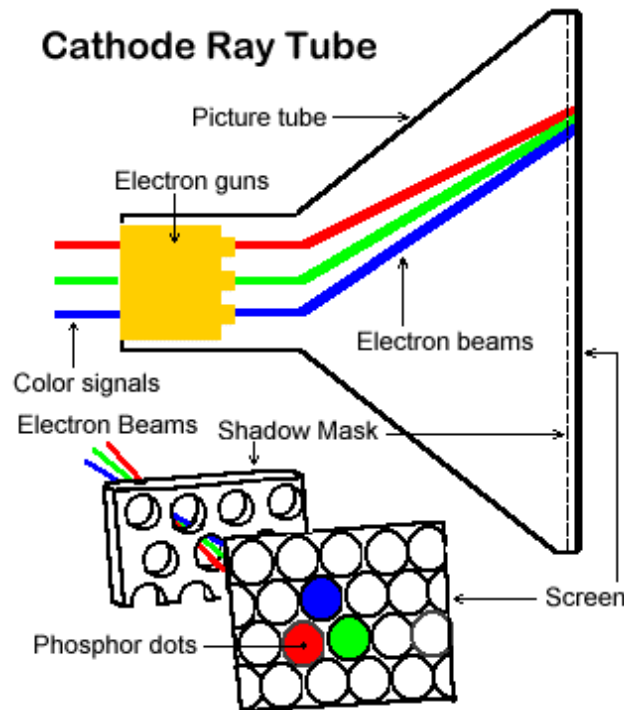


Fig. 2.17 CRT structure [42].

2.6.2 Basic principle and structure of LCD

Liquid crystal displays are categorised as a transmissive class of displays, as they are dependent on light passing through them, whereas most other screens (e.g. CRT) are emissive as they produce light themselves. Furthermore, they exhibit the double refraction phenomena. An LCD panel is a thin flat panel device wherein a number of coloured pixels are arrayed in front of a light source or reflector. These optical properties are highly related to the characteristic response of the liquid crystals [179]. A very small amount of electricity has been used in addition frequently used in battery-powered electronic devices. Liquid crystals form a phase between liquid and crystal, which is generally called a "mesophase" [36]. LCD displays contain many columns of liquid crystal molecules which are evenly distributed to form a uniform layer between two transparent electrodes and two polarising filters with axes of polarity that are perpendicular to each other. In the

case of colour LCD, between the upper substrate and transparent electrode, a colour filter layer is formed to represent colour, as shown in Fig. 2.18.

A colour LCD is obtained by subdividing the pixel into three sub-pixels with red, green, and blue colour filters. Since the colour filters absorb a large portion of the light, these colour LCDs require a backlight to operate in a transmissive rather than a reflective mode in order to be useful in most ambient lighting conditions [44].

Liquid crystal is one of the most successful materials in applied molecular electronics. Various technologies are implemented in Liquid crystal displays, especially ones which provide high performance and low power. Moreover, Active-Matrix LCD (AMLCD) displays have been developed which results in higher performing LCD screens. 'Active matrix' term refers to the active capacitors which control each individual pixel in the display, resulting in a faster response time and clearer picture. Peter Brody and coworkers [21] constructed the first so-called active matrix LCDs (AMLCDs) with CdSe thin film transistors (TFTs) as the switching elements. Moreover, AMLCDs are capable of displaying fast-moving images with the use of thin film transistors (TFTs) and capacitors. The TFTs in the array act merely as ON/OFF switches and do not have an amplifying function [44]. Hence, with this advantage TFTs display a clearer picture, especially with moving images.

Some further developments which have resulted in higher performing LCD displays are overridden (OD) technology [120, 87], dimming technology for low-power consumption [64, 51], and wide viewing LCD characteristics for large-size TVs and 3D applications [184, 153].

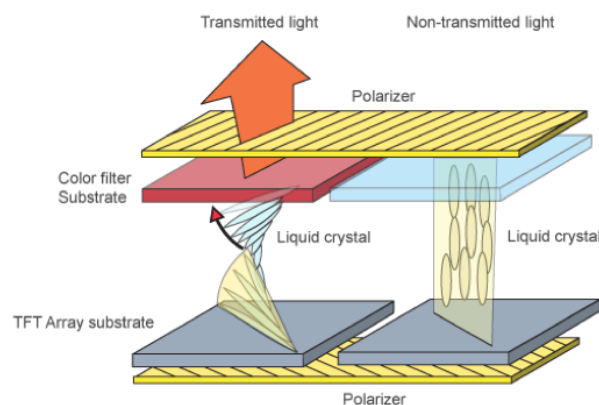


Fig. 2.18 LCD structure [94].

2.6.3 LED display

During the last four decades, much technical progress has taken place in the field of LEDs (Light Emitting Diodes). The advantages of LEDs are that they are small, rugged, reliable, bright, and efficient. As a result, LEDs play an increasingly important role in a vast range of applications and technologies. LEDs have the potential to convert electricity to light with an efficiency nearing unity [147].

LED displays are created by the use of dot-matrix, 7-segment, star-burst and similar LED component packages. The dot matrix module can display one or more dots, numbers, graphics and symbols. The 7-segment package can be used to illuminate a number between 0 and 9, and are commonly used in devices such as clock radios. The third module (star-burst LED components) can represent numbers from 1 to 15 lines. Star-burst can also be programmed to represent both numeric symbols as well as certain other graphics [164, 186]. In order to create a high-resolution colour display, thousands of LEDs are placed together to form a display panel. The light emitting diode can be designed to emit either red, green or blue lights. As a consequence of the small size of the diodes, they can be easily mounted in arrays in order to blend together and reproduce a given colour by mixing light which is to be seen from a distance. White can be obtained by a mixture of twice as many green units as red or blue. As a result, arrays of such LEDs can provide displays of very high luminance which can be used outdoors [73, 95]. Brown [22] and his co-workers developed the idea of producing a white light by mixing red, green and blue LEDs in order to produce any colour on the visible spectrum (from 380nm to 780nm).

2.6.3.1 OLED

OLED displays are made from organic (carbon-based) light emitting diodes. OLED is a flat light emitting technology, made by placing a series of organic thin films between two conductors. When an electrical current is applied, a bright light is emitted. Since OLEDs do not require a backlight and filters (unlike LCD displays), they are more efficient, thinner and much simpler to make. Moreover, the other advantages of OLEDs are wide viewing angle, fast response rate, superior picture quality with greater colour accuracy and better power efficiency. Fig. 2.19 illustrates the structure of the OLED. OLED technology opens a whole world of possibilities

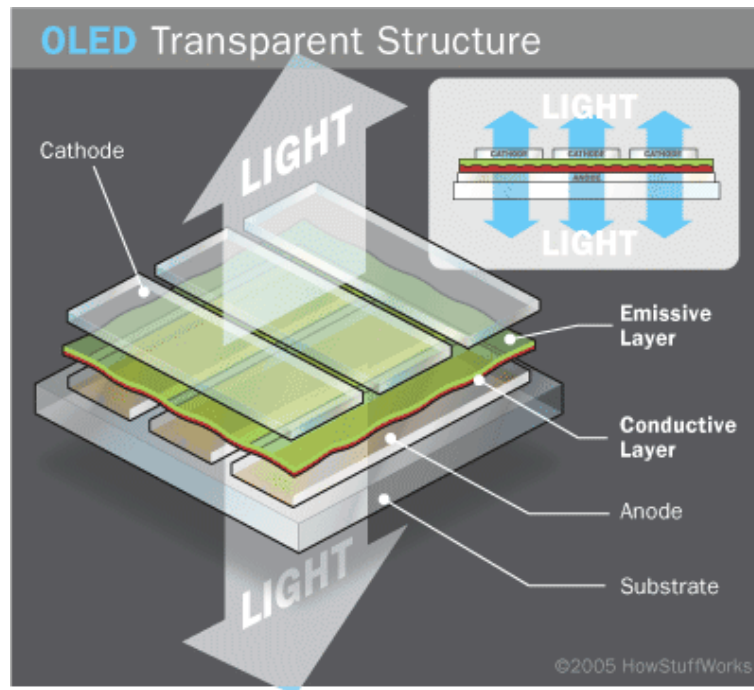


Fig. 2.19 Structure of OLED [121].

through their potential for the construction of transparent and flexible imaging devices. Amongst other applications, they may be used in curved OLED displays, wearable OLEDs, and transparent OLEDs embedded in windows [123]. OLED displays can be used in either passive-matrix or active-matrix addressing schemes. An AMOLED uses an active-matrix TFT (thin-film-transistor) array and storage capacitors. While these displays are more efficient and can be made in larger sizes, it makes them more complicated to build [144].

2.6.4 PDP

A Plasma Display Panel (PDP) is a type of flat panel display which produces each pixel in a separate cell. These cells contain electrically charged ionised gasses which are plasmas. Each cell is covered with one of three different fluorescent powders which convert the radiation (including its ultra-violet content) into either red, green or blue light [73, 176]. By placing red, green or blue filters over the cell, the contrast of the pictures can be increased. The reproduction of colour in a PDP depends on combining the discharge with phosphors since it is not possible to have discharger cells containing different gases in the same panel in order to produce different

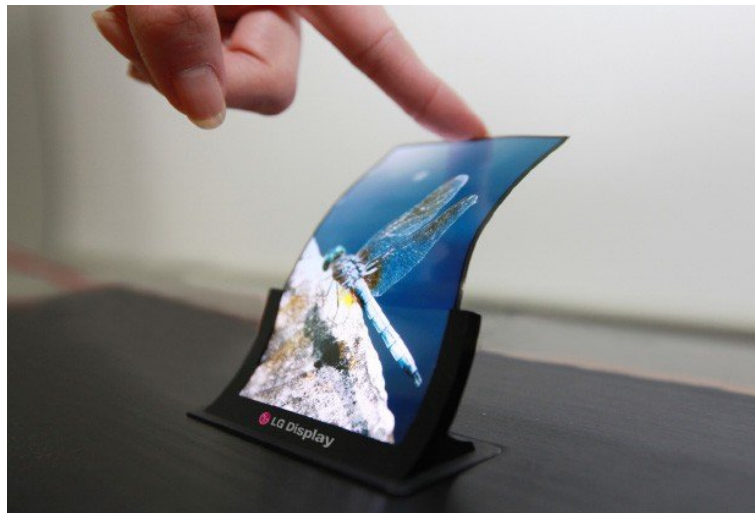


Fig. 2.20 Flexible OLED [96].

colours. One of the advantages of PDPs is that the displayed black is much blacker than those found in an LCD display, which tends to display the same colour as grey. Plasma displays can be produced in any large size and need only be a few inches deep.

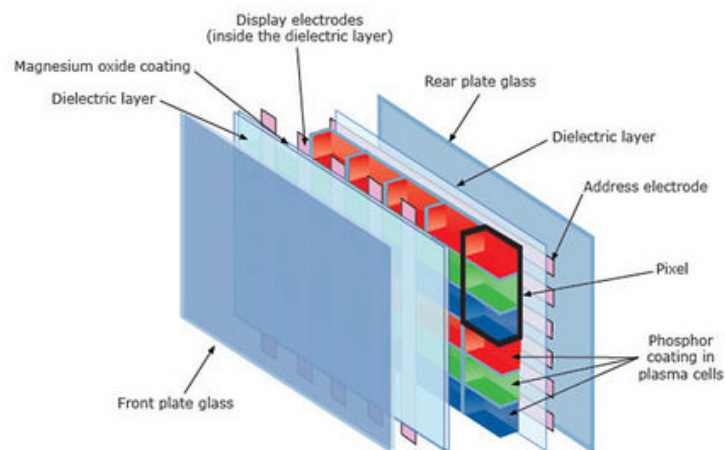


Fig. 2.21 PDP structure [125].

Fig. 2.22 summarises the display specifications of all display technologies which described.

Display technologies	Specifications
CRT (Cathode Ray Tube)	<ul style="list-style-type: none"> ➤ CRT is a specialised vacuum tube in which images are produced when an electron beam strikes a phosphorescent surface. ➤ The red, green and blue phosphors are arranged in very close spatial proximity. The calibration of a CRT displays including brightness and contrast adjustment to pre set nominal values.
LCD (Liquid Crystal Displays)	<ul style="list-style-type: none"> ➤ An LCD Panel is a thin flat panel device where in a number of coloured pixels are arrayed in front of a light source or reflector. ➤ A colour LCD is obtained by subdividing the pixel into three sub- pixels red, green, and blue colour filters. ➤ Liquid Crystal is one of the most successful materials in applied molecular electronics. ➤ Various technologies are implemented in LCD with high performance and low power. ➤ Active Matrix LCD (AMLCD) displays have been developed which results in higher performance LCD Screens.
LEDs (Light Emitting Diodes)	<ul style="list-style-type: none"> ➤ The advantages of LEDs are that they are small rugged, reliable, bright, and efficient. ➤ LEDs have the Potential to convert electricity to light with an efficiency nearing unity. ➤ LEDs play important role in a vast range of applications.
OLED (Organic Light Emitting Diodes)	<ul style="list-style-type: none"> ➤ OLED displays are made from organic (carbon based) light emitting diodes. ➤ OLED is a flat light emitting technology, made by placing a series of organic thin films between two conductors. ➤ OLEDs do not require a backlight and filters (unlike LCD displays), they are more efficient, thinner and much simpler to make. ➤ The other advantages of OLEDs are: wide viewing angle, fast response rate, superior picture quality with greater colour accuracy and better power efficiency. ➤ OLED Displays can be used in either passive-matrix or active-matrix addressing schemes.
AMOLEDs (Active-Matrix Organic Light Emitting Diodes)	<ul style="list-style-type: none"> ➤ An AMOLED uses an active-matrix TFT (thin-film-transistor) array and storage Capacitors. ➤ This displays are more efficient, can be made larger sizes.
PDP (Plasma Display Panel)	<ul style="list-style-type: none"> ➤ PDP is a type of flat panel display which produces each pixel in a separate cell. ➤ The advantage of PDPs is that the displayed black is much blacker than those found in an LCD display, which tend to display the same colour as grey. ➤ Plasma displays can be produced in any large size and need only be a few inches deep.

Fig. 2.22 Display specifications.

2.7 Device characterisation

Device characterisation converts the device dependent colour specification to device independent coordinates. The relationship between device-dependent coordinates such as *RGB* or *CMYK* and some device-independent colour space such as *CIEXYZ* for a calibrated device is called characterisation [172, 80]. In the design of a colour reproduction system, the characterisation of colour-imaging devices is essential [103]. Display characterisation with a colour appearance model provides a means for accurate colour communication [143]. The signal output of colour in each device depends on the manufacturer settings or hardware design. The manufacturing process could affect the colour even with the same specification and identical product models.

Device characterisation often requires two procedures [75]:

- Calibration: Fixing the setting on the device (or any other process) in order to ensure repeatable performance with regards to the colour response, is given on each subsequent use [80]. Calibration is often the most practical way of setting parameters such as white point and brightness of a display. In a case of display calibration, the calibration information is often stored in a display profile. The calibration is the basis for an additional colour characterisation of the device and later profiling, in International Colour Consortium (ICC) terms [95].
- Characterisation: The relationship between device colour space and the device-independent colour space, e.g., CIE tristimulus values.

The calibration of a device means configuring the device in order to produce colours specified in CIE 1931 (or other physical absolute) spaces with the transformations from the *RGB* space used by the computer display to CIE 1931 colour space. Hence the examination of the current setting of a display before starting any colour measurement or running the experiment is very important. The effect of changing settings, such as 'Brightness', 'Contrast' and 'colour temperature', will affect colour but the effect may vary from one device to another. Before making radiometric measurements for characterisation, the monitor should be placed in the position where it will be used and then turned on. Sufficient time should be allowed for the monitor to warm up. The warm-up time required for a monitor

to stabilise after initial power up varies for different devices but can range from fifteen minutes to three or more hours [13]. Allowing sufficient time for the display to warm up is required before doing any calibration. It helps for all devices to be stabilised in order to keep these devices with a fixed characteristic colour response and is fundamental to characterisation. Calibration is necessary for viewing the same colour on different devices or in different graphics systems [40]. In this study, the effect of changing the calibration of display devices has been checked in order to determine the optimum level before running the experiments.

The characterisation of a device involves estimating a tone-reproduction curve (TRC) for each colour channel as well as the so-called optoelectronic transfer function (OETF) and driving a colour transform between the device-dependent signals and the device independent coordinates [67]. The OptoElectronic Transfer Function (OETF) describes a non-linear tone-reproduction function for each colour channel of the imaging device [76]. There are three main characterisation methods; Physical Model, Look-up Tables and Numerical Models [58]. In the Physical model, the colour response of the device should be modelled physically by a chosen model, which are, in many cases, based on the total independence between channels and the chromaticity constancy of primaries. Therefore, a combination of full intensity of the primaries by the luminance response of the display can be used to perform the colorimetric transform. Follow the assumption cited by Berns *et al.*, [15, 13, 11] Brainard [18], Cowan and Rowel [41], Sharma [150] the physical models widely used for displays especially the old CRT technologies.

There are two stages of the process of the characterisation based on the physical model [135, 174].

- Linearisation

The first step is to linearise the intensity response of the device. This can be done by establishing a gamma curve model which follow the mathematical function for CRT displays [15, 13, 11, 41, 150, 19], or an S-shaped curve for LCD displays [90, 91, 183]. Post and Calhoun [131] introduced the linearisation method by generalising the measurements by interpolation along the luminance for each primary. The spectroradiometer can measure the luminance levels in order to estimate a visual response curve, where for each channel the 50% luminance point is determined to estimate the

gamma value [41]. In regards of using halftone patches in order to have more luminance levels, this method is highly recommended [110, 117].

- Transformation of the linearised values into the *CIEXYZ* tristimulus values. The second step is to build the colorimetric transform from luminance to an additive reference colour space by using the 3×3 matrices including primary tristimulus values at full intensity. The three primaries of the device channel can be measured at a full intensity by spectroradiometer, assuming their chromaticity constancy. However, this assumption is not perfect hence, the accuracy of the model affected. By applying a black-correction, the non-constancy of primaries can be corrected [79]. Day *et al.* [43], tried to minimise the chromaticity non-constancy by optimising the components of the 3×3 matrices. It is also possible to use the defined primaries such as *sRGB* [2] depending on the level of required accuracy for some application [6, 7].

The second model is based on 3D Look Up Tables (LUT). The third category is based on the use of training data sets, in order to establish a transform by optimisation of the parameters of a polynomial function. The advantage of the numerical models is, by applying cross components factors in the establishment of the function, the channel inter-dependence takes into account [161, 84]. Wen and Wu [170] reducing the number of measurements by considering that the interdependence channel is only due to two-channel crosstalk, therefore they conclude to remove the three-channel crosstalk from the model. The results accuracy has remained considering the three-channel crosstalk.

The following section presents the different methods of device characterisation which have been used in this study.

2.7.1 Device independent colour reproduction

Achieving the same visual colour in different media devices through a single, standard representation of colour rendering is the purpose of device independent colour reproduction [159]. Defining an image independently is an attribute of device-independence. Colorimetric-based programming bridges the input capturing device (like a camera or scanner) with the output device (like a display or printer). In this way, device-independent data, which is based on colorimetric standards, such as *CIELAB* or *CIEXYZ*, is obtained [9]. Sometimes gamut mapping

is required to take into account the different colour gamut between an input and output device (see Fig. 2.23).

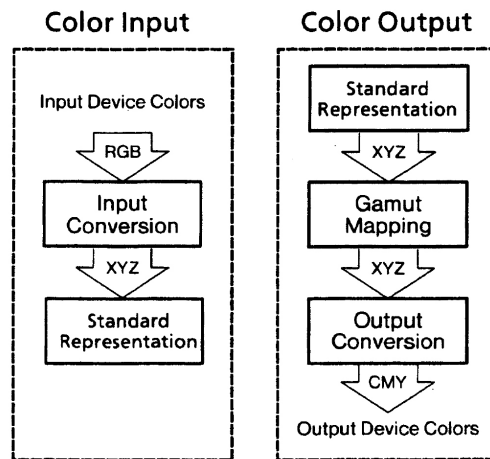


Fig. 2.23 System diagram for input and output components of a colorimetric colour reproduction system [159].

2.7.2 GOG model

The GOG model was developed for use with CRT displays but these have been almost entirely replaced in the consumer computer and television markets by newer technologies such as LCD and plasma. CRT displays are still frequently used in research laboratories, where high colour fidelity is required and where the research teams may have substantial experience with characterising CRT display devices. LCD displays are increasing in popularity, however, even in research environments. Reproduction of the colour of natural objects can be achieved by the relative scalar values (RGB) of each colour channel obtained from the GOG model of the calibrated CRT [9, 127, 135].

2.7.2.1 Gamma

The luminance generated by a computer monitor is generally not a linear function of the applied signal. Most CRT (cathode ray tube) devices exhibit a power-law response to voltage so that the luminance produced at the face of the display is approximately proportional to the applied voltage raised to a power in the range 2.35-2.55 [134]. The value of the exponent of this power function is sometimes called

the gamma of the CRT or monitor. In a typical 8-bit digital-to-analogue converter, the lowest voltage will be coded by the value 0 whereas the highest voltage will be coded by the value 255 ($2^8 - 1$). The relationship between the voltage applied to the CRT's phosphors and the displayed luminance can be approximated by the gamma relationship;

$$L = V^\gamma \quad (2.30)$$

where L is the luminance of the display, V is the applied voltage (this is linearly related to the RGB values) and γ is the gamma.

High-end CRT displays were considered to be state of the art in the 1990s. However, CRT technology has now been almost entirely replaced by various new technologies. LCD (liquid crystal display) devices are now commonplace, were early models used a CCFL (cold cathode fluorescent lamp) backlight. Various other technologies compete for the market including plasma displays and LED front-projection systems. Although most display devices exhibit non-linearity it is not clear that the power law in Equation 2.30 is appropriate [43].

Although CRTs exhibit an inherent non-linearity, the term gamma is commonly used to represent the non-linearity of the entire opto-electronic transfer function of the display system [43, 15, 13] have studied the relationship between the digital monitor values (sometimes referred to as DAC values) and the displayed luminance for a range of typical CRT devices. Though reasonably accurate models of display behaviour exist [14] they are generally not used for the purposes of characterisation. Rather, the relationship between luminance L and normalised DAC value $d/(2^N - 1)$ is generalised to yield:

$$L = (ad/(2^N - 1) + b)^\gamma \quad (2.31)$$

where it can be useful to think of the coefficients a and b as the system gain and offset respectively. This generalised relationship is known as the gain-offset-gamma or GOG model [14]. The implication of this equation is that although the CRT has an inherently fixed gamma, the effective gamma of a system will be dependent

upon how the offset and gain controls are set. In practice, a relationship of the form shown as Equation 2.31 is used to map the normalised DAC values ($d_r/(2^N - 1)$, $d_g/(2^N - 1)$, and $d_b/(2^N - 1)$) to the linearised normalised DAC values (R, G, and B). Thus, for the red channel of a 24-bit system, the following equation can be used,

$$R = (ad_r/255 + b)^\gamma \quad (2.32)$$

where the sum of the system gain (a) and offset (b) are constrained to equal unity. Since there are three model parameters but only two degrees of freedom a minimum of two radiometric measurements is required per channel. The advantage of minimising the number of measurements required to characterise the monitor is important since it is widely recognised that when making measurements a time of at least 80s must be allowed for the colour to stabilise [13]. It is only practicable to allow this time for relatively small numbers of measurements. Berns [13] recommend measuring neutral colours where the load is placed equally across all three channels rather than highly chromatic colours where the load is placed on only one of the gun amplifiers. As few as two neutral colours need be measured in order to be able to determine the parameters of Equation 2.32 for all three of the channels (although the use of so few measurements may not generate accurate results).

2.7.3 Device-independent transformation

Once the GOG model (Equation 2.31) has been used to linearise the DAC values, the linearised DAC values can be related to tristimulus values using a simple linear transform.

$$\begin{bmatrix} X \\ Y \\ Z \end{bmatrix} = \begin{bmatrix} X_{r,max} & X_{g,max} & X_{b,max} \\ Y_{r,max} & Y_{g,max} & Y_{b,max} \\ Z_{r,max} & Z_{g,max} & Z_{b,max} \end{bmatrix} \begin{bmatrix} R \\ G \\ B \end{bmatrix} \quad (2.33)$$

where R , G and B are the linearised and normalised (in the range 0 to 1) DAC values. Three measurements are required in order to specify the system matrix

for Equation 2.33. The tristimulus values XYZ must be measured for each of the guns at the maximum DAC value (255 for a 24-bit system). The XYZ values of the red gun at maximum intensity form the first column of the system matrix (Equation 2.33) and the XYZ values for the green and blue guns for the second and third columns respectively. The main parameters which are important to consider in Equation 2.33 are that the returned proportion of RGB must be converted into appropriate DAC values when converting XYZ to RGB .

Perfect channel independence and chromaticity constancy of primaries, required for using the colorimetric transform matrix 2.33. CRT technologies have been highly tested using the colorimetric transform matrix in previous studies [41, 19]. Considering the assumption of chromaticity constancy, it is evident that there is a flare [84], either an internal flare (black offset) or an external flare (ambient flare), added to the signal, therefore the assumption of chromaticity constancy is not valid anymore. The flare can be removed by changing the input level of black to (0, 0, 0). Any light source reflecting on the display screen can cause the ambient flare. This ambient flare remains constant if the viewing conditions do not change. The internal flare which is the main part of the chromaticity inconstancy is coming from the black levels especially in CRT technology [84]. In LC technology, due to a leakage of the crystal, an amount of light passing through a panel. By setting the measurements to be placed in the dark room the external flare or ambient flare is minimised. Furthermore, the black level subtraction can help to minimise the internal flare, therefore, the chromaticity become more constant. A new model can be set up in taking these two flares into account [84, 79, 66] Hence, the gamma model reviewed and extended by adding an offset term. Therefore, the GOG model can become a Gain-Offset-Gamma-Offset (GOGO) model [85, 84].

2.7.4 PLCC

PLCC (Piecewise Linear Chromaticity Constancy) is an alternative method to the GOG model. The DAC linear curve with interpolative methods, unlike gamma correction, is not made by fitting one of a series of mathematical functions. Instead, a look-up table of various DAC measurements is stored, such that in any DAC value requirements, a search will have been made through all of these stored DAC data points for each gun. For example, in a case where 50% of the maximum

luminance of a gun is required, a look-up table data is searched until the appropriate DAC value is found. For DAC values which are not explicitly tabulated, then the value is interpolated, typically based on the nearest points tabulated. The Interpolation method (PLCC) is based on a functional approximation by applying a linear interpolation between measurements [131], followed by a colorimetric transformation between the chromaticity matrix and the luminance responses of primaries. The actual interpolation method depends on the required accuracy and the complexity of the interpolation can vary. There are three methods of estimating the curvature between nearest tabulated points such as Linear, Logarithmic and Lagrange Polynomial.

In this study, simple linear interpolation is used. Imagine a series of N values of R and N corresponding values of R' . The corresponding values are obtained in exactly the same way as is described in the previous section for the GOG model. The interpolated linear value y for any non-linear value x is given by the Equation 2.34.

$$y = R'_i + \frac{x - R_i}{R_j - R_i} (R'_j - R'_i) \quad (2.34)$$

where $R_i < x < R_j$. Clearly, some additional consideration needs to be taken if $x = R_1$ or $x = R_N$ and either $x < R_1$ or $x > R_N$. In addition the value of y is constrained to be $0 \leq y \leq 1$.

2.7.5 3D-Look-Up-Table

The inversion of a display colour characterisation model is essential for colour reproduction since it provides the set of digital values to input into the device in order to display the desired colour. Among those models or routines utilised to accomplish colour characterisation, we might recognise two classes. The first one contains models that are practically invertible (either analytically, or by using simple 1D LUT) [15, 13, 41, 79, 84, 131], such as the PLCC and GOG models. The second category contains the models or methods which are not practically invertible directly like LUT (look-up-table). The 3D LUT is a three-dimensional table that maps colours into a different colour space. The full 3D LUT requires a high number of measurements. However, these models do have the possibility to take device

colour-reproduction features into account more precisely, such as the interaction between channels or chromaticity inconsistency of the primaries. Therefore, such these kind of model needs computational power and high storage capacity to handle the 3D data. Graphic processor units can perform the computational power easily [35].

2.7.6 Review of previous studies of the display characterisation

An information base on past investigations of display characterisation is reviewed in this study. A major issue for the accurate colour reproduction of the display devices is the colour characterisation. The main purpose of colour characterisation of a device is to define the transformation between the *RGB* (the device colour space), and a *CIEXYZ* or *CIELAB* (reference colour space), based on the *CIE* standard observer [176]. According to the literature which has been reviewed in the section Section 2.7, the physical model which contain the two-step of Linearisation and Transformation highly used for the display characterisation. However, due to lack of channel independence and chromaticity constancy of primaries, colorimetric transformation using a simple 3×3 matrix leads to be inaccurate especially in the LCD technologies [19, 91]. The cross-talk between channels have been taken to account by using the masking model and modified masking model introduced by Tamura *et al.* [161]. The other characterisation models have been introduced such as the 2-step parametric models purposed by Blonde *et al.* [17] particularly for the other technologies which based on the separation between chromaticity and intensity. This colorimetric transform is based on two dimensional interpolations in the chromaticity plane based on a set of saturated measured colours, the luminance level is retrieved. In addition, there are another two models such as the Piecewise assuming Variation in Chromaticity called PLVC [50] and PLCC which are not subject to this effect. Post and Calhoun [131] demonstrates these models and tested the accuracy for the CRT displays, since then it has been commonly used in the studies (The PLVC model is described in Chapter 7 of this thesis and used).

2.8 Summary relevant to the current research

The main purpose of the current research is to investigate the effect of using the different characterisation methods for LCD display systems. To achieve this goal, the basic principle of the colour science, the CIE system, different RGB colour spaces, and the different aspects of display technologies, as well as the different characterisation models, have been described. Colour management systems, ICC profiling and, more importantly, many previous studies investigating and testing different models and samples were reviewed. The associated process of choosing the right sets of samples are another part of this literature review which can be found in chapters 3 and 4 respectively.

Chapter 3

Overview of Experimental Work

3.1 Introduction

This chapter provides an overview of the experimental work that is contained in this thesis. Chapter 4 describes the key methodology for the experimental work that is presented in Chapters 5-8. This is to enable a large amount of data that was collected as part of the work to be shown and discussed clearly. The work in Chapters 5-8 is concerned with methods for the colorimetric characterisation of displays.

3.2 Research Questions

The experimental work in this thesis is contained in Chapter 5-8 and is concerned with the colorimetric characterisation of displays. Traditionally, the GOG model has been used to characterise CRT displays. However, CRT displays are now seldom used and difficult to obtain; they have been replaced by several technologies including LCD displays. The GOG model assumes that the tone-reproduction curve (TRC) of a display can be modelled by a power function but it has been noted [14] that this model may not be appropriate for modern LCD displays (and for displays based on other technologies). This work, therefore, explores different ways to characterise the TRC of displays. The performance of the GOG model (which is based on a power function) is compared with PLCC (which is based

on interpolation). In addition, regardless of whether GOG or PLCC is used, it is possible to base the characterisation on either grey-ramp samples (256 steps) or on so-called colour-ramps (where each primary colours are displayed on 256 steps, 768 levels in total). There is no published data that provides robust findings on whether grey-ramp or colour-ramps should best be used (although Berns [14] recommended the neutral samples). In this thesis, the effect of these parameters on the characterisation performance is evaluated for 20 different displays in order to try to arrive at some recommendations for best practice. As part of this work, additional different sets of samples such as Macbeth ColorChecker chart, Chart4 and Matlab60 (described in Chapter 4) were specified and used for evaluation of characterisation performance.

The GOG and PLCC methods employ different approaches to address the TRCs of the displays; however, both then employ a matrix to convert linear *RGB* values to *XYZ* values. Explicit in this matrix is an assumption that the chromaticities of the primaries remain constant as the drive input to the primaries is increased. For displays that do not meet this assumption a different model, known as Piecewise Linear model assuming Variation in Chromaticity (PLVC), has been developed. The performance of the 20 different displays have been evaluated therefore another additional model, the PLVC tested to improve the characterisation of the displays which did not work with the GOG or PLCC. In addition, the effect of using different background conditions on colour calibration patches has been tested. Furthermore, the display characterisation is tested for moving images.

The research questions addressed in this thesis can, therefore, be listed below:

- What are relative merits of the GOG, PLCC and PLVC models for colour characterisation of modern displays and how can they be optimally used?
- What is the effect of using different test charts on the evaluation of different characterisation methods?
- What is the effect of using different sets of linearisation samples?
- What is the effect of using different N (number of linearisation samples) sub-sampling linearisation data?
- What is the effect of using different background conditions on a colour of calibration patches?

- What is the effect of using whether the static or moving background on a colour of calibration patches?

The main novelty of the work comes from the meta-analysis of 20 physical displays that will allow conclusions and recommendations that are more robust and meaningful than those from previous studies.

3.3 Colour-Measurement Equipment

There are broadly three types of colour measurement devices such as Colorimeter, Spectrophotometer and Spectroradiometer. CIE tristimulus values are obtained by colour measuring devices. A colorimeter directly measures colorimetric quantities, whilst the spectrophotometer and spectroradiometers calculate colorimetric quantities from spectral data measured across the visible spectrum, e.g. in the wavelength range from $360nm$ to $780nm$ [14]. A spectroradiometer is an instrument designed to measure radiometric quantities as a function of wavelength in a narrow spectral bandpass. The wavelength range, spectral bandwidth, wavelength sampling increment, dynamic range and measurement area are the critical factors for designing a spectroradiometer [20]. A tele-spectroradiometer incorporates a telescopic input module. This instrument is specially used to measure the colour of a distance object [187]. In this work, the spectral radiance from a patch in a display was measured using a Konica Minolta CS-2000 tele-spectroradiometer. The colour matching functions to convert measured SPD to XYZ values used were the CIE 1931 standard colorimetric observer (2°) computed by the tele-spectroradiometer software. This instrument records radiance in watts per steradian per square meter ($W.sr^{-1}.m^{-2}$) in $10nm$ intervals in the range $380nm$ to $780nm$. Fig 3.4 shows the specification of the Konica Minolta CS-2000 device. Measuring colour with a tele-spectroradiometer gives the advantage of measuring the colour of a distant object from its usual observing position under its usual viewing conditions [187]. However, since only trichromatic data were required, the Yxy (luminance and chromaticity) values (that were calculated by the instrument onboard software) only were recorded. These data were converted to CIE tristimulus values and other colours spaces (as required) using *ASTM(2001) E308-01* [173] standard method.

All the XYZ measured converted to the relative values using Equation 3.1-3.3 and then normalised by using Equation 3.4-3.6:

$$X = 100 \times X_a / Y_{max} \quad (3.1)$$

$$Y = 100 \times Y_a / Y_{max} \quad (3.2)$$

$$Z = 100 \times Z_a / Y_{max} \quad (3.3)$$

where the X_a , Y_a and Z_a are the absolute values, while the XYZ obtained is the relative values.

$$X = X_r / X_{max} \quad (3.4)$$

$$Y = Y_r / Y_{max} \quad (3.5)$$

$$Z = Z_r / Z_{max} \quad (3.6)$$

where the X_r , Y_r and Z_r are the relative values, while the XYZ is normalised. Y_{max} is also the luminance of white for each display.

The Konica Minolta CS-2000 tele-spectroradiometer was mounted on a tripod (see Fig. 3.1), so that it is free of vibration and cannot wobble. In practice, all measurements were carried out in a fully darkened measuring room so that ambient light does not affect the measured values. Figs 3.2 and 3.3 show the structure of the instrument. A recently purchased Konica Minolta CS-2000 was used to carry out all the measurements of this thesis. The device was turned on and left to warm up for one hour (recommended by manufacturer to warm up for 20 minutes at least after switching power on when the object luminance is 2 cd/m^2 or lower (measuring angle 1°) [111]) and then the temporal precision was assessed by measuring the white patch from displays every five seconds for at least 40 minutes. Note that all the measurements took place in a dark surrounding room. Fig 3.5 illustrates the graphs shows that the measurements luminance $L_v(\text{cd/m}^2)$ over the time are stable.



Fig. 3.1 Experimental setup using the Konica Minolta CS-2000.

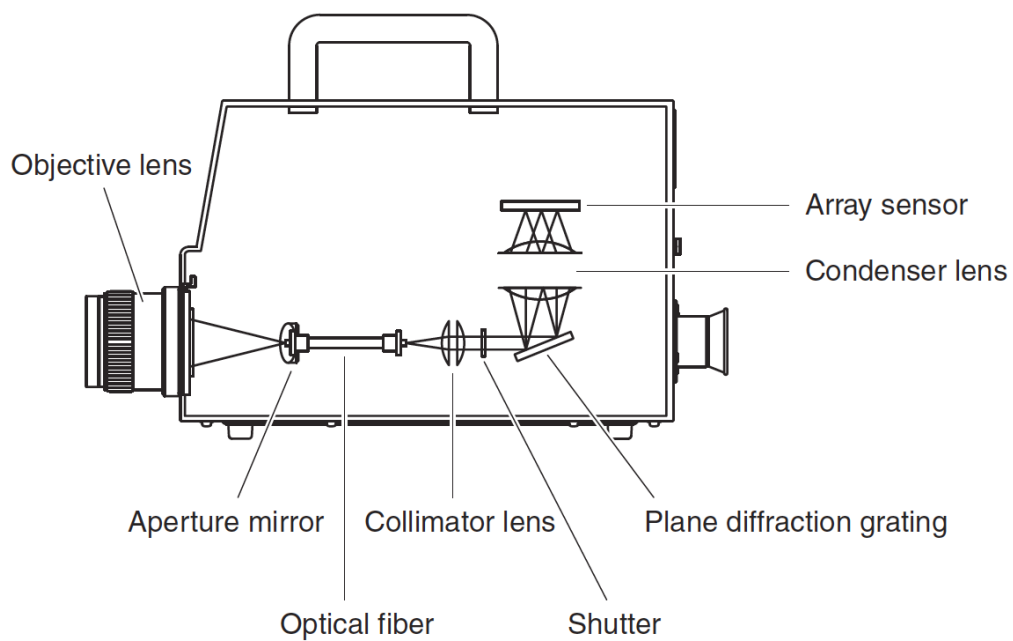


Fig. 3.2 The structure of the Konica Minolta CS-2000 [111].

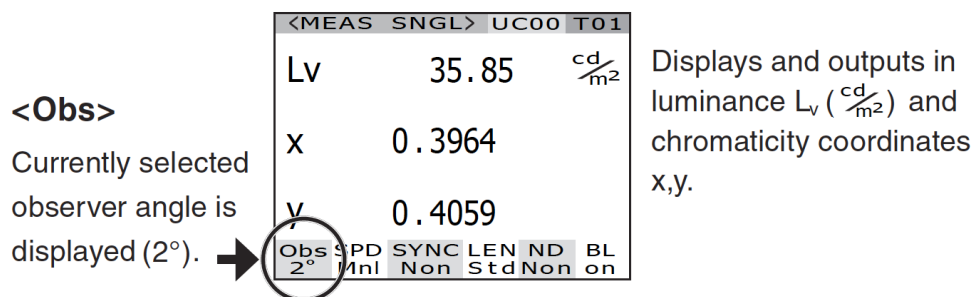


Fig. 3.3 The Display example of the Minolta CS-2000, measurement result is displayed in the currently $Lvxy$ colour space and the standard colorimetric 2° observer [111].

3.3.1 Repeatability of Konica Minolta CS-2000 device

Repeatability of Konica Minolta CS-2000 tele-spectroradiometer was also checked by measuring the pure white patch ($RGB = 255, 255, 255$) for one of the displays (A), considering the warming up time of the display which is 30 minutes recommended by the manufacturer, 20 times in 40 minutes. Table 3.1 shows the results data and the colour differences ΔE_{ab}^* from the mean value. Table 3.1 shows the resulting XYZ data and their colour differences (ΔE_{ab}^*) from the mean XYZ. According to the results of the Table 3.1, having very small ΔE_{ab}^* values. it can be seen that the Konica Minolta CS-2000 tele-spectroradiometer is highly repeatable.

Model	CS-2000		
Wavelength range	380 to 780 nm		
Wavelength resolution	0.9 nm/pixel		
Display wavelength bandwidth	1.0 nm		
Wavelength precision	±0.3 nm (median wavelength: 435.8 nm, 546.1 nm, 643.8 nm Hg-Cd lamp)		
Spectral bandwidth	5 nm or less (half bandwidth)		
Measuring angle (selectable)	1°	0.2°	0.1°
Measurement luminance range (Standard light source A)	0.003 to 5,000 cd/m ²	0.075 to 125,000 cd/m ²	0.3 to 500,000 cd/m ²
Minimum measuring area	∅5 mm (∅1 mm when using closeup lens)	∅1 mm (∅0.2 mm when using closeup lens)	∅0.5 mm (∅0.1 mm when using closeup lens)
Minimum measuring distance	350 mm (55 mm when using closeup lens)		
Minimum luminance display	0.00002 cd/m ²		
Minimum spectral radiance display	1.0×10 ⁻⁹ W/sr, m ² , nm		
Accuracy: Luminance (Standard light source A) ^{*1}	±2%		
Accuracy: Chromaticity (Standard light source A) ^{*1}	x,y : ±0.003 (0.003 to 0.005 cd/m ²) x,y : ±0.002 (0.005 to 0.05 cd/m ²) x : ±0.0015 (0.05 cd/m ² or more) y : ±0.001	x,y : ±0.003 (0.075 to 0.125 cd/m ²) x,y : ±0.002 (0.125 to 1.25 cd/m ²) x : ±0.0015 (1.25 cd/m ² or more) y : ±0.001	x,y : ±0.003 (0.3 to 0.5 cd/m ²) x,y : ±0.002 (0.5 to 5 cd/m ²) x : ±0.0015 (5 cd/m ² or more) y : ±0.001
Repeatability: Luminance (2 σ)	0.4% (0.003 to 0.05 cd/m ²) 0.3% (0.05 to 0.1 cd/m ²) 0.15% (0.1 to 5,000 cd/m ²)	0.4% (0.075 to 1.25 cd/m ²) 0.3% (1.25 to 2.5 cd/m ²) 0.15% (2.5 to 125,000 cd/m ²)	0.4% (0.3 to 5 cd/m ²) 0.3% (5 to 10 cd/m ²) 0.15% (10 to 500,000 cd/m ²)
Repeatability: Chromaticity (2 σ)	0.002 (0.003 to 0.005 cd/m ²) 0.001 (0.005 to 0.1 cd/m ²) 0.0006 (0.1 to 0.2 cd/m ²) 0.0004 (0.2 to 5,000 cd/m ²)	0.002 (0.075 to 0.125 cd/m ²) 0.001 (0.125 to 2.5 cd/m ²) 0.0006 (2.5 to 5 cd/m ²) 0.0004 (5 to 125,000 cd/m ²)	0.002 (0.3 to 0.5 cd/m ²) 0.001 (0.5 to 10 cd/m ²) 0.0006 (10 to 20 cd/m ²) 0.0004 (20 to 500,000 cd/m ²)
Polarization error	1°: 2% or less (400 to 780 nm); 0.1° and 0.2°: 3% or less (400 to 780 nm)		
Integration time	Fast: 0.005 to 16 sec.; Normal: 0.005 to 120 sec.		
Measurement time	2 sec. min. (Manual mode) to 243 sec. max. (Normal mode)		
Color space mode	L _v x y, L _v u'v', L _v T Δuv, XYZ, dominant wavelength, spectral graph		
Interface	USB 1.1		
Operating temperature/humidity range	5 to 35°C, relative humidity 80% or less with no condensation		
Storage temperature/humidity range	0 to 35°C, relative humidity 80% or less with no condensation		
Size	Main unit: 158 (W) x 200 (H) x 300 (D) mm; Lens: ∅70 x 95 mm		
Weight	6.2 kg		

*1: Average of 10 measurements in Normal mode at a temperature of 23±2°C and a relative humidity of 65% or less.

Fig. 3.4 The Minolta CS-2000 device specification [111].

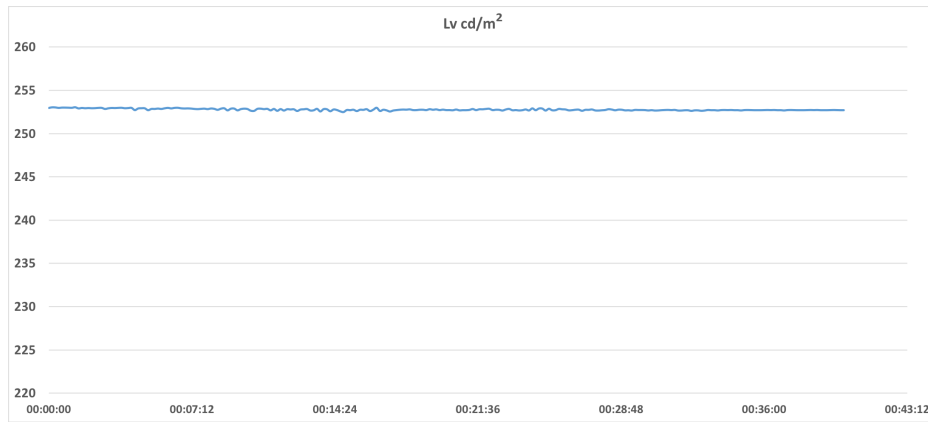


Fig. 3.5 Konica Minolta CS-2000 measurements of white luminance from display A for 40 minutes.

Table 3.1 Repeatability measurement of the Konica Minolta CS-2000 tele-spectroradiometer.

Measurement	X	Y	Z	ΔE_{ab}^*
1 st	258.00	262.00	287.40	0.09
2 nd	258.20	262.00	287.80	0.08
3 rd	258.10	261.90	287.50	0.08
4 th	258.00	261.90	287.70	0.02
5 th	258.20	262.00	287.80	0.08
6 th	258.00	262.00	287.70	0.05
7 th	258.00	261.90	287.70	0.02
8 th	257.90	262.00	287.60	0.12
9 th	258.20	261.90	287.90	0.16
10 th	258.10	261.90	287.70	0.08
11 th	258.00	261.90	287.60	0.01
12 th	257.80	261.90	287.50	0.12
13 th	257.90	262.00	287.40	0.14
14 th	257.90	261.90	287.60	0.05
15 th	258.00	261.90	287.60	0.01
16 th	257.90	261.90	287.60	0.05
17 th	258.00	261.90	287.80	0.04
18 th	257.90	261.90	287.70	0.06
19 th	257.90	261.80	287.70	0.05
20 th	258.00	261.80	287.70	0.09

3.4 Implementation Details

In the literature review, some characterisation models were described. However, in this section, the implementation details for the experimental work are given.

3.4.1 General Approach

One way to evaluate a characterisation approach for a particular display would be to use it to derive the display *RGB* values required to show a set of test samples defined by *CIEXYZ* values (See Fig. 3.6). The *RGB* values would then be used to display the test samples and the colours that were actually displayed would be measured using the Minolta CS-2000 tele-spectroradiometer device. The measured *XYZ* values would be compared with the target *XYZ* values and colour differences calculated (by first converting the *XYZ* values into *CIELAB* values) and used as a measure of performance (the smaller, the better, of course). Fig. 3.6 shows the *XYZ* conversion procedure leading to do the target *XYZ* and measured *XYZ* comparison.



Fig. 3.6 The *XYZ* conversion procedure and comparison between the target *XYZ* and measured *XYZ*.

Although this approach may sound natural, it is not the approach that was used. The main reason is to reduce the risk of having additional measurement errors. Furthermore, for every variant of each characterisation model, it would require the test samples to be measured separately. For example, the work was carried out over a number of years and this approach would assume that everything (the displays and the measurement device) remained constant over that time. Instead, a different (and more efficient) approach was used to evaluate performance. In this approach, the samples used for the characterisation process and the test samples were all displayed and measured once for each display devices individually. This means that the test samples were defined in terms of *RGB* values. The *XYZ* values of the displayed samples were measured and are considered to be the ground

truth. The characterisation process was then used to convert display RGB values to $CIEXYZ$ values and the colour difference between the predicted XYZ values and the ground-truth measured XYZ values was used as a measure of performance. Characterisation performance was therefore evaluated in terms of ΔE_{ab}^* values between measured and predicted XYZ values. Fig. 3.7 illustrates the comparison between the predicted XYZ and the measured XYZ . For characterisation in typical ambient or office situations, it may be more important to include a black correction. As it noted from previous studies, black-subtraction, in general, is necessary and causes the chromaticity to be constant [12, 79, 66].

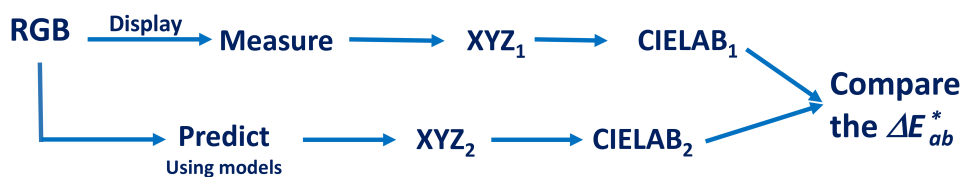


Fig. 3.7 The RGB conversion procedure and comparison between the predicted XYZ and measured XYZ .

3.4.2 Characterisation Process

There are two steps in the characterisation process for using either GOG and PLCC models (Fig. 3.7) that converts display RGB to $CIEXYZ$. The first step is to convert non-linear RGB values into the linear RGB tristimulus values. In this, linear RGB tristimulus values will be denoted as R , G and B and nonlinear RGB values will be denoted as R' , G' and B' . This requires that pairs of corresponding values are obtained (for example, pairs of R and R' , for the red channel) that can be used as a calibration set. Consider a colour ramp that is produced with 256 steps of R' . In this case, the R' are known as they were used to generate the samples and XYZ can be measured; however, how can we know the corresponding values of R ? The answer is to use Equation 3.8. Equation 3.8 can be used to calculate R' for each XYZ measurement.

The second step is to convert the linear RGB values to XYZ values. Assuming that the XYZ values are close to zero when $R = G = B = 0$ (this was justified because all measurements were made in a darkened room) then a simple linear transform can be used for this step, thus:

$$\mathbf{T} = \mathbf{M}\mathbf{D} \quad (3.7)$$

where \mathbf{T} is a $3 \times N$ matrix of XYZ values, \mathbf{D} is a $3 \times N$ matrix of normalised display RGB tristimulus values (normalising requires dividing by 255 so that the values are in the range 0 - 1) and \mathbf{M} is a 3×3 system matrix. The entries of \mathbf{M} can be simply written down since each column of \mathbf{M} corresponds to the XYZ tristimulus values of the red primary ($R = 1; G = B = 0$), the green primary ($G = 1; R = B = 0$) and the blue primary respectively ($B = 1; R = G = 0$). Of course, whereas this equation will convert RGB into XYZ, our work also requires the inverse relationship; however, this can be achieved by inverting the system matrix \mathbf{M} , thus:

$$\mathbf{D} = \mathbf{M}^{-1}\mathbf{T} \quad (3.8)$$

The inversion of \mathbf{M} , and related calculations were carried out in MATLAB. Once corresponding values of R and R' are established several methods are available to enable R' to be predicted for any value of R . The first method is to use the GOG model. This fits the relation of R' to R using a parametric equation with two variables (see Equation 2.32 in literature review). A second method is to use Piecewise Linear-assuming Chromaticity Constancy (PLCC). In this model, piecewise linear interpolation between the measurements has been approximated by the function f . The attribute of using this model is particularly useful when there is no information about the shape of the TRC of the display. A linear PLCC function was written in MATLAB and this is now described. Consider n known values of R'_i and R_i ($i = 1$ to n) and a target value of R , denoted as t , for which we want to find the corresponding value of R' , known as t' . The PLCC process has two steps. The first step is to determine which two values of R_i bracket t ; denote these as R_j and R_{j+1} . The second step is to estimate t' based on these two values this:

$$t' = R'_j + (R'_{j+1} - R'_j)(t - R_j)/(R_{j+1} - R_j) \quad (3.9)$$

The MATLAB code that was written also handles cases where $t < R_1$ and where $t > R_n$; however, in practice these cases are not required. Irrespective of whether

the GOG model or PLCC is used, it is possible to obtain the corresponding pairs of R and R' either from three pure colour-ramps (one for each channel) or from one set of grey-ramp samples. The question of which of these sets of samples is better is one of the aims of this thesis. The example above is given for the red channel but, of course, the process is carried out separately for each of the three channels.

A third method is to use Piecewise Linear model assuming Variation in Chromaticity (PLVC). In this model, by knowing the XYZ tristimulus values for each primary as a function of the digital input, assuming additivity, the resulting colour tristimulus values can be expressed as the sum of tristimulus values for each component (i.e. primary) at the given input level. A linear PLVC function was written in MATLAB. Note that in order not to have an effect of the black level, the black is subtracted from all calculation used to define the model. Then, it is added to the result, to return to a correct standard observer colour space [79, 132]. The model is summarised and generalised in Chapter 7 precisely.

3.4.3 Result analysis

Characterisation performance which has been obtained using the GOG, PLCC or PLVC, therefore, needs to be evaluated in terms of ΔE_{ab}^* values between measured and predicted XYZ values to show how good or bad are they. There is some literature that defines these evaluations by introducing the term Just Noticeable Differences (JND) such as; Kang [82] noted in his book that the good term used when the JND is of 1 ΔE_{ab}^* unit. However, the other study assessed that the JND is of 2.3 ΔE_{ab}^* Mahy *et al.* [106]. In addition, many other thresholds have been used. It proposed by Abrardo *et al.* [1] that the ΔE_{ab}^* between 0 and 1 is out of perception, from 1 to 3 is very good quality, from 3 to 6 is good quality, from 6 to 10 is sufficient and over 10 is insufficient. The different thresholds sets have been defined by Hardeberg in 1999 [65] noted that the ΔE_{ab}^* between 0 to 3 is hardly perceptible, from 3 to 6 is perceptible, but acceptable, over 6 it is not acceptable. However, acceptable ΔE_{94}^* of 1.98 and maximum of 5.57, while the best average error of non-acceptable ΔE_{94}^* is 3.73 and a maximum of 7.63 have been founded by Gibson and Fairchild [54].

In this thesis considering the professional reproduction, the following rules will be used. Fig 3.8 illustrates the histograms of the display A using three different

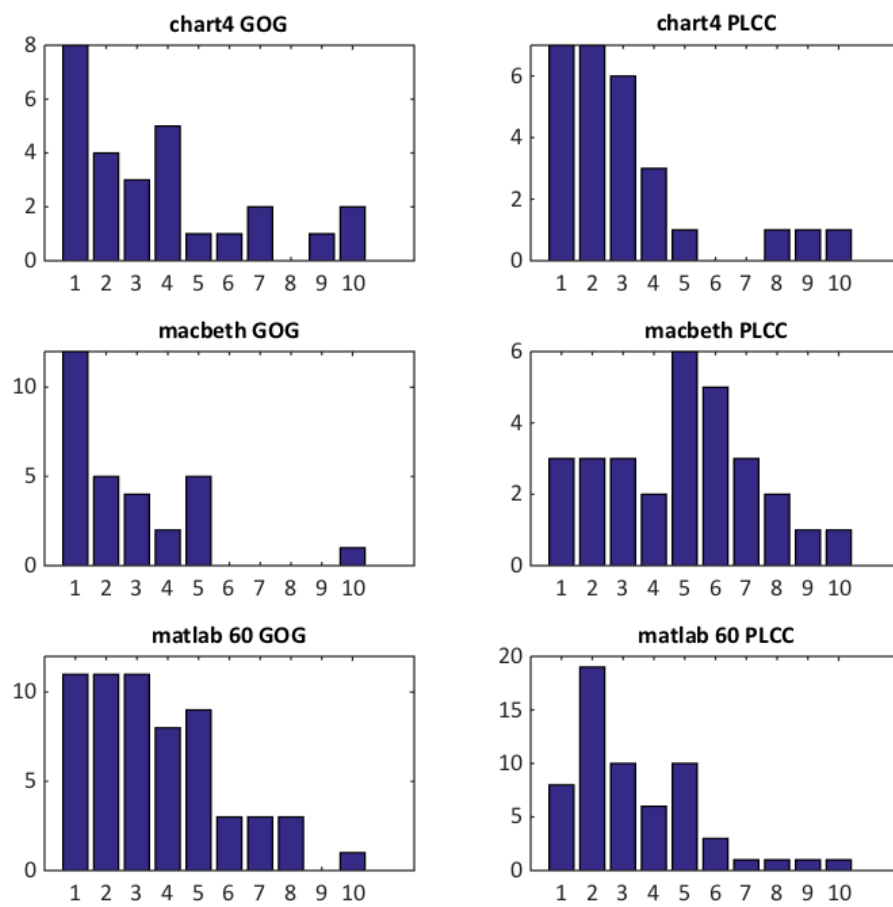


Fig. 3.8 the histograms of the display A using three different sets of samples.

sets of samples and two models (GOG and PLCC). It is clear that these data are not normally distributed; it has been decided to take the median values rather than the mean values between errors. The *Excellent* characterised display median ΔE_{ab}^* error is less than 1 ($\Delta E_{ab}^* < 1$) while the *good* one is between 1 and 2, hence the median ΔE_{ab}^* is between 2 and 4 is considered as *acceptable* and over the ceiling > 4 is considered as *not acceptable* (Table 3.2).

Table 3.2 The set of thresholds we used to assess the quality of a colour characterisation model depending on the purpose.

ΔE_{ab}^*	Quality
$\Delta E_{ab}^* < 1$	Excellent
$1 < \Delta E_{ab}^* < 2$	Good
$2 < \Delta E_{ab}^* < 4$	Acceptable
$4 < \Delta E_{ab}^*$	Not acceptable

Chapter 4

Methodology

4.1 Introduction

This section describes the methodology and experimental details that relate to Chapters 5-7. The performance of a characterisation method for a certain display is assessed by predicting the *CIEXYZ* values for a set of test samples (defined by *RGB* values) and comparing the prediction with measurements of the *CIEXYZ* values for a display showing the test samples. This means that the *XYZ* values of the test samples are generally only measured once for each display to obtain the *XYZ* value of each sample, of course, this is a requirement of the characterisation process. In this work, 20 physical displays were used.

4.2 Different types of samples

There are two types of test samples used for this study. The first sets of samples called Linearisation samples which have been used for linearisation process and defined as Grey-ramp as well as the Colour-ramps. The second types are defined as the Macbeth, Chart4 and Matlab60 were specified and the colour differences (between measured and predicted *XYZ* values) were calculated for each set of samples. Test samples were defined by *RGB* values.




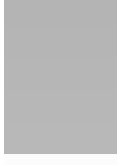

4.2.1 Linearisation samples

There are two different linearisation sample sets which have been widely used in this study called the grey-ramp and the colour-ramps.

4.2.1.1 Grey-ramp

The simplest linearisation sample set used was the grey-ramp. The grey-ramp test set is the 256 step of equal values of each RGB channel ($R = G = B$), in total there are 256 samples (Table 4.1) in this set. The grey-ramp samples were used (in some cases) to characterise the TRC (Tone Reproduction Curve) using either the GOG model or PLCC. The main characteristic of this data set is that the samples are obviously achromatic.

Table 4.1 RGB values of grey-ramp samples.

R	G	B	Colour
0	0	0	
1	1	1	
2	2	2	
3	3	3	
4	4	4	
⋮	⋮	⋮	
⋮	⋮	⋮	
⋮	⋮	⋮	
⋮	⋮	⋮	
⋮	⋮	⋮	
126	126	126	
127	127	127	
128	128	128	
129	129	129	
130	130	130	
⋮	⋮	⋮	
⋮	⋮	⋮	
⋮	⋮	⋮	
⋮	⋮	⋮	
⋮	⋮	⋮	
252	252	252	
253	253	253	
254	254	254	
255	255	255	
256	256	256	

4.2.1.2 Colour-ramps

The second linearisation test set used was the set of three colour ramps. The *RGB* values of the samples in this set is starting from 0 to 256 (Table 4.2) for each channel. A total number of 768 of samples are in this set. The colour-ramps were used (in some cases) to characterise the TRC using either the GOG model, PLCC and PLVC. The main characteristic of this data set is that the samples are very chromatic.

Table 4.2 RGB values of colour-ramps samples.

R	G	B	Colour	R	G	B	Colour	R	G	B	Colour
1	0	0		0	1	0		0	0	1	
2	0	0		0	2	0		0	0	2	
3	0	0		0	3	0		0	0	3	
4	0	0		0	4	0		0	0	4	
5	0	0		0	5	0		0	0	5	
.	0	0		0	.	0		0	0	.	
.	0	0		0	.	0		0	0	.	
.	0	0		0	.	0		0	0	.	
.	0	0		0	.	0		0	0	.	
.	0	0		0	.	0		0	0	.	
126	0	0		0	126	0		0	0	126	
127	0	0		0	127	0		0	0	127	
128	0	0		0	128	0		0	0	128	
129	0	0		0	129	0		0	0	129	
130	0	0		0	130	0		0	0	130	
.	0	0		0	.	0		0	0	.	
.	0	0		0	.	0		0	0	.	
.	0	0		0	.	0		0	0	.	
.	0	0		0	.	0		0	0	.	
.	0	0		0	.	0		0	0	.	
252	0	0		0	252	0		0	0	252	
253	0	0		0	253	0		0	0	253	
254	0	0		0	254	0		0	0	254	
255	0	0		0	255	0		0	0	255	
256	0	0		0	256	0		0	0	256	

4.2.2 Test samples

There are three different test samples describe in this section which have been used for this study.

4.2.2.1 Macbeth ColorChecker chart

The first test set used was the Macbeth ColorChecker. Table 4.3 shows the *RGB* values of the samples in this set. The Macbeth ColorChecker chart (which contains 24 patches) was developed in 1976 and its patches include six neutral colours, red-green-blue and cyan-magenta-yellow primaries, and other important colours such as light and dark skin, sky blue, and foliage etc. [109, 124]. The pigments were selected to be optimally colour constant. This chart contains both saturated and neutral colours but there is some doubt about whether it is optimal for characterisation purposes [24].

Table 4.3 RGB values of Macbeth ColorChecker samples.











































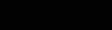
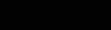
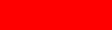







R	G	B	Colour
116	81	67	
199	147	129	
91	122	156	
90	108	64	
130	128	176	
92	190	172	
224	124	47	
68	91	170	
198	82	97	
94	58	106	
159	189	63	
230	162	39	
35	63	147	
67	149	74	
180	49	57	
238	198	20	
193	84	151	
0	136	170	
245	245	243	
200	202	202	
161	163	163	
121	121	122	
82	84	86	
49	49	51	

4.2.2.2 Chart4

One approach to developing a colour chart for characterisation purposes is to select a set of colours that are maximally different in terms of *RGB* values to each other. For example, one method [24] has been published and is available to select any

number N of samples from a pool of M samples (where $M \geq N$) based on a criterion of the samples being maximally distant in RGB colour space. One possible way to select a colour chart would be to use this method to select 24 samples (since the Macbeth ColorChecker chart has 24 samples it seems reasonable to keep the same number for comparison purposes) from all the possible RGB samples (the possible set of samples is 256^3 for a 24-bit colour display). However, the algorithm is slow and it is not practical to select 24 colours from 256^3 using this approach. Therefore, the full set of colours was first sub-sampled by taking RGB steps of 4; that is, RGB values of $[0\ 0\ 0]$, $[4\ 0\ 0]$, $[8\ 0\ 0]$, $[12\ 0\ 0]$, etc. This generates a subset of 64^3 samples which is 262,144 rather than 16,777,216. The 24 samples selected using the Cheung and Westland [24] method from this sub-sample of all possible RGB values is referred to as the Chart4. Table 4.4 shows the RGB values of the samples in this set.

Table 4.4 RGB values of the Chart4 and Chart2 samples.

Chart4				Chart2			
R	G	B	Colour	R	G	B	Colour
255	255	255		255	255	255	
0	124	252		0	126	254	
124	252	0		126	254	0	
252	0	124		254	0	126	
144	144	144		148	148	148	
0	252	128		0	254	128	
128	0	252		128	0	254	
252	128	0		254	128	0	
0	156	4		0	158	2	
4	0	156		2	0	158	
96	248	252		158	2	0	
156	4	0		96	254	254	
248	252	96		254	96	254	
252	96	248		254	254	96	
20	124	124		22	126	126	
124	20	124		126	22	126	
124	124	20		126	126	22	
116	116	252		116	116	254	
116	252	116		116	254	116	
252	116	116		254	116	116	
0	224	228		0	226	228	
24	252	28		226	228	0	
28	24	252		228	0	226	
0	0	0		0	0	0	
255	0	0		255	0	0	
0	255	0		0	255	0	
0	0	255		0	0	255	



























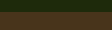

































4.2.2.3 Chart2

A Chart2 sample set was also created using the same method as the Chart4, but from a sub-sample of 128^3 (or 2,097,152) samples from the full *RGB* colour space. Table 4.4 shows the *RGB* values of the samples in this set.

4.2.2.4 Matlab60

A Matlab60 chart was created using the 450 different high-quality images selected from a various scene with the wide variety of different colours. In this method, a Matlab code defines the colour pallets based on the random selection of the most used colours from the *RGB* colour space in the image. Table 4.5 shows the *RGB* values of the 60 selected samples in this set.

Table 4.5 The *RGB* values of the Matlab60 sample set.

Matlab60							
R	G	B	Colour	R	G	B	Colour
87	101	15		106	105	77	
117	157	218		126	51	47	
157	166	113		95	83	65	
46	68	21		27	86	180	
39	49	53		118	153	140	
26	90	202		105	130	71	
82	113	180		168	163	156	
127	146	63		233	194	67	
62	144	226		211	213	215	
213	185	135		54	68	99	
183	188	200		158	31	48	
1	4	49		177	161	57	
142	122	91		15	33	80	
30	42	11		155	108	57	
72	52	27		125	165	84	
126	106	78		170	78	95	
190	70	37		11	11	10	
48	70	60		81	70	54	
154	150	142		116	79	82	
103	72	40		55	133	163	
129	87	54		142	173	201	
179	178	176		161	102	128	
95	97	103		118	113	104	
165	92	42		229	226	219	
1	43	126		65	93	148	
109	105	31		87	75	27	
50	48	31		183	109	65	
249	248	247		223	204	167	
178	13	6		110	135	14	
31	89	111		173	157	128	

4.3 Experimental Settings

There are a plethora of settings that can be adjusted for most displays which were used in the experiments. Most of these settings will affect the colours that are displayed. It is therefore important to keep the settings fixed during a characterisation process and afterwards whilst the characterisation is used. This is sometimes referred to as device calibration and is a prerequisite for colour characterisation. However, that does still leave the question of what the settings should be in order to test the display?

Setting up the brightness and contrast of the display devices would be changed by the illuminant condition of the environment as it has been noted in the previous studies [4, 56]. However, in this study, the optimum setting condition of the brightness and contrast level of display A was evaluated. Consequently, the fixed contrast and brightness levels have been used. A total number of 20 LCD displays listed in Table 4.6 were used in this study. Some specification of displays are listed in Table 4.6, However, some of these specifications are evaluated in Chapter 6.

Table 4.6 Age, Luminance of black level (cd/m^2), the chromaticity of white point, gamut size and contrast ratio specification of each display.

Display	Age	Luminance of black level cd/m^2	White point		Gamut size	Contrast ratio
			x	y		
A	2015	0.2800	0.3097	0.2873	0.1210	0.9989
B	2016	0.3499	0.3133	0.3196	0.1199	0.9985
C	2006	0.1781	0.3227	0.3537	0.1173	0.9991
D	2015	0.2277	0.3249	0.3404	0.1169	0.9989
E	2007	0.2263	0.3404	0.3582	0.1162	0.9988
F	2015	0.2303	0.3278	0.3511	0.1159	0.9990
G	2013	0.3234	0.3234	0.3249	0.1146	0.9974
H	2012	0.1487	0.3199	0.3274	0.1146	0.9983
I	2014	0.1622	0.3416	0.3536	0.1140	0.9989
J	2012	0.2074	0.3048	0.2982	0.1140	0.9990
K	2014	0.2233	0.2953	0.3265	0.1137	0.9978
L	2013	0.3159	0.3188	0.3297	0.1134	0.9990
M	2011	0.3363	0.3224	0.3308	0.1129	0.9980
N	2010	0.3330	0.3201	0.3308	0.1128	0.9953
O	2012	0.1900	0.3118	0.3262	0.1118	0.9982
P	2008	0.2955	0.3263	0.3375	0.1106	0.9981
Q	2009	4.5656	0.3400	0.3611	0.1080	0.9752
R	2012	6.2033	0.3419	0.3590	0.1035	0.9672
S	2011	0.2811	0.3427	0.3469	0.1002	0.9983
T	2013	0.3650	0.3126	0.3343	0.0950	0.9979

4.4 Summary

In this research, 20 different displays with an identical calibrated setting, two different linearisation sets of samples and three different colour sample sets were conducted. The general experimental settings that were applied to these test samples were described. These include the tele-spectroradiometer performance. The colorimetric characteristic and the characterisation models for all 20 displays which have been used are described.

Chapter 5

Display Characterisation

5.1 Introduction

In this chapter, the colorimetric properties of a single display are analysed in detail. The data processing is shown in full along with all of the processing stages. This is done so that in the following chapter it will be possible to concisely summarise results from a number of displays. The display that is considered in this chapter is displayed A which is a high-performance device, although note that in principle any the displays considered in this thesis could have been selected as the focus of the study in this chapter. Specifically, *CIEXYZ* values were measured for display A and were used to estimate various performance metrics and characteristics. These include the white point of the display, the grey-scale tracking, contrast ratio, size of the gamut, spatial uniformity, channel and spatial independence, tone-reproduction curve, linearisation and colour characterisation performance. Specifically, the effect of the number of samples used in the linearisation is considered for two linearisation methods. Some insights are made regarding best practice; however, these are based on the findings from a single display and the following chapter will present data from a larger population of displays to allow more robust insights (and recommendations) to be derived.

5.2 Colour measurements

The colorimetric characteristics of different aspects of display A device are introduced. A tele-spectroradiometer (TSR) Minolta CS-2000 (Measuring angle: 1° , Accuracy: Luminance: $\pm 2\%$, x : ± 0.0015 , y : ± 0.001 , Repeatability: Luminance: $\pm 0.15\%$, xy : ± 0.002 for standard light source A) was used to measure stimuli displayed on the display in a dark room. The devices were warmed up for at least one hour before any measurements taken place. The 2° CIE observer was used to measure *CIEXYZ* values for various stimuli defined by test sample sets such as Macbeth ColorChecker chart, Matlab60 and Chart4 (these were described in Chapter 4) and for certain samples to assess characteristics such as spatial uniformity. All the data measured by the Minolta CS-2000 were obtained in *Yxy* colour space and were converted to absolute *XYZ* measurements where the units of the *Y* tristimulus value are candelas per meter squared (cd/m^2).

5.3 White point and Grey-scale tracking

The chromaticity of the white point of display A, is $x = 0.3098$ and $y = 0.2874$. Fig. 5.1 shows the position of the display white point (shown as a green circle) in the CIE $u'v'$ chromaticity diagram. It is evident from the figure that the white point is a little yellower than D65 (red square). Both the GOG model and the PLCC model assume that the chromaticities of the primaries are constant as the intensity of the display is increased. If the three channels also have identical tone-reproduction characteristics then the chromaticity coordinates of the grey (where $R = G = B$) will be constant no matter what the values of RGB are. A display where the chromaticity of the neutral point ($R = G = B$) remains constant is said to exhibit perfect grey-scale tracking. Deviation from perfect grey-scale tracking might, therefore, be assumed to be indicative of a poorer performance of GOG and PLCC than would be obtained with perfect grey-scale tracking (colour balance). In this section, the quality of grey-scale tracking is explored. The chromaticities of the grey-scale, on a scale of $RGB = 0, \dots, 256$, with 0 for black and 255 for peak white, are shown in Fig. 5.1. For a device, with perfect grey-scale tracking, the chromaticities of all of these points would be coincident. It is evident, however, that there is some deviation from this and this occurs notably for the very dark colours.

Fig. 5.1 also shows any deviation from the chromaticity of the white point (denoted as a green symbol) and D65 (denoted as a red symbol).

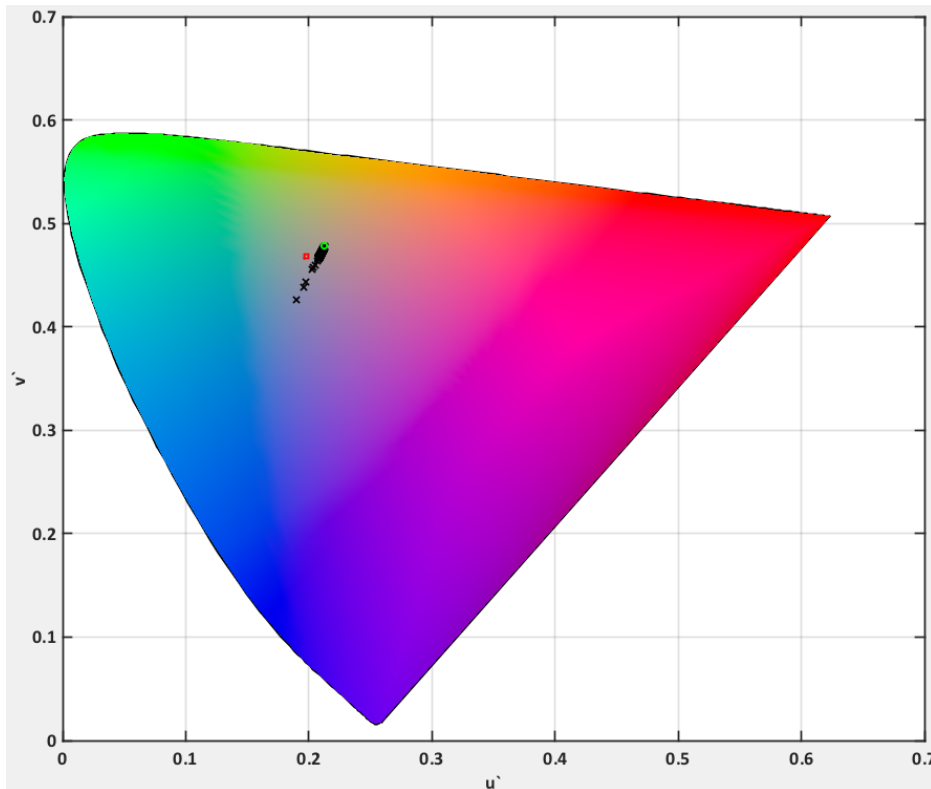


Fig. 5.1 Chromaticities of white point (green circle) and grey levels (black crosses) for the display A without black correction. The chromaticity of D65 (red square) is also shown for reference.

Black Level in displays is the capability of producing black in the display technologies and is a major challenge for all the display technologies. No display can produce a perfect black. An error occurs in both intensity and colour throughout the entire lower end of the scale with poor black-level the display's intensity-scale is lifted the bottom end. Fig. 5.2 illustrates the grey-scale tracking after doing the black correction. It is evident from the graph that the black crosses are much closer together in comparison to Fig. 5.1 which shows the greyscale tracking before doing the black correction. Therefore, for this reason, it has been decided to do the black-correction for all the displays.

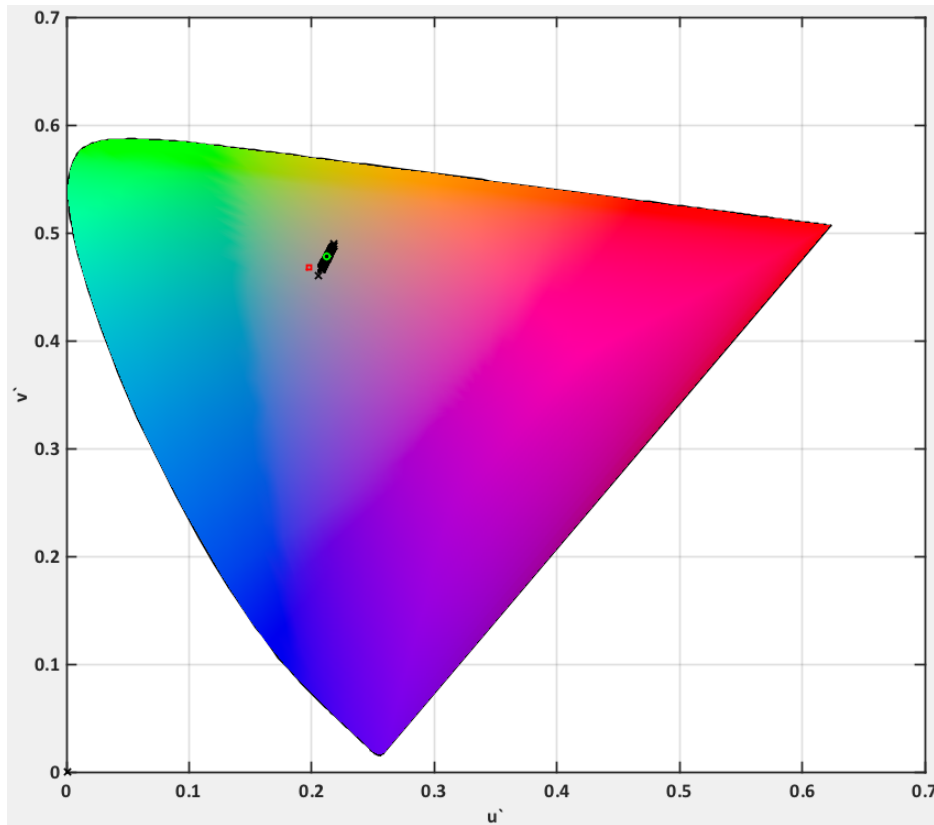


Fig. 5.2 Chromaticities of white point (green circle) and grey levels (black crosses) for display A after the black correction. The chromaticity of D65 (red square) is also shown for reference.

5.4 Colour tracking (Chromaticity changes of primaries)

Colour tracking describes the ability of a display to reproduce the locus of chromaticity of primary colours by changing the input digital value of each channel. In liquid-crystal displays (LCDs), colour tracking is dependent on brightness [165]. To evaluate the colour tracking of each display 256 steps of the primaries (RGB) were measured. All the results are plotted in a CIE1976 $u'v'$ diagram.

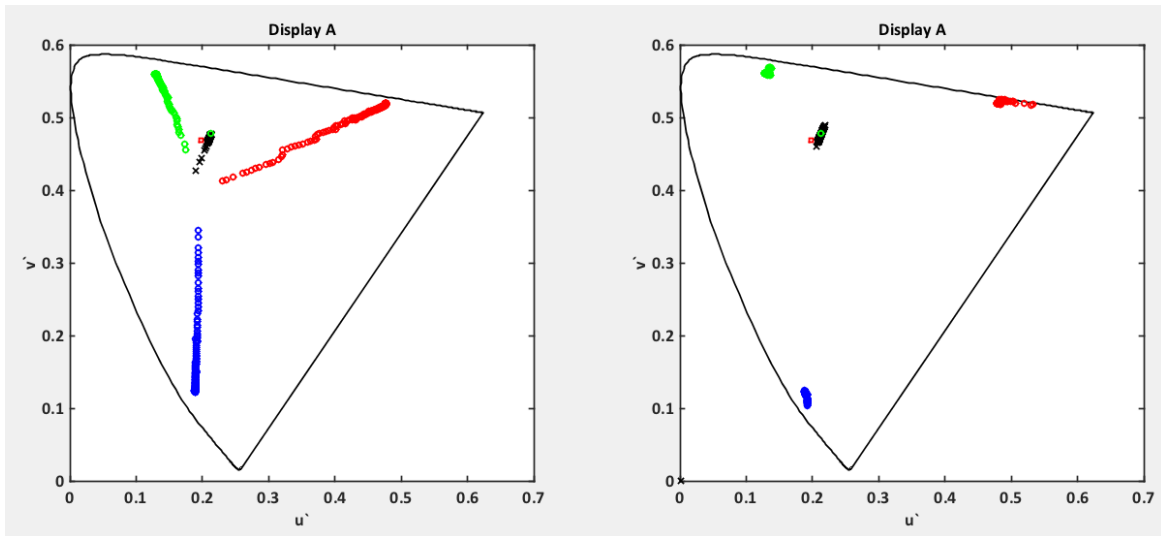


Fig. 5.3 Colour and greyscale tracking and chromaticities of white point (green circle) before (left) and after (right) black correction in $u'v'$ -diagram.

5.5 Colour Gamut

The colour gamut of each display shows the range of colours which can be reproduced by a display under a specified set of viewing conditions [114]. Fig. 5.4 shows the plotted $u'v'$ -diagram of the primaries colour coordinates (RGB) of the display A primaries were measured under the dark surrounding condition. The gamut of display A is larger than $sRGB$ especially in the red and blue regions whereas it is a little smaller in the green region.

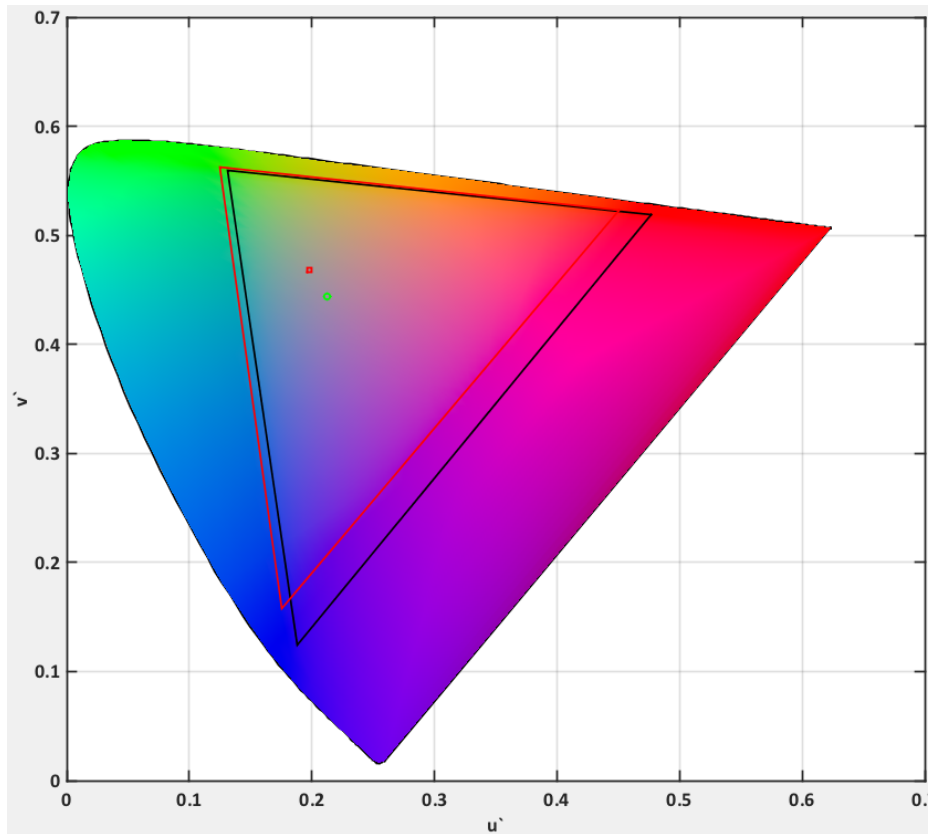


Fig. 5.4 Colour gamut of display A (black line) and chromaticities of white point (green circle) in comparison with the *sRGB* (red line and red square) plotted in $u'v'$ -diagram.

5.6 Spatial Uniformity

Spatial uniformity of the device by displaying a nominally spatially uniform white across the whole display and then measuring the colour in the centre and at each of 8 different surrounding positions across the display. Fig. 5.6 illustrates these 9 measurement points. The white colour positioned in the centre of the display, which in this case is number 5, was taken as a reference. Colour differences were then computed from the white colours between the centre and in each surrounding position. Table 5.1 shows these colour differences in CIELAB (ΔE_{ab}^*) units. The mean colour difference across the 8 locations compared to the centre was $2.16 \Delta E_{ab}^*$. The largest colour-difference (ΔE_{ab}^*) was found at the top left corner with a colour difference of 5.26 (position 1). The smallest difference was seen at the centre of the display in the horizontal and vertical directions. Table 5.1 indicates the extent of colour variation according to the position. The colour cast between corners

and centre of the screen suggests some defects in the illumination system of this particular LCD.



Fig. 5.5 Position of white measurements.

Table 5.1 Spatial uniformity of display A.

Spatial Uniformity	
Measurements position	ΔE_{ab}^*
1	5.26
2	2.66
3	2.88
4	1.56
5	0.00
6	1.63
7	0.72
8	2.50
9	2.22
Mean	2.16

5.26	2.66	2.88
1.56	0.00	1.63
0.72	2.50	2.22

Fig. 5.6 Spatial uniformity checking a colour difference (ΔE_{ab}^*) between the centre and the different position of the display.

5.7 Channel Independence

The three channels of a display (red, green and blue), ideally, should perform independently. Therefore the output of any one colour channel (e.g. red) should not be affected by the signals from the other two (e.g. green or blue) channels. Table 5.2 shows the *XYZ* values and *CIELAB* values for the pure primaries, the white, and the sum of the three primaries. All stimuli were shown using the full screen as discussed earlier and measurement was in the centre of the display. The white point for the *CIELAB* calculations was the white stimulus itself of course. If the display has excellent channel independence then the colour difference between the white and the sum *RGB* stimuli should be close to zero. In this case, the colour difference is 0.80 ΔE_{ab}^* units.

Table 5.2 Channel Independency test for display A.

Display A Channel Independence						
	X	Y	Z	L^*	a^*	b^*
Red	46.56	22.53	2.11	54.58	73.71	72.29
Green	37.61	70.94	13.33	87.45	-93.92	87.09
Blue	24.10	7.06	127.17	31.95	96.79	-110.90
Sum RGB	108.27	100.53	142.62	100.20	-0.15	-0.76
White	100.00	100.00	140.27	100	0	0
ΔE_{ab}^*	0.80					

5.8 Spatial Independence

Table 5.3 shows the colorimetric measurements for the display white as full screen (referred to as White vs White) and as a patch on a black background (referred to as White vs Black). The dimensions of the patch were 500×500 pixels. If the display has excellent spatial independence then the colour difference between these two stimuli should be close to zero and this can be seen to be the case, here. In this case, the colour difference is $0.15 \Delta E_{ab}^*$ units.

Table 5.3 Spatial Independence of the display A.

Display A Spatial Independence						
Colour patch	X	Y	Z	L^*	a^*	b^*
White vs Black	275.19	255.36	358.59	99.88	-0.05	-0.07
White vs White	276.14	256.17	359.33	100.00	0.00	0.00
ΔE_{ab}^*	0.15					

5.9 Non-Linearity of Response

Fig. 5.7 shows the tone-reproduction curves (TRC) for the three channels in the display A. In each case, the R , G or B value for the stimulus is plotted against the linear R , G or B value respectively (recall that these linear values are obtained from a linear transform of the measured XYZ values).

The plot is shown in two ways; with the linear values on the x-axis on the left and the linear values on the y-axis on the right. It is evident that the TRC for this display (A) is highly nonlinear and that it exhibits a gamma-type curve that has often been associated with older CRT displays. Fig. 5.7 is obtained from the grey-ramp linearisation data set. Fig. 5.8 shows the TRC obtained from the pure colour-ramps linearisation data sets of the display A. As mentioned previously, it is possible to obtain these corresponding sets of linear and non-linear values in two ways; either using the grey-ramp values or using the colour-ramps. In both cases, we use Equation 2.33 to convert measured XYZ values into linear RGB values. The two sets of plots look rather similar. One of the aims of this work is to explore whether the use of one set of samples or another (grey vs. colour) makes a

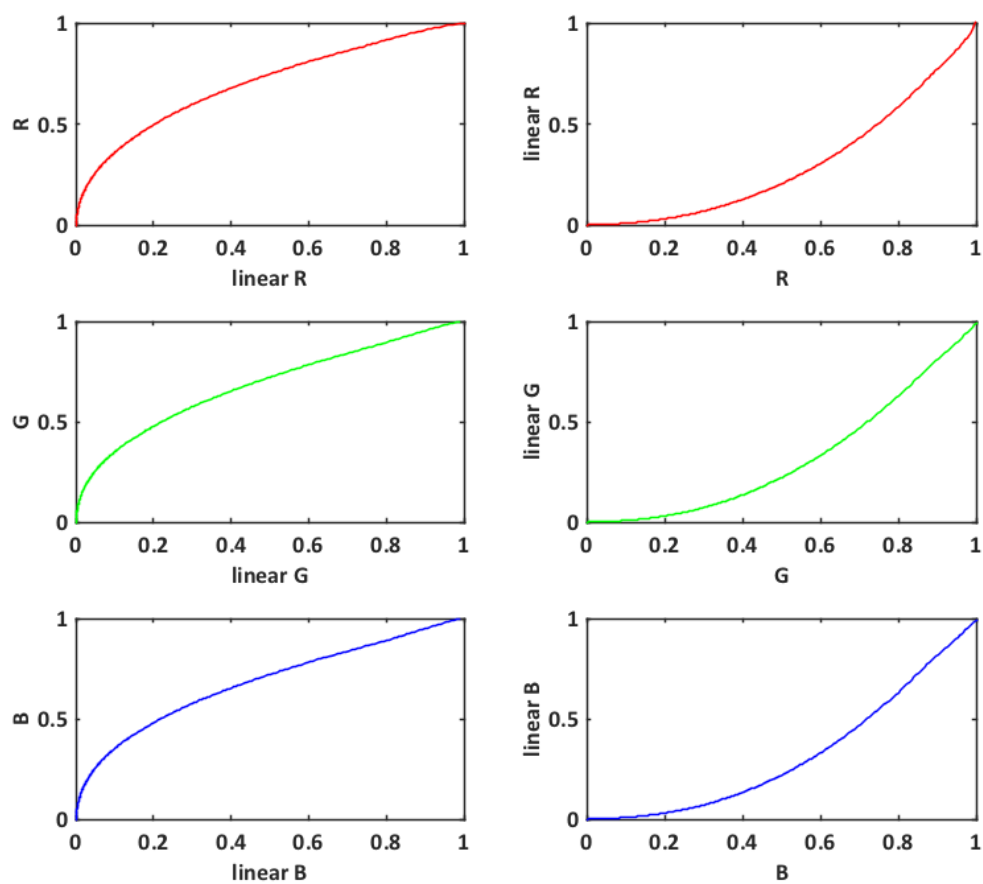


Fig. 5.7 The tone-reproduction curves (TRC) of display A for the three channels (obtained using grey-ramp linearisation sample set). Note that actual points are plotted but there is so many level (256) that it appears as a solid line.

difference to the characterisation performance and, if it does, to ascertain which leads to the better characterisation performance.

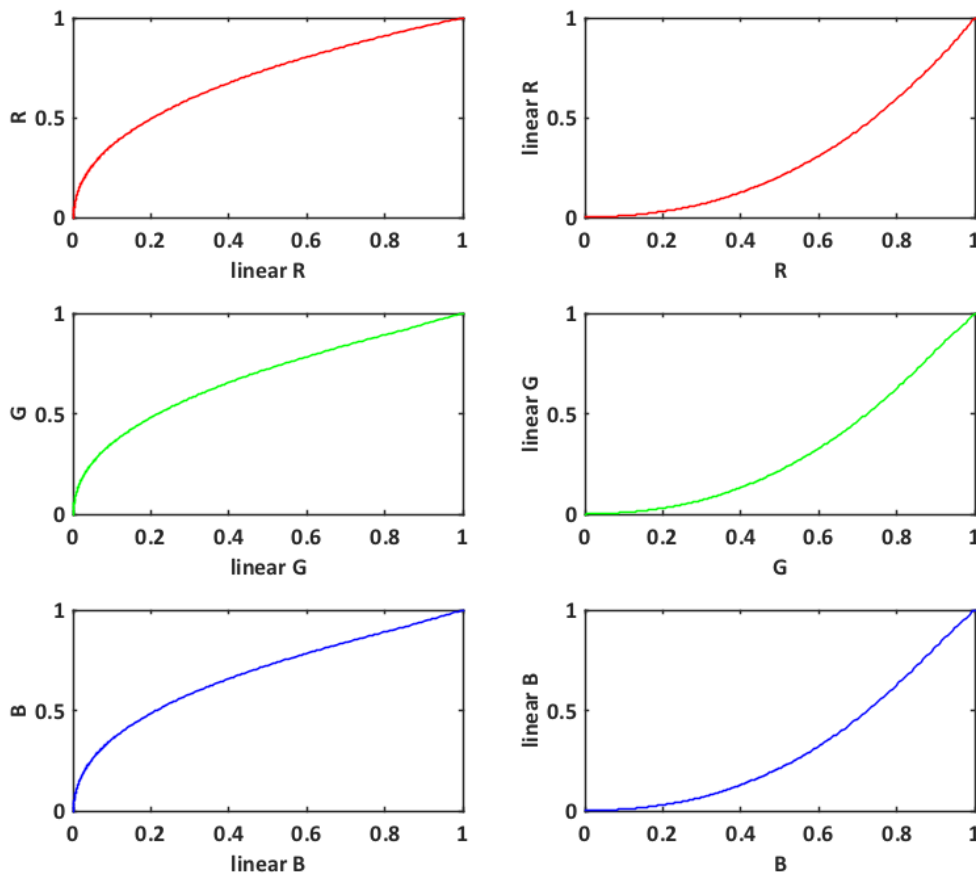


Fig. 5.8 The tone-reproduction curves (TRC) of display A for the three channels (obtained using colour-ramps linearisation sample set). Note that actual points are plotted but there are so many levels (256) that it appears as a solid line.

5.10 Linearisation

In this study different colour characterisation methods have been used, referred to as GOG, PLCC and PLVC in this thesis. The GOG and PLCC methods are two-stage methods where linearisation is followed by a linear (matrix) transform. The difference between GOG and PLCC is simply in how the linearisation is performed. The GOG model (discussed in Section 2.7.1) fits the TRC with a parametric model; the PLCC uses interpolation between known points to ‘fit’ the data (PLVC also uses interpolation but does not separate the linearisation stage from the colour transform stage in the way that PLCC does). In this study, the starting point was

to convert nonlinear *RGB* to linear *RGB* since the aim is to convert from *RGB* to *XYZ*. In contrast, if users wanted to go from *XYZ* to *RGB* (which is probably more common in practice) then this would be done by mathematical inversion for the GOG model whereas for the PLCC model a separate interpolation would be required on, for example, the left-hand plots of Fig. 5.7 (so that PLCC is strictly not invertible). In this study, there are 256 levels of *RGB* and these have all been measured. For PLCC, when all 256 points per channel are used, the linearisation is a simple look-up table. For both GOG and PLCC (and for PLVC in a later chapter), the 256 data are sub-sampled (resulting in fewer and fewer used points) to allow the performance of the models to be investigated as the number of calibration points is reduced. There are different statistical methods available to calculate the agreement between two variables. For example, there is the work of Luo *et. al* [60] who have developed *PF/4* and *PF/3* methods. However, there is no clear consensus over which method is better than any other in a specific circumstance and coefficient of determination r^2 is widely used and accepted in many studies. In this work, r^2 is used.

Table 5.4 r^2 linearisation values (display A) for the methods when all 256 levels are used in the training using either grey or colour ramps.

	Display A r^2			
	R	G	B	Mean
Grey_PLCC	0.9999	0.9998	0.9998	0.9998
Grey_GOG	0.9999	0.9996	0.9992	0.9996
Colour_PLCC	1.0000	1.0000	1.0000	1.0000
Colour_GOG	1.0000	0.9997	0.9995	0.9997

It is useful to look more detail at the implementation of interpolation (PLCC) or parametric modelling (GOG) on the data with various numbers N . Fig. 5.10 shows the effect of linearisation using both GOG and PLCC methods (with the grey samples being used). In each case, the predicted linear *RGB* values are plotted against the actual linear *RGB* values; if linearisation is perfect then these data should fall on a straight line. Performance can, therefore, be measured using the coefficient of determination r^2 which is shown on each of the graphs. Table 5.4 shows the r^2 values obtained when each of the three methods is used with all of the training data available (that is, all 256 measured samples). Note that for PLCC and GOG there is the option of using the grey-ramp linearisation samples as the training data to derive the parameters or using the colour-ramps and therefore the

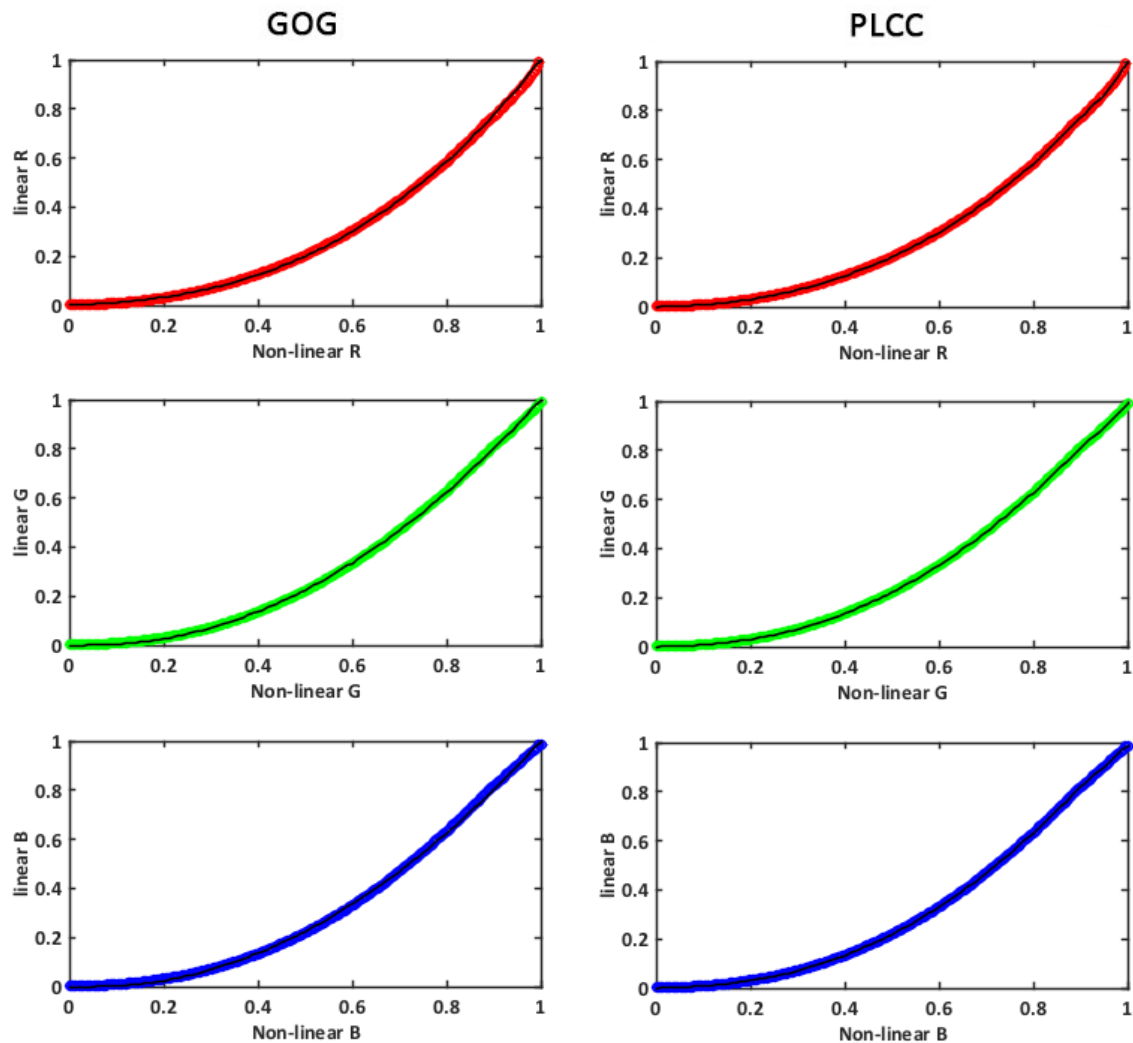


Fig. 5.9 The data from Fig. 5.7, fitted with GOG and PLCC (using grey-ramp linearisation samples with 256 steps).

models are denoted with a prefix of Grey or Colour accordingly. Table 5.4 indicates that when all 256 training data are measured and used all of the methods perform well. The interesting thing is what happens when fewer than 256 training samples are used with either the Grey or Colour method.

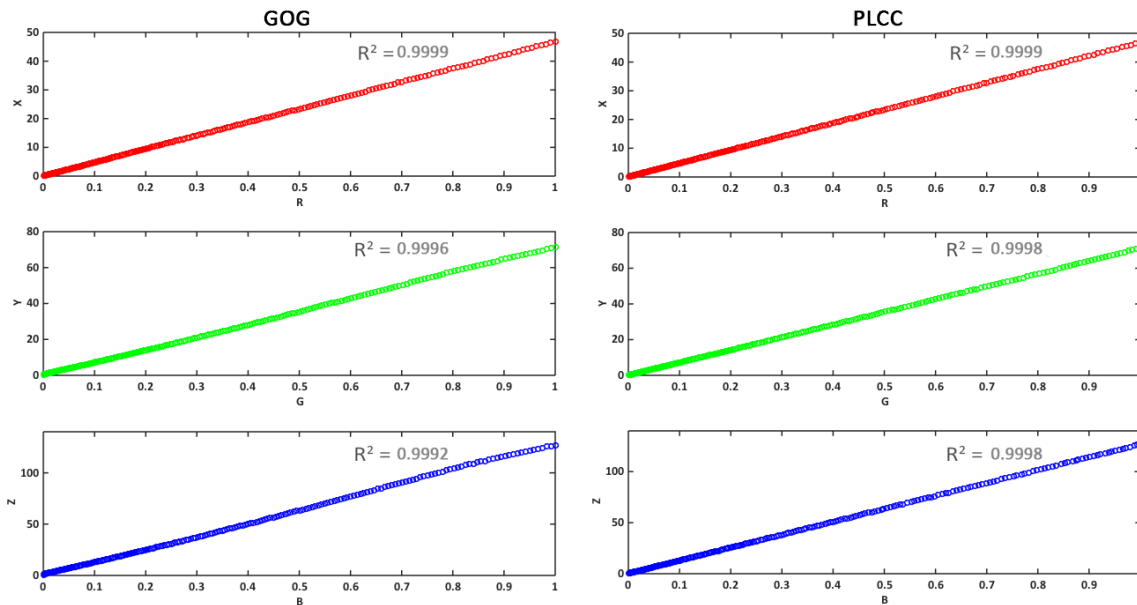


Fig. 5.10 The effect of linearisation using both GOG and PLCC method.

5.10.1 Effect of using a various number of samples on data linearisation

The 256 colour-ramp and grey-ramp values were subsampled to generate 7 sets of training data with 256, 129, 66, 34, 18, 10 and 6 samples. In all cases, the extreme values were always present (0 and 256) and the other values were uniformly spaced between them. The data in Table 5.4 were recalculated for each of these 7 training sets (this was not done for the LUT method since this requires all of the 256 training samples). Table 5.5 shows the r^2 values obtained when each of four methods (Grey_PLCC, Colour_PLCC, Grey_GOG and Colour_GOG) is used with the various training sets (note that although the number of samples in the training (that is, in the calculation of the fitting parameters or as the basis of the interpolation) is varied, the r^2 value is always calculated using all of the available data). All of the r^2 values are quite high and it is easier to understand the trends by looking at the Fig. 5.11. From this figure, it is evident that irrespective of whether colour or grey-ramp samples are used for the training when the number of training samples N is high, the PLCC method performs much better than the GOG method. However, when N is small the difference between GOG and PLCC is less evident. However, what is not clear is how important the differences in Fig. 5.11 are in practical terms of

Table 5.5 The r^2 values for using each of four methods with various training sets of data.

Number of samples	Method	R	G	B	Mean
N=256	Grey_GOG	0.9999	0.9996	0.9992	0.9996
	Grey_PLCC	0.9999	0.9998	0.9998	0.9998
	Colour_GOG	1.0000	0.9997	0.9995	0.9997
	Colour_PLCC	1.0000	1.0000	1.0000	1.0000
N=129	Grey_GOG	0.9999	0.9996	0.9992	0.9996
	Grey_PLCC	0.9999	0.9998	0.9998	0.9998
	Colour_GOG	1.0000	0.9997	0.9995	0.9997
	Colour_PLCC	1.0000	1.0000	1.0000	1.0000
N=66	Grey_GOG	0.9999	0.9996	0.9992	0.9996
	Grey_PLCC	0.9999	0.9998	0.9998	0.9998
	Colour_GOG	1.0000	0.9997	0.9995	0.9997
	Colour_PLCC	1.0000	1.0000	1.0000	1.0000
N=34	Grey_GOG	0.9999	0.9996	0.9992	0.9996
	Grey_PLCC	0.9999	0.9998	0.9998	0.9998
	Colour_GOG	1.0000	0.9997	0.9995	0.9997
	Colour_PLCC	1.0000	1.0000	1.0000	1.0000
N=18	Grey_GOG	0.9999	0.9996	0.9992	0.9996
	Grey_PLCC	0.9999	0.9998	0.9997	0.9998
	Colour_GOG	1.0000	0.9997	0.9995	0.9997
	Colour_PLCC	1.0000	1.0000	1.0000	1.0000
N=10	Grey_GOG	0.9999	0.9996	0.9991	0.9995
	Grey_PLCC	0.9999	0.9997	0.9996	0.9998
	Colour_GOG	1.0000	0.9997	0.9995	0.9997
	Colour_PLCC	1.0000	0.9999	0.9999	0.9999
N=6	Grey_GOG	0.9999	0.9996	0.9992	0.9996
	Grey_PLCC	0.9996	0.9992	0.9989	0.9992
	Colour_GOG	1.0000	0.9997	0.9995	0.9997
	Colour_PLCC	0.9996	0.9995	0.9995	0.9995

characterisation; this is evaluated in the next section where the characterisation performance is assessed for varying amounts of training data N in the linearisation process.

Fig. 5.12 - 5.17 shows the effect of choosing the various number of linearisation samples when using either the GOG or PLCC method (with the grey-ramp linearisation samples being used). It is evident from Fig. 5.12 that the number of linearisation samples N has a much greater effect on the PLCC model than it does on the GOG model. The GOG model is quite invariant to changes in N and has better performance than the PLCC model when the number of linearisation samples is small ($N = 6$). In general, however, when $N \geq 10$ the performance of

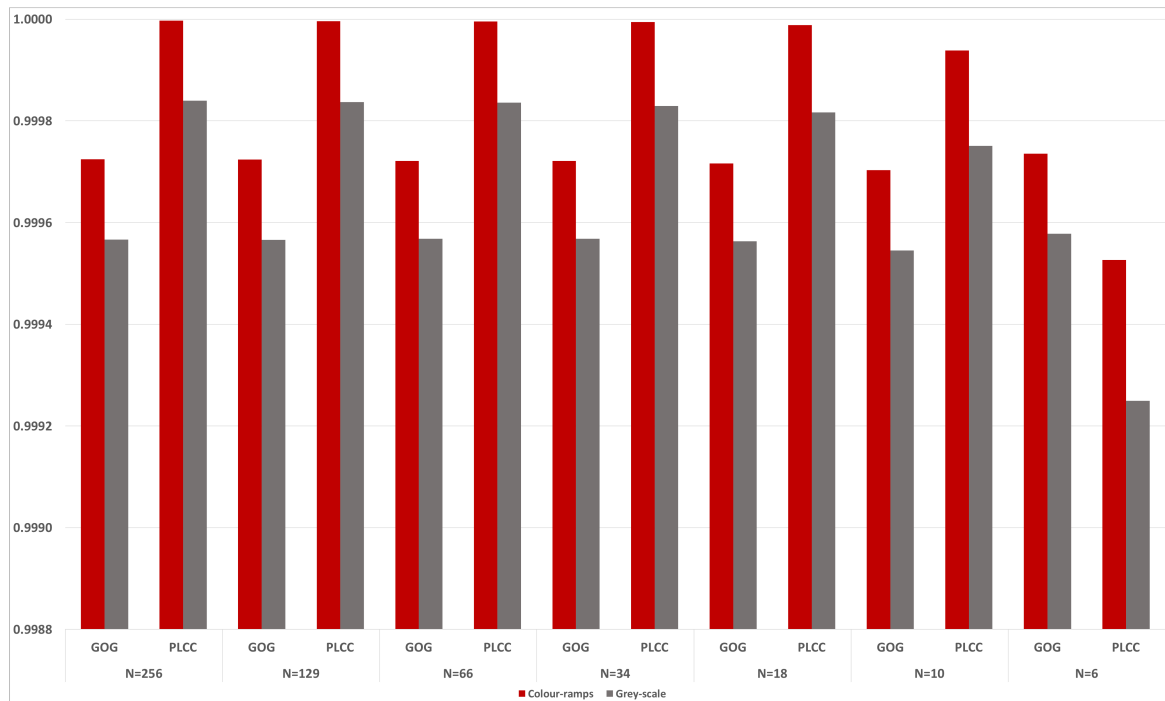


Fig. 5.11 The r^2 values for four different methods using the various training data sets (N is the number of samples used in the linearisation).

the PLCC model is better than for the GOG model (no matter whether using the grey-ramp samples or colour-ramps samples for linearisation).

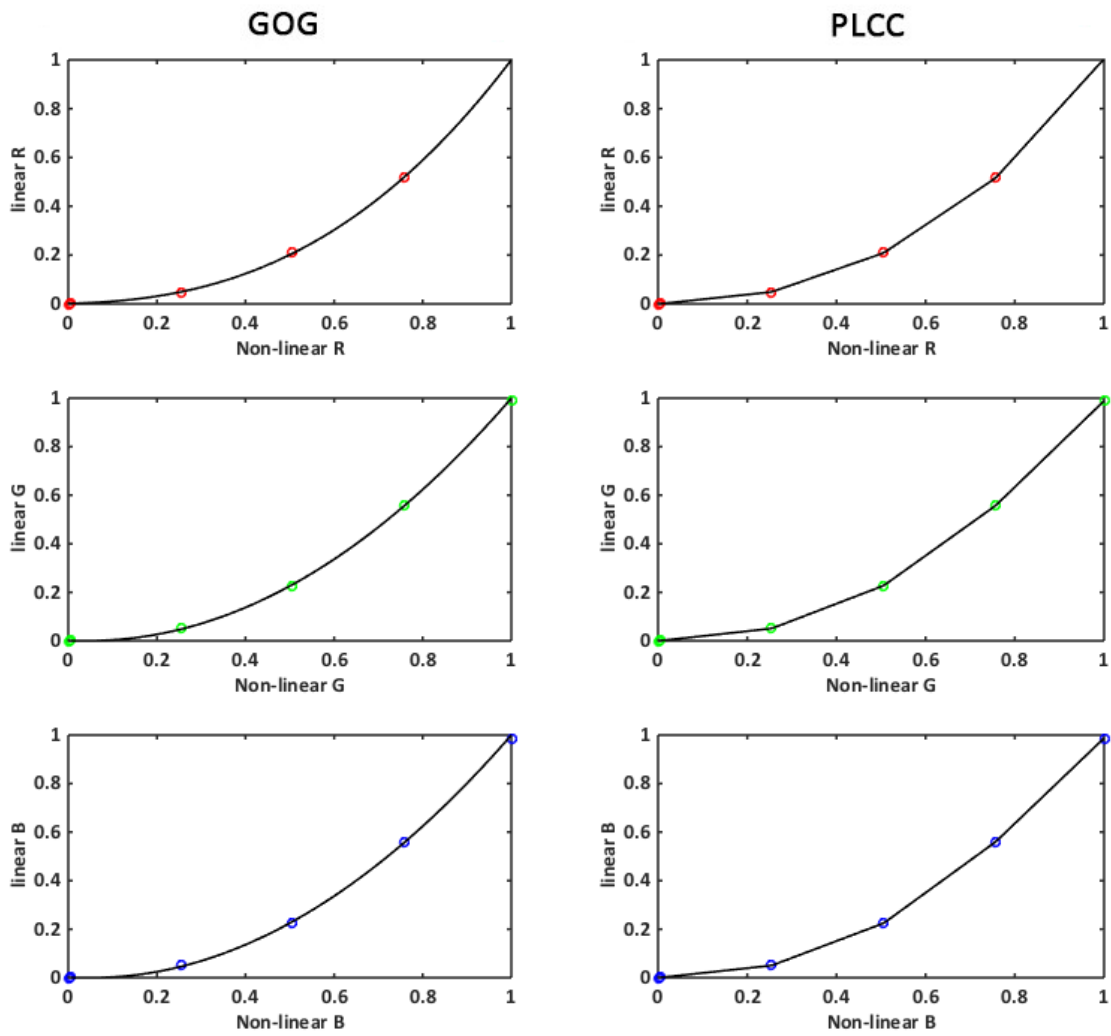


Fig. 5.12 The effect of choosing 6 linearisation samples ($N = 6$) by using either the GOG or PLCC method (with the grey samples being used).

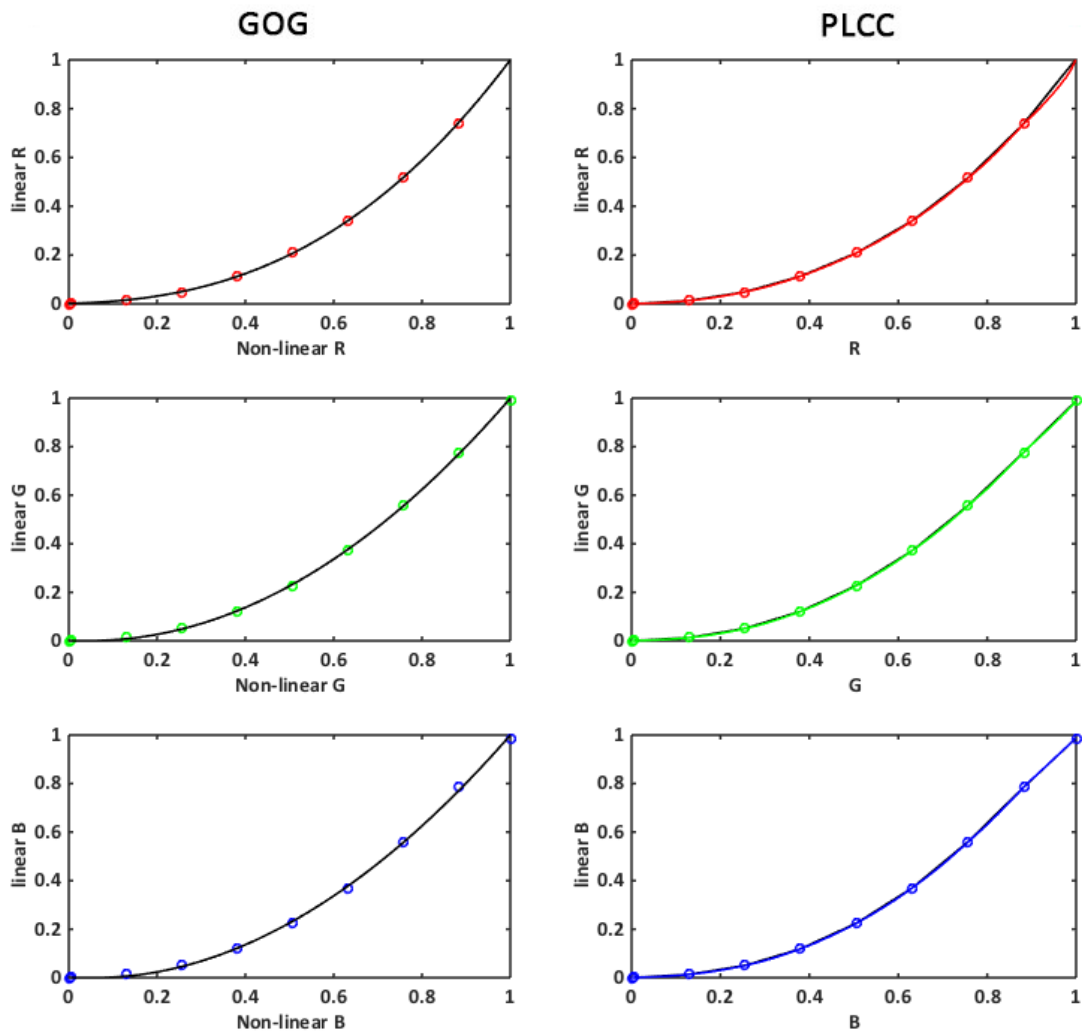


Fig. 5.13 The effect of choosing 10 linearisation samples ($N = 10$) by using either the GOG or PLCC method (with the grey samples being used).

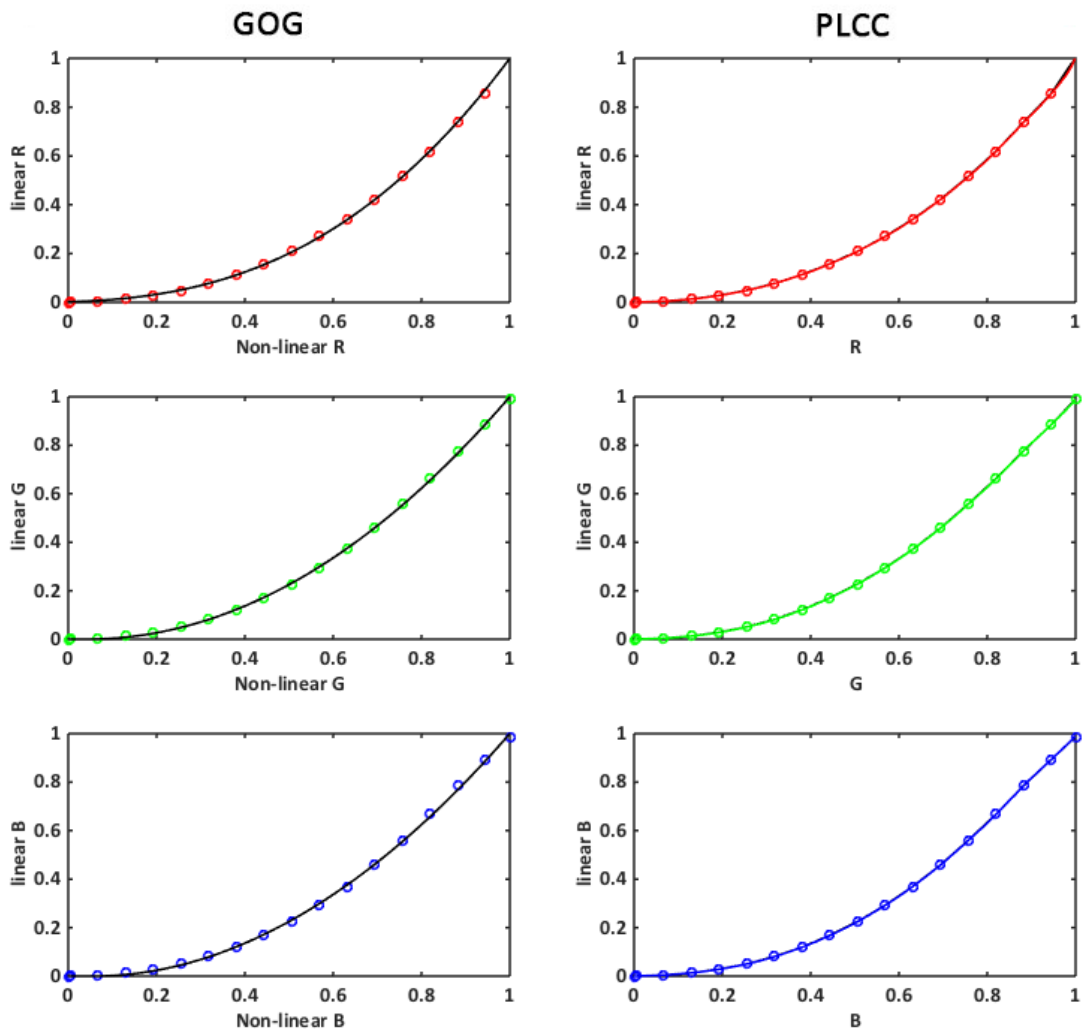


Fig. 5.14 The effect of choosing 18 linearisation samples ($N = 18$) by using either the GOG or PLCC method (with the grey samples being used).

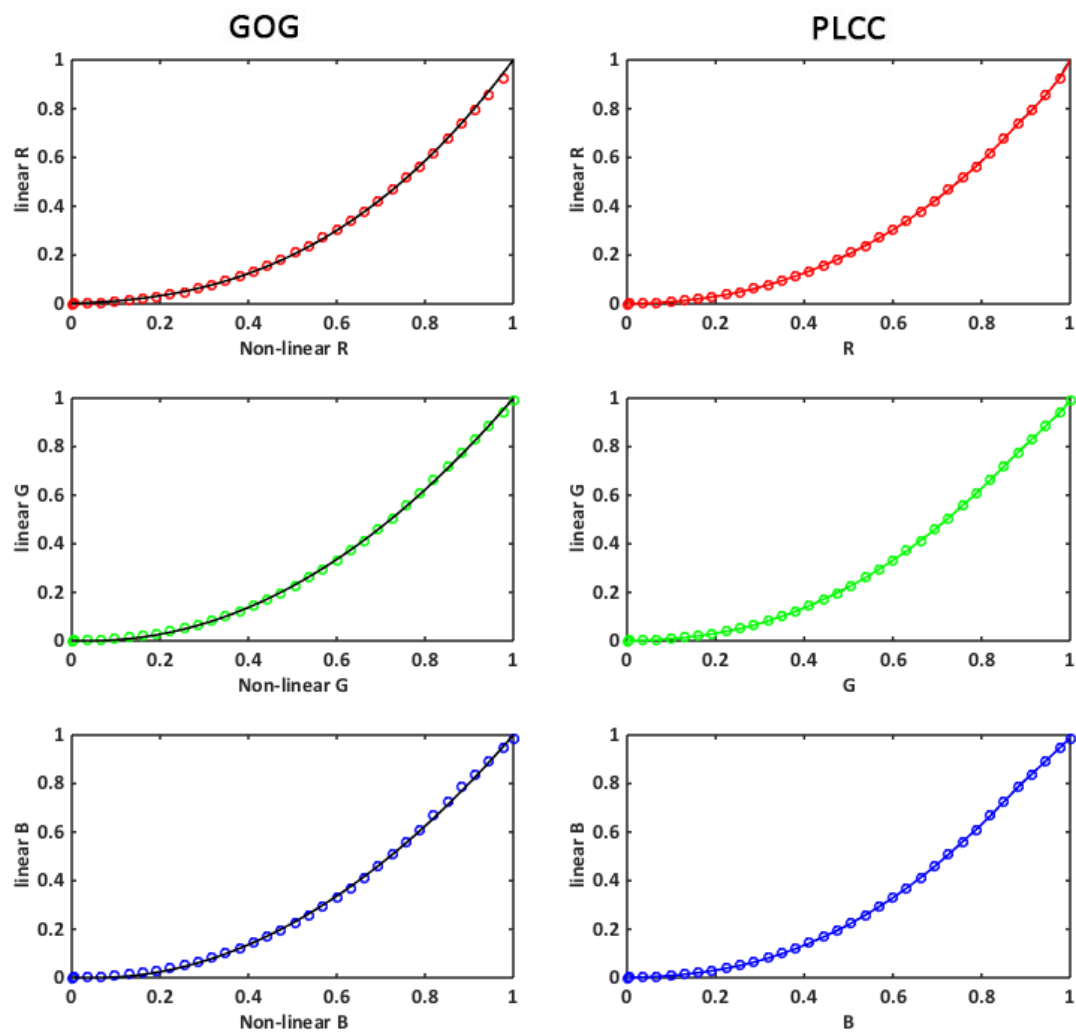


Fig. 5.15 The effect of choosing 34 linearisation samples ($N = 34$) by using either the GOG or PLCC method (with the grey samples being used).

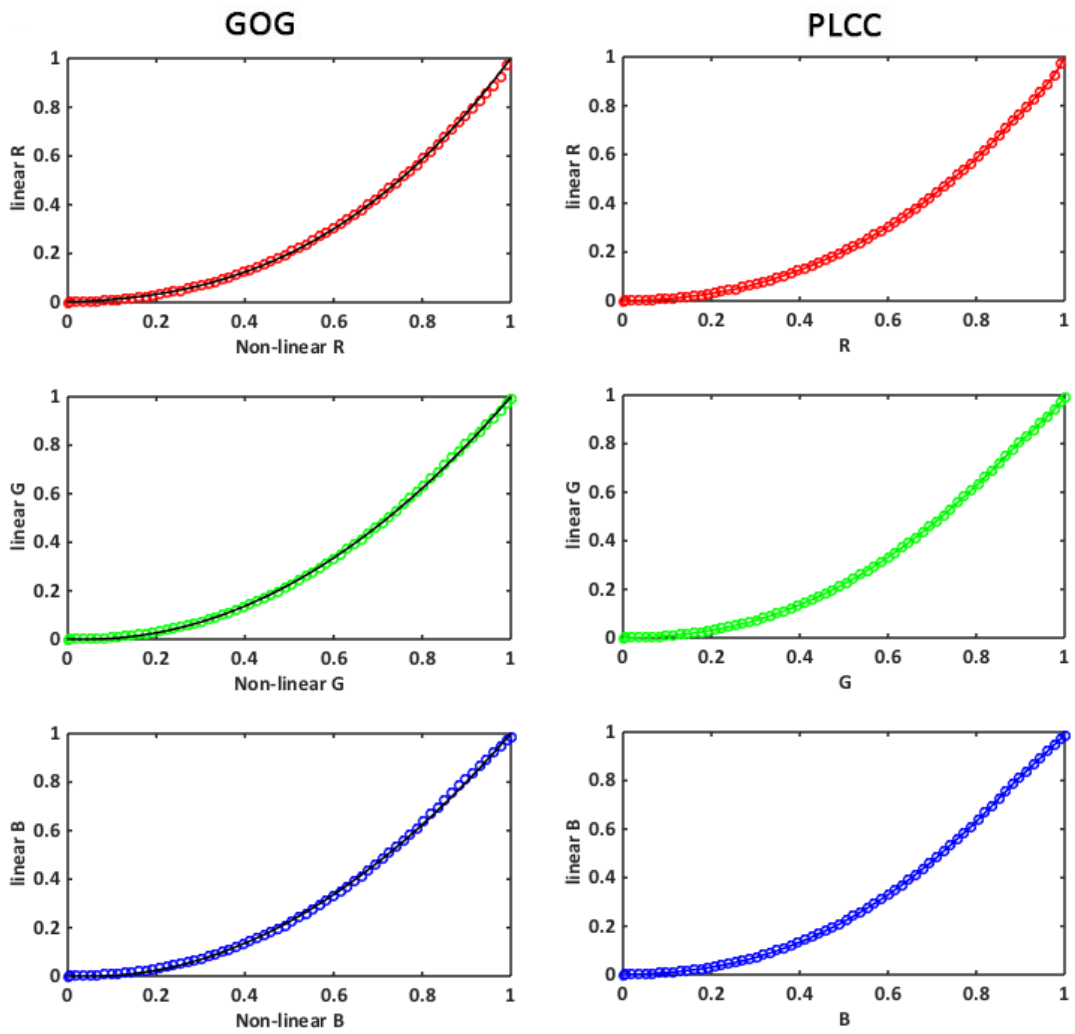


Fig. 5.16 The effect of choosing 66 linearisation samples ($N = 66$) by using either the GOG or PLCC method (with the grey samples being used).

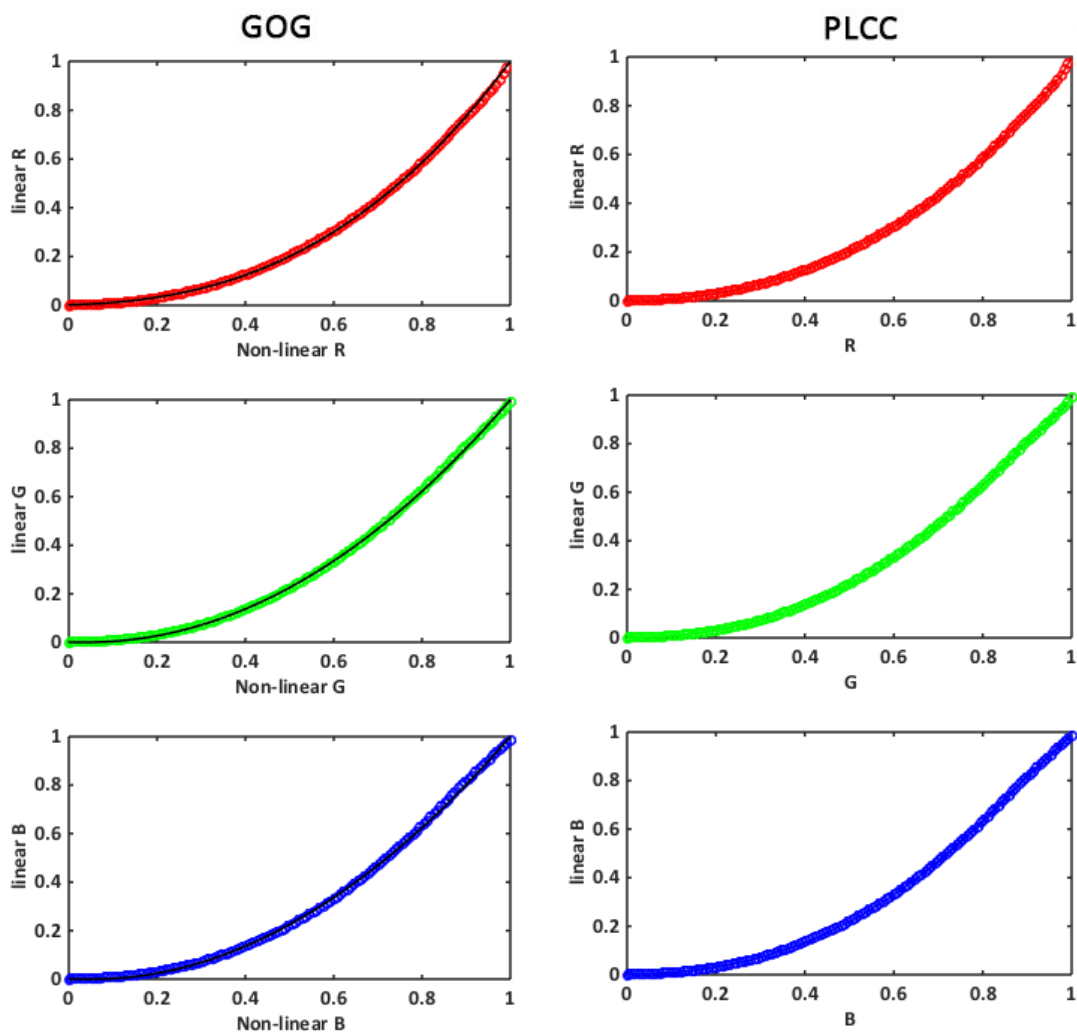


Fig. 5.17 The effect of choosing 129 linearisation samples ($N = 129$) by using either the GOG or PLCC method (with the grey samples being used).

5.11 Characterisation Performance

In this section characterisation performance is reported for the four different models (two ways of obtaining data using either colour-ramps or grey-ramp linearising samples). For each of these models, the effect of a number of linearisation samples N (256, 129, 66, 34, 18, 10 and 6) is explored. Performance is tested using three different sets of test samples named as Chart4, Macbeth and Matlab60 (these were defined and discussed earlier in Section 4.2). The performance of each method was compared by computing the colour difference between measured and predicted values for all sets of samples in ΔE_{ab}^* units.

Table 5.6 shows the characterisation performance of using the Macbeth ColorChecker chart sample set with both, the grey-ramp and colour-ramps linearisation samples ($N = 256$). It is evident that the best performing model is to use grey-ramp linearisation sample set and the PLCC linearisation method in the Macbeth data sets. However, the same pattern is shown for the Chart4 and Matlab60 datasets (Table 5.9).

Table 5.7 listed the overall results in ΔE_{ab}^* units in terms of mean, median, standard deviation minimum and maximum values of all three different sample sets with using all ($N=256, 129, 66, 34, 18, 10$ and 6) linearisation sub-sample sets for display A. The results show that the PLCC method gives the best predictions compared with the other models in terms of the mean and median colour difference (ΔE_{ab}^*) and the PLCC method also shows the best accuracy in terms of standard deviation and minimum values. However, the PLCC method shows the worse accuracy in terms of the mean and median colour difference (ΔE_{ab}^*) values when the number of linearisation samples is less than 6 ($N < 6$). Fig. 5.18 illustrates the max ΔE_{ab}^* over the median ΔE_{ab}^* .

Tables 5.8 and 5.9 show the characterisation performance of the three sets of the sample (Chart4, Macbeth and Matlab60). It is evident that the best performance is obtained for the grey-ramp linearisation samples and the PLCC method (Table 5.8). A similar pattern is found, the PLCC model is again the best method but in this case using the colour-ramps linearisation samples (Table 5.9). However, note that the GOG is performing better when the number of samples is low ($N = 6$). In addition, the performance using the grey-ramp linearisation samples is very similar to that when using the colour-ramps linearisation samples. Taking these two

Table 5.6 CIELAB colour differences (ΔE_{ab}^*) for each set of the linearisation samples in the Macbeth ColorChecker sample set.




















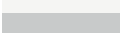




Display A				
Macbeth				
Sample	Grey		Colour	
	GOG	PLCC	GOG	PLCC
	1.58	0.36	1.90	0.58
	0.67	0.39	0.37	1.09
	0.48	0.44	0.25	0.62
	2.45	0.19	2.85	0.41
	0.35	0.39	0.30	0.83
	1.04	0.80	0.82	0.89
	3.49	0.40	4.03	1.08
	1.17	0.86	1.35	1.01
	0.89	0.70	1.27	1.24
	2.66	0.38	3.19	0.54
	1.70	0.59	2.32	0.91
	3.52	0.76	3.84	0.87
	3.08	0.65	3.65	0.58
	1.74	0.64	2.32	0.92
	2.30	0.57	3.69	0.91
	2.11	0.76	2.22	0.47
	7.21	6.60	7.45	6.68
	1.55	1.36	1.31	1.39
	0.83	0.05	0.96	0.66
	0.49	0.16	1.01	0.73
	0.42	0.10	0.38	0.75
	0.73	0.05	0.05	0.72
	0.23	0.09	0.75	0.62
	3.31	0.02	3.44	0.39

Table 5.7 CIELAB colour differences (ΔE_{ab}^*) of different statistic parametric for each set of the linearisation samples in the Macbeth ColorChecker sample set using grey-ramp linearisation samples.

Macbeth ColourChecker Chart											
ΔE_{ab}^*	Mean		Median		Std		Min		Max		
N	GOG	PLCC	GOG	PLCC	GOG	PLCC	GOG	PLCC	GOG	PLCC	
256	1.66	0.66	1.17	0.40	1.49	1.19	0.23	0.00	7.21	6.60	
129	1.65	0.66	1.17	0.41	1.49	1.19	0.23	0.00	7.21	6.63	
66	1.65	0.65	1.16	0.41	1.49	1.19	0.23	0.00	7.20	6.63	
34	1.65	0.64	1.15	0.41	1.49	1.17	0.22	0.00	7.20	6.54	
18	1.66	0.65	1.13	0.41	1.50	1.17	0.24	0.00	7.21	6.55	
10	1.75	0.85	1.22	0.79	1.60	1.04	0.23	0.00	7.37	5.88	
6	1.61	2.12	1.06	2.29	1.52	1.22	0.13	0.00	7.27	4.88	

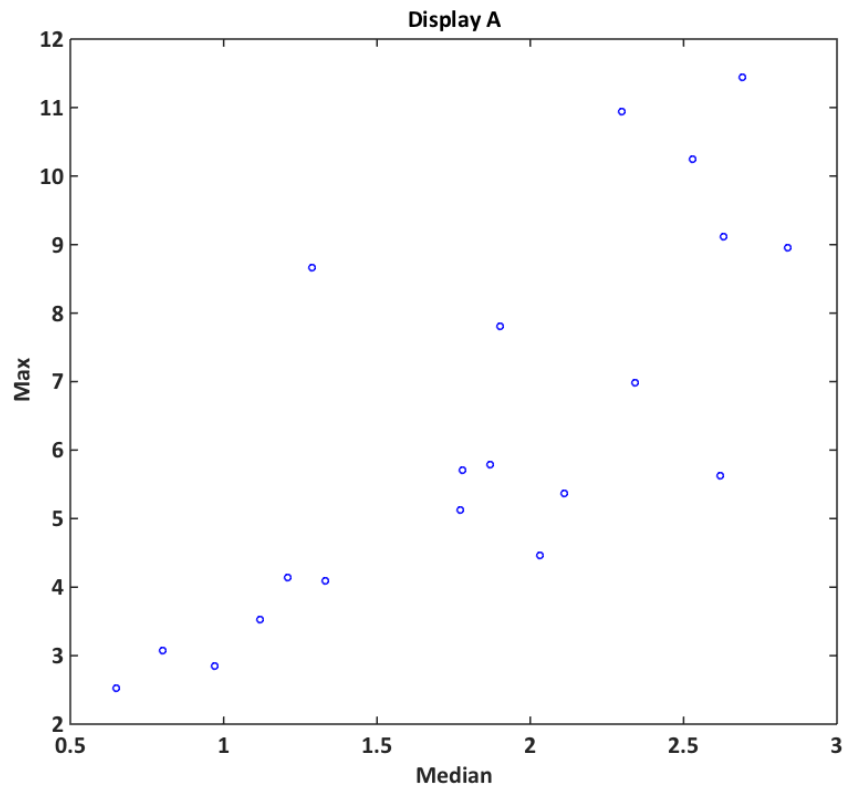


Fig. 5.18 Max ΔE_{ab}^* over the Median ΔE_{ab}^* .

tables together would strongly suggest that the optimal characterisation process is to use grey-ramp samples for the linearisation process and to use PLCC for the linearisation method. This is especially the case when one considers that most real-world images, for example, do not contain lots of highly saturated colours.

Fig. 5.19 and 5.20 show the characterisation performance of display A, obtained using the GOG and PLCC models with the grey-ramp and colour-ramps linearisation samples respectively. It is evident that the GOG model is performing better when the number of samples is low whereas the PLCC model gives lower colour differences when N is greater.

Fig. 5.21 - 5.24 show the characterisation performance (ΔE_{ab}^*) obtained using the GOG and PLCC models with the grey-ramp and colour-ramps linearisation samples with the maximum use of $N = 256$ and minimum use of $N = 6$, for all different sets of samples (Chart4, Macbeth and Matlab60) over the Lightness and Chroma of display A respectively.

Table 5.8 The Overall results of median ΔE_{ab}^* units for display A using the grey-ramp linearisation samples and three different set of samples (Chart4, Macbeth and Matlab60).

Display A						
Grey linearisation samples						
Number of samples	Chart4		Macbeth		Matlab60	
	GOG	PLCC	GOG	PLCC	GOG	PLCC
256	0.80	0.46	0.83	0.30	1.58	0.82
129	0.80	0.45	0.83	0.30	1.58	0.82
66	0.80	0.43	0.83	0.30	1.58	0.81
34	0.79	0.43	0.81	0.30	1.58	0.82
18	0.76	0.46	0.76	0.30	1.61	0.85
10	0.59	0.56	0.70	0.58	1.65	0.99
6	0.52	0.87	0.64	1.68	1.56	2.12

Table 5.9 The Overall results of median ΔE_{ab}^* units for display A using the Colour-ramp linearisation samples and three different set of samples (Chart4, Macbeth and Matlab60).

A						
Colour linearisation samples						
Number of samples	Chart4		Macbeth		Matlab60	
	GOG	PLCC	GOG	PLCC	GOG	PLCC
256	0.75	0.75	0.93	0.53	1.67	0.79
129	0.75	0.77	0.93	0.53	1.68	0.76
66	0.74	0.74	0.93	0.52	1.70	0.76
34	0.74	0.71	0.93	0.52	1.69	0.78
18	0.74	0.70	0.91	0.48	1.67	0.73
10	0.72	0.72	0.89	0.50	1.70	0.83
6	0.78	0.87	0.77	1.53	1.60	2.12

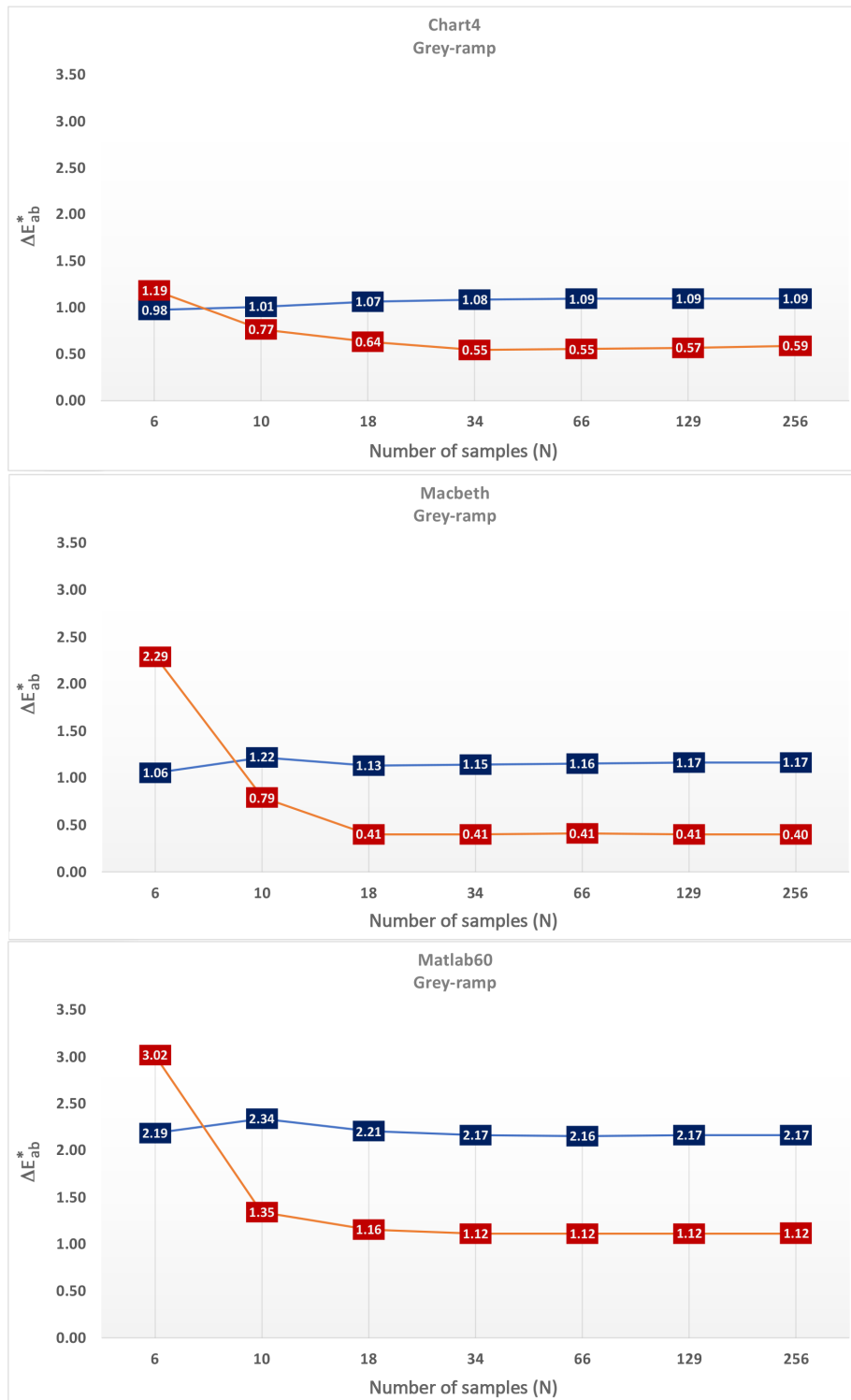


Fig. 5.19 Characterisation performances of the GOG and PLCC models using the grey-ramp linearisation samples for the three different set of samples (Chart4, Macbeth and Matlab60).

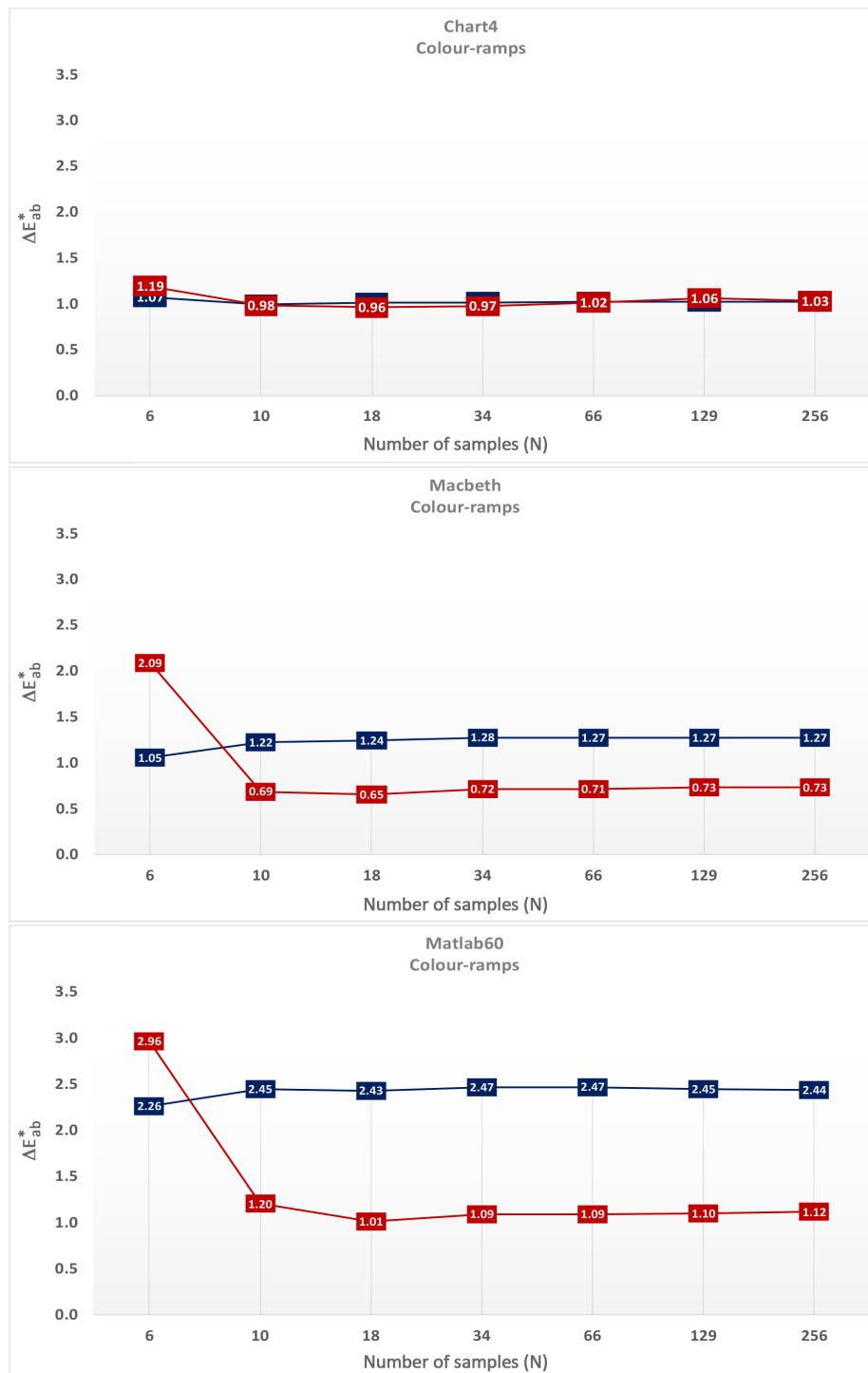


Fig. 5.20 Characterisation performances of the GOG and PLCC models using the colour-ramps linearisation samples for the three different set of samples (Chart4, Macbeth and Matlab60).

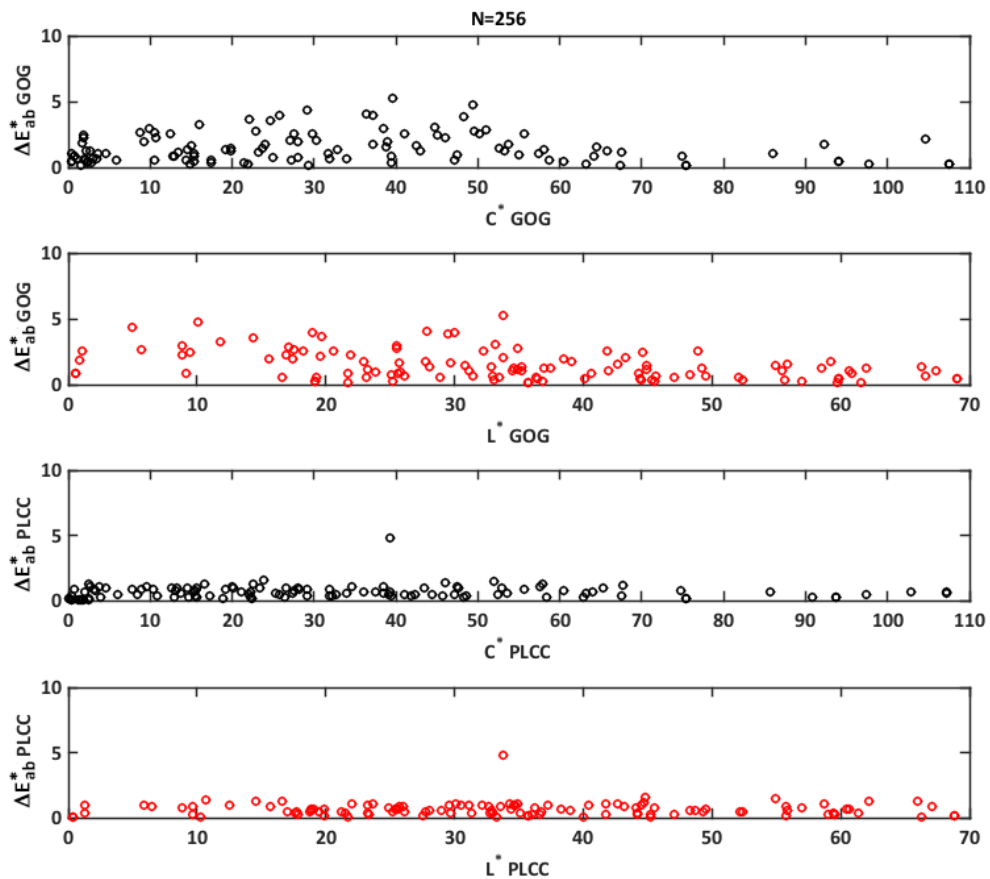


Fig. 5.21 Characterisation performances (ΔE_{ab}^*) of the GOG and PLCC models using the grey-ramp linearisation samples with 256 linearisation samples for all different set of samples (Chart 4, Macbeth and Matlab 60) over the Lightness and Chroma of display A.

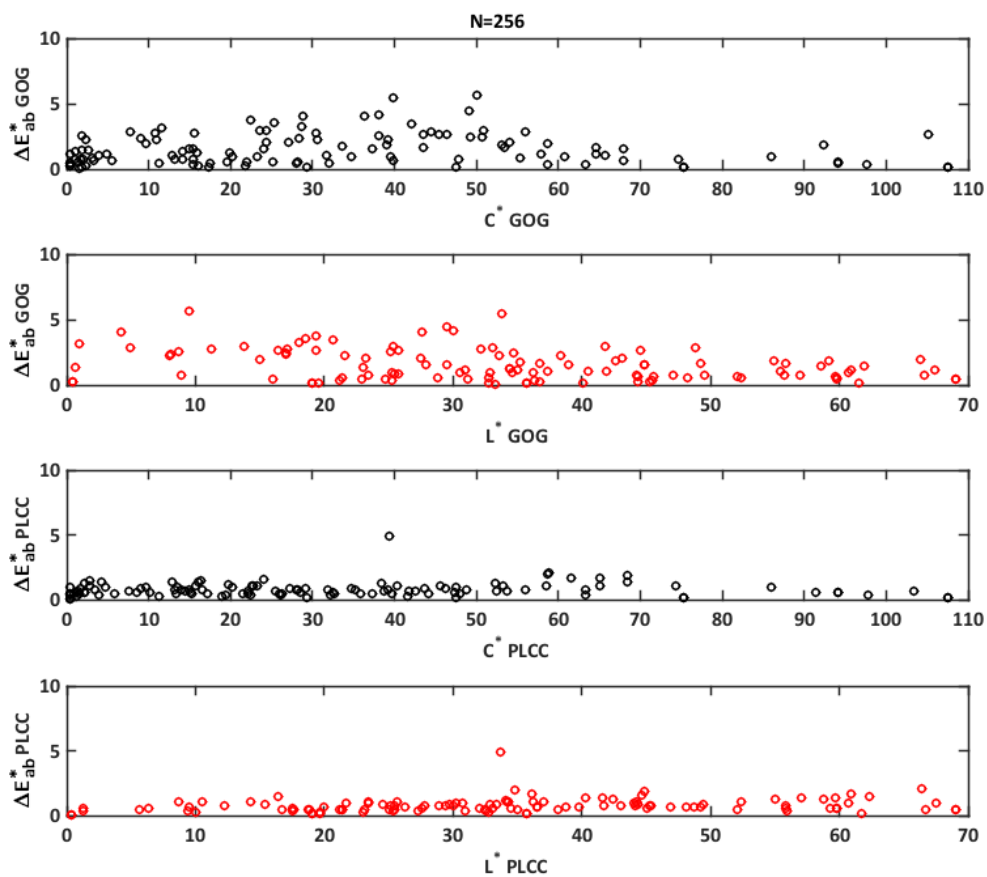


Fig. 5.22 Characterisation performances (ΔE_{ab}^*) of the GOG and PLCC models using the colour-ramps linearisation samples with 256 linearisation samples for all different set of samples (Chart4, Macbeth and Matlab60) over the Lightness and Chroma of display A.

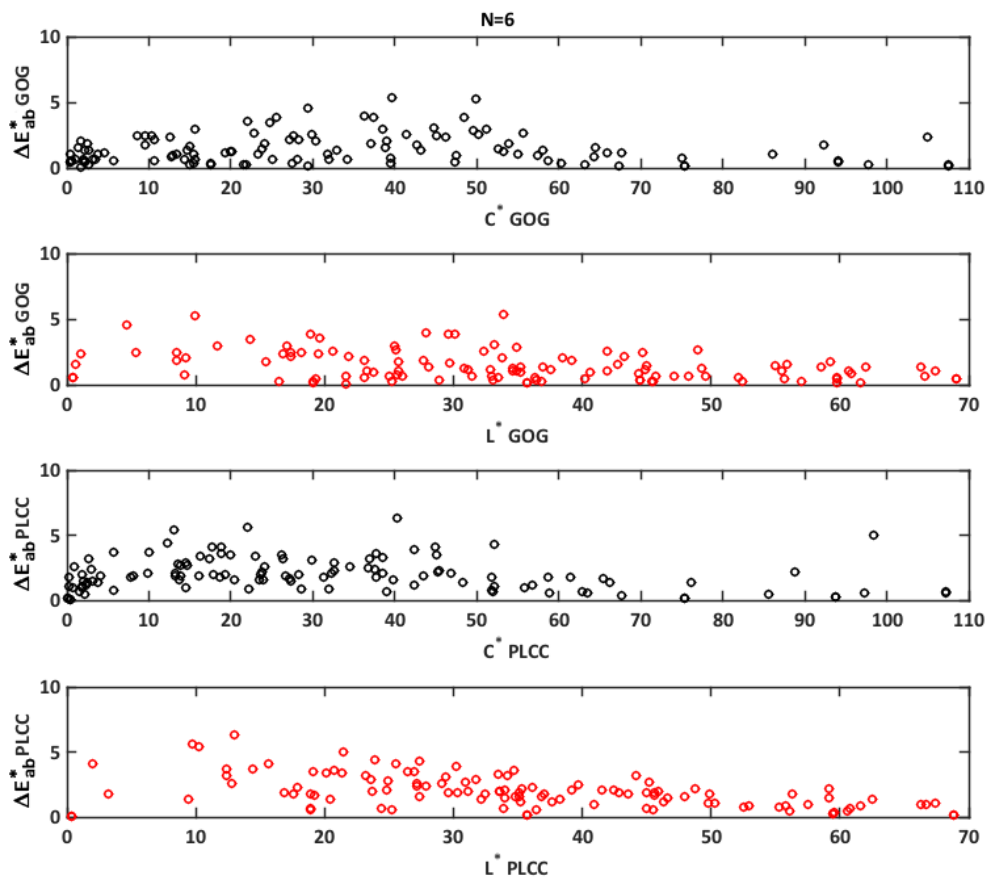


Fig. 5.23 Characterisation performances (ΔE_{ab}^*) of the GOG and PLCC models using the grey-ramps linearisation samples with 256 linearisation samples for all different set of samples (Chart4, Macbeth and Matlab60) over the Lightness and Chroma of display A.

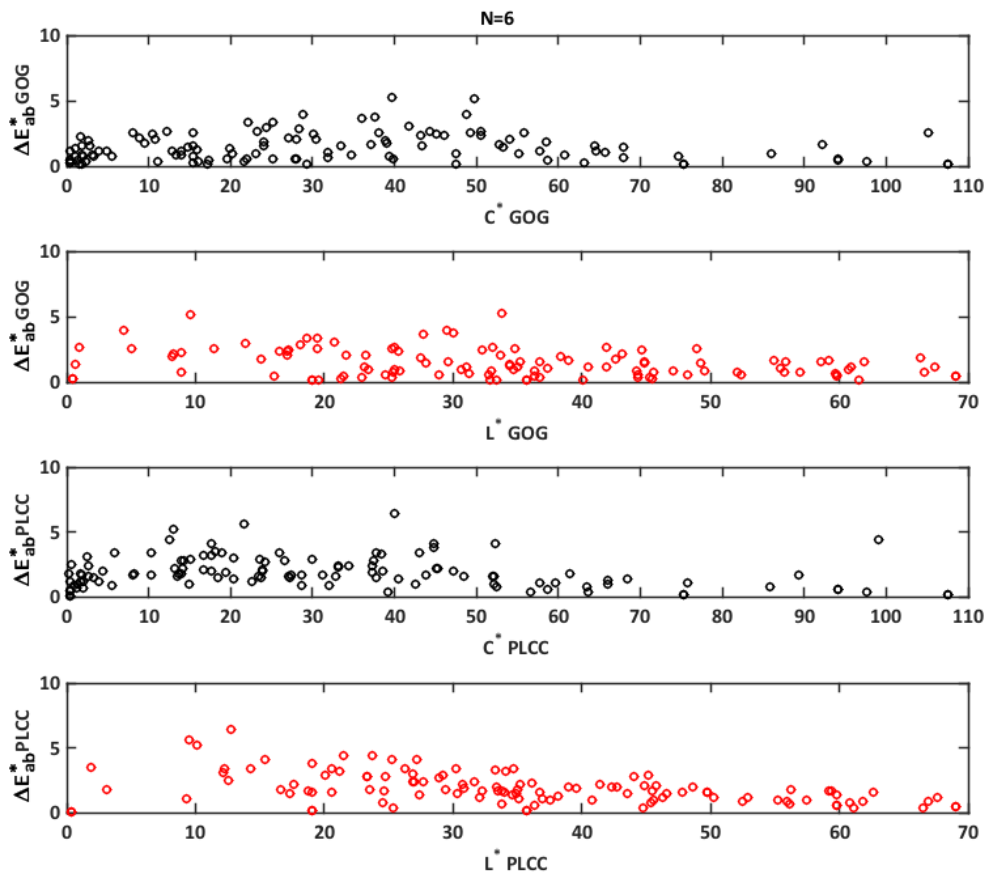


Fig. 5.24 Characterisation performances (ΔE_{ab}^*) of the GOG and PLCC models using the colour-ramps linearisation samples with 256 linearisation samples for all different set of samples (Chart4, Macbeth and Matlab60) over the Lightness and Chroma of display A.

5.12 Summary and Conclusion

This chapter has examined the characteristics and colour characterisation in some detail for a particular display (display A). Several different ways of performing the characterisation have been explored; specifically, whether to use the GOG model or the PLCC model for the linearisation part, and whether to use colour-ramps or grey-ramp samples for the linearisation data that is used by GOG or PLCC model. This produced four variants of the characterisation process. The grey-scale tracking and the colour tracking properties of the display were demonstrated and some deviation in chromaticity at low luminance levels was observed. The spatial and channel independence of display A was quantified using methods that are widely used in the literature. The channel independence was $0.80 \Delta E_{ab}^*$ units and the spatial independence was $0.15 \Delta E_{ab}^*$ units. The spatial independence is excellent. The colour gamut and the white point of the display have been evaluated.

The non-linearity of the response of the display (the TRC) was also shown. There was little evidence of an S-shaped TRC in the display. The data from both colour-ramps and grey-ramp linearisation samples are fitted quite well (at least on visual inspection) by both PLCC and GOG models. However, the degree of linearisation was also quantified by the coefficient of determination r^2 and these values were shown to be very close to 1. In other words, both PLCC and GOG models seem to do a good job of linearising the data whether colour-ramps or grey-ramp samples are used. However, the r^2 values for PLCC were generally higher than those for GOG in all but the $N = 6$ case.

Characterisation performance was assessed by calculating the ΔE_{ab}^* between the measurements that were made for a set of test samples displayed on the screen and the colorimetric values that were predicted by the models based on the input *RGB* values. Three different test sets were used: the Macbeth ColorChecker chart, Matlab60, and a specially designed chart known as Chart4. When predicting data for the Macbeth set of samples, the best performance was obtained using grey-ramp linearisation samples and the PLCC model. The differences between PLCC and GOG was surprisingly large (especially given the similarity in the r^2 values cited earlier that were used to quantify linearisation effectiveness); when predicting the Macbeth samples the median ΔE_{ab}^* was 0.40 for the PLCC model and 1.17 for the GOG model (in other words, it seems that very small differences in the apparent

goodness of fit of the linearisation process can result in quite large differences in characterisation performance). When predicting data for the Macbeth using the colour-ramps linearisation samples, the best performance was also for the PLCC. Hence, the PLCC model with the grey-ramp linearisation samples performed better in all sets of samples (apart from when $N = 6$). Taken together, the results of using these two test sets would strongly suggest that PLCC performs better than GOG and the grey-ramp samples should be used for the linearisation. The Macbeth ColorChecker sample set results, Matlab60 set results and the results from the Chart4 sample set confirm this finding; that PLCC is better than GOG and that grey-ramp samples should be used for the linearisation. Berns has previously suggested [13] that grey-ramp samples are better than coloured samples for the linearisation because this "applies load evenly across all channels"; however, an alternative explanation may be that the matrix transform on 'pure colour-ramps' measured XYZ data does not always produce zero for the two non-active channels and this causes error.

The GOG and PLCC methods that were presented in this chapter include the black-level correction. The black correction has been recommended by a number of authors [12, 66], especially for LCD displays. However, although all measurements were made in a very dark room there could still be internal flare [163]. Therefore, the black correction was always applied to the work in this thesis.

There are three main findings from this chapter. Firstly, characterisation results with the PLCC model are generally better than for the GOG model unless only very few linearisation samples are available. Secondly, grey-ramp samples work better than colour-ramp samples for the linearisation which agrees with the earlier suggestion by Berns [12, 66]. Thirdly, there was a better performance of using the GOG model rather than the PLCC when the number of test samples is very low. It is perhaps interesting that PLCC is generally better than GOG even though the TRC did not seem to exhibit an S-shaped curve; the difference between PLCC and GOG may be even greater for some other displays.

The results presented in this chapter, although interesting, have little significance other than in terms of the particular display that was tested. They have been presented in some detail to demonstrate the methods and techniques that will be used in the following chapters. How one particular display works and which characterisation methods work best is not of general interest. The significance of the

work in this thesis is that a similar analysis has been carried out for a population of displays and a meta-analysis of this is presented in Chapter 6. This will allow insights about the relative merits of the various methods that have been used to be developed and recommendations of wider interest to be made.

Chapter 6

Display Characterisation Meta-Analysis

6.1 Introduction

In this chapter 20 different displays are considered. Although the previous chapter enabled some insights into the relative merits of the GOG and PLCC models and of using either colour-ramps or grey-ramp in the linearisation process, it is only by comparing such results for a population of displays that meaningful conclusions and recommendations can be made. The purpose of this chapter, therefore, is to carry out a meta-analysis of characterisation performance on a population of 20 different displays. The effect of using the different number of linearisation samples will be shown for all 20 displays.

6.2 Colour measurements

The tele-spectroradiometer (TSR) Konica Minolta CS-2000 was used to measure stimuli displayed on displays in a dark room. The devices were warmed up for at least one hour before any measurements took place. The 2° CIE observer was used to measure *CIEXYZ* values for various stimuli defined by test sample sets such as Macbeth, Matlab60 and Chart4 (these were described in Chapter 4) which were displayed on each device and generated by a computer-controlled graphic

card equipped with Digital Visual Interface (DVI) output. All the data measured by the Konica Minolta CS-2000 are in Yxy colour space as well as the absolute XYZ measurements where the unit of the Y tristimulus value are candelas per meter squared (cd/m^2).

6.3 White-point evaluation

The chromaticities of the white-point for each device are shown in Table 6.1. Each display is identified simply by a letter, A-T (all of the displays used were LCD or LCD/backlight). Although each display was nominally set for $D65$ there were some substantial departures. In order to categorise the performance of each display in this regard, the mean difference in CIE x and y space of the white-point from $D65$ was calculated. Displays, where this distance was more than $15 \Delta E_{ab}^*$ units are considered poor, displays, where this distance is less than $3 \Delta E_{ab}^*$ units are considered excellent and displays where this distance is between 5 and $15 \Delta E_{ab}^*$ units are considered average. This boundary is somewhat arbitrary of course but does allow the classification as shown in Table 6.1. Fig. 6.1 shows an example of an excellent, average, and poor white-points of the display.

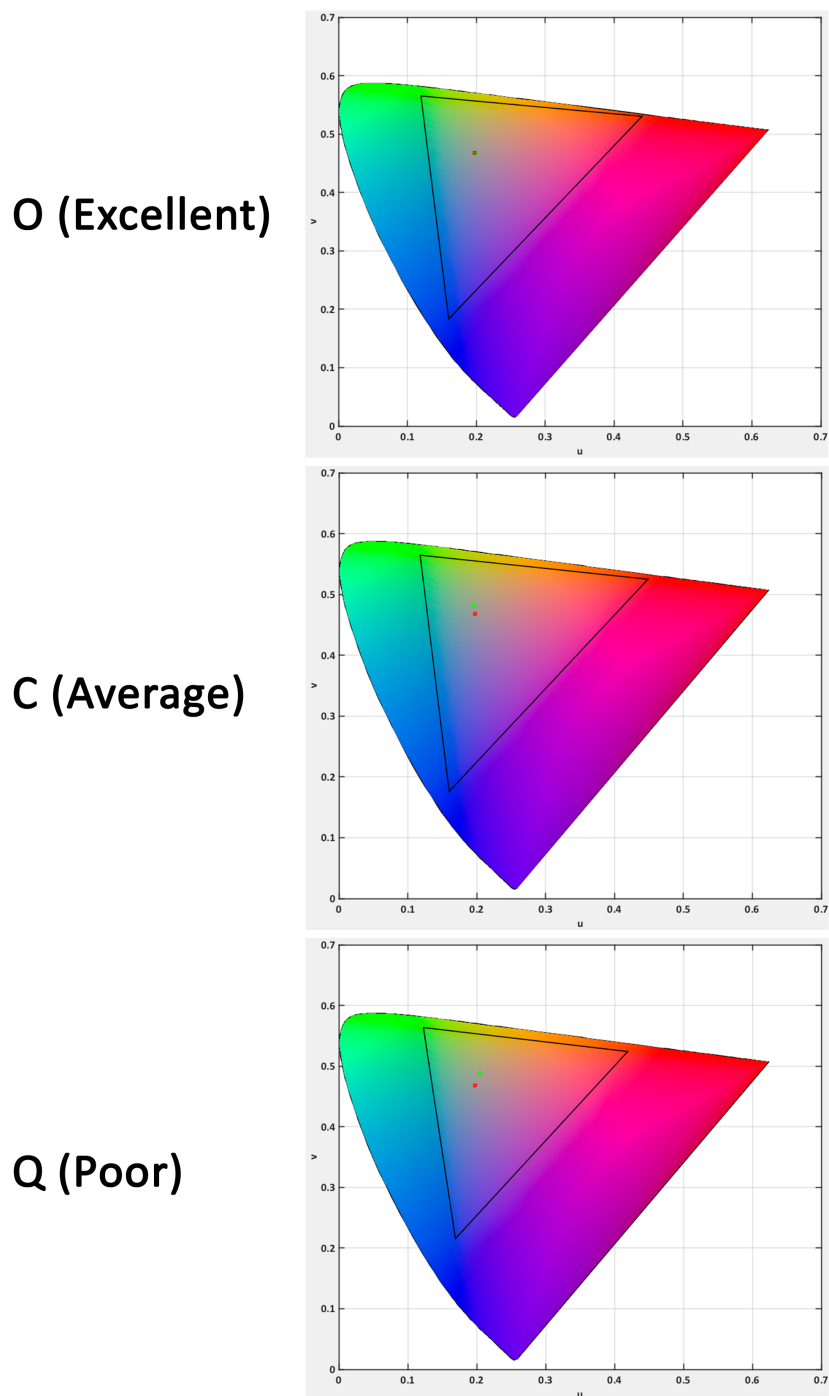


Fig. 6.1 White-point Evaluation of three displays plotted in $CIEu'v'$ diagram. In each case, D65 is shown (red symbols) along with the white point of the display (green symbols). Display O is categorised as an excellent, C is Average and Q is poor in terms of D65 representation.

Table 6.1 Whitepoint evaluation of display devices.

Display	Chromaticity of whitepoint		x,y Differences	ΔE_{ab}^*	Evaluation
	x	y			
	A	0.3098	0.2874	0.2874	27.74
B	0.3133	0.3196	0.3196	6.32	Average
C	0.3227	0.3537	0.3537	13.17	Average
D	0.3249	0.3404	0.3404	6.72	Average
E	0.3404	0.3582	0.3582	16.47	Poor
F	0.3278	0.3511	0.3511	11.67	Average
G	0.3234	0.3249	0.3249	7.77	Average
H	0.3199	0.3274	0.3274	4.66	Excellent
I	0.3416	0.3536	0.3536	15.25	Poor
J	0.3048	0.2982	0.2982	18.50	Poor
K	0.2953	0.3265	0.3265	9.23	Average
L	0.3188	0.3297	0.3297	3.22	Excellent
M	0.3224	0.3308	0.3308	4.88	Excellent
N	0.3201	0.3308	0.3308	3.63	Excellent
O	0.3118	0.3262	0.3262	1.57	Excellent
P	0.3263	0.3375	0.3375	6.50	Average
Q	0.3400	0.3611	0.3611	17.53	Poor
R	0.3419	0.3590	0.3590	17.08	Poor
S	0.3427	0.3469	0.3469	14.25	Average
T	0.3126	0.3343	0.3343	3.40	Excellent

6.4 Channel and Spatial Independence

Table 6.2 shows the channel independence of each display devices. Colour differences are shown between the white ($R=G=B=255$) and the additive sum of the three primaries (R, G and B). All stimuli were measured using the full screen as discussed earlier. The white point for the *CIELAB* calculations was the white stimulus itself of course. If the display has excellent channel independence then the colour difference between the white and the sum RGB stimuli should be close to zero. Table 6.2 also shows colour differences between the display white as full screen (referred to as White vs White) and as a patch on a black background (referred to as White vs Black). Fig 6.2 shows the patches measuring for testing the spatial independence of each display. The dimensions of the patch were described earlier. If the display has excellent spatial independence then these colour differences should be close to zero. Table 6.2 shows that display *U* exhibits poor channel independence. Display *L* shows the best spatial independence among all 20 displays.



Fig. 6.2 Measuring the white over two different backgrounds to evaluate the Spatial Independence.

The other test that has been done to evaluate the spatial dependence of each display is to measure grey patches with R, G and B backgrounds as illustrated in Fig 6.3.

Table 6.3 shows the results for the spatial independence test for all 20 displays. The table shows that the best performance among all 20 displays is for display *R*. However, the poor spatial independence is belonged to display *S*.



Fig. 6.3 Measuring the grey over three different backgrounds to evaluate the Spatial dependence.

Table 6.2 Channel and Spatial Independence in all display devices (the spatial independence was measured as the colour difference between a white patch with a white and black background; channel independence - or additivity - is the colour difference between the white and the additive sum of the three primaries).

Display	Channel independence		Spatial independence	
	ΔE_{ab}^*	ΔE_{00}^*	ΔE_{ab}^*	ΔE_{00}^*
A	0.80	0.79	0.15	0.13
B	0.59	0.47	0.19	0.12
C	0.17	0.11	0.12	0.07
D	0.15	0.11	0.15	0.11
E	0.14	0.09	0.10	0.06
F	0.14	0.09	0.08	0.05
G	0.82	0.58	0.17	0.12
H	0.70	0.52	0.17	0.11
I	0.65	0.38	0.17	0.10
J	0.34	0.19	0.13	0.08
K	0.78	0.57	0.27	0.25
L	0.10	0.07	0.13	0.08
M	0.48	0.49	0.22	0.15
N	1.27	0.81	0.08	0.06
O	0.46	0.43	0.11	0.07
P	0.34	0.31	0.08	0.05
Q	1.88	1.07	0.12	0.09
R	2.54	1.44	0.11	0.07
S	0.24	0.21	0.14	0.09
T	2.89	1.69	0.20	0.13

Table 6.3 Spatial dependency in all display devices (in this table the colour differences are between grey patches measured with a red, green or blue background).

Display	Spatial independence					
	ΔE_{ab}^*			ΔE_{00}^*		
	R vs G	R vs B	G vs B	R vs G	R vs B	G vs B
A	1.04	0.68	1.21	1.32	0.66	1.36
B	1.19	0.82	1.33	1.43	0.67	1.31
C	1.04	0.59	0.89	1.30	0.66	0.97
D	0.77	0.53	0.86	0.85	0.38	0.84
E	0.82	0.52	0.63	0.80	0.44	0.48
F	0.69	0.41	0.62	0.93	0.46	0.65
G	1.18	0.94	1.17	1.54	1.03	1.15
H	0.78	0.67	0.91	0.94	0.45	0.97
I	1.18	0.75	1.17	1.31	0.72	1.17
J	1.11	0.73	1.25	1.08	0.59	0.77
K	0.70	0.42	0.83	0.65	0.30	0.75
L	1.14	0.85	1.43	1.36	0.66	1.46
M	1.47	0.91	1.17	1.86	1.08	1.18
N	0.45	0.51	0.59	0.51	0.40	0.66
O	0.51	0.40	0.45	0.60	0.40	0.44
P	0.61	0.44	0.44	0.68	0.43	0.43
Q	0.45	0.35	0.42	0.42	0.29	0.32
R	0.24	0.20	0.21	0.22	0.17	0.17
S	1.85	1.17	1.68	2.14	1.24	1.40
T	1.17	0.82	1.27	1.07	0.65	1.13

6.5 Colour Gamut

Fig. 6.4 illustrates the colour gamut of each device in a uniform $u'v'$ -diagram. The triangular boundary of the colour gamut is determined by chromaticity converted to $u'v'$ of each primary colour for each display. The standard *RGB* colour space and the *D65* white-point is also illustrated in each diagram. It is evident that in displays *E*, *Q* and *R* the size of the display's colour gamut is smaller than the *sRGB* gamut. There is no evidence of having wide gamut in these displays.

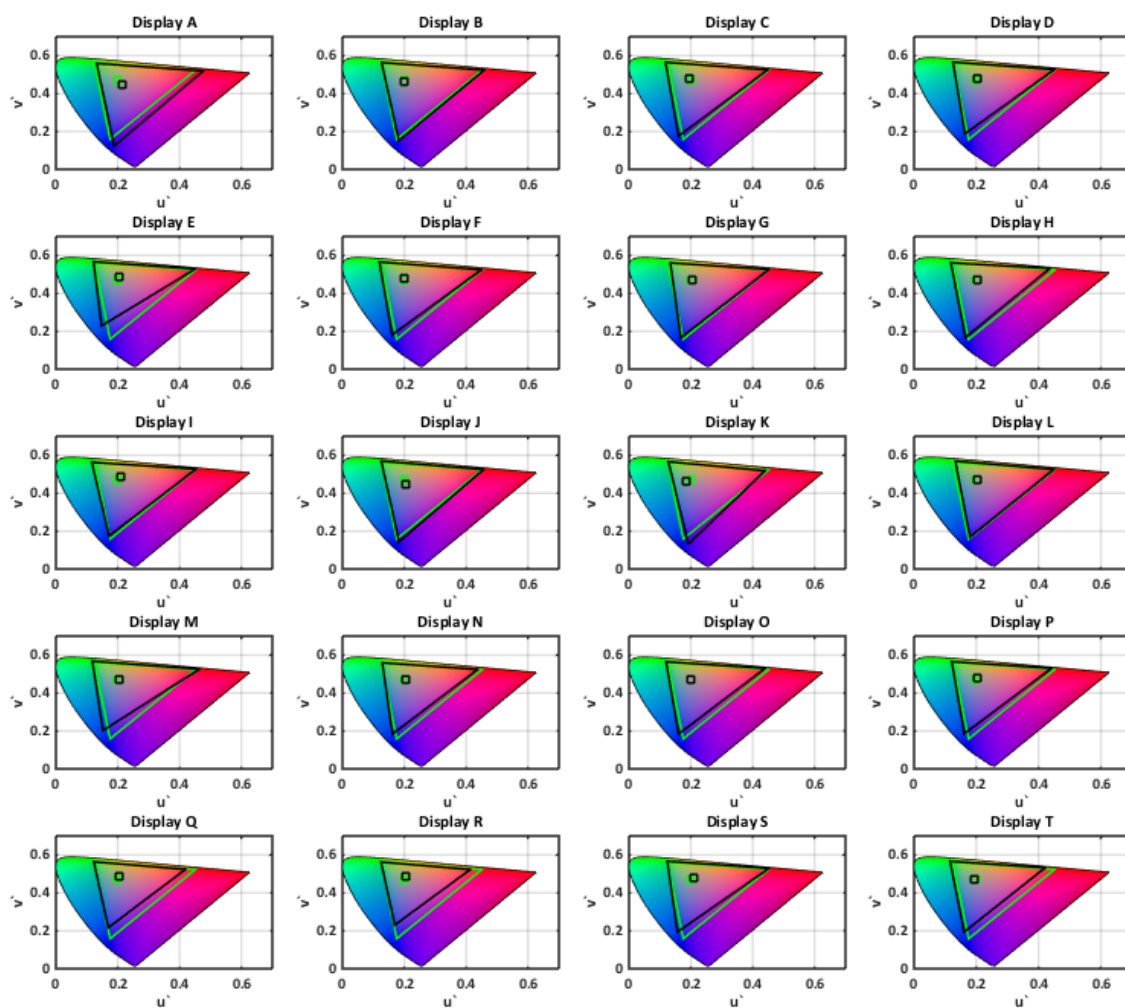


Fig. 6.4 *sRGB* colour gamut (green line triangle) and all display gamuts (black line triangle) in CIE 1976 $u'v'$ chromaticity diagram. *D65* (green square) and each display white-point (black square) is illustrated.

6.6 Contrast ratio

The contrast ratio of each display is calculated in Equation 6.1:

$$C = \frac{L_0 - L_b}{L_b} \quad (6.1)$$

where L_0 and L_b are the CIE luminance (Y value) for white and black.

Note that all patches are measured in dark ambient illumination. Table 6.4 shows that the best contrast ratio is for display C as it is closer to 1 (where $C=1$ is perfect performance). In many cases, the contrast ratio is greater than 0.99.

Table 6.4 Contrast ratio of 20 displays.

Display	Contrast ratio
A	0.9989
B	0.9985
C	0.9991
D	0.9989
E	0.9988
F	0.9990
G	0.9974
H	0.9983
I	0.9989
J	0.9990
K	0.9978
L	0.9990
M	0.9980
N	0.9953
O	0.9982
P	0.9981
Q	0.9752
R	0.9672
S	0.9983
T	0.9979

6.7 Linearisation

Two methods, referred to as GOG and PLCC, have been used to perform a linearisation of RGB values using either colour-ramps or grey-ramp of 256 linearisation

samples. The performance can be assessed using r^2 values between linear and predicted linear values (where $r^2=1$ is perfect performance). Table 6.5 shows the average r^2 values for each of the four conditions in all devices. In many cases, r^2 is greater than 0.999 using the colour-ramps linearisation samples as well as the PLCC model. The linearisation is least effective for the four display devices C, E, F and S.

Table 6.5 The average r^2 values for all displays using all ($N = 256$) samples.

Display	r^2 ($N = 256$)			
	Grey_ramp		Colour_ramp	
	GOG	PLCC	GOG	PLCC
A	0.9996	0.9998	0.9997	1.0000
B	0.9998	1.0000	1.0000	1.0000
C	0.9887	0.9995	0.9916	1.0000
D	0.9932	0.9995	0.9947	0.9999
E	0.9864	0.9983	0.9915	0.9999
F	0.9876	0.9993	0.9893	1.0000
G	0.9993	0.9996	1.0000	1.0000
H	0.9970	0.9993	0.9996	1.0000
I	0.9992	0.9999	0.9999	1.0000
J	0.9993	0.9996	0.9999	1.0000
K	0.9995	0.9997	0.9998	1.0000
L	0.9990	0.9998	1.0000	1.0000
M	0.9998	0.9998	0.9997	1.0000
N	0.9973	0.9997	0.9991	1.0000
O	0.9987	1.0000	0.9986	1.0000
P	0.9950	1.0000	0.9950	1.0000
Q	0.9992	0.9999	0.9994	1.0000
R	0.9946	0.9998	0.9953	1.0000
S	0.9891	0.9949	0.9971	1.0000
T	0.9959	0.9989	0.9993	1.0000

6.8 Characterisation Performance

The characterisation performance of all 20 displays are assessed for each three sample sets using two different linearisation sets of samples that have been previously described. Tables 6.6 to 6.12 show the median colour differences based on ΔE_{ab}^* units for each of the three test sets of samples in all 20 number of displays using various numbers of samples for the linearisation. For the sets using all the linearisation samples ($N = 256$) and using the Macbeth set of samples (Table 6.6)

the PLCC model consistently performs better than GOG model and the grey-ramp linearisation samples perform better than the colour-ramps. For the other two sets of samples, the PLCC again consistently performs better than GOG and there is little to choose between grey-ramp linearisation samples and colour-ramps linearisation samples (although the latter are, of course, marginally better). The advantage of the PLCC method is evident for the Macbeth, Matlab60 and the Chart4 test samples (Table 6.6). In all the test samples there is clear evidence that using the grey-ramp linearisation samples is preferable to using the colour-ramps linearisation samples. Performance of the display *K* is *excellent* as the ΔE_{ab}^* is less than 1, and *B, Q, A, M, L, I, N, O, G, J* devices is *good* as the ΔE_{ab}^* is between 1 and 2 by using the all sample sets as well as PLCC and GOG considering the grey-ramp and colour-ramp linearisation samples, however, with the same condition the performance of the *E* display is *not acceptable* ($\Delta E_{ab}^* > 4$). It is evident from Fig. 6.12 that the characterisation performance of the *C, D, E, F, P, S* are not acceptable ($\Delta E_{ab}^* > 4$) especially by using the GOG model while using the PLCC and the grey-ramp linearisation sample, reduced this error down to the *good* range ($\Delta E_{ab}^* < 2$).

Fig. 6.5- 6.9 illustrates the TRC (Tone Reproduction Curve) of all the displays. It is clear that the response curve could be a gamma-shaped curve (defined by an offset and a gain) for displays *A, G, I, J, K, L, M, N, O, S* and *T* or a S-shaped curve for displays *B, C, D, E, F, H, P, Q* and *R*.

It is evident that the PLCC is always better than the GOG using the grey-ramp linearisation samples, no matter which type of samples sets were used in all display devices (Fig. 6.10- 6.11). However, by having the colour-ramps linearisation samples and using Chart4 samples, with display *A, B, E* and *G*, the GOG is better to perform than the PLCC. In the rest of sets of samples (Macbeth and Matlab60) the PLCC is always better in all display devices. Fig. 6.12 shows that the best characterisation performance considering both linearisation samples (grey-ramp and colour-ramps) and both models (GOG and PLCC) for all display devices and using all linearisation samples ($N = 256$) is for using the PLCC with grey-ramp linearisation samples.

It is interesting to try to relate the colour characterisation performances to the other characteristics that have been measured. Is there evidence that some characteristics are more important than others? The *K* display device has the best characterisation performance either by using the grey or colour-ramp linearisation samples as well as using the GOG or PLCC model in all sets of samples, but it

Table 6.6 Median ΔE_{ab}^* values for 20 displays using the grey-ramp and colour-ramps linearisation samples and three different test sets for all linearisation samples ($N = 256$).

N=256												
Display	Grey_ramp						Colour_ramp					
	Chart4		Macbeth		Matlab60		Chart4		Macbeth		Matlab60	
	GOG	PLCC	GOG	PLCC	GOG	PLCC	GOG	PLCC	GOG	PLCC	GOG	PLCC
A	1.09	0.59	1.17	0.40	2.17	1.12	1.03	1.03	1.27	0.73	2.44	1.12
B	0.87	1.05	1.00	0.79	1.83	1.28	0.98	1.09	0.90	1.00	1.14	1.07
C	2.32	0.77	5.42	0.86	9.04	1.69	2.01	0.97	6.11	2.61	8.62	2.95
D	4.19	1.17	4.64	0.97	8.21	1.27	2.85	1.73	4.75	2.57	9.19	2.73
E	3.33	1.73	5.83	1.16	8.17	1.94	2.74	3.11	5.45	3.61	8.24	3.23
F	3.74	0.76	4.23	0.91	8.61	1.51	3.60	1.75	5.00	3.78	9.36	4.14
G	2.20	0.73	1.53	0.74	2.08	1.13	1.67	1.79	1.67	1.55	2.16	2.17
H	2.27	1.15	2.42	0.71	4.03	1.00	1.80	1.62	2.48	2.06	3.05	2.03
I	1.52	0.76	1.34	0.47	2.45	0.95	0.96	0.91	1.46	1.54	2.43	1.95
J	2.30	1.48	1.62	0.71	2.13	1.10	2.34	2.12	2.38	2.23	2.62	2.69
K	0.98	0.66	0.96	0.57	1.21	0.77	0.98	0.91	0.93	0.88	1.12	1.04
L	2.04	1.63	1.84	0.86	2.56	0.86	1.19	1.16	0.90	0.83	1.09	0.97
M	1.34	0.71	1.31	0.64	1.39	0.81	2.16	0.88	1.62	1.16	1.73	1.10
N	1.59	1.21	2.84	0.58	3.03	0.64	1.66	1.01	1.60	0.87	1.99	1.08
O	2.15	0.27	2.32	0.25	3.06	0.81	2.20	0.34	2.38	0.30	3.37	0.97
P	2.36	0.46	3.61	0.44	6.58	0.72	2.40	0.45	3.63	0.47	6.54	0.72
Q	1.49	0.89	1.12	0.47	1.25	0.81	1.34	0.94	1.28	1.13	1.74	1.38
R	2.82	0.70	2.51	0.33	3.01	0.75	2.82	1.15	2.47	2.22	3.48	2.42
S	2.99	2.61	4.40	1.71	5.40	2.16	5.88	3.75	5.16	4.27	5.20	3.85
T	3.07	2.61	2.98	1.07	3.33	1.21	3.86	3.20	4.16	3.48	4.33	3.28

Table 6.7 Median ΔE_{ab}^* values for 20 displays using the grey-ramp and colour-ramps linearisation samples and three different test sets for 129 linearisation samples ($N = 129$).

N=129												
Display	Grey_ramp						Colour_ramp					
	Chart4		Macbeth		Matlab60		Chart4		Macbeth		Matlab60	
	GOG	PLCC	GOG	PLCC	GOG	PLCC	GOG	PLCC	GOG	PLCC	GOG	PLCC
A	1.09	0.57	1.17	0.41	2.17	1.12	1.02	1.06	1.27	0.73	2.45	1.10
B	0.87	1.05	1.00	0.77	1.83	1.24	0.98	1.10	0.89	0.98	1.14	1.08
C	2.30	0.76	5.41	0.84	9.03	1.66	2.00	0.99	6.11	2.62	8.60	2.96
D	4.19	1.21	4.70	0.97	8.34	1.29	2.88	1.78	4.77	2.52	9.10	2.75
E	3.33	1.74	6.09	1.15	8.27	1.94	2.74	3.12	5.45	3.60	8.25	3.23
F	3.74	0.76	4.24	0.92	8.59	1.55	3.60	1.75	5.01	3.78	9.39	4.21
G	2.16	0.72	1.53	0.74	2.06	1.13	1.66	1.90	1.68	1.55	2.14	2.14
H	2.27	1.14	2.44	0.69	4.02	1.03	1.80	1.61	2.48	2.06	3.06	2.00
I	1.52	0.69	1.35	0.47	2.46	0.91	0.96	0.92	1.45	1.54	2.41	1.96
J	2.30	1.48	1.62	0.80	2.14	1.09	2.35	2.25	2.39	2.33	2.63	2.74
K	0.98	0.74	0.93	0.49	1.14	0.77	0.98	0.94	0.94	0.93	1.11	1.01
L	2.04	1.60	1.84	0.88	2.55	0.89	1.18	1.15	0.91	0.85	1.09	1.00
M	1.33	0.75	1.28	0.62	1.40	0.79	2.14	0.94	1.62	1.22	1.74	1.07
N	1.61	1.22	2.85	0.59	3.02	0.73	1.66	1.01	1.61	0.88	2.00	1.08
O	2.14	0.34	2.32	0.28	3.05	0.81	2.19	0.40	2.38	0.39	3.36	0.91
P	2.33	0.47	3.58	0.45	6.55	0.73	2.30	0.45	3.53	0.47	6.51	0.71
Q	1.49	0.86	1.13	0.52	1.26	0.86	1.33	1.00	1.27	1.12	1.73	1.44
R	2.81	0.75	2.48	0.50	3.00	0.76	2.82	1.13	2.48	2.15	3.55	2.45
S	2.98	2.66	4.41	1.71	5.41	2.04	5.88	3.75	5.13	4.28	5.19	3.79
T	3.06	2.61	2.98	1.08	3.33	1.17	3.86	3.24	4.16	3.48	4.34	3.26

Table 6.8 Median ΔE_{ab}^* values for 20 displays using the grey-ramp and colour-ramps linearisation samples and three different test sets for 66 linearisation samples ($N = 66$).

N=66													
Display	Grey_ramp						Colour_ramp						
	Chart4		Macbeth		Matlab60		Chart4		Macbeth		Matlab60		
	GOG	PLCC	GOG	PLCC	GOG	PLCC	GOG	PLCC	GOG	PLCC	GOG	PLCC	
A	1.09	0.55	1.16	0.41	2.16	1.12	1.02	1.02	1.27	0.71	2.47	1.09	
B	0.87	1.05	1.01	0.75	1.83	1.22	0.98	1.10	0.88	0.92	1.14	1.08	
C	2.27	0.77	5.39	0.83	9.11	1.72	2.01	1.03	6.13	2.58	8.63	3.01	
D	4.19	1.23	4.73	0.97	8.46	1.27	2.85	1.85	4.76	2.54	9.25	2.79	
E	3.33	1.70	6.16	1.16	8.19	1.91	2.74	3.11	5.45	3.60	8.26	3.23	
F	3.75	0.77	4.17	0.88	8.64	1.55	3.60	1.75	5.00	3.78	9.44	4.24	
G	2.15	0.71	1.52	0.69	2.07	1.07	1.66	1.86	1.67	1.61	2.13	2.12	
H	2.27	1.14	2.27	0.72	4.02	1.00	1.80	1.58	2.49	2.11	3.06	2.01	
I	1.52	0.74	1.34	0.49	2.46	0.90	0.96	0.92	1.44	1.54	2.42	1.95	
J	2.31	1.45	1.58	0.82	2.11	1.08	2.33	2.25	2.39	2.27	2.58	2.66	
K	0.98	0.67	0.89	0.52	1.13	0.80	0.98	0.93	0.95	0.87	1.10	0.98	
L	2.05	1.60	1.84	0.85	2.53	0.94	1.19	1.12	0.93	0.90	1.13	0.98	
M	1.33	0.71	1.27	0.62	1.41	0.78	2.13	0.91	1.63	1.21	1.74	1.09	
N	1.59	1.24	2.84	0.59	3.05	0.74	1.67	1.08	1.62	0.87	1.99	1.08	
O	2.14	0.43	2.33	0.44	2.99	0.87	2.13	0.41	2.38	0.44	3.23	0.94	
P	2.38	0.45	3.60	0.45	6.61	0.70	2.27	0.45	3.70	0.47	6.58	0.71	
Q	1.46	0.84	1.11	0.57	1.26	0.85	1.30	1.05	1.27	0.89	1.71	1.41	
R	2.83	0.76	2.57	0.53	3.02	0.78	2.87	1.08	2.45	2.09	3.26	2.39	
S	2.97	2.92	4.35	1.68	5.42	2.03	5.90	3.74	5.07	4.28	5.22	3.77	
T	3.08	2.57	2.96	1.09	3.32	1.19	3.86	3.21	4.17	3.53	4.34	3.24	

Table 6.9 Median ΔE_{ab}^* values for 20 displays using the grey-ramp and colour-ramps linearisation samples and three different test sets for 34 linearisation samples ($N = 34$).

N=34													
Display	Grey_ramp						Colour_ramp						
	Chart4		Macbeth		Matlab60		Chart4		Macbeth		Matlab60		
	GOG	PLCC	GOG	PLCC	GOG	PLCC	GOG	PLCC	GOG	PLCC	GOG	PLCC	
A	1.08	0.55	1.15	0.41	2.17	1.12	1.02	0.97	1.28	0.72	2.47	1.09	
B	0.88	1.03	1.01	0.74	1.84	1.21	0.98	1.07	0.88	0.95	1.14	1.06	
C	2.28	0.82	5.40	0.83	9.10	1.71	2.00	1.00	6.15	2.61	8.65	2.95	
D	4.19	1.21	4.68	0.95	8.18	1.28	3.16	1.99	4.80	2.52	9.05	2.74	
E	3.33	1.67	5.76	1.20	8.21	1.89	2.74	3.07	5.45	3.61	8.29	3.23	
F	3.74	0.79	4.07	0.88	8.72	1.55	3.60	1.78	5.02	3.80	9.29	4.24	
G	2.13	0.68	1.50	0.67	2.04	1.06	1.66	1.66	1.67	1.58	2.11	2.09	
H	2.27	1.14	2.12	0.69	4.14	1.02	1.81	1.58	2.50	2.09	3.07	2.02	
I	1.53	0.76	1.34	0.55	2.45	0.94	0.97	0.95	1.43	1.53	2.38	1.93	
J	2.30	1.44	1.62	0.81	2.09	1.12	2.34	2.27	2.36	2.24	2.61	2.66	
K	0.98	0.72	0.90	0.53	1.14	0.76	0.98	0.95	0.93	0.93	1.08	0.99	
L	2.03	1.61	1.84	0.85	2.50	0.90	1.25	1.11	0.92	0.84	1.13	0.98	
M	1.31	0.80	1.25	0.62	1.41	0.76	2.11	0.99	1.65	1.17	1.75	1.10	
N	1.57	1.24	2.85	0.59	3.10	0.73	1.66	1.15	1.61	0.85	2.01	1.11	
O	2.15	0.35	2.33	0.42	2.96	0.84	2.11	0.49	2.39	0.36	3.20	0.94	
P	2.59	0.45	4.12	0.46	6.11	0.73	2.44	0.45	4.16	0.45	6.14	0.70	
Q	1.37	0.70	1.09	0.59	1.26	0.81	1.30	0.97	1.30	0.87	1.75	1.44	
R	2.86	0.76	2.45	0.56	2.96	0.82	2.84	1.03	2.42	1.94	3.77	2.37	
S	2.90	3.28	4.12	1.81	5.48	2.01	5.80	3.74	4.93	4.28	5.22	3.76	
T	3.10	2.56	2.96	1.09	3.32	1.20	3.86	3.22	4.18	3.55	4.36	3.19	

Table 6.10 Median ΔE_{ab}^* values for 20 displays using the grey and colour-ramp linearisation samples and five different test sets for 18 linearisation samples ($N = 18$).

N=18												
Display	Grey_ramp						Colour_ramp					
	Chart4		Macbeth		Matlab60		Chart4		Macbeth		Matlab60	
	GOG	PLCC	GOG	PLCC	GOG	PLCC	GOG	PLCC	GOG	PLCC	GOG	PLCC
A	1.07	0.64	1.13	0.41	2.21	1.16	1.01	0.96	1.24	0.65	2.43	1.01
B	0.87	0.96	0.97	0.73	1.80	1.25	0.98	1.02	0.88	0.80	1.13	1.04
C	2.28	0.87	5.45	0.87	9.11	1.71	1.99	1.23	6.19	2.59	8.70	2.88
D	4.19	1.22	4.92	0.80	7.57	1.25	3.28	1.86	4.94	2.56	9.06	2.76
E	3.33	1.23	5.80	1.16	8.27	1.92	2.74	3.04	5.49	3.47	8.33	3.27
F	3.69	0.85	4.08	0.83	8.48	1.58	3.60	1.85	5.08	3.75	8.86	4.17
G	2.07	0.68	1.46	0.65	2.00	1.01	1.65	1.71	1.66	1.60	2.10	2.06
H	2.26	1.10	2.01	0.79	4.20	0.99	1.84	1.56	2.49	2.07	3.08	1.92
I	1.55	0.76	1.39	0.40	2.51	0.92	0.98	1.03	1.45	1.61	2.36	1.74
J	2.30	1.39	1.61	0.72	2.05	1.05	2.38	2.25	2.37	2.27	2.59	2.63
K	0.98	0.74	0.91	0.54	1.13	0.73	0.98	0.88	0.94	0.78	1.06	0.94
L	2.02	1.61	1.84	0.74	2.42	0.89	1.26	1.04	0.87	0.81	1.12	0.97
M	1.27	0.78	1.21	0.61	1.42	0.75	2.04	1.01	1.69	1.08	1.76	1.03
N	1.60	1.26	2.81	0.61	3.06	0.73	1.64	1.40	1.58	0.89	1.93	1.01
O	2.15	0.48	2.33	0.31	2.98	0.85	2.11	0.40	2.39	0.45	3.21	0.95
P	2.38	0.53	4.24	0.46	6.09	0.74	2.39	0.45	4.28	0.49	6.02	0.74
Q	1.26	0.83	1.07	0.59	1.24	0.89	1.29	0.97	1.31	0.96	1.77	1.43
R	2.86	0.77	2.70	0.58	3.08	0.84	2.84	1.04	2.26	1.91	3.20	2.26
S	3.10	2.33	4.33	1.68	5.21	2.02	5.93	3.56	5.21	4.22	5.28	3.81
T	3.03	2.58	2.68	1.01	3.30	1.25	3.86	3.26	4.22	3.54	4.32	3.23

Table 6.11 Median ΔE_{ab}^* values for 20 displays using the grey-ramp and colour-ramps linearisation samples and three different test sets for 10 linearisation samples ($N = 10$).

N=10												
Display	Grey_ramp						Colour_ramp					
	Chart4		Macbeth		Matlab60		Chart4		Macbeth		Matlab60	
	GOG	PLCC	GOG	PLCC	GOG	PLCC	GOG	PLCC	GOG	PLCC	GOG	PLCC
A	1.01	0.77	1.22	0.79	2.34	1.35	0.99	0.98	1.22	0.69	2.45	1.20
B	0.88	0.84	0.86	0.79	1.75	1.33	0.98	0.76	0.90	0.71	1.12	1.21
C	2.33	1.69	5.56	1.51	8.66	1.85	1.98	1.51	5.82	2.61	8.56	2.65
D	4.18	1.56	5.15	1.12	7.60	1.45	3.54	2.32	5.11	2.89	8.27	2.75
E	3.33	1.39	5.92	1.49	8.49	2.45	3.17	2.72	5.50	3.67	7.75	3.45
F	3.71	1.37	4.54	1.07	8.53	1.70	3.49	1.65	4.83	3.50	9.46	3.91
G	1.83	0.67	1.39	0.79	1.96	1.06	1.69	1.74	1.64	1.53	2.13	2.23
H	2.26	1.31	2.48	1.12	3.95	1.25	1.86	1.46	2.39	2.01	3.34	1.81
I	1.48	0.89	1.08	0.98	2.43	1.31	0.96	1.34	1.51	1.83	2.54	1.95
J	2.31	1.42	1.55	1.28	2.10	1.69	2.37	2.28	2.40	2.45	2.64	2.70
K	1.01	0.84	0.75	0.71	0.99	0.97	0.96	0.95	0.98	0.95	1.16	1.18
L	2.03	1.45	1.84	1.07	2.27	1.28	1.32	1.08	0.84	1.13	1.11	1.38
M	1.38	1.06	1.33	0.71	1.52	0.90	2.00	1.24	1.72	0.86	1.84	1.15
N	1.62	1.28	2.42	1.21	2.64	1.04	1.62	1.29	1.42	0.96	1.70	1.18
O	1.99	0.58	2.08	0.59	2.88	1.28	1.86	0.62	2.27	0.69	2.98	1.38
P	2.59	0.72	3.85	0.76	5.64	1.28	2.44	0.64	3.94	0.73	5.67	1.29
Q	1.32	0.84	1.15	0.66	1.25	1.01	1.28	1.13	1.21	0.95	1.80	1.50
R	2.89	0.99	2.78	0.84	3.20	0.99	2.88	1.49	2.45	2.07	3.26	2.24
S	3.06	2.23	3.92	1.85	5.19	2.99	5.98	3.51	5.23	4.12	5.36	3.91
T	3.07	2.68	2.96	1.45	3.29	1.88	3.86	3.12	4.19	3.54	4.39	3.36

Table 6.12 Median ΔE_{ab}^* values for 20 displays using the grey-ramp and colour-ramps linearisation samples and three different test sets for 6 linearisation samples ($N = 6$).

N=6												
Display	Grey_ramp						Colour_ramp					
	Chart4		Macbeth		Matlab60		Chart4		Macbeth		Matlab60	
	GOG	PLCC	GOG	PLCC	GOG	PLCC	GOG	PLCC	GOG	PLCC	GOG	PLCC
A	0.98	1.19	1.06	2.29	2.19	3.02	1.07	1.19	1.05	2.09	2.26	2.96
B	0.81	1.28	0.68	2.01	1.48	3.19	0.96	1.18	0.93	1.74	1.11	3.09
C	2.78	3.20	2.36	3.18	4.23	3.46	2.17	2.42	2.49	2.97	3.63	3.72
D	4.32	2.23	4.66	2.20	7.42	3.25	3.59	2.74	5.38	2.96	7.91	4.09
E	3.32	2.55	5.73	2.74	7.67	4.36	2.97	2.48	5.12	4.91	6.93	6.33
F	3.44	2.86	3.83	2.54	5.42	3.01	3.41	2.97	4.86	3.60	15.12	4.51
G	1.55	0.81	1.08	2.11	1.63	2.44	1.65	2.17	1.65	2.55	2.20	2.91
H	2.27	2.51	2.47	1.94	3.57	3.44	1.92	2.18	2.64	2.19	3.11	3.45
I	1.53	1.93	1.71	2.11	2.29	2.76	1.00	2.34	1.43	2.35	2.35	3.07
J	2.34	2.83	1.49	2.69	1.96	3.17	2.19	2.68	2.22	2.86	2.58	3.71
K	0.95	1.58	0.74	2.40	0.90	2.53	0.98	1.28	0.95	2.30	1.08	2.33
L	1.95	2.09	1.73	2.21	2.18	2.60	1.29	1.90	0.96	1.96	1.16	2.58
M	1.20	1.00	1.09	2.26	1.32	2.65	1.77	1.45	1.62	1.79	1.74	2.40
N	1.84	1.92	1.42	2.56	1.62	3.01	1.76	2.03	1.36	2.18	1.91	2.76
O	1.81	1.35	1.66	2.21	2.31	3.24	1.78	1.36	1.79	2.20	2.45	3.39
P	2.42	1.49	3.69	1.74	5.00	2.72	2.41	1.17	3.48	1.69	5.13	2.75
Q	1.42	0.86	1.28	0.92	1.61	1.58	1.32	1.03	1.26	1.11	1.98	1.83
R	2.73	1.42	2.51	1.22	3.18	1.52	2.67	1.75	2.57	2.19	4.31	2.55
S	2.94	2.55	6.10	3.12	8.42	4.75	6.95	3.59	10.48	3.92	16.71	5.04
T	3.08	3.83	2.19	2.60	3.17	3.89	3.71	3.86	4.01	3.44	4.29	4.20

does not have the lowest channel independence, spatial independence or contrast ratio nor does it have the best white-point tracking. It is likely that all of these factors could be related to overall characterisation performance. However, it is not clear that there is any definitive relationship between any of these factors and characterisation performance although it is interesting to note that the display *K* did result not in the best but in one of the highest r^2 values for linearisation.

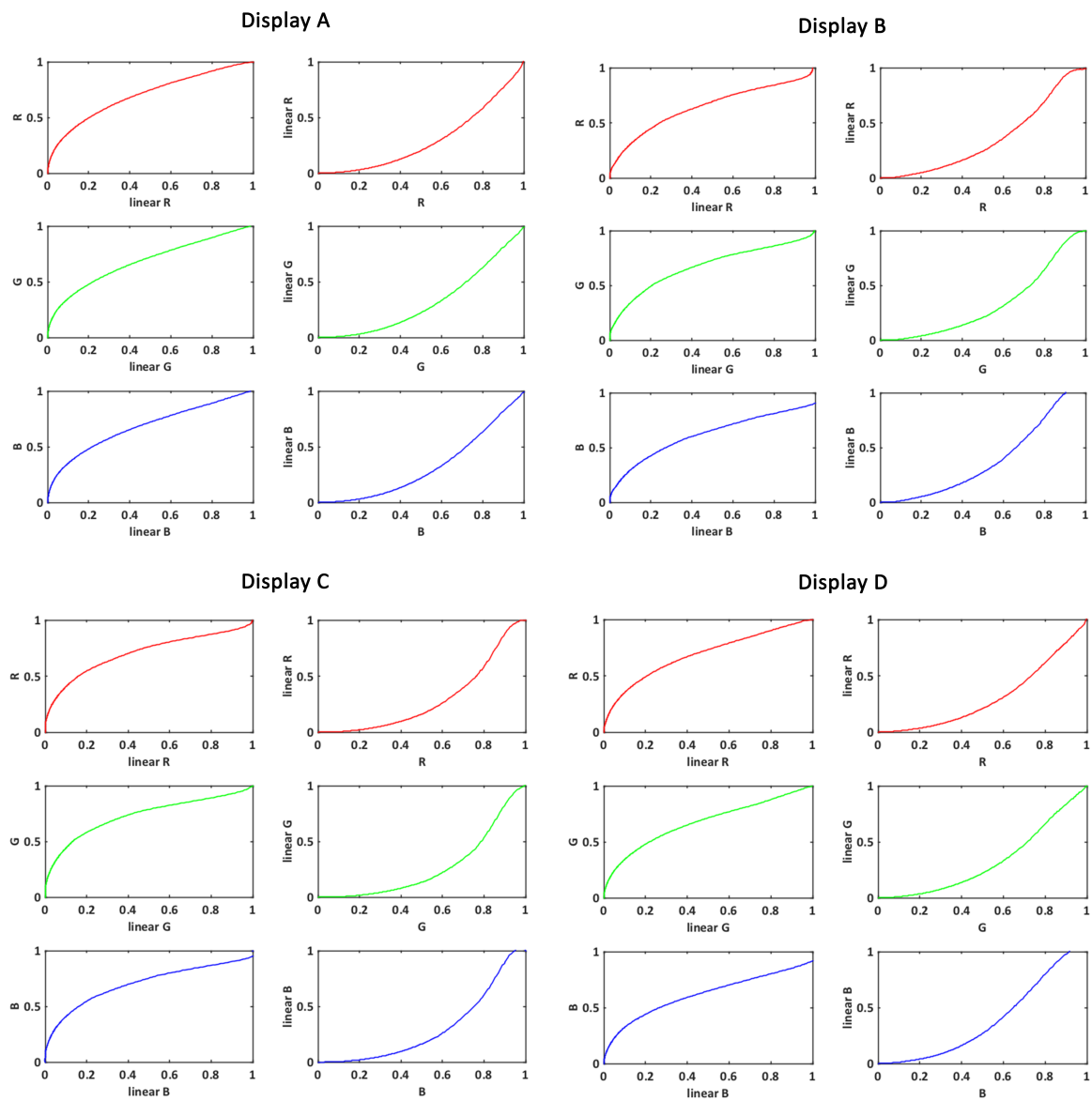


Fig. 6.5 TRC of A-D display.

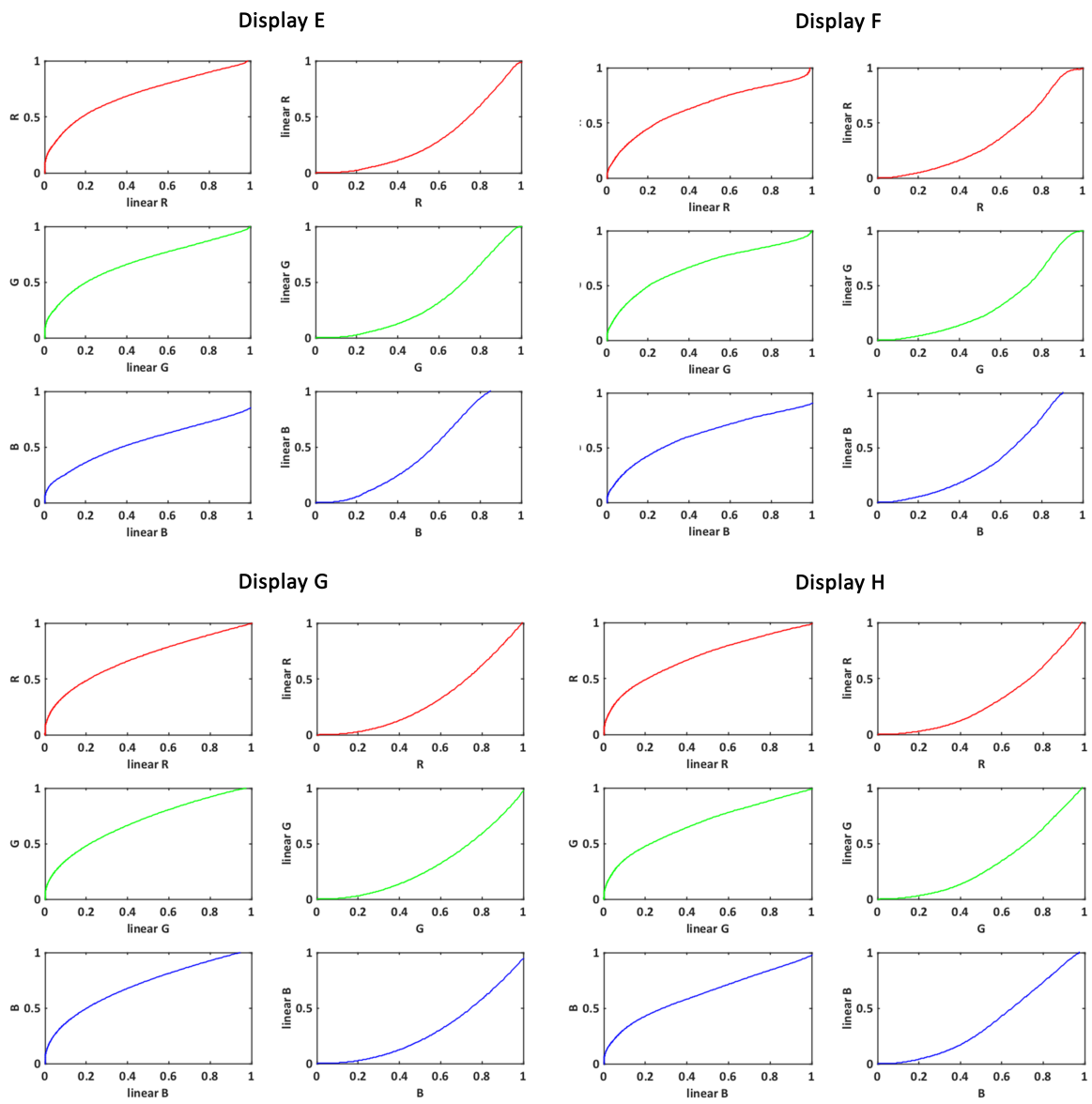


Fig. 6.6 TRC of E-H display.

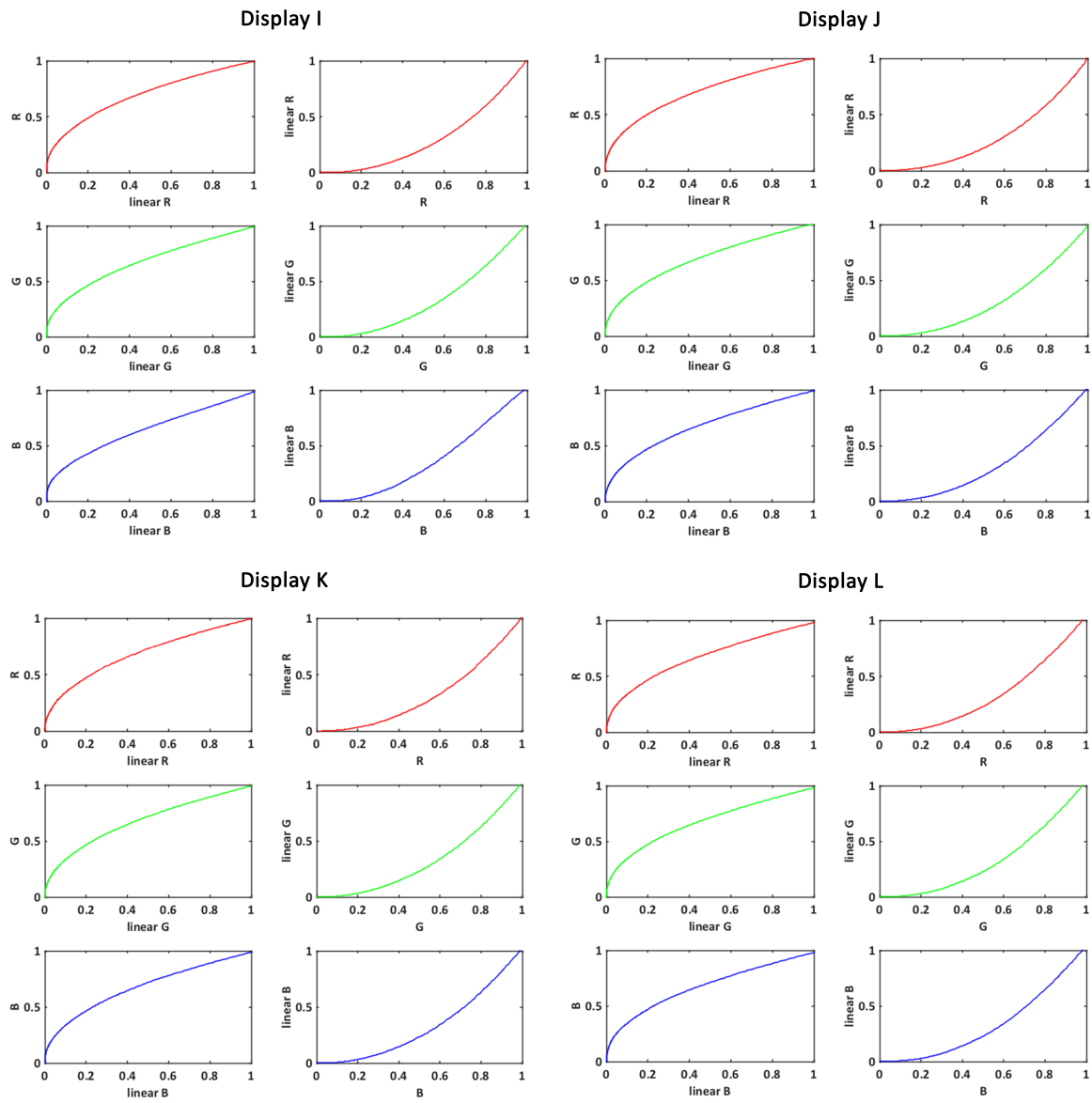


Fig. 6.7 TRC of I-L display.

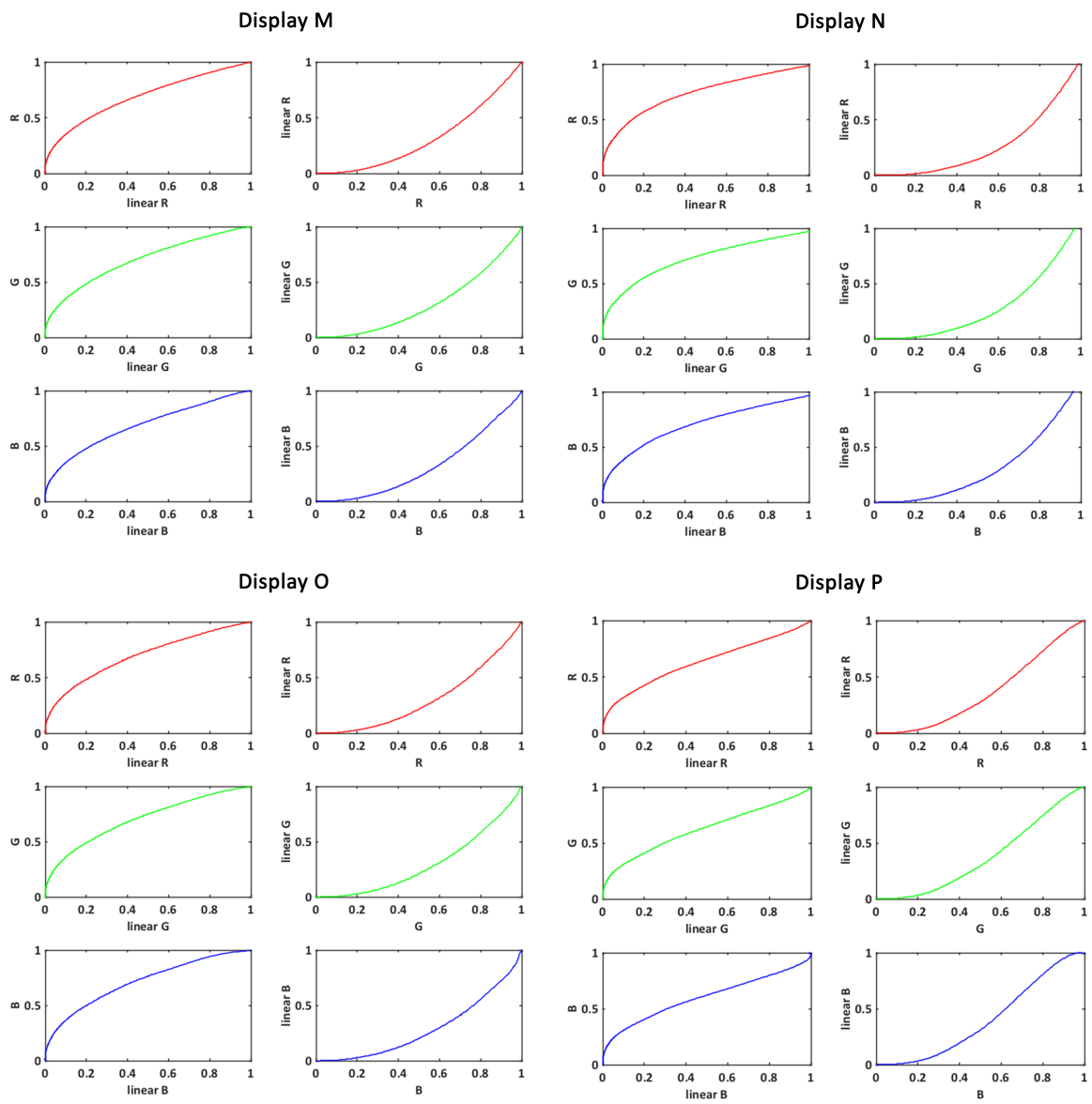


Fig. 6.8 TRC of M-P display.

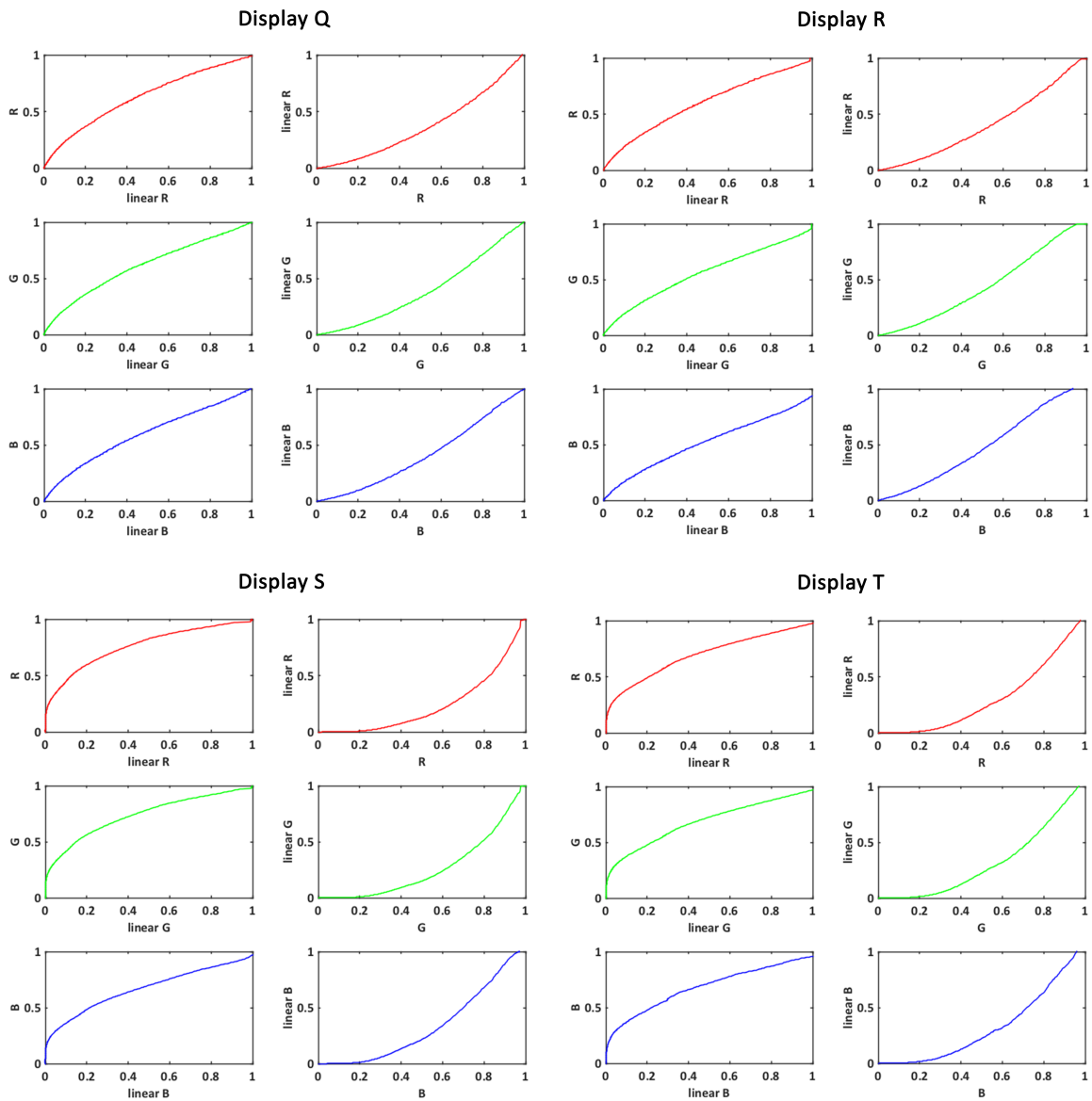


Fig. 6.9 TRC of Q-T display.

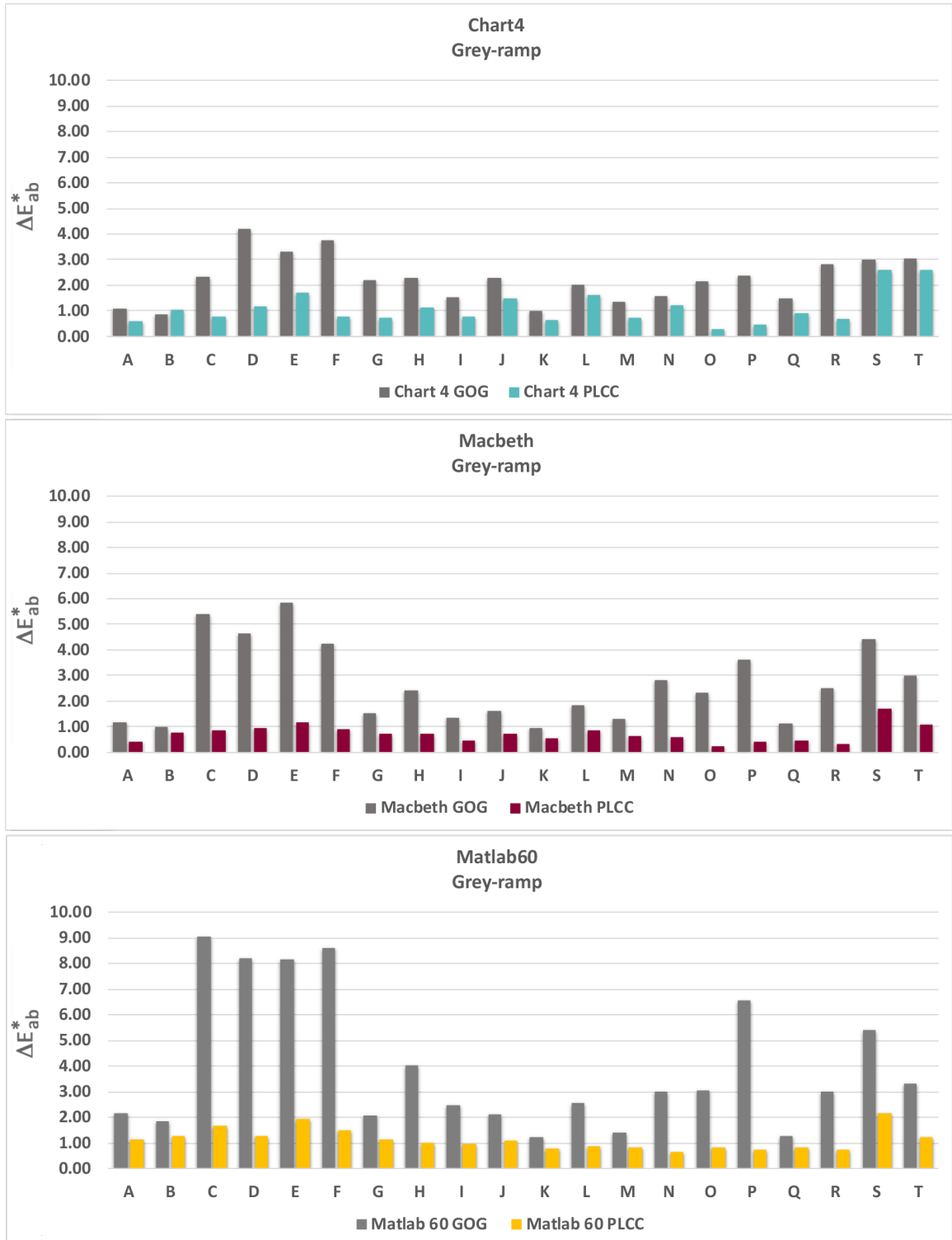


Fig. 6.10 Characterisation result using grey-ramp linearisation samples for all display devices and all samples (N=256).

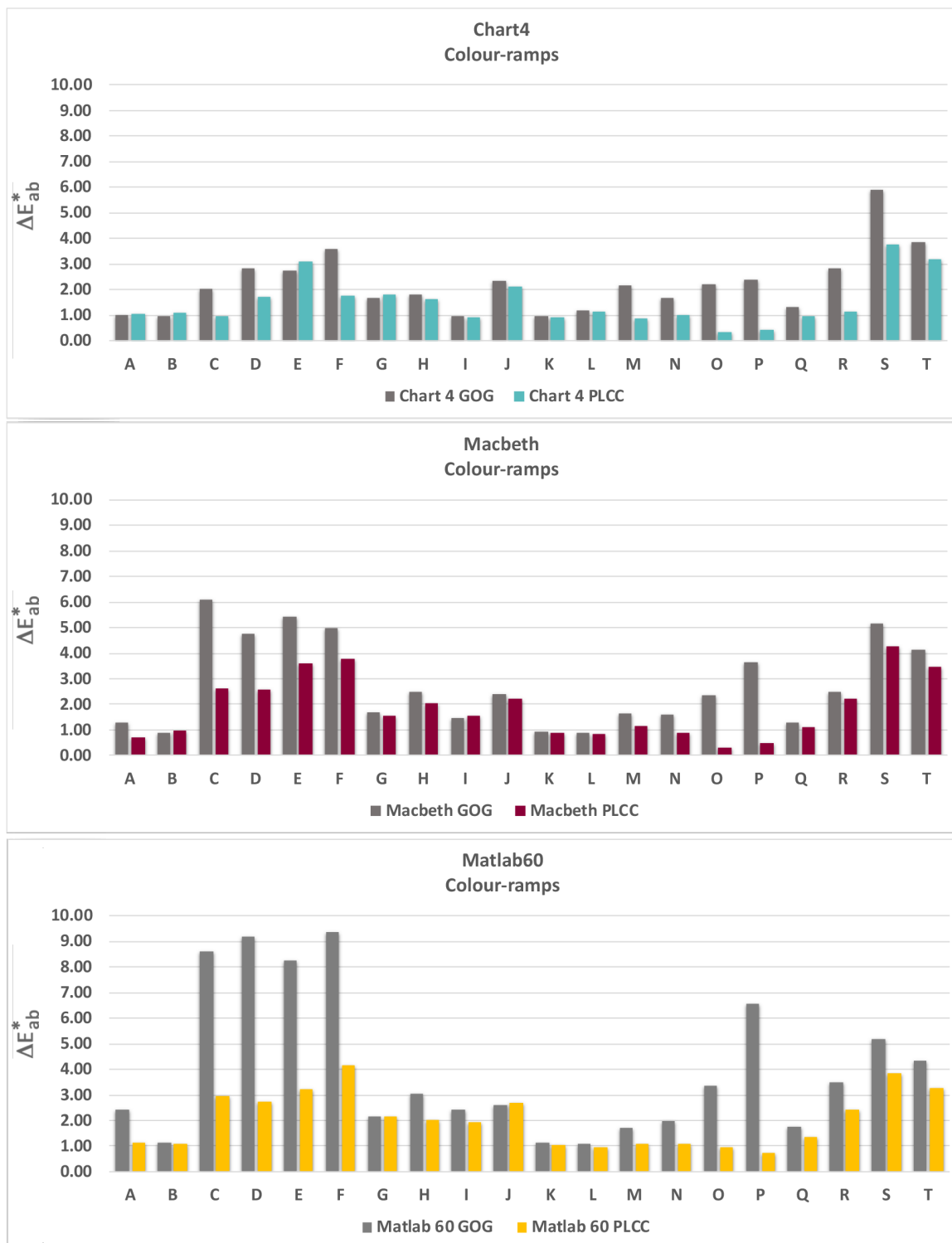


Fig. 6.11 Characterisation result using colour-ramp linearisation samples for all display devices and all samples (N=256).

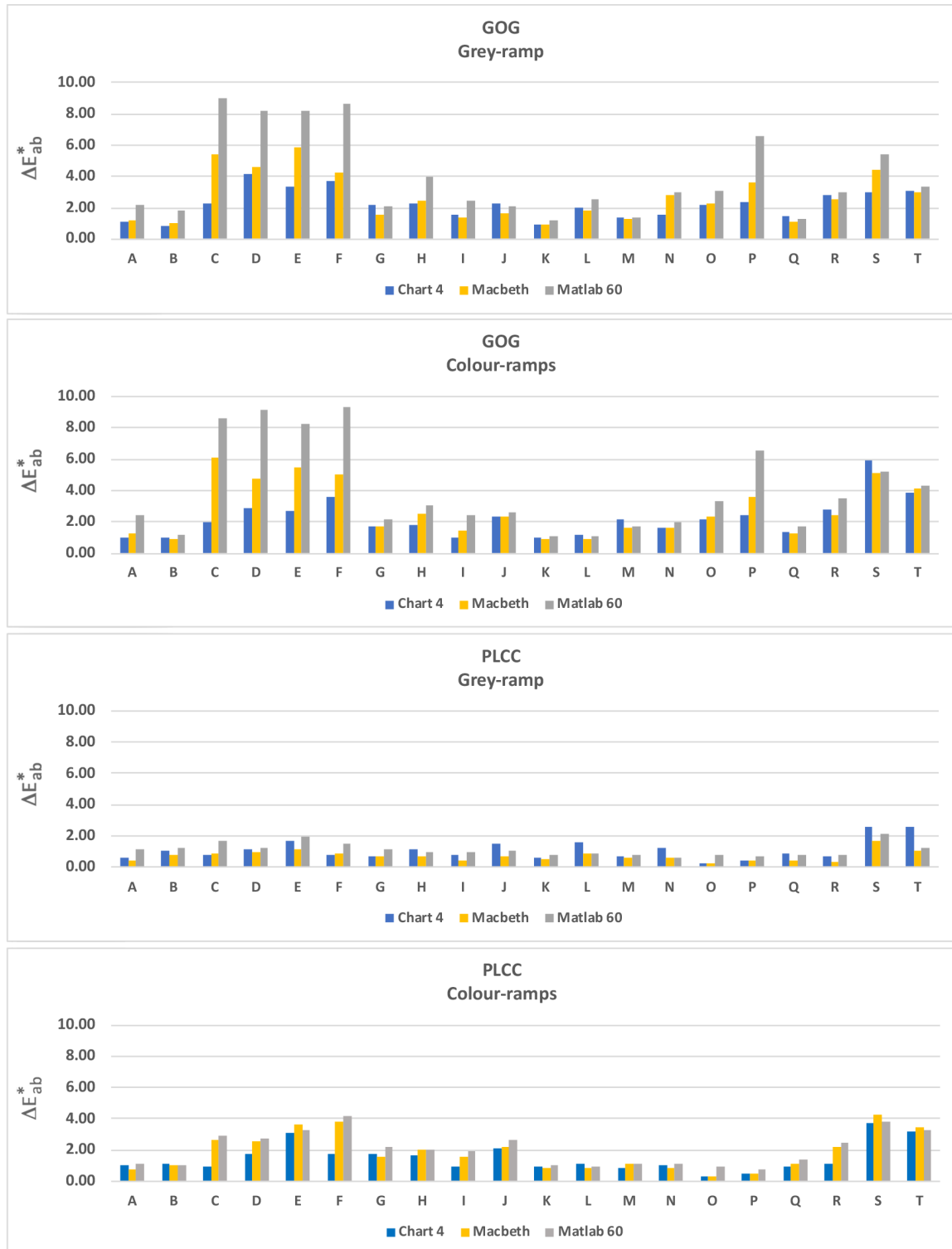


Fig. 6.12 Characterisation result using both linearisation samples and both models for all display devices and all samples (N=256).

6.9 Statistical analysis

The t-distribution is used when the σ value (population standard deviation calculated from $\sigma = \sqrt{\mu_2}$) is unknown. Two different t.test have been conducted to look at the effects of using the GOG and PLCC as well as the grey-ramp or colour-ramps linearisation samples for the Macbeth set of samples considering to use all linearisation samples ($N = 256$). Table 6.13 and Table 6.14 show a significant effect of using model (GOG or PLCC) and a significant effect of using linearisation characterisation samples (grey-ramp or colour-ramps) with p values of less than 0.05 in both cases for the majority of displays.

It is evident from this formal statistical analysis that PLCC is better than GOG and grey-ramp linearisation samples are better than colour-ramps linearisation samples.

Table 6.13 Statistical t.test for GOG vs PLCC linearisation samples for all displays using Macbeth set of samples.

GOG vs. PLCC		
Display	GreyRamp	ColourRamp
A	0.0000	0.0009
B	0.0008	0.1146
C	0.0000	0.0001
D	0.0005	0.0022
E	0.0007	0.0063
F	0.0000	0.0011
G	0.0006	0.8463
H	0.0010	0.0090
I	0.0004	0.0418
J	0.0001	0.1524
K	0.0001	0.0347
L	0.0000	0.0152
M	0.0012	0.0010
N	0.0000	0.0000
O	0.0000	0.0000
P	0.0003	0.0003
Q	0.0003	0.0620
R	0.0000	0.0101
S	0.0009	0.0037
T	0.0021	0.0064

Table 6.14 Statistical t.test for Grey vs Colour linearisation samples for all displays using Macbeth set of samples.

Grey vs. Colour		
Display	GOG	PLCC
A	0.1226	0.0001
B	0.0337	0.2277
C	0.0261	0.0000
D	0.8036	0.0000
E	0.2183	0.0000
F	0.8378	0.0000
G	0.5830	0.0000
H	0.0161	0.0012
I	0.0524	0.0000
J	0.0247	0.0000
K	0.2986	0.0014
L	0.0001	0.6290
M	0.0002	0.0001
N	0.0001	0.2785
O	0.8636	0.3047
P	0.0585	0.5680
Q	0.1275	0.0000
R	0.0873	0.0000
S	0.9865	0.0000
T	0.0376	0.0000

6.10 Effect of using different number of samples (Sub sampling).

The effect of using the different number of linearisation samples on the characterisation performance of all 20 displays are tested. There are two main questions needed to be answered in this section. Firstly, is there any evidence that PLCC improves with choosing different numbers of linearisation samples ($N = 256, 129, 66, 34, 18, 10$ and 6)? Secondly, is there a trade-off value of N ?

Table 6.15 shows the median colour differences (ΔE_{ab}^*) for colour characterisation using different numbers of linearisation samples (N) and the Macbeth test samples. It is evident that the PLCC consistently perform better than GOG in most of the cases. This table also shows that using GOG with fewer linearisation samples tends to results in smaller colour differences than when there are more linearisation samples. Fig. 6.13 and 6.14 illustrate the result of the Table 6.15. It is clear that most displays, PLCC works better than GOG, especially when the number of linearisation samples is greater than 10 ($N > 10$). The same pattern has been shown when using the Macbeth set of samples and colour-ramps linearisation samples on the characterisation performance of all 20 displays which can be seen from Table. 6.16 and visualised in Fig. 6.15 and 6.16.

Table 6.15 The median ΔE_{ab}^* values for a various number of linearisation samples using grey-ramp linearisation samples for all displays testing Macbeth set of samples.

Display	Macbeth													
	N=256		N=129		N=66		N=34		N=18		N=10		N=6	
	GOG	PLCC	GOG	PLCC	GOG	PLCC	GOG	PLCC	GOG	PLCC	GOG	PLCC	GOG	PLCC
A	1.17	0.40	1.17	0.41	1.16	0.41	1.15	0.41	1.13	0.41	1.22	0.79	1.06	2.29
B	1.00	0.79	1.00	0.77	1.01	0.75	1.01	0.74	0.97	0.73	0.86	0.79	0.68	2.01
C	5.42	0.86	5.41	0.84	5.39	0.83	5.40	0.83	5.45	0.87	5.56	1.51	2.36	3.18
D	4.64	0.97	4.70	0.97	4.73	0.97	4.68	0.95	4.92	0.80	5.15	1.12	4.66	2.20
E	5.83	1.16	6.09	1.15	6.16	1.16	5.76	1.20	5.80	1.16	5.92	1.49	5.73	2.74
F	4.23	0.91	4.24	0.92	4.17	0.88	4.07	0.88	4.08	0.83	4.54	1.07	3.83	2.54
G	1.53	0.74	1.53	0.74	1.52	0.69	1.50	0.67	1.46	0.65	1.39	0.79	1.08	2.11
H	2.42	0.71	2.44	0.69	2.27	0.72	2.12	0.69	2.01	0.79	2.48	1.12	2.47	1.94
I	1.34	0.47	1.35	0.47	1.34	0.49	1.34	0.55	1.39	0.40	1.08	0.98	1.71	2.11
J	1.62	0.71	1.62	0.80	1.58	0.82	1.62	0.81	1.61	0.72	1.55	1.28	1.49	2.69
K	0.96	0.57	0.93	0.49	0.89	0.52	0.90	0.53	0.91	0.54	0.75	0.71	0.74	2.40
L	1.84	0.86	1.84	0.88	1.84	0.85	1.84	0.85	1.84	0.74	1.84	1.07	1.73	2.21
M	1.31	0.64	1.28	0.62	1.27	0.62	1.25	0.62	1.21	0.61	1.33	0.71	1.09	2.26
N	2.84	0.58	2.85	0.59	2.84	0.59	2.85	0.59	2.81	0.61	2.42	1.21	1.42	2.56
O	2.32	0.25	2.32	0.28	2.33	0.44	2.33	0.42	2.33	0.31	2.08	0.59	1.66	2.21
P	3.61	0.44	3.58	0.45	3.60	0.45	4.12	0.46	4.24	0.46	3.85	0.76	3.69	1.74
Q	1.12	0.47	1.13	0.52	1.11	0.57	1.09	0.59	1.07	0.59	1.15	0.66	1.28	0.92
R	2.51	0.33	2.48	0.50	2.57	0.53	2.45	0.56	2.70	0.58	2.78	0.84	2.51	1.22
S	4.40	1.71	4.41	1.71	4.35	1.68	4.12	1.81	4.33	1.68	3.92	1.85	6.10	3.12
T	2.98	1.07	2.98	1.08	2.96	1.09	2.96	1.09	2.68	1.01	2.96	1.45	2.19	2.60

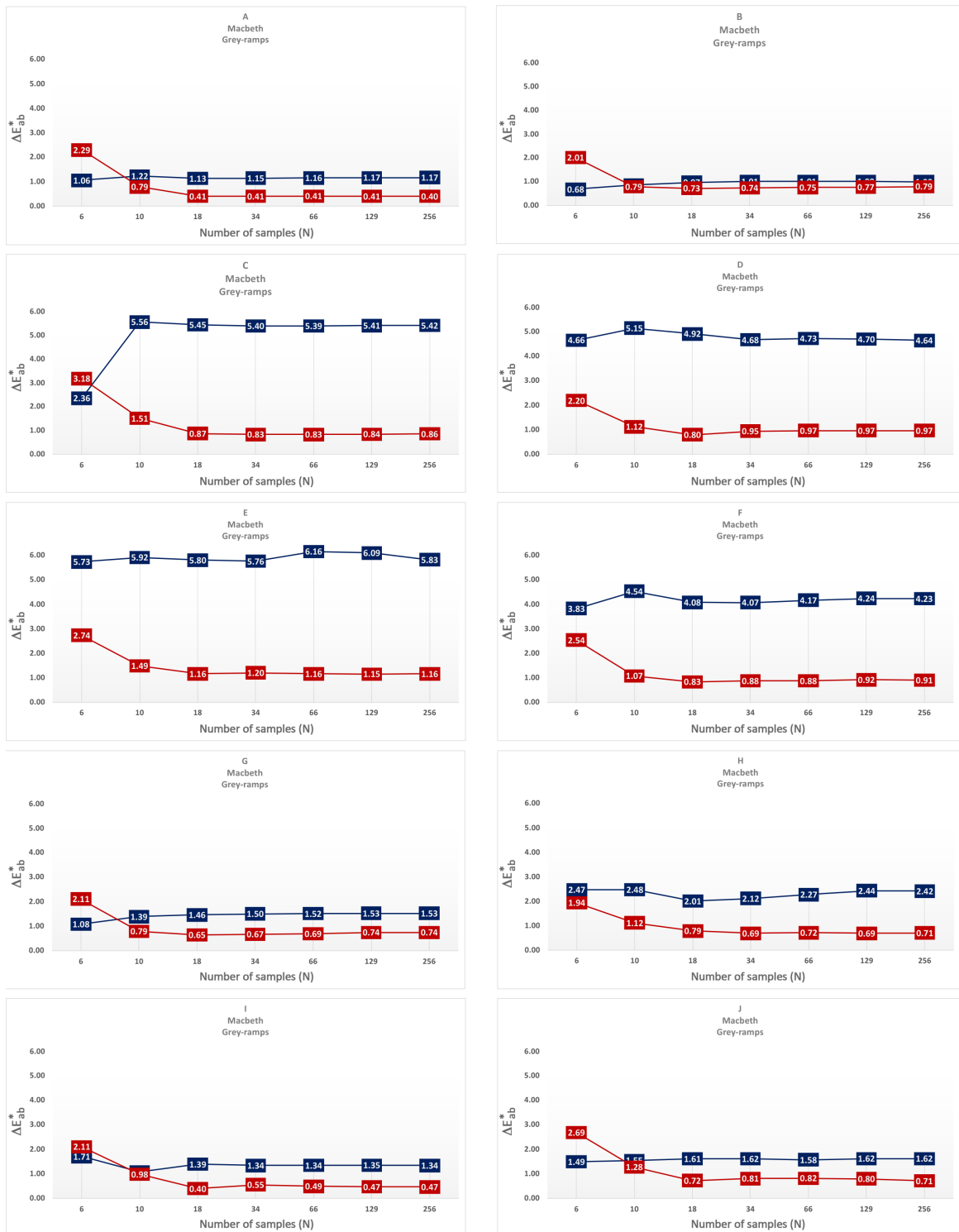


Fig. 6.13 Characterisation result using grey-ramp linearisation samples testing GOG and PLCC for A-J display devices using different linearisation samples ($N = 256, 129, 66, 34, 18, 10, 6$).

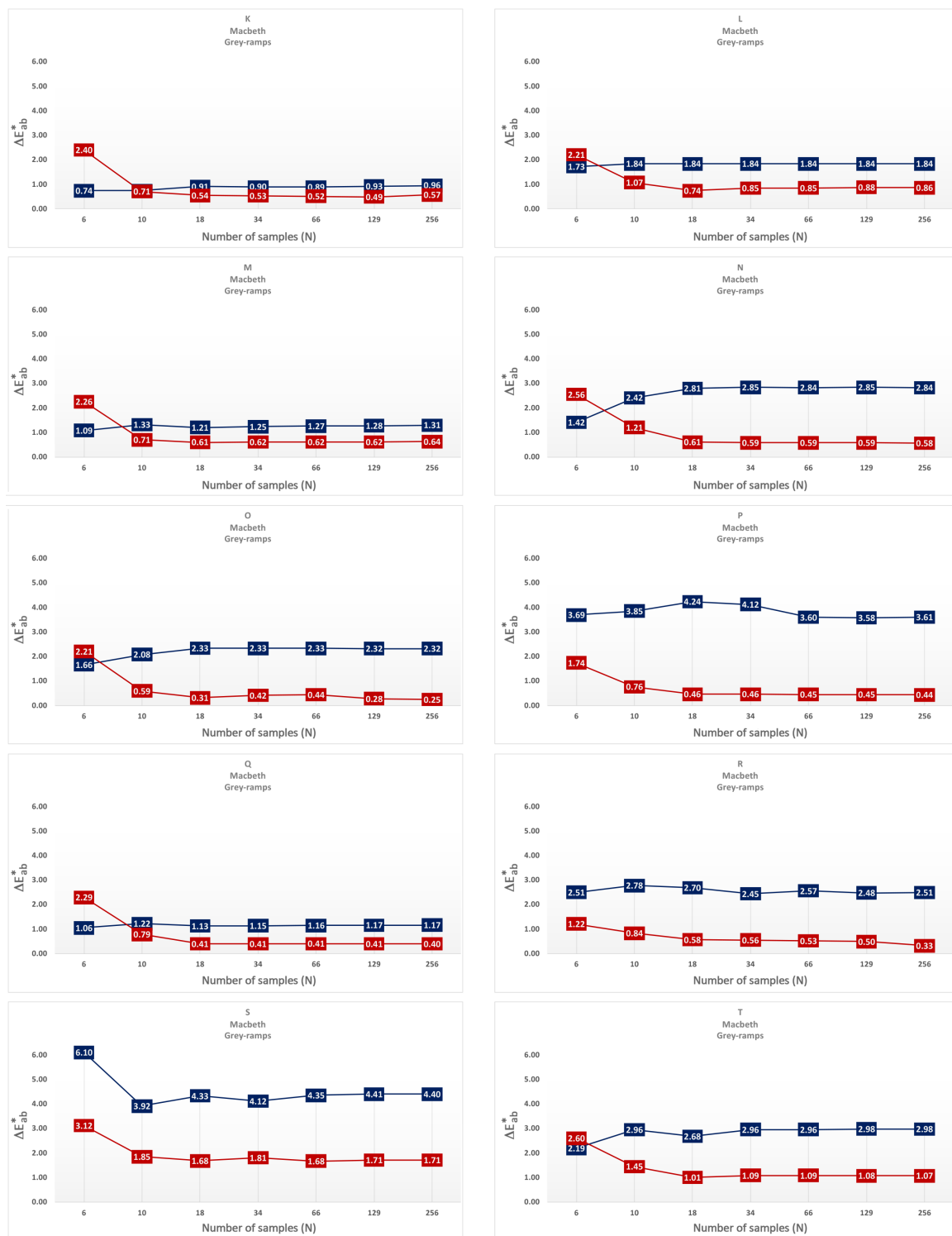


Fig. 6.14 Characterisation result using grey-ramp linearisation samples testing GOG and PLCC for K-T display devices using different linearisation samples ($N = 256, 129, 66, 34, 18, 10, 6$).

Table 6.16 The median ΔE_{ab}^* values for various number of linearisation samples using colour-ramps linearisation samples for all displays testing Macbeth set of samples.

Macbeth														
Display	N=256		N=129		N=66		N=34		N=18		N=10		N=6	
	GOG	PLCC	GOG	PLCC	GOG	PLCC	GOG	PLCC	GOG	PLCC	GOG	PLCC	GOG	PLCC
A	1.27	0.73	1.27	0.73	1.27	0.71	1.28	0.72	1.24	0.65	1.22	0.69	1.05	2.09
B	0.90	1.00	0.89	0.98	0.88	0.92	0.88	0.95	0.88	0.80	0.90	0.71	0.93	1.74
C	6.11	2.61	6.11	2.62	6.13	2.58	6.15	2.61	6.19	2.59	5.82	2.61	2.49	2.97
D	4.75	2.57	4.77	2.52	4.76	2.54	4.80	2.52	4.94	2.56	5.11	2.89	5.38	2.96
E	5.45	3.61	5.45	3.60	5.45	3.60	5.45	3.61	5.49	3.47	5.50	3.67	5.12	4.91
F	5.00	3.78	5.01	3.78	5.00	3.78	5.02	3.80	5.08	3.75	4.83	3.50	4.86	3.60
G	1.67	1.55	1.68	1.55	1.67	1.61	1.67	1.58	1.66	1.60	1.64	1.53	1.65	2.55
H	2.48	2.06	2.48	2.06	2.49	2.11	2.50	2.09	2.49	2.07	2.39	2.01	2.64	2.19
I	1.46	1.54	1.45	1.54	1.44	1.54	1.43	1.53	1.45	1.61	1.51	1.83	1.43	2.35
J	2.38	2.23	2.39	2.33	2.39	2.27	2.36	2.24	2.37	2.27	2.40	2.45	2.22	2.86
K	0.93	0.88	0.94	0.93	0.95	0.87	0.93	0.93	0.94	0.78	0.98	0.95	0.95	2.30
L	0.90	0.83	0.91	0.85	0.93	0.90	0.92	0.84	0.87	0.81	0.84	1.13	0.96	1.96
M	1.62	1.16	1.62	1.22	1.63	1.21	1.65	1.17	1.69	1.08	1.72	0.86	1.62	1.79
N	1.60	0.87	1.61	0.88	1.62	0.87	1.61	0.85	1.58	0.89	1.42	0.96	1.36	2.18
O	2.38	0.30	2.38	0.39	2.38	0.44	2.39	0.36	2.39	0.45	2.27	0.69	1.79	2.20
P	3.63	0.47	3.53	0.47	3.70	0.47	4.16	0.45	4.28	0.49	3.94	0.73	3.48	1.69
Q	1.28	1.13	1.27	1.12	1.27	0.89	1.30	0.87	1.31	0.96	1.21	0.95	1.26	1.11
R	2.47	2.22	2.48	2.15	2.45	2.09	2.42	1.94	2.26	1.91	2.45	2.07	2.57	2.19
S	5.16	4.27	5.13	4.28	5.07	4.28	4.93	4.28	5.21	4.22	5.23	4.12	10.48	3.92
T	4.16	3.48	4.16	3.48	4.17	3.53	4.18	3.55	4.22	3.54	4.19	3.54	4.01	3.44

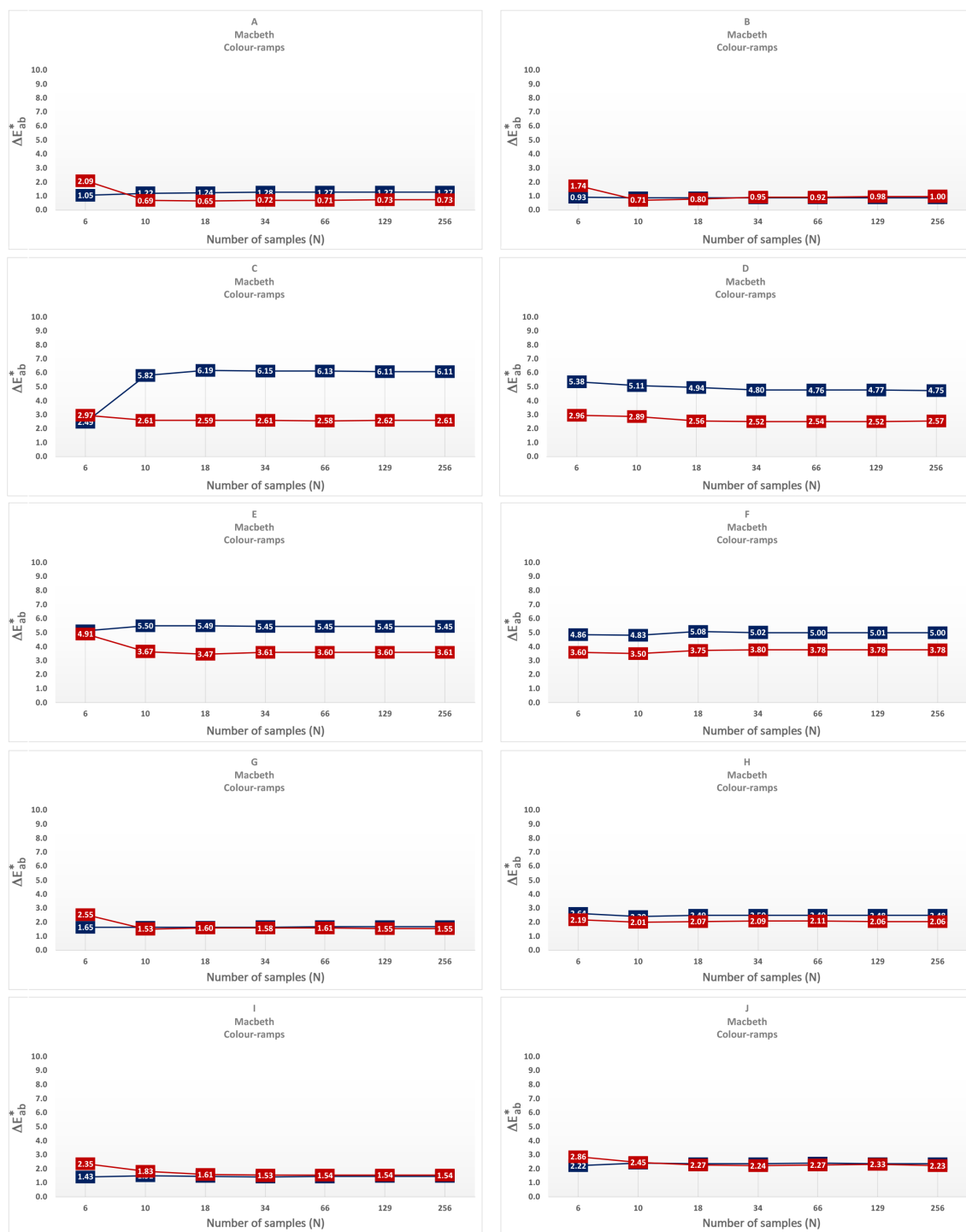


Fig. 6.15 Characterisation result using colour-ramp linearisation samples testing GOG and PLCC for A-J display devices using different linearisation samples ($N = 256, 129, 66, 34, 18, 10, 6$).

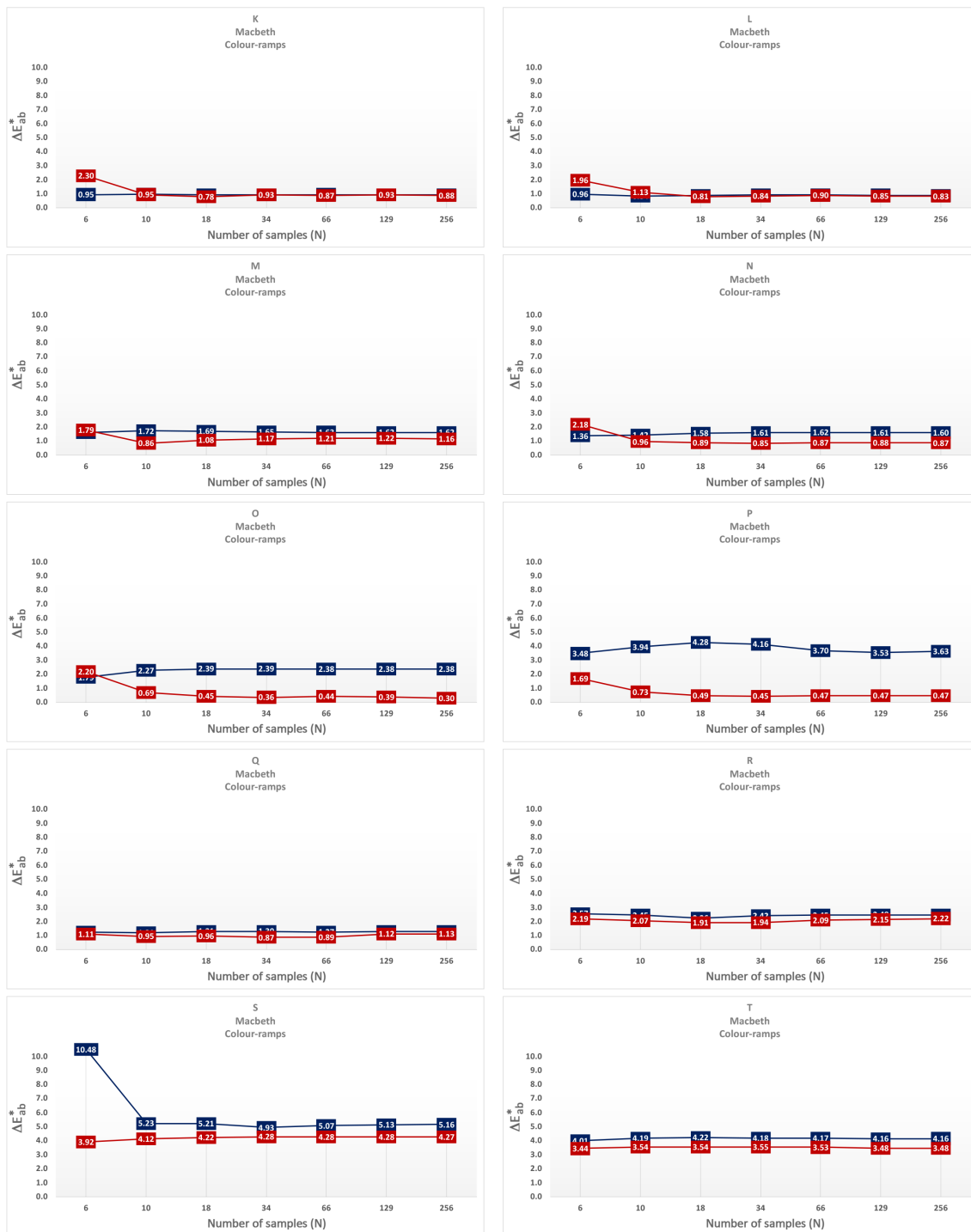


Fig. 6.16 Characterisation result using colour-ramp linearisation samples testing GOG and PLCC for K-T display devices using different linearisation samples ($N = 256, 129, 66, 34, 18, 10, 6$).

6.11 Chromaticity Constancy

To evaluate the chromaticity constancy of the displays, the grey-ramp chromaticities (x, y) are plotted against the luminance of the display ($Y(\text{cd}/\text{m}^2)$). Fig. 6.17 and 6.18 illustrate the chromaticity constancy of all the display devices. It is evident that for displays A, B, C, D, F, J , the chromaticities are quite constant until the very dark samples. However, some other displays ($E, G, H, I, K, L, M, N, O, P, Q, R, S, T$) have very varying chromaticities.

This suggests that other characterisation models may be needed to improve characterisation performances where the assumption for constant chromaticity (inherent in matrix M) is not required. Therefore, the PLVC model has been implemented and is described in the next Chapter.

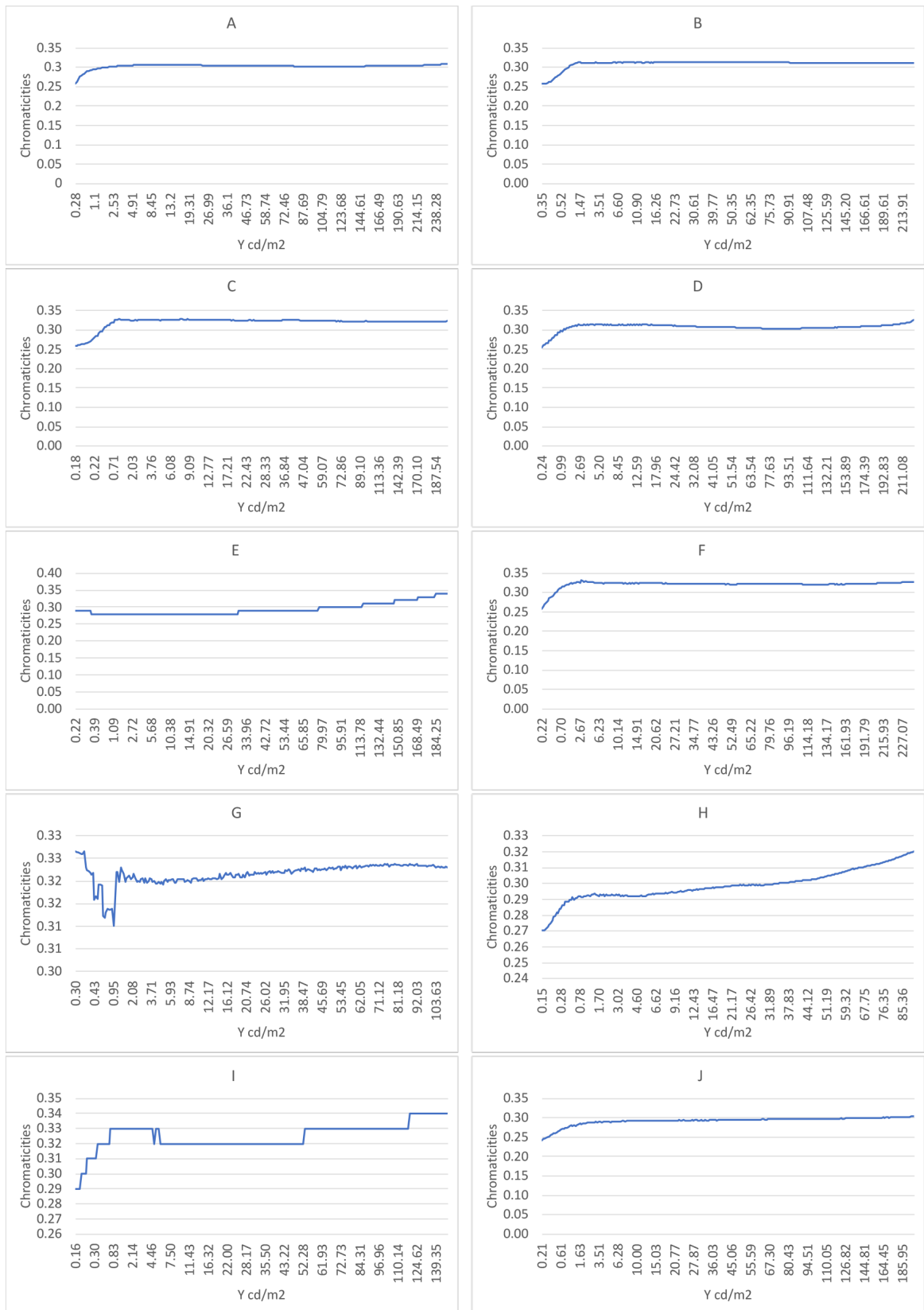


Fig. 6.17 The chromaticity graph for display A – J.

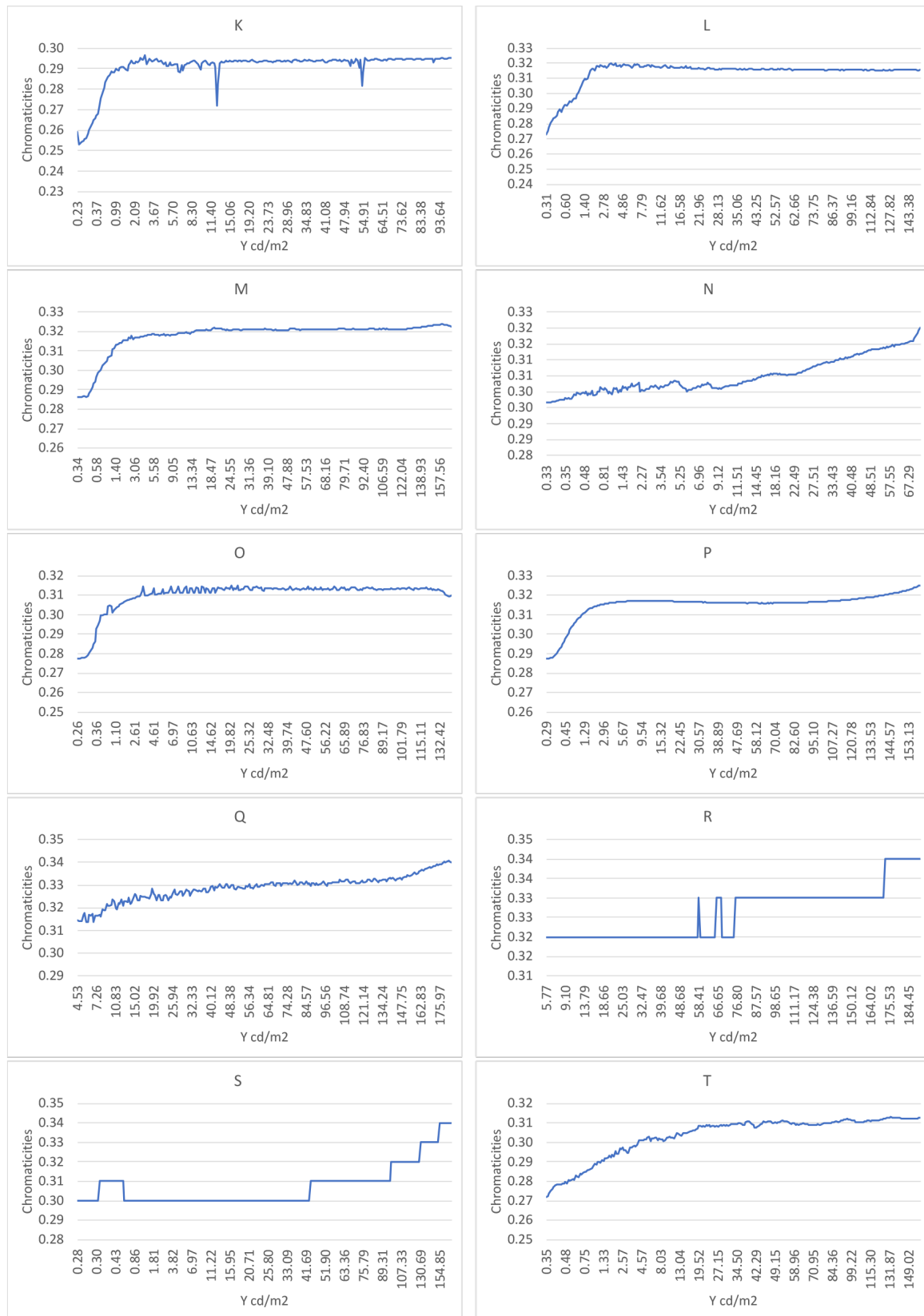


Fig. 6.18 The chromaticity graph for display K – T.

6.12 Conclusions

An analysis of 20 displays has allowed a robust study of characterisation performance. There is clear evidence from this analysis that the PLCC method is superior to the GOG model and should be preferred. There is also clear evidence that the grey-ramp linearisation samples produce better performance than the colour-ramps linearisation samples; this was true for Chart4, Macbeth and Matlab60 test sets. There is, therefore, a clear recommendation to use the PLCC method with grey-ramp linearisation samples. A preference for grey-ramp samples has been suggested by Berns [13].

Having determined that PLCC gives lower characterisation errors (ΔE_{ab}^*) than GOG when all 256 tonal steps are available for the linearisation and that linearisation using grey-ramp linearisation samples results in better results than linearisation with colour-ramps, it is also interesting to explore how relative performance changes as the number of tonal steps (N) is reduced. How robust are the methods as $N \rightarrow 0$? For the PLCC, characterisation errors (ΔE_{ab}^*) tend to rise as N decreases which are perhaps not surprising. Two specific conclusions can be drawn from the analysis. Firstly, that although the PLCC characterisation performance tends to improve with N , the change in performance is not linear; as N increases performances initially changes quickly but changes much more slowly after $N = 25$. This suggests that although better results are probably possible with high values of N , an N of about 25 is a practical and effective method. Secondly, that in general when $N > 10$ the PLCC method superior to the GOG methods but that for $N < 10$ sometimes the GOG method can give the better performance in a few numbers of displays using Chart4 (highly chromatic) set of samples. It seems that empirical experimentation is necessary to ascertain whether GOG or PLCC should be preferred if few linearisation samples are available. There is some suggestion in this work that the linearisation performance is one of the most important factors that contributes to overall colour characterisation.

Chapter 7

Testing the PLVC model

7.1 Introduction

In this chapter, the effect of using an additional model called PLVC is considered. The analysis and experimental validation of this model and comparison with the other models such as two GOGs model using grey-ramp and colour-ramp linearisation samples and two PLCC models using the grey-ramp and colour-ramp linearisation are evaluated. As before, seven sub-sets of linearisation samples are considered to allow the effect of N to be explored.

7.2 The PLVC model

The Piecewise Linear model assuming Variation in Chromaticity (PLVC) was introduced for the first time by Farley and Gutmann [50]. Note that it preceded the well-known article from Cowan [40]. Post and Calhoun [131] widely used this model with CRT technologies. Further studies have been performed with CRTs [79, 131, 132], and later on more recent technologies [162, 163] such as LCD. The other modification including the black correction has been added to this model by Del Barco *et al.* [79]. According to Thomas *et al.* [163] the accuracy of the PLVC model for the display based on liquid crystal technologies is more accurate. In addition, the PLVC model does model the chromaticity shift of the primaries but does not consider the channel inter-dependence.

In this section, we recall the principles of this model and some features that characterise it. Knowing the tristimulus values of XYZ for each primary as a function of the digital input, assuming additivity, the resulting colour tristimulus values can be expressed as the sum of tristimulus values for each component (i.e. primary) at the given input level. Note that in order not to have an effect of the black level, it is subtracted from all calculation used to define the model. Then, it is added to the result, to return to a correct standard observer colour space [79, 132]. The model is summarised and generalised in Equation 7.1- 7.3 for N primaries, and illustrated in Equation 7.4- 7.6 for a trichromatic RGB device, using an equivalent formulation to Del Barco *et al.* [79]. Considering the chromaticity coordinates of the channel as a function of digital input value has been taken by using the PLVC model [185]. The relationship between the channel luminance and the digital input value of primaries have been described by using this model to eliminates the influence of non-constant chromaticity and uses a piecewise linear interpolation method [185, 163, 132].

For an N primary device, we consider the digital input to the i^{th} primary, $d_i(m_i)$, with i an integer $\in [0, N]$, and m_i an integer limited by the resolution of the device (i.e. $m_i \in [0, 255]$ for a channel coded on 8 bits). Then, a colour $XYZ(\dots, d_i(m_i), \dots)$ can be expressed by :

$$X(\dots, d_i(m_i), \dots) = \sum_{i=0, j=m_i}^{(i=N-1)} [X(d_i(j)) - X_k] + X_k \quad (7.1)$$

$$Y(\dots, d_i(m_i), \dots) = \sum_{i=0, j=m_i}^{(i=N-1)} [Y(d_i(j)) - Y_k] + Y_k \quad (7.2)$$

$$Z(\dots, d_i(m_i), \dots) = \sum_{i=0, j=m_i}^{(i=N-1)} [Z(d_i(j)) - Z_k] + Z_k \quad (7.3)$$

where the X_k, Y_k, Z_k are the colour tristimulus values of black.

It has been illustrated for RGB primaries of the devices. Therefore the XYZ of each digital input which shows as $d_r(i), d_g(j), d_b(l)$, with i, j, l integers $\in [0, 255]$, can be expressed by:

$$X(d_r(i), d_g(j), d_b(l)) = [X(d_r(i)) - X_k] + [X(d_g(j)) - X_k] + [X(d_b(l)) - X_k] + X_k \quad (7.4)$$

$$Y(d_r(i), d_g(j), d_b(l)) = [Y(d_r(i)) - Y_k] + [Y(d_g(j)) - Y_k] + [Y(d_b(l)) - Y_k] + Y_k \quad (7.5)$$

$$Z(d_r(i), d_g(j), d_b(l)) = [Z(d_r(i)) - Z_k] + [Z(d_g(j)) - Z_k] + [Z(d_b(l)) - Z_k] + Z_k \quad (7.6)$$

The transformation between digital *RGB* values and *RGB* device's primaries is as direct as possible if the considered device is a *RGB* primaries device. The X_k , Y_k and Z_k are obtained by accurate measurement of the black level for each device. The $X(d_r(i))$, $X(d_g(j))$, $X(d_b(l))$, $Y(d_r(i))$, $Y(d_g(j))$, $Y(d_b(l))$ and $Z(d_r(i))$, $Z(d_g(j))$, $Z(d_b(l))$ are all obtained by one dimensional linear interpolation with the measurement of a colour ramp along each primary. Post and Calhoun [131, 132] stated that chromaticity error is lower for the PLVC than for the PLCC in low luminance. This is due to the setting of primaries colorimetric values at maximum intensity in the PLCC. In the other hand, Jimenez Del Barco *et al.* [79] stated that both models show inaccuracy for high luminance colours due to channel interdependence. Since it takes into account that the chromaticity shift of primaries that is a key feature for characterising LCD displays, Thomas, *et al.* [163] demonstrated that the PLVC model is more accurate than usual linear models (PLCC, GOGO).

7.3 Experimental work

In this chapter, the 20 displays described in Chapter 4 were evaluated. For each display, the Y_{xy} values were measured for the colour channels at each of the 256 steps (in order to implement the PLVC model) and also for the other sets of samples (e.g. Macbeth, Chart4 and Matlab60) that were described in Chapter 4. All the measurements were carried out using the spectroradiometer CS-2000 from Konica Minolta described in Chapter 3. The device was warmed up for at least one hour before any measurement taken place. Experiments were performed in a dark room. The 2 degrees CIE observer and the white point of the display used. Performance was evaluated using median ΔE_{ab}^* primarily on the Macbeth set of samples and is

presented in this Chapter for seven different sub-sampling regimes ($N = 6, 10, 18, 34, 66, 129$ and 256) as was done in the previous Chapter. This allows a comparison between the GOG and PLCC models (Chapter 5 and 6) and the PLVC model.

7.4 Performance of the PLVC model

Table 7.1 summarises the results that were obtained for all the data sets using the PLVC model and the seven levels of sub-sampling ($N = 256, 129, 66, 34, 18, 10, 6$). Table 7.2 illustrates the average results between the three different sets of samples (Chart4, Macbeth and Matlab60) shown in Table 7.1. An increase in the error ΔE_{ab}^* is seen when the number of linearisation samples is reduced, especially when $N < 18$ in most of the displays; however, note that for display *B* the best result is obtained when $N = 10$.

Fig. 7.1 shows the median ΔE_{ab}^* for the Macbeth set of samples (averaged over all 20 displays) as a function of N (the number of linearisation samples) from which it is evident that the performance of the model is relatively stable for values of $N > 18$. Fig. 7.2 illustrates the effect of using a different number of linearisation samples with all sample sets (Chart4, Macbeth and Matlab60) using the PLVC model. It is evident that there are not more differences in the results of using either 256 nor 18 number of linearisation samples for the PLVC model. However, display *B*, *C*, *F*, and *H* give a better performance with the 18 number of linearisation samples. In summary, there is trade-off point of 18 samples when using the PLVC model.

Table 7.1 Median ΔE_{ab}^* values for all displays testing all sets of samples for N=256, 129, 66, 34, 18, 10 and 6 sub-sampling using PLVC model.

		PLVC																				
		N=256			N=129			N=66			N=34			N=18			N=10			N=6		
	Chart 4	Matlab 60	Mac- beth	Chart 4	Matlab 60	Mac- beth	Chart 4	Matlab 60	Mac- beth	Chart 4	Matlab 60	Mac- beth	Chart 4	Matlab 60	Mac- beth	Chart 4	Matlab 60	Mac- beth	Chart 4	Matlab 60	Mac- beth	
A	1.00	0.66	1.07	0.96	0.68	0.95	0.98	0.67	1.07	0.61	1.00	0.62	0.95	0.93	0.81	1.00	1.38	0.81	1.12	1.38	2.29	3.00
B	1.26	1.18	1.18	1.23	1.18	1.19	1.24	1.15	1.29	1.16	1.17	1.14	1.14	1.20	0.86	1.00	1.35	0.86	1.56	1.35	1.82	3.45
C	0.96	0.98	1.30	0.93	0.91	1.31	0.96	0.91	0.95	0.94	1.27	0.85	0.85	1.26	0.84	1.48	1.68	0.84	2.49	1.68	2.35	3.38
D	0.85	0.64	1.03	0.84	0.63	0.96	0.82	0.63	0.82	0.61	0.99	0.82	0.82	0.99	0.73	1.18	1.42	0.73	2.04	1.42	2.21	3.56
E	1.42	1.65	1.83	1.43	1.66	1.81	1.44	1.66	1.84	1.46	1.84	1.52	1.63	1.84	1.75	1.62	1.75	1.75	2.06	2.06	2.75	4.34
F	1.16	1.23	1.39	1.16	1.24	1.41	1.16	1.24	1.40	1.16	1.22	1.36	1.17	1.41	1.28	1.20	1.51	1.28	2.30	2.30	2.31	3.27
G	2.11	1.66	2.29	2.04	1.66	2.32	2.04	1.67	2.29	2.03	2.25	2.05	2.05	2.24	2.12	2.12	2.35	2.12	2.38	2.38	2.78	3.17
H	1.65	1.54	1.86	1.68	1.60	1.89	1.72	1.57	1.86	1.72	1.87	1.70	1.53	1.91	1.68	1.67	2.12	1.68	2.06	2.12	2.63	3.39
I	0.72	0.79	1.05	0.77	0.79	1.10	0.80	0.78	1.11	0.81	1.12	0.84	0.84	1.27	1.00	1.00	1.83	1.00	1.64	2.00	2.00	2.79
J	1.00	1.28	1.46	1.01	1.30	1.42	1.16	1.24	1.44	1.23	1.45	1.53	1.33	1.46	1.21	1.58	1.80	1.21	1.95	2.24	2.24	2.81
K	1.79	1.56	2.02	2.20	1.88	2.15	2.35	1.95	2.41	1.72	2.32	1.77	2.01	2.48	2.11	2.53	2.66	2.11	2.77	2.86	3.42	3.42
L	1.52	1.57	1.74	1.61	1.56	1.80	1.62	1.65	1.81	1.57	1.82	1.64	1.64	1.97	1.81	1.89	2.62	1.81	2.13	2.44	2.44	3.23
M	1.77	0.95	1.13	1.78	0.97	1.10	1.78	0.94	1.13	1.81	1.13	1.96	0.92	1.16	0.97	1.23	1.63	0.97	1.63	2.15	2.15	2.55
N	1.98	1.95	2.12	1.95	1.79	2.17	2.10	1.81	2.17	2.40	1.80	2.62	1.92	2.43	3.35	3.35	2.58	1.96	3.57	3.11	3.11	3.64
O	0.82	0.91	1.75	0.92	0.90	1.82	0.90	0.86	1.78	0.98	1.80	0.88	0.88	1.85	1.09	1.34	2.15	1.34	1.98	2.78	2.78	3.89
P	0.78	0.80	1.19	0.78	0.80	1.20	0.78	0.77	1.30	0.77	1.31	0.85	0.85	1.46	1.11	1.00	2.23	1.11	1.95	1.86	3.34	3.34
Q	6.53	3.67	3.77	6.66	3.62	3.65	6.62	3.55	3.68	6.40	3.56	6.45	3.73	3.68	6.77	3.84	3.70	6.77	7.09	3.93	3.93	3.99
R	7.82	4.27	4.51	8.10	4.28	4.50	8.13	4.63	4.55	8.31	4.68	8.40	4.75	4.70	8.95	4.81	4.81	8.95	9.10	5.06	5.06	5.20
S	3.17	3.51	3.87	3.12	3.51	3.75	3.07	3.51	3.79	3.13	3.52	3.01	3.62	3.99	2.84	3.62	4.20	2.84	3.33	3.33	3.39	5.12
T	3.15	3.40	3.41	3.20	3.42	3.44	3.24	3.39	3.45	3.24	3.45	3.26	3.45	3.45	3.29	3.54	3.74	3.29	3.76	3.60	3.60	4.61

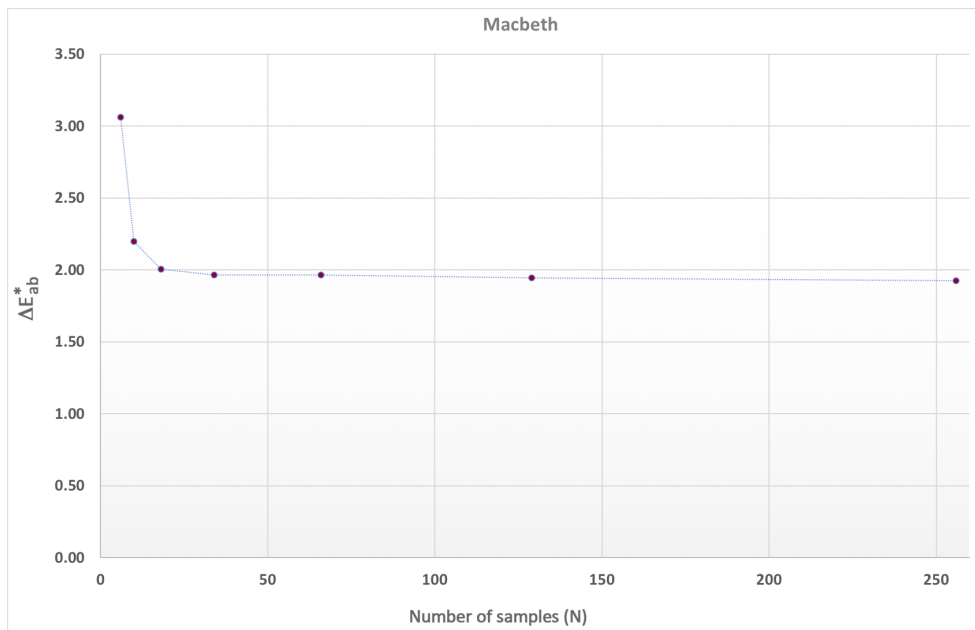


Fig. 7.1 The median ΔE_{ab}^* for the Macbeth chart (averaged over 20 displays) as a function of N (the number of linearisation samples) using PLVC model.

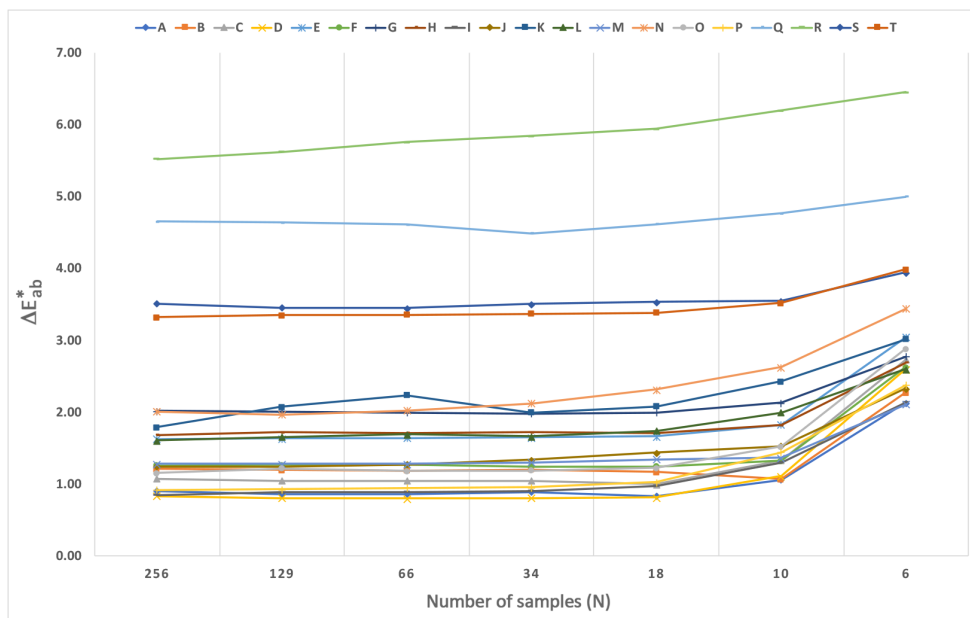


Fig. 7.2 The median ΔE_{ab}^* using all sets of samples (Chart4, Macbeth and Matlab60) as a function of N (the number of linearisation samples).

Table 7.2 The effect of using different sub-sampling sets (N) on the median ΔE_{ab}^* values of using different sets of samples (Chart4, Macbeth and Matlab60) for all displays using PLVC model (the lowest value in each row is highlighted).

Display	256	129	66	34	18	10	6
A	0.91	0.87	0.86	0.89	0.83	1.06	2.14
B	1.21	1.20	1.19	1.21	1.17	1.07	2.28
C	1.08	1.05	1.05	1.05	1.00	1.33	2.74
D	0.84	0.81	0.80	0.81	0.81	1.11	2.60
E	1.63	1.64	1.65	1.65	1.66	1.83	3.05
F	1.26	1.27	1.27	1.25	1.25	1.33	2.63
G	2.02	2.01	2.00	1.99	2.00	2.13	2.78
H	1.69	1.72	1.72	1.72	1.71	1.82	2.69
I	0.85	0.89	0.90	0.91	0.98	1.30	2.14
J	1.25	1.24	1.28	1.34	1.44	1.53	2.33
K	1.79	2.08	2.24	2.00	2.09	2.43	3.02
L	1.61	1.66	1.69	1.67	1.74	2.00	2.60
M	1.28	1.28	1.29	1.30	1.35	1.37	2.11
N	2.02	1.97	2.03	2.12	2.32	2.63	3.44
O	1.16	1.22	1.18	1.19	1.23	1.53	2.88
P	0.92	0.93	0.95	0.96	1.03	1.45	2.38
Q	4.66	4.65	4.62	4.49	4.62	4.77	5.00
R	5.53	5.63	5.77	5.84	5.95	6.20	6.45
S	3.51	3.46	3.45	3.51	3.54	3.55	3.95
T	3.32	3.35	3.36	3.37	3.39	3.53	3.99

7.5 The effect of using different models

In this section, the results from the Macbeth chart will be focussed on in order to allow a clear comparison between the different models that have been evaluated in this thesis. Table 7.3 and 7.4 show the median ΔE_{ab}^* results for the Macbeth sample set for the five models (two GOG models, two PLCC models and PLVC). The data are visualised for each display as Fig. 7.3 and Fig. 7.4.

Table 7.3 and 7.4 also summarises the results from this thesis using the standard Macbeth sample set. The median ΔE_{ab}^* values for the Macbeth chart are shown for each display and for each of the five models (at each of the seven sub-sampling values). The best-performing model for each display has been highlighted at each value of N (number of linearisation samples). Clearly, there is no single model that is guaranteed to give the best performance. Note that for almost every display it is possible to reach ΔE_{ab}^* values that are less than 1.5 ($\Delta E_{ab}^* < 1.5$, 90%) or $\Delta E_{ab}^* < 1.0$ (75%); however, the model that yields the best performance is difficult to ascertain in advance (a good strategy would be to evaluate all five models and select the one that performs best for the characterisation of any particular display). However, a number of observations can be made:

1. increasing the number of samples used for the linearisation allows increasingly better results to be obtained (for best results all 256 levels should be used);
2. for the PLCC model using the grey samples rather than the colour samples in the linearisation produces better results;
3. if fewer than 10 linearisation samples are used then GOG may be the best-performing model (and it is unclear whether grey or colour linearisation samples should be preferred) but for if more linearisation samples are available GOG is less effective than PLCC and PLVC);
4. when all 256 linearisation samples are used the PLCC model using grey linearisation samples is almost always the best technique. Although much fewer than 256 samples can be used it needs to be understood that is almost always accompanied by a cost of higher characterisation error.

Table 7.3 The median ΔE_{ab}^* results for the Macbeth sample set for the five models (two GOG models, two PLCC models and PLVC) for $N=256$, 129, 66 and 34 sub-sampling data sets.

Display	N=256					N=129					N=66					N=34				
	Grey GOG	Grey PLCC	Colour GOG	Colour PLCC	PLVC	Grey GOG	Grey PLCC	Colour GOG	Colour PLCC	PLVC	Grey GOG	Grey PLCC	Colour GOG	Colour PLCC	PLVC	Grey GOG	Grey PLCC	Colour GOG	Colour PLCC	PLVC
A	1.17	0.40	1.27	0.73	0.66	1.17	0.41	1.27	0.73	0.68	1.16	0.41	1.27	0.71	1.15	0.41	1.28	0.72	0.61	
B	1.00	0.79	0.90	1.00	1.18	1.00	0.77	0.89	0.98	1.18	1.01	0.75	0.88	0.92	1.15	0.74	0.88	0.95	1.16	
C	5.42	0.86	6.11	2.61	0.98	5.41	0.84	6.11	2.62	0.91	5.39	0.83	6.13	2.58	0.91	5.40	6.15	2.61	0.94	
D	4.64	0.97	4.75	2.57	0.64	4.70	0.97	4.77	2.52	0.63	4.73	0.97	4.76	2.54	0.63	4.68	4.80	2.52	0.61	
E	5.83	1.16	5.45	3.61	1.65	6.09	1.15	5.45	3.60	1.66	6.16	1.16	5.45	3.60	1.66	5.76	5.45	3.61	1.65	
F	4.23	0.91	5.00	3.78	1.23	4.24	0.92	5.01	3.78	1.24	4.17	0.88	5.00	3.78	1.24	4.07	5.02	3.80	1.22	
G	1.53	0.74	1.67	1.55	1.66	1.53	0.74	1.68	1.55	1.66	1.52	0.69	1.67	1.61	1.67	1.50	1.67	1.58	1.67	
H	2.42	0.71	2.48	2.06	1.54	2.44	0.69	2.48	2.06	1.60	2.27	0.72	2.49	2.11	1.57	2.12	2.09	1.57	1.67	
I	1.34	0.47	1.46	1.54	0.79	1.35	0.47	1.45	1.54	0.79	1.34	0.49	1.44	1.54	0.78	1.34	1.43	1.53	0.81	
J	1.62	0.71	2.38	2.23	1.28	1.62	0.80	2.39	2.33	1.30	1.58	0.82	2.39	2.27	1.24	1.62	2.36	2.24	1.34	
K	0.96	0.57	0.93	0.88	1.56	0.93	0.49	0.94	0.93	1.88	0.89	0.52	0.95	0.87	1.95	0.90	0.53	0.93	1.97	
L	1.84	0.86	0.90	0.83	1.57	1.84	0.88	0.91	0.85	1.56	1.84	0.85	0.93	0.90	1.65	1.84	0.85	0.92	1.62	
M	1.31	0.64	1.62	1.16	0.95	1.28	0.62	1.62	1.22	0.97	1.27	0.62	1.63	1.21	0.94	1.25	1.65	1.17	0.96	
N	2.84	0.58	1.60	0.87	1.95	2.85	0.59	1.61	0.88	1.79	2.84	0.59	1.62	0.87	1.81	2.85	1.61	0.85	1.80	
O	2.32	0.25	2.38	0.30	0.91	2.32	0.28	2.38	0.39	0.90	2.33	0.44	2.38	0.44	0.86	2.33	0.42	0.36	0.80	
P	3.61	0.44	3.63	0.47	0.80	3.58	0.45	3.53	0.47	0.80	3.60	0.45	3.70	0.47	0.77	4.12	4.16	0.45	0.79	
Q	1.12	0.47	1.28	1.13	3.67	1.13	0.52	1.27	1.12	3.62	1.11	0.57	1.27	0.89	1.09	1.09	1.30	0.87	3.52	
R	2.51	0.33	2.47	2.22	4.27	2.48	0.50	2.48	2.15	4.28	2.57	0.53	2.45	2.09	2.45	2.45	2.42	1.94	4.68	
S	4.40	1.71	5.16	4.27	3.51	4.41	1.71	5.13	4.28	3.51	4.35	1.68	5.07	4.28	4.12	4.12	4.93	4.28	3.52	
T	2.98	1.07	4.16	3.48	3.40	2.98	1.08	4.16	3.48	3.42	2.96	1.09	4.17	3.53	2.96	2.96	4.18	3.55	3.45	

Table 7.4 The median ΔE_{ab}^* results for the Macbeth sample set for the five models (two GOG models, two PLCC models and PLVC) for $N=18$, 10 and 6 sub-sampling data sets.

Display	N=18					N=10					N=6				
	Grey GOG	Grey PLCC	Colour GOG	Colour PLCC	PLVC	Grey GOG	Grey PLCC	Colour GOG	Colour PLCC	PLVC	Grey GOG	Grey PLCC	Colour GOG	Colour PLCC	PLVC
A	1.13	0.41	1.24	0.65	0.62	1.22	0.79	1.22	0.69	0.81	1.06	2.29	1.05	2.09	2.29
B	0.97	0.73	0.88	0.80	1.16	0.86	0.79	0.90	0.71	0.86	0.68	2.01	0.93	1.74	1.82
C	5.45	0.87	6.19	2.59	0.89	5.56	1.51	5.82	2.61	0.84	2.36	3.18	2.49	2.97	2.35
D	4.92	0.80	4.94	2.56	0.63	5.15	1.12	5.11	2.89	0.73	4.66	2.20	5.38	2.96	2.21
E	5.80	1.16	5.49	3.47	1.63	5.92	1.49	5.30	3.67	1.75	5.73	2.74	5.12	4.91	2.75
F	4.08	0.83	5.08	3.75	1.16	4.54	1.07	4.83	3.50	1.28	3.83	2.54	4.86	4.60	2.31
G	1.46	0.65	1.66	1.60	1.71	1.39	0.79	1.64	1.53	1.92	1.08	2.11	1.65	2.55	2.78
H	2.01	0.79	2.49	2.07	1.53	2.48	1.12	2.39	2.01	1.68	2.47	1.94	2.64	2.19	2.63
I	1.39	0.40	1.45	1.61	0.82	1.08	0.98	1.51	1.83	1.07	1.71	2.11	1.43	2.35	2.00
J	1.61	0.72	2.37	2.27	1.33	1.55	1.28	2.40	2.45	1.21	1.49	2.69	2.22	2.86	2.24
K	0.91	0.54	0.94	0.78	2.01	0.75	0.71	0.98	0.95	2.53	0.74	2.40	0.95	2.30	2.86
L	1.84	0.74	0.87	0.81	1.61	1.84	1.07	0.84	1.13	1.56	1.73	2.21	0.96	1.96	2.44
M	1.21	0.61	1.69	1.08	0.92	2.42	1.33	1.72	0.86	0.97	1.09	2.26	1.62	1.79	2.15
N	2.81	0.61	1.58	0.89	1.92	2.42	1.21	1.42	0.96	1.96	1.42	2.56	1.36	2.18	3.11
O	2.33	0.31	2.39	0.45	0.96	2.08	0.59	2.27	0.69	1.34	1.66	2.21	1.79	2.20	2.78
P	4.24	0.46	4.28	0.49	0.77	3.85	0.76	3.94	0.73	1.00	3.69	1.74	3.48	1.69	1.86
Q	1.07	0.59	1.31	0.96	3.73	1.15	0.66	1.21	0.95	3.84	1.28	0.92	1.26	1.11	3.93
R	2.70	0.58	2.26	1.91	4.75	2.78	0.84	2.45	2.07	4.84	2.51	1.22	2.57	2.19	5.06
S	4.33	1.68	5.21	4.22	3.62	3.92	1.85	5.23	4.12	3.62	6.10	3.12	10.48	3.92	3.39
T	2.68	1.01	4.22	3.54	3.45	2.96	1.45	4.19	3.54	3.54	2.19	2.60	4.01	3.44	3.60



Fig. 7.3 The average ΔE_{ab}^* for the Macbeth sample set for display A – J as a function of N (the number of linearisation samples).

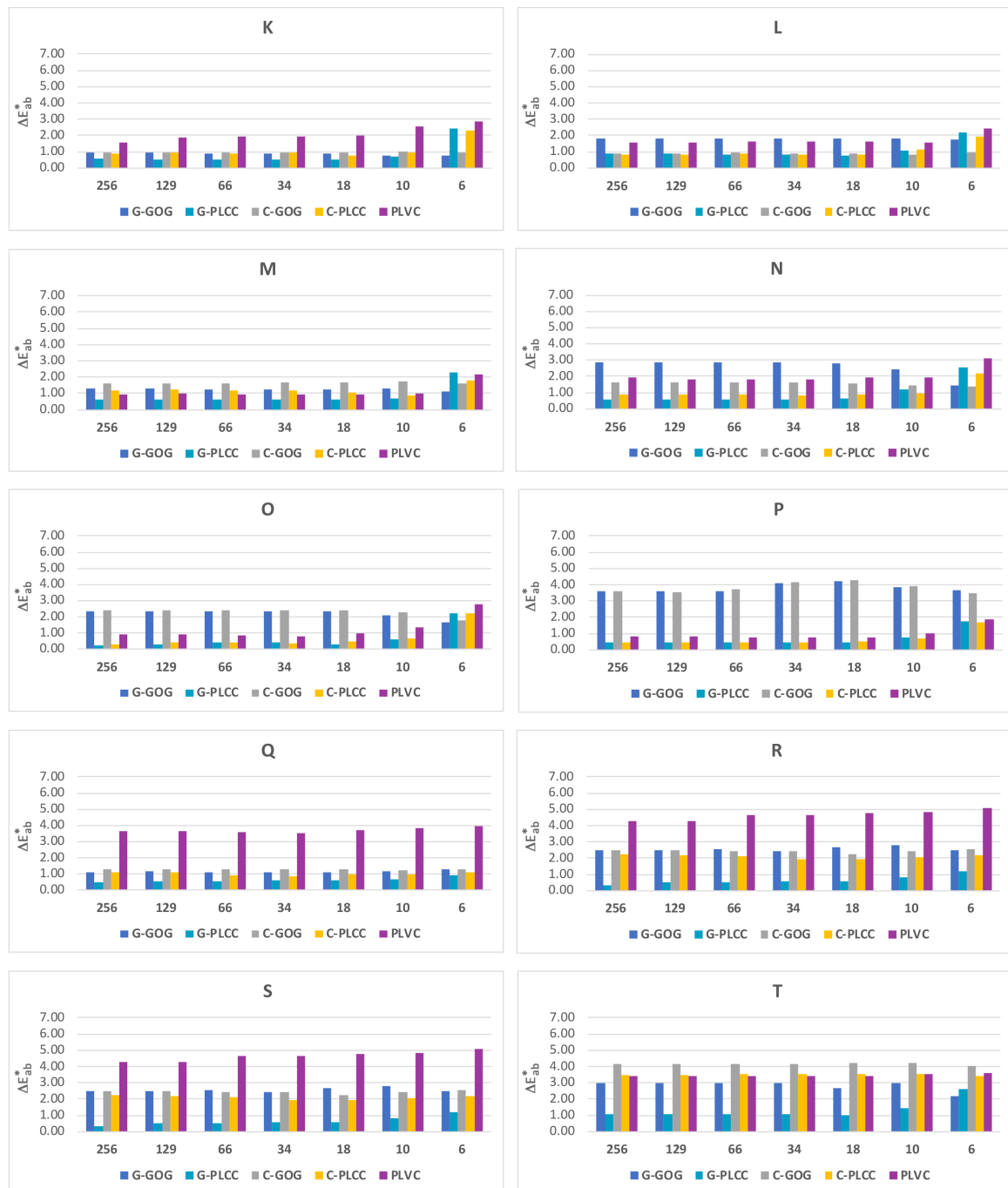


Fig. 7.4 The average ΔE_{ab}^* for the Macbeth sample set for display $K - T$ as a function of N (the number of linearisation samples).

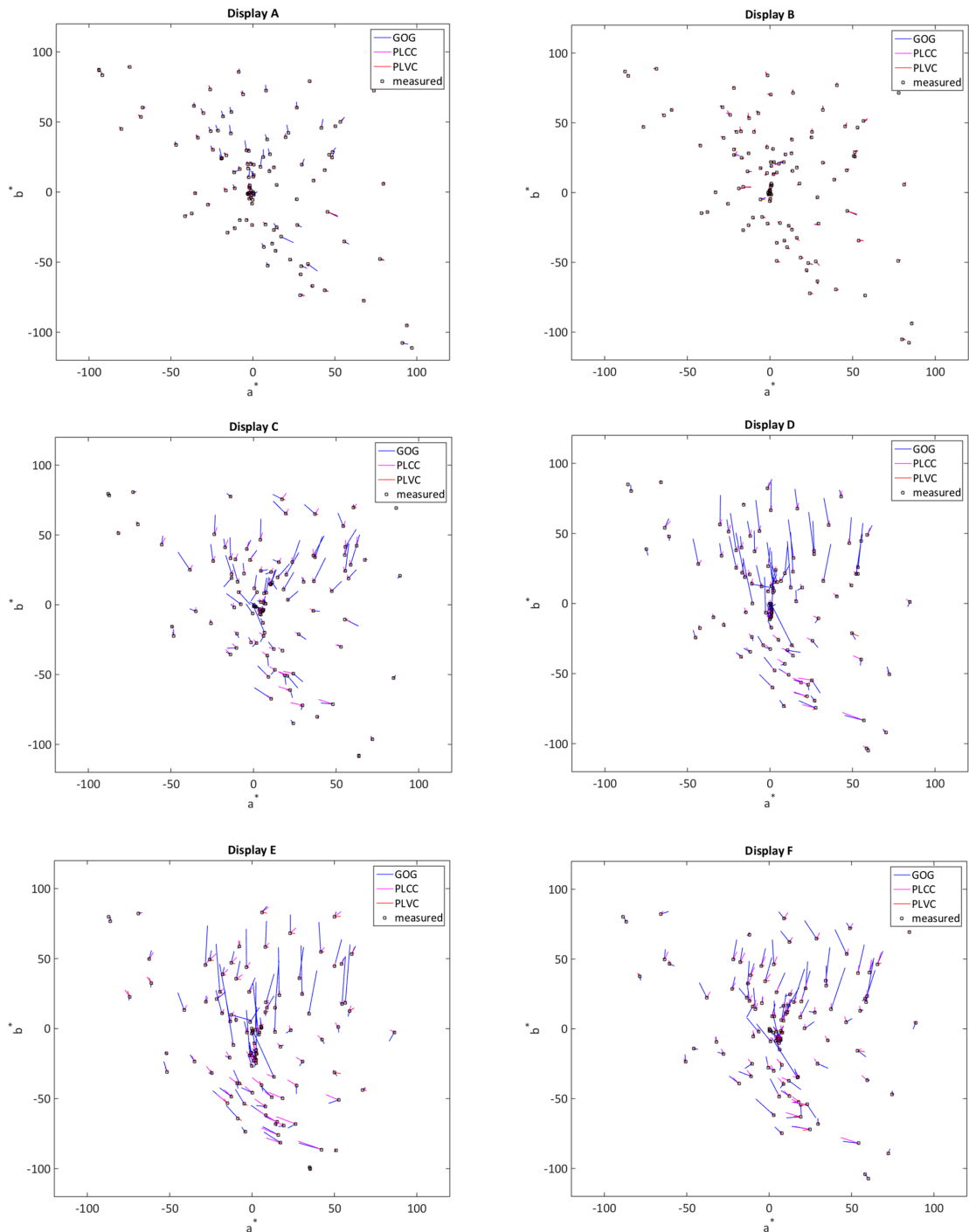


Fig. 7.5 Visualisation of errors using three different models (GOG, PLCC and PLVC) for all three testing sample sets on the a^*b^* diagram for displays A – F.

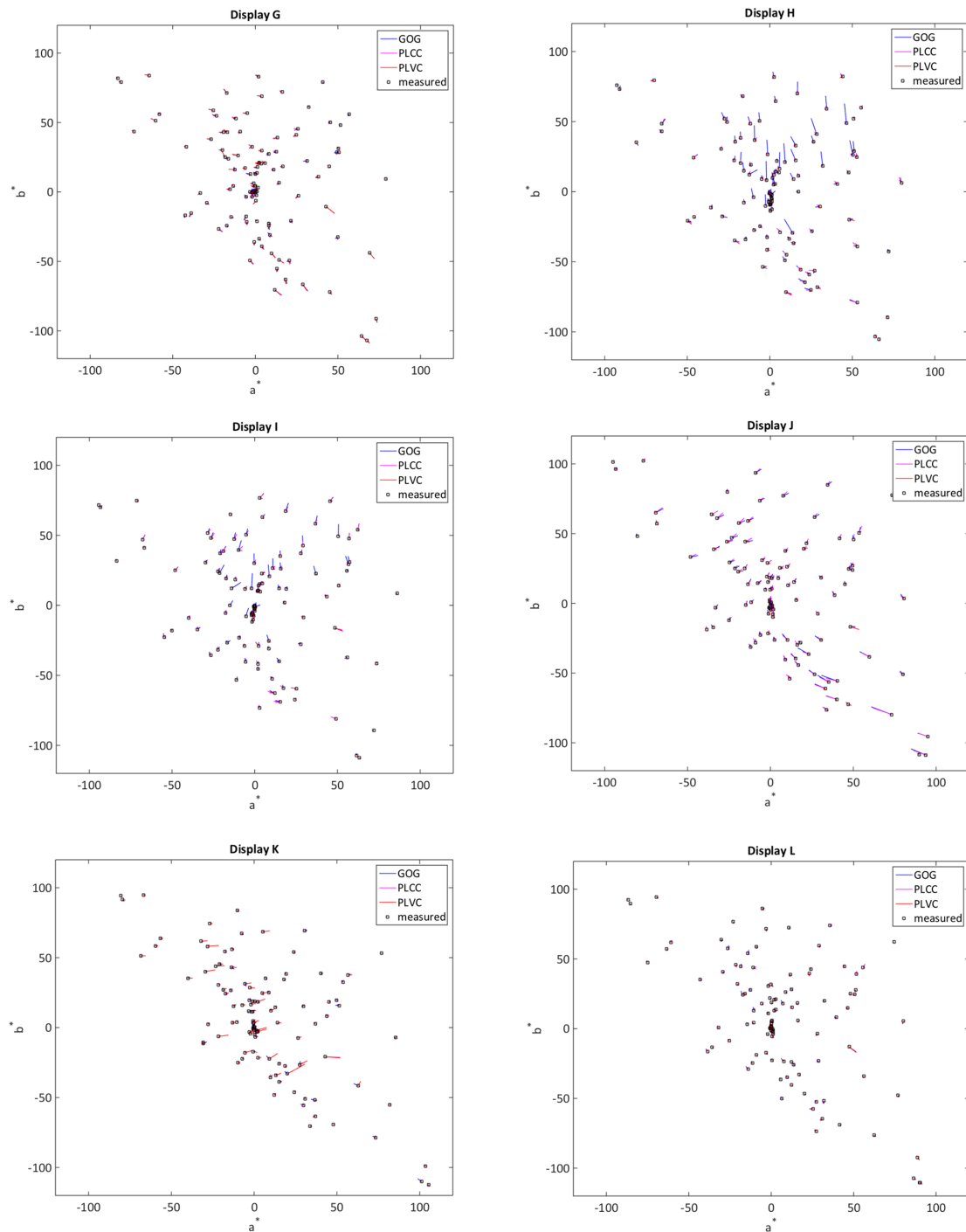


Fig. 7.6 Visualisation of errors using three different models (GOG, PLCC and PLVC) for all three testing sample sets on the a^*b^* diagram for displays $G - L$.

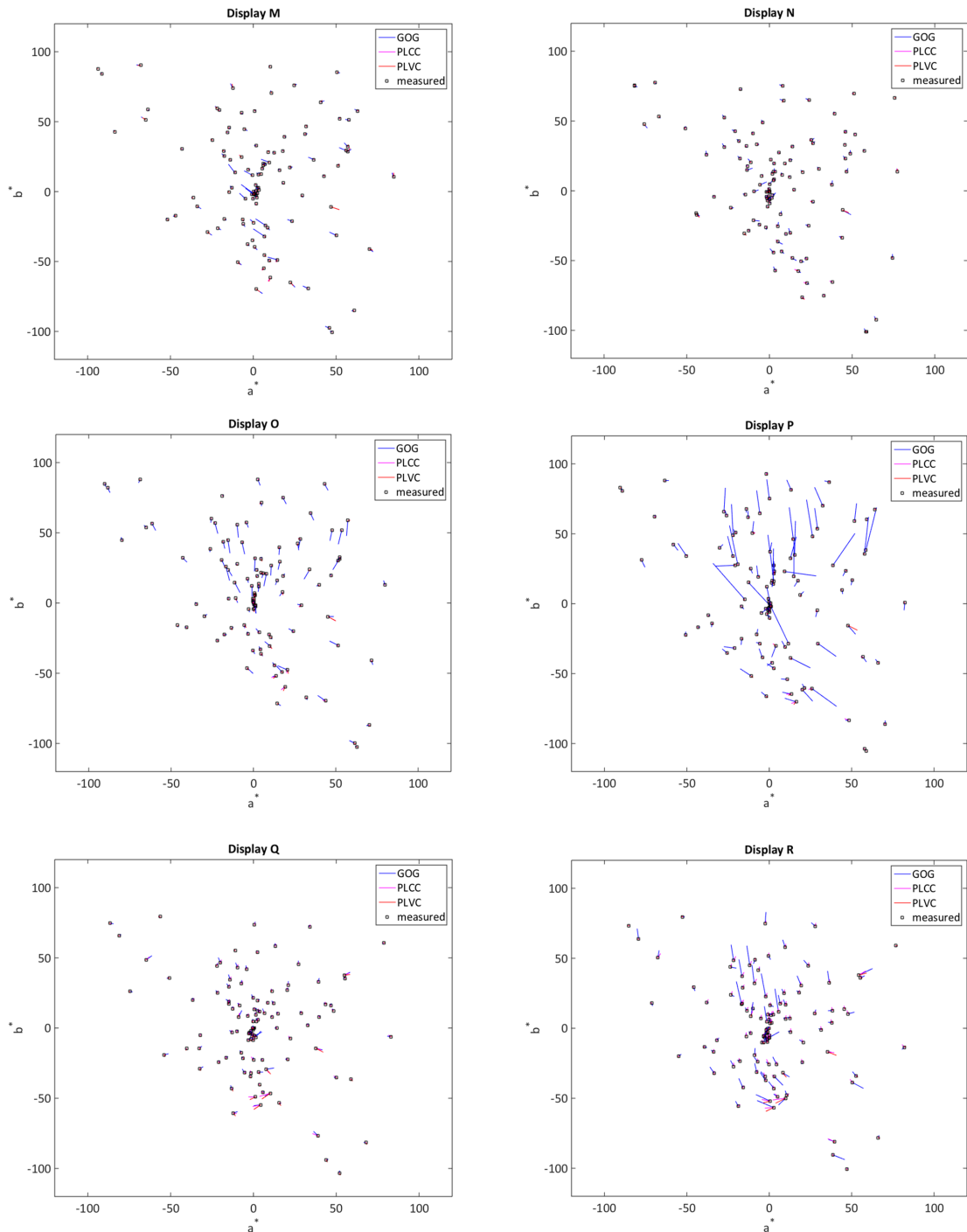


Fig. 7.7 Visualisation of errors using three different models (GOG, PLCC and PLVC) for all three testing sample sets on the a^*b^* diagram for displays $M - R$.

Fig 7.5- 7.8 illustrates the location of errors in the device gamut using three different models (GOG, PLCC and PLVC) for all three different sets of samples

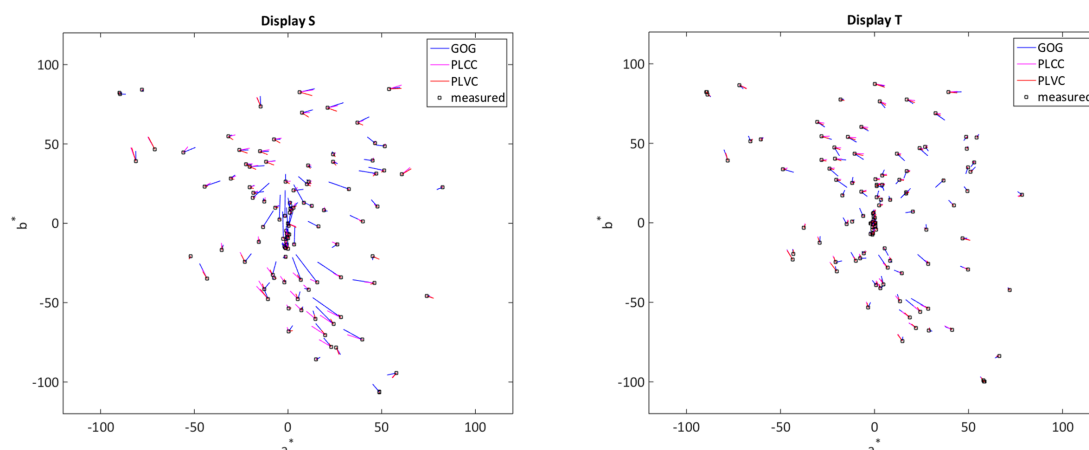


Fig. 7.8 Visualisation of errors using three different models (GOG, PLCC and PLVC) for all three testing sample sets on the a^*b^* diagram for displays *S* and *T*.

(Chart4, Macbeth and Matlab60) using 256 colour-ramps linearisation samples on the a^*b^* diagram for all 20 display devices.

It is evident that the most errors for the *C*, *D*, *E*, *F*, *P* and *S* displays are for the GOG model, which is shown by the blue line. The error location for display *D* is mainly along the $+b^*$ and $-b^*$ (blue/yellow) area. It is difficult to find any systematic type of errors about the PLCC model, as they are really small in the a^*b^* diagram in most of the displays. However, in *C*, *D*, *E*, *F*, *R* and *S* very minor errors can be seen along the a^* line. The PLVC errors cannot be found easily in majority of display, However, display *K* shows the biggest PLVC errors along the $+a^*$ line while there are no noticeable errors for the same display using the GOG and PLCC models. Furthermore, there are no noticeable errors in the a^*b^* diagram for displays *L* and *N* (the same pattern can be seen with the *Q* and *B* displays with very minor errors).

The C^*L^* diagram is illustrated in Fig 7.9- 7.12 for all 20 display devices using three different model, GOG, PLCC and PLVC with all 256 step of linearisation colour-ramps samples. This diagram is mainly looking at the luminance factor in each display. For displays *A*, *C*, *D*, *E*, *F*, *H*, *M*, *O*, *P*, *S* and *T* from high to medium luminance, the accuracy is good, while the results are getting worst when the luminance is low. Display *S* shows the worst shifting in the luminance. It is evident that in a majority of the displays the errors of using GOG model appears

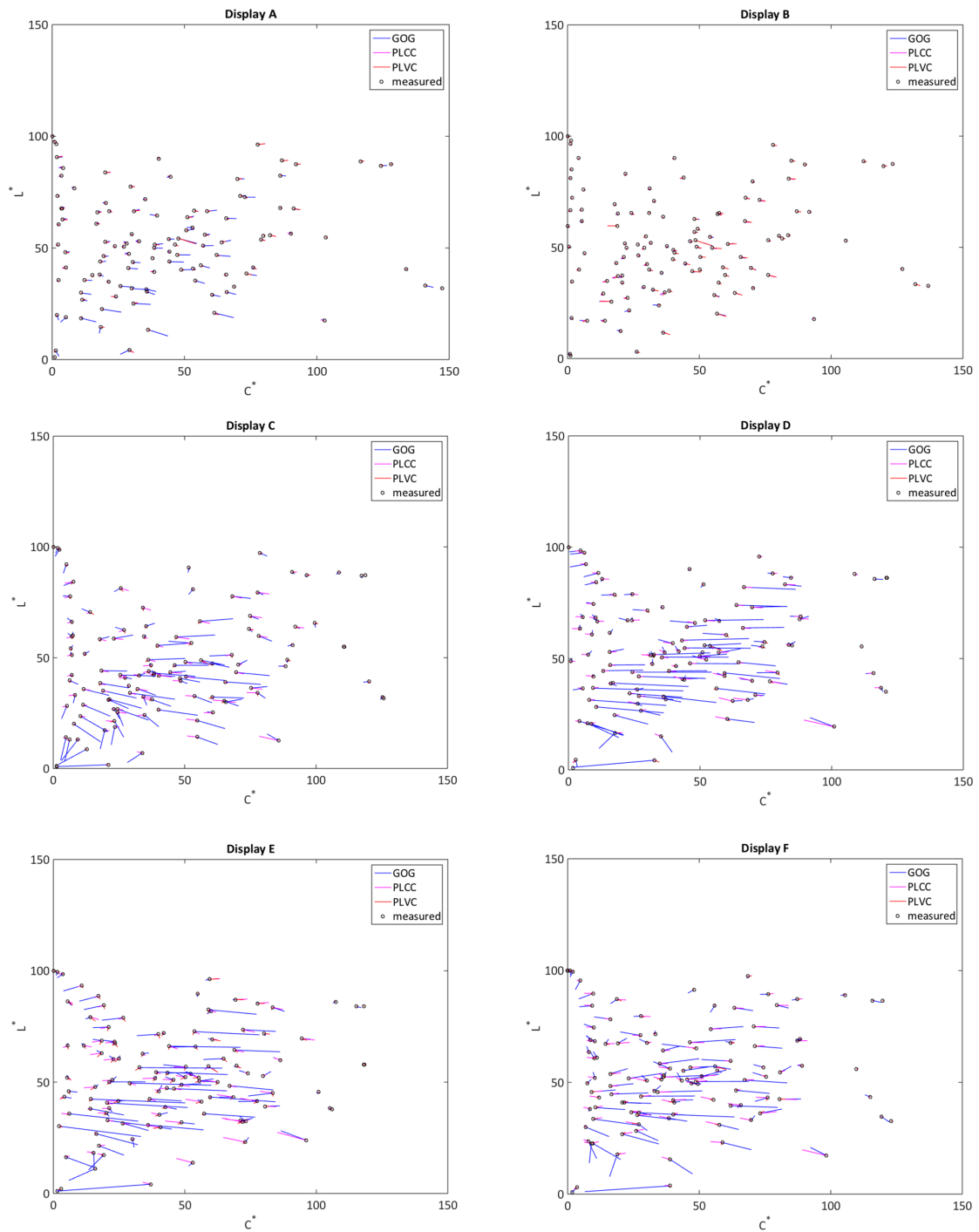


Fig. 7.9 Visualisation of errors using three different models (GOG, PLCC and PLVC) for all three testing sample sets on the C^*L^* diagram for displays A – F.

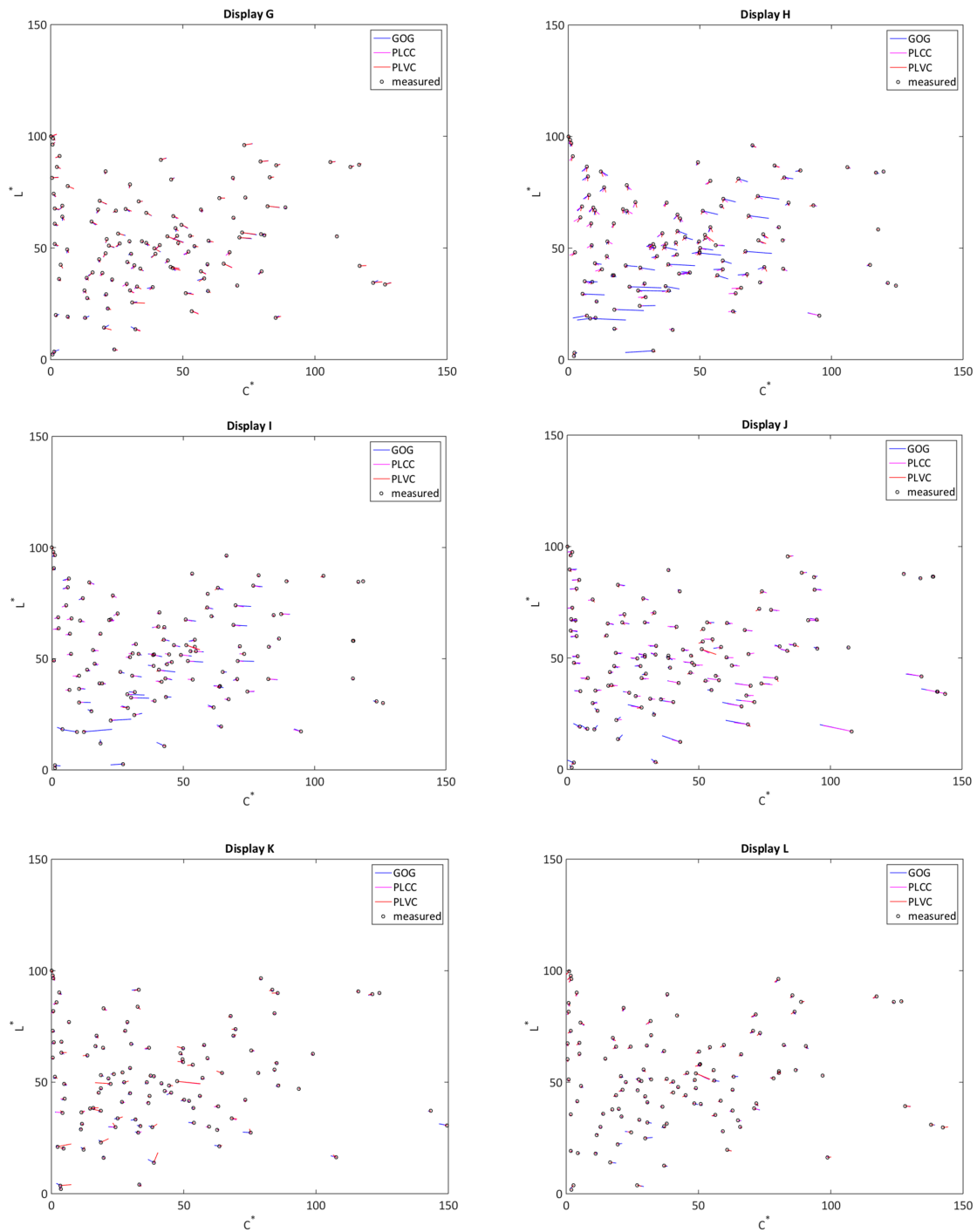


Fig. 7.10 Visualisation of errors using three different models (GOG, PLCC and PLVC) for all three testing sample sets on the C^*L^* diagram for displays G – L.

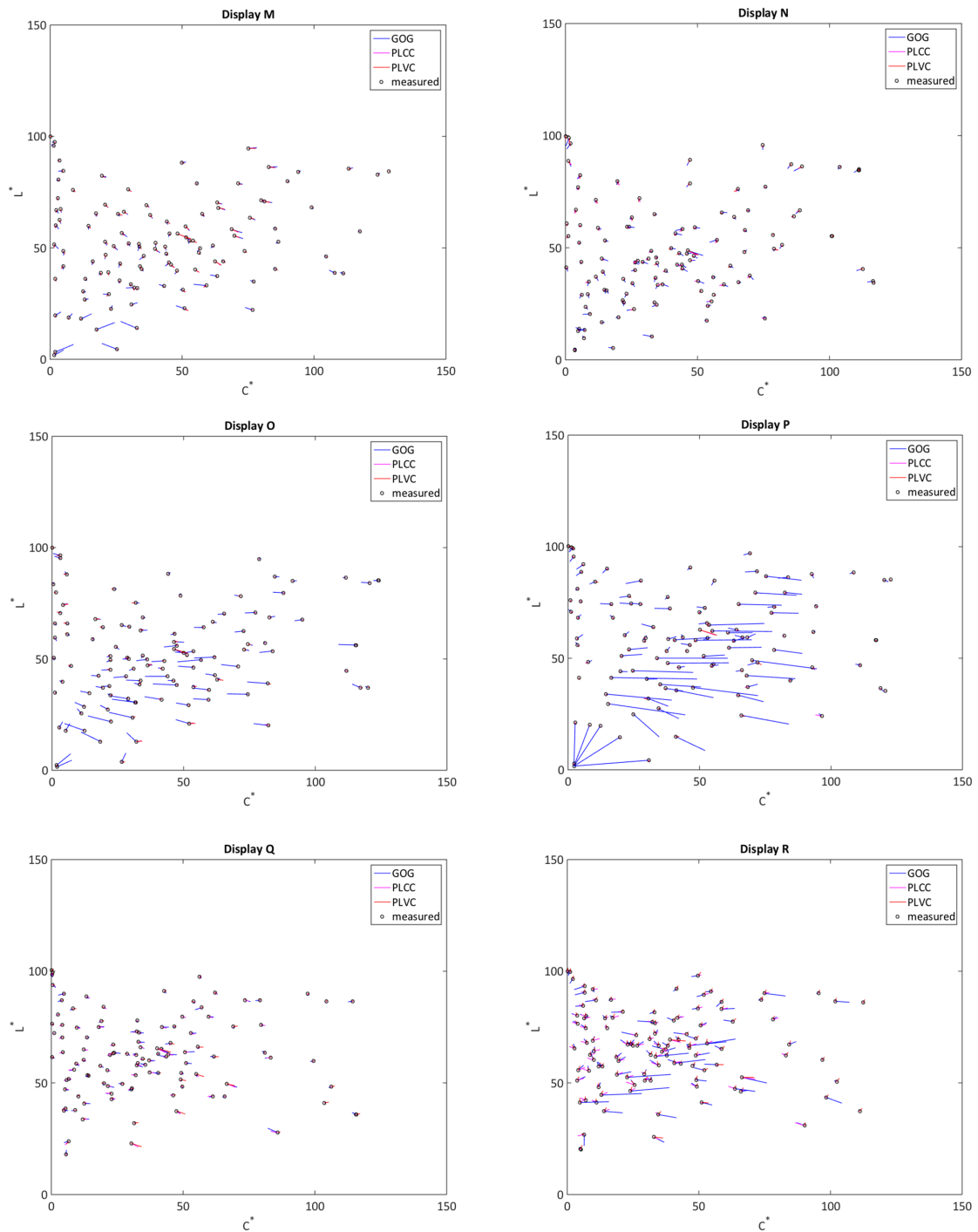


Fig. 7.11 Visualisation of errors using three different models (GOG, PLCC and PLVC) for all three testing sample sets on the C^*L^* diagram for displays M – R.

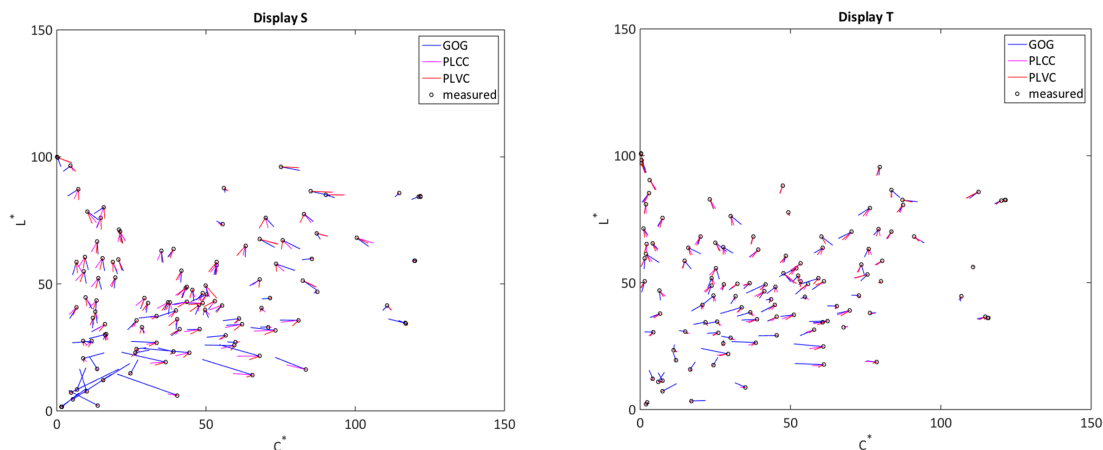


Fig. 7.12 Visualisation of errors using three different models (GOG, PLCC and PLVC) for all three testing sample sets on the C^*L^* diagram for displays S and T .

mainly in medium or low luminance area. The measured luminance is higher than the estimated one when there is a difference in using any models (e.g. display S).

The location of errors appears to be different for different displays. The interdependence between channels could explain these differences in behaviours. Yoshida and Yamamoto [183] claim that the luminance shift follows the shape of the derivative of an S-shape curve.

7.6 Conclusion

This chapter summarises the results that were obtained for all the data sets using the PLVC model and the seven levels of sub-sampling ($N = 256, 129, 66, 34, 18, 10, 6$). The median results between the three different sets of samples (Chart4, Macbeth and Matlab60) is shown that there is an increased error of ΔE_{ab}^* by reducing the number of linearisation samples especially when $N < 18$ in most of the displays, however, in display B the best result is obtained when $N = 10$. To evaluate the PLVC model in detail, the results from the Macbeth sample set focussed on in order to allow a clear comparison between the different models that have been evaluated in this thesis. The median ΔE_{ab}^* errors for the Macbeth set of samples (averaged over all 20 displays) as a function of N (the number of linearisation samples) from which it is evident that the performance of the model is relatively stable for values of $N > 18$. The effect of using the different number of samples using the PLVC

model is also evaluated. It is evident that there are not many differences in the results of using either 256 nor 18 number of samples for the PLVC model. However, display *B*, *C*, *F*, and *H* give a better performance with the 18 number of samples. In summary, there is trade point of 18 number of samples in using the PLVC model. In summary, using the PLVC model, resulting in the excellent characterisation performances when $N = 256$ for display *A*, *D*, *I* and *P* ($\Delta E_{ab}^* < 1$), characterisation performances is good for display *B*, *C*, *E*, *F*, *H*, *J*, *K*, *L*, *M* and *O* which $1 < \Delta E_{ab}^* < 2$ and acceptable for *G*, *N*, *S* and *T* $2 < \Delta E_{ab}^* < 4$ and not acceptable for *Q* and *R* as the $\Delta E_{ab}^* > 4$.

This Chapter is also summarised the results of using different models (GOG, PLCC and PLVC) in this thesis. The median ΔE_{ab}^* error unit result values for the Macbeth testing on each display and for all of the five models (at each of the seven sub-sampling linearisation sets) describes clearly that there is no single model that is guaranteed to give the best performance. Note that for almost every display it is possible to reach ΔE_{ab}^* values that are less than 1.5 ($\Delta E_{ab}^* < 1.5$, 90%) or $\Delta E_{ab}^* < 1.0$ (75%); however, the model that yields the best performance is difficult to ascertain in advance (a good strategy would be to evaluate all five models and select the one that performs best for the characterisation of any particular display).

Chapter 8

Effect of background colour on monitor characterisation

8.1 Introduction

In the previous chapters, different methods of display characterisation, as well as the linearisation samples, were described. However, it is known that the colour measurements of the patches may vary with the colour and luminance of the background against which they are displayed. Lack of spatial independence is one of the factors that can cause this phenomenon. This raises the question of what the nature of the background should be for an optimal characterisation of a display system. It is likely that what is optimal will depend upon the intended application of the characterised display (for example, is it being used to display simple images in a psychophysical experiment or more complex images in some other setting). The effect of using grey, white or black backgrounds are well known in the literature [14] and variations in colour as a result of the background are described as lack of spatial independence. There is no evidence, whether motion in the background field could affect the colour of a central calibration patch. One of the background conditions that we have explored is that where the background is not static. Two different experiments have been conducted to test the effect of using different background condition on the colour of calibration patches which describes in this chapter.

8.2 Experiment I






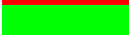








The first experiment considers the effect of using five different background conditions (white, grey, black, Mondrian and a new Mondrian-like coloured background with movement) on colour of a central calibration patches and on the usefulness of the colour characterisation in various imaging scenarios. The HP DreamColour LP2480zx display was used particularly for the first experiment.

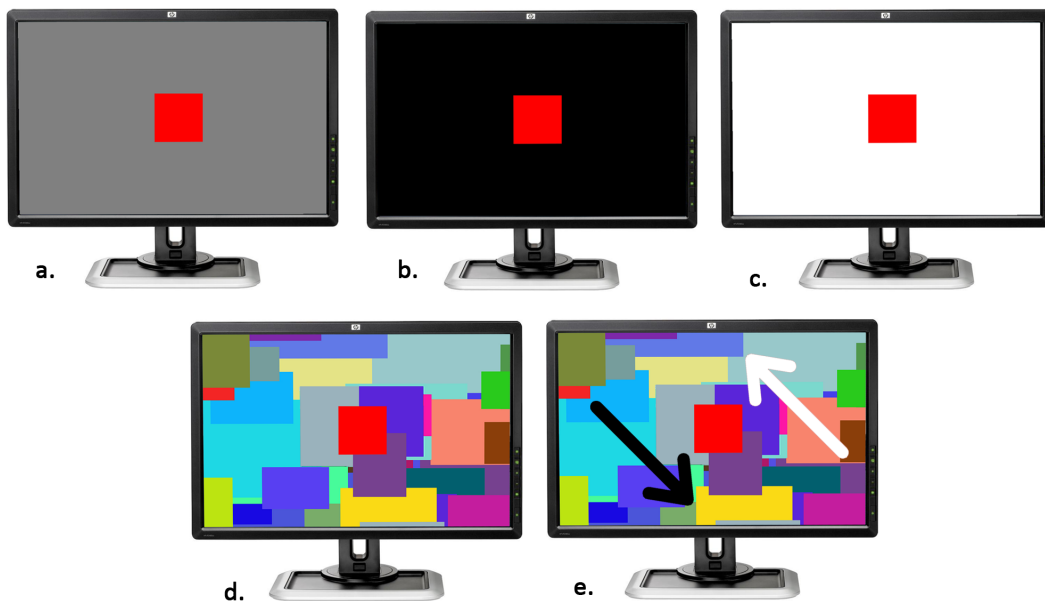
8.2.1 Experimental setting

A PhotoResearch CS-1000 spectroradiometer was used to make measurements of stimuli displayed on a HP DreamColour LP2480zx display housed in a darkened room. Measurements were made using the spectroradiometer mounted on a tripod so that the measuring distance was one meter. Stimuli were generated on the display using a MATLAB GUI so that specific colours (generated with known *RGB* values) with different backgrounds were displayed. The colours were 6cm by 6cm displayed on a background that otherwise filled the display screen. Measurements were made using the spectroradiometer of the centre of the colour stimulus. The spectroradiometer setting was such that the instrument automatically integrated light from the display until a sufficiently accurate reading was taken. Fourteen colours were measured (see Table 8.1 for the *RGB* specifications) and these were chosen to include black, white, different greys, the additive primary colours (red, green and blue) and a few colours where all three primaries were moderately active. Measurements were taken for each colour displayed against five backgrounds: (a) grey, (b) black, (c) white, (d) Mondrian, (e) moving Mondrian. The spectroradiometer measured *CIEXYZ* values (1964 standard observer) which were downloaded to a computer and subsequently analysed.

Fig. 8.1 shows an illustration of a typical colour stimulus displayed against a neutral grey, black, white, Mondrian and moving Mondrian background. The white *RGB* value of $[255, 255, 255]$, the black *RGB* value $[0, 0, 0]$ and the grey background *RGB* values were $[128, 128, 128]$. The Mondrian was generated using a specially developed algorithm and each patch of the Mondrian pattern had a random colour.

Table 8.1 Colour samples of fourteen stimuli.

R	G	B	Colour
0	0	0	
255	255	255	
50	50	50	
128	128	128	
200	200	200	
255	0	0	
0	255	0	
0	0	255	
128	180	50	
128	50	180	
50	128	180	
180	128	50	
50	180	128	
180	50	128	

**Fig. 8.1** Typical colour stimuli displayed against a neutral grey (a), black (b), white (c), Mondrian (d), moving Mondrian (e) background.

8.2.2 Results

Table 8.2- 8.5 shows the *CIEXYZ* values that were measured for each of the colour stimuli in each of the five conditions (background). These values are absolute colorimetric measurements so that the luminance of the white, for example, when displayed on the grey background was 174.67 cd/m^2 . These absolute data are

converted to relative XYZ value and as it illustrates in Table 8.2- 8.5 were converted to CIELAB values (using the white from the grey-background condition as the white point) so that the white for the grey-background condition (only) had values of $L^* = 100$ and $a^* = b^* = 0$. CIELAB (ΔE_{ab}^*) values were computed between the colours with the Mondrian, moving Mondrian, white, black backgrounds and the corresponding colours with the grey background. Table 8.7 shows the colour differences that resulted.

Table 8.2 CIEXYZ measurements of the stimuli and CIELAB values of the grey background condition.






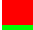
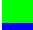







Colour values			Grey background						
R	G	B	X	Y	Z	L*	a*	b*	
0	0	0		0.65	0.63	0.86	3.25	0.68	-1.61
255	255	255		171.23	174.67	184.60	100.00	0.00	0.00
50	50	50		4.98	5.07	5.51	19.64	0.13	-0.56
128	128	128		39.41	40.93	42.60	55.52	-1.88	0.64
200	200	200		106.00	109.83	116.23	83.38	-2.21	-0.08
255	0	0		96.47	44.86	1.91	57.73	95.15	83.59
0	255	0		43.35	116.73	9.34	85.42	-120.83	100.87
0	0	255		33.08	14.76	175.60	34.90	69.64	-108.93
128	180	50		44.28	69.20	9.98	69.20	-48.68	71.24
128	50	180		39.13	20.42	87.28	40.72	61.20	-58.02
50	128	180		29.00	35.89	88.67	52.45	-18.44	-38.60
180	128	50		57.45	49.40	7.99	60.14	19.24	61.03
50	180	128		31.75	63.32	44.50	66.71	-71.38	18.13
180	50	128		55.01	28.03	41.13	47.04	70.71	-12.56

Table 8.3 *CIEXYZ* measurements of the stimuli and *CIELAB* values of the Mondrian background condition.







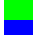







Colour values			Mondrian background						
R	G	B	X	Y	Z	L*	a*	b*	
0	0	0		0.65	0.64	0.92	3.34	0.29	-2.05
255	255	255		171.10	174.60	184.60	99.98	-0.05	-0.03
50	50	50		5.07	5.19	5.53	19.92	-0.20	-0.20
128	128	128		39.48	41.03	42.70	55.57	-1.92	0.64
200	200	200		106.00	109.87	116.30	83.39	-2.26	-0.09
255	0	0		96.35	44.81	1.99	57.70	95.10	82.89
0	255	0		43.43	116.77	9.47	85.43	-120.66	100.57
0	0	255		33.04	14.74	175.47	34.88	69.63	-108.92
128	180	50		44.29	69.22	10.08	69.21	-48.67	71.03
128	50	180		39.17	20.48	87.22	40.78	61.06	-57.87
50	128	180		29.09	35.95	88.63	52.49	-18.30	-38.52
180	128	50		57.42	49.38	8.12	60.13	19.24	60.66
50	180	128		31.81	63.37	44.62	66.73	-71.32	18.05
180	50	128		55.05	28.09	41.25	47.08	70.65	-12.60

Table 8.4 *CIEXYZ* measurements of the stimuli and *CIELAB* values of the black background condition.















Colour values			Black Background						
R	G	B	X	Y	Z	L*	a*	b*	
0	0	0		0.47	0.47	0.65	2.44	0.58	-1.17
255	255	255		170.67	174.23	184.30	99.90	5.46	0.95
50	50	50		4.80	4.91	5.29	19.27	1.61	-0.10
128	128	128		39.33	40.91	42.56	55.50	1.45	1.26
200	200	200		105.93	109.83	116.37	83.38	2.46	0.72
255	0	0		96.01	44.55	1.70	57.57	99.82	85.18
0	255	0		43.15	116.53	9.13	85.36	-117.53	101.75
0	0	255		32.88	14.60	175.30	34.72	73.04	-108.14
128	180	50		44.14	69.15	9.79	69.18	-45.37	72.12
128	50	180		38.96	20.28	87.16	40.59	64.77	-57.38
50	128	180		28.88	35.82	88.57	52.41	-15.54	-37.84
180	128	50		57.30	49.32	7.80	60.10	23.00	61.94
50	180	128		31.65	63.32	44.43	66.71	-68.50	18.82
180	50	128		54.87	27.90	41.06	46.94	74.74	-12.06

Table 8.5 *CIEXYZ* measurements of the stimuli and *CIELAB* values of the white background condition.



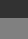
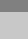










Colour values			White Background						
R	G	B	X	Y	Z	L*	a*	b*	
0	0	0		1.22	1.14	1.56	5.87	3.44	-2.79
255	255	255		171.17	174.73	185.10	100.02	5.48	0.86
50	50	50		5.55	5.58	6.21	20.83	2.51	-0.77
128	128	128		39.81	41.33	43.21	55.75	1.64	1.06
200	200	200		106.20	110.03	116.77	83.44	2.54	0.64
255	0	0		96.53	45.12	2.62	57.88	99.23	79.19
0	255	0		43.86	117.10	10.05	85.52	-116.51	99.64
0	0	255		33.62	15.27	176.17	35.48	71.98	-107.16
128	180	50		44.71	69.57	10.69	69.35	-44.71	70.17
128	50	180		39.55	20.87	87.80	41.14	63.92	-56.82
50	128	180		29.52	36.31	89.22	52.72	-14.81	-37.68
180	128	50		57.70	49.71	8.70	60.30	22.97	59.68
50	180	128		32.26	63.71	45.15	66.89	-67.41	18.46
180	50	128		55.34	28.43	41.80	47.33	74.00	-12.10

Table 8.6 *CIEXYZ* measurements of the stimuli and *CIELAB* values of the moving Mondrian background condition.















Colour values			Moving Mondrian						
R	G	B	X	Y	Z	L*	a*	b*	
0	0	0		0.77	0.75	1.02	3.88	0.73	-2.00
255	255	255		169.29	172.96	183.81	99.62	-0.26	-0.36
50	50	50		4.91	4.98	5.51	19.43	0.29	-0.98
128	128	128		38.61	40.09	41.86	55.02	-1.77	0.50
200	200	200		104.67	108.45	115.15	82.96	-2.22	-0.27
255	0	0		95.07	44.25	2.14	57.40	94.60	81.22
0	255	0		43.07	115.84	9.46	85.16	-120.40	100.15
0	0	255		32.98	14.77	174.73	34.92	69.25	-108.57
128	180	50		43.55	68.26	9.87	68.81	-48.73	70.88
128	50	180		38.51	20.09	86.46	40.41	60.93	-58.06
50	128	180		28.60	35.24	87.78	52.03	-17.89	-38.82
180	128	50		56.55	48.55	7.88	59.70	19.34	60.63
50	180	128		31.28	62.47	43.73	66.34	-71.18	18.22
180	50	128		54.27	27.61	40.59	46.72	70.54	-12.57

Table 8.7 Colour differences between Mondrian- and movie-condition backgrounds and the grey-condition backgrounds as well as the black-condition and white-condition background.

ΔE_{ab}^*					
Grey vs Mon	Grey vs Mov	Grey vs black	Grey vs white	Black vs White	
0.59	0.74	0.93	3.98	4.75	
0.06	0.58	5.54	5.55	0.15	
0.56	0.50	1.59	2.67	1.92	
0.06	0.53	3.39	3.55	0.37	
0.05	0.46	4.74	4.80	0.13	
0.70	2.46	4.94	6.00	6.03	
0.34	0.88	3.42	4.49	2.35	
0.02	0.53	3.50	2.99	1.63	
0.21	0.53	3.43	4.11	2.07	
0.21	0.41	3.63	3.00	1.16	
0.17	0.73	3.00	3.75	0.81	
0.37	0.60	3.87	3.97	2.27	
0.10	0.43	2.96	3.99	1.16	
0.08	0.36	4.06	3.33	0.84	
Average	0.25	0.70	3.50	4.01	1.83





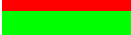














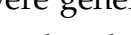
8.3 Experiment II

The second experiment is a wider project to explore characterisation methods for modern display technology. It has been shown in experiment I, that the colour may change with the background. The implication of this is that a characterisation model calculated using one background may not perform well in the case of a different background or in the case of a real image. Therefore, experiment II mainly focused on testing the effect of motion in the background on the colour of a central calibration patch using different display devices. However, some preliminary results based on one display device and a small number of colour stimuli were previously tested and published [167], the effect of motion on the background mainly focussed on this experiment.

8.3.1 Experimental setup

A Konica Minolta CS-1000 spectroradiometer was used to make measurements of stimuli displayed on three displays: HP DreamColour LP2480zx, EIZO ColorEdge CG220 and NEC Multisync 1960Nxi. Measurements were made in a darkened room using the spectroradiometer mounted on a tripod so that the measuring





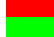
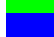













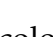
Table 8.8 Colour samples of 20 stimuli.

R	G	B	Colour
50	50	50	
255	255	255	
128	128	128	
200	200	200	
255	0	0	
0	255	0	
0	0	255	
0	255	255	
255	0	255	
255	255	0	
128	180	50	
235	225	150	
50	128	180	
180	128	50	
50	180	128	
125	0	10	
245	85	10	
205	165	255	
115	45	0	
0	0	0	

distance was fixed at one meter. Stimuli were generated on the display using a MATLAB GUI. Twenty colours were measured and these were chosen to include black, white, different greys, the additive primary colours (red, green and blue), secondary colours (cyan, magenta and yellow) and a few colours where all three primaries were moderately active. Table 8.8 shows the specific colours (generated with known *RGB* values). Measurements were taken for each colour displayed against two backgrounds: (d) Mondrian and (e) Mondrian with movement (Fig. 8.1). The colour patches were 6 cm by 6 cm displayed on a background that otherwise filled the display screen. Measurements were made using the spectroradiometer from the centre of each colour stimulus.

Fig. 8.1 (d and e) shows an illustration of a typical colour stimulus displayed against Mondrian-like background. In one condition (Mondrian) the background is static whereas in the other condition (Movie) the Mondrian-like background pattern drifts diagonally across the screen at a rate of about 0.01 m/s. In both conditions, the central patch (stimulus) remains stationary. The Mondrian was generated using a specially developed algorithm so that each patch of the Mondrian pattern had a random colour and size (within certain constraints). The central patches were measured and the measurements were compared using the *CIELAB*

Table 8.9 XYZ values for measuring the Mondrian condition of 20 stimuli.

	Mondrian Background								
	HP			EIZO			NEC		
	X	Y	Z	X	Y	Z	X	Y	Z
	2.91	2.95	3.29	3.67	3.74	3.84	2.62	2.71	3.09
	98.51	100.00	107.04	98.02	100.00	110.83	96.38	100.00	107.86
	22.80	23.64	24.91	23.33	23.68	25.77	23.47	24.70	26.72
	61.17	63.14	67.78	59.07	59.66	66.68	59.71	62.17	68.44
	59.39	26.34	1.20	61.42	31.78	2.15	47.31	25.32	1.20
	21.20	69.32	7.34	19.25	62.28	6.77	31.69	66.06	10.39
	19.08	5.44	99.99	19.53	9.04	104.38	18.15	9.32	97.48
	39.74	74.19	106.59	37.70	69.72	109.59	49.43	75.06	107.34
	77.81	31.24	100.47	79.95	39.99	105.67	65.12	34.28	98.19
	80.09	95.13	7.95	79.93	92.73	8.15	78.76	91.21	10.92
	24.61	41.09	6.79	24.18	36.55	7.09	27.52	39.43	7.92
	73.47	79.86	39.46	71.77	75.08	40.27	71.08	76.69	41.24
	16.02	19.75	51.22	15.69	19.39	50.11	18.23	21.77	52.09
	34.12	29.18	5.15	34.12	29.33	5.94	31.37	29.07	5.54
	16.57	36.94	26.53	15.61	31.98	26.76	21.47	36.10	29.17
	12.74	5.81	0.78	13.26	7.08	1.10	10.75	5.88	0.80
	56.53	30.47	1.82	58.10	34.76	2.62	46.84	29.55	2.05
	63.53	50.08	103.14	63.12	51.64	107.07	59.94	51.93	102.54
	11.11	6.27	0.84	11.85	7.61	1.12	9.52	6.17	0.98
	0.42	0.39	0.60	0.63	0.62	0.76	0.45	0.42	0.67

(ΔE_{ab}^*) colour-difference equations. Measurements were made three times for each of the three displays and each of the two conditions. The order of measurement was totally randomised each time. The XYZ values were averaged for each display and monitor and were then multiplied by $100/Y_W$ where Y_W was the Y (cd/m^2) value of the white sample so that $Y = 100$ (cd/m^2) for the white in each case.

8.3.2 Results

Tables 8.9 and 8.10 show the average relative XYZ values of the colour patches for each of the three displays for the Mondrian and Movie conditions respectively. Table 8.11 shows the *CIELAB* (ΔE_{ab}^*) colour differences between the Mondrian and Movie conditions for each of the three monitors. The average colour differences are 0.50, 0.62 and 0.77 for the HP, EIZO and NEC displays respectively.

Fig. 8.2 shows a plot of the difference between the Mondrian and Movie condition against the Y value of the Mondrian condition for the HP display. The

Table 8.10 XYZ values for measuring the Mondrian with moving condition of 20 stimuli.





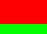
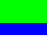

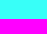











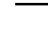



















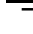
Moving Mondrian Background									
	HP			EIZO			NEC		
	X	Y	Z	X	Y	Z	X	Y	Z
	3.00	3.03	3.29	4.82	4.86	5.28	3.88	3.91	4.25
	98.64	100.00	107.09	98.12	100.00	110.93	96.42	100.00	108.36
	22.51	23.27	24.53	23.12	23.40	25.74	23.15	24.36	26.46
	60.99	62.83	67.41	58.90	59.53	66.54	59.98	62.46	69.03
	59.26	26.31	1.23	61.50	31.82	2.16	47.16	25.22	1.19
	21.17	69.16	7.38	19.28	62.26	6.84	31.64	66.01	10.37
	19.10	5.43	99.95	19.55	9.05	104.36	18.24	9.33	97.97
	39.70	74.02	106.35	37.75	69.74	109.56	49.48	75.01	107.80
	77.65	31.19	100.36	79.94	39.99	105.55	65.02	34.17	98.67
	79.74	94.79	7.97	79.91	92.60	8.17	78.49	90.98	10.91
	24.26	40.65	6.69	23.91	36.33	6.91	27.16	39.00	7.84
	73.09	79.43	39.05	71.64	74.95	39.83	70.99	76.37	41.44
	15.80	19.41	50.76	15.61	19.24	49.93	18.02	21.46	51.78
	33.78	28.78	4.99	33.98	29.13	5.75	30.92	28.62	5.51
	16.36	36.54	26.16	15.53	31.86	26.45	21.24	35.72	28.89
	12.61	5.79	0.83	13.10	7.03	1.11	10.56	5.80	0.82
	56.11	30.17	1.84	57.92	34.64	2.67	46.37	29.10	2.04
	63.05	49.61	102.76	63.11	51.51	107.30	59.84	51.58	102.86
	10.93	6.18	0.87	11.59	7.47	1.12	9.27	5.97	0.94
	0.48	0.46	0.61	0.76	0.74	0.97	0.61	0.60	0.78

Table 8.11 *CIELAB* (ΔE_{ab}^*) colour differences between the two conditions (solid Mondrian vs. Moving Mondrian).

Solid v Movie CIELAB						
	R	G	B	HP	EIZO	NEC
	50	50	50	0.67	3.89	4.91
	255	255	255	0.23	0.18	0.32
	128	128	128	0.49	0.64	0.37
	200	200	200	0.33	0.15	0.28
	255	0	0	0.50	0.06	0.12
	0	255	0	0.39	0.32	0.10
	0	0	255	0.18	0.07	0.47
	0	255	255	0.24	0.13	0.38
	255	0	255	0.14	0.10	0.49
	255	255	0	0.38	0.23	0.20
	128	180	50	0.39	0.65	0.42
	235	225	150	0.26	0.42	0.69
	50	128	180	0.57	0.31	0.56
	180	128	50	0.54	0.63	0.66
	50	180	128	0.35	0.34	0.34
	125	0	10	1.09	0.64	0.85
	245	85	10	0.74	0.52	0.79
	205	165	255	0.42	0.42	0.90
	115	45	0	0.94	0.85	0.51
	0	0	0	1.17	1.82	1.94

differences are almost all positive which indicates that the Y values of the Mondrian display were consistently greater than the corresponding Y values of the Movie display.

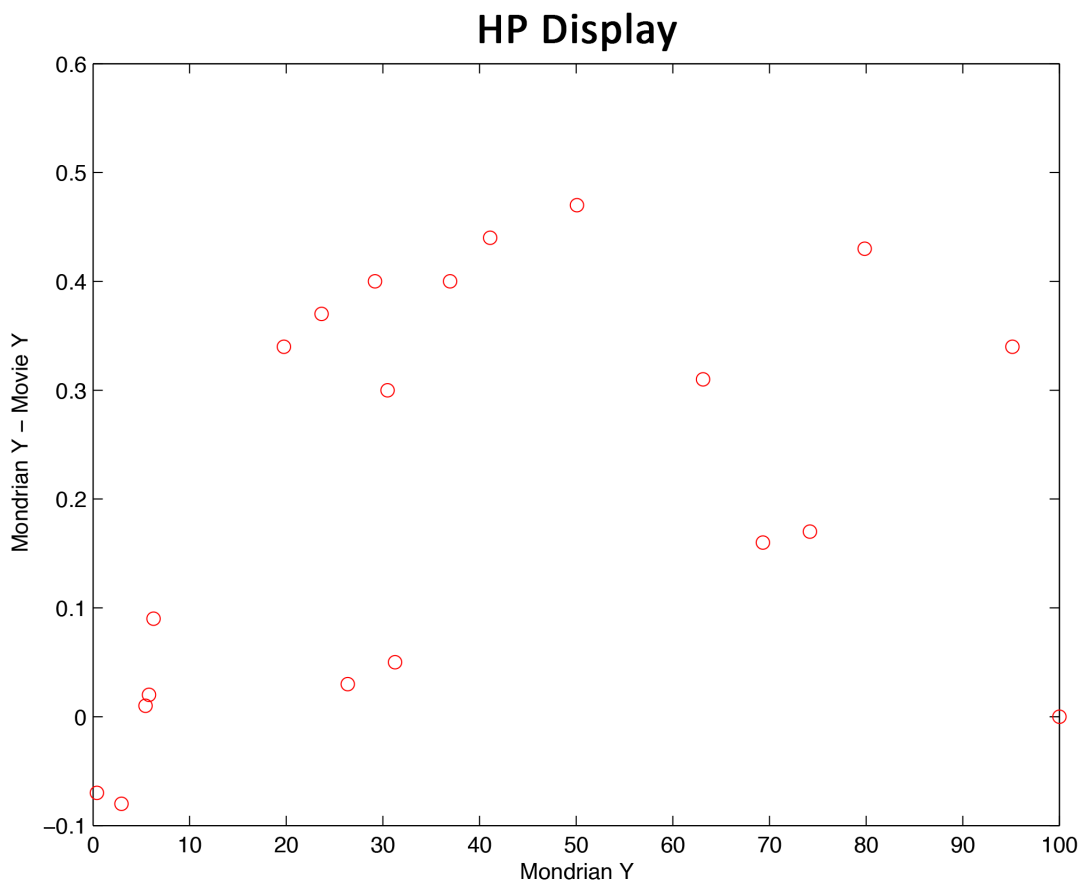


Fig. 8.2 Difference between Mondrian and Movie Y value plotted against Mondrian Y value for each colour stimulus (HP display).

Fig. 8.5 indicates the CIE chromaticities of the Mondrian and Movie conditions for the HP display. With the exception of the black sample, there are very few differences between the two conditions. Fig. 8.5 and 8.2 would seem to indicate that the effect of the moving background is to reduce the Y value of the colour stimuli with little or no effect on chromaticity. Fig. 8.6 and 8.7 also illustrate the CIE chromaticity coordinates for Mondrian (black circle symbols) and Movie (white triangle symbols) conditions for EIZO and NEC displays respectively. The differences between two conditions (Mondrian and Moving Mondrian) are mainly in the dark samples and in total, four samples for NEC and five for EIZO are problematic.

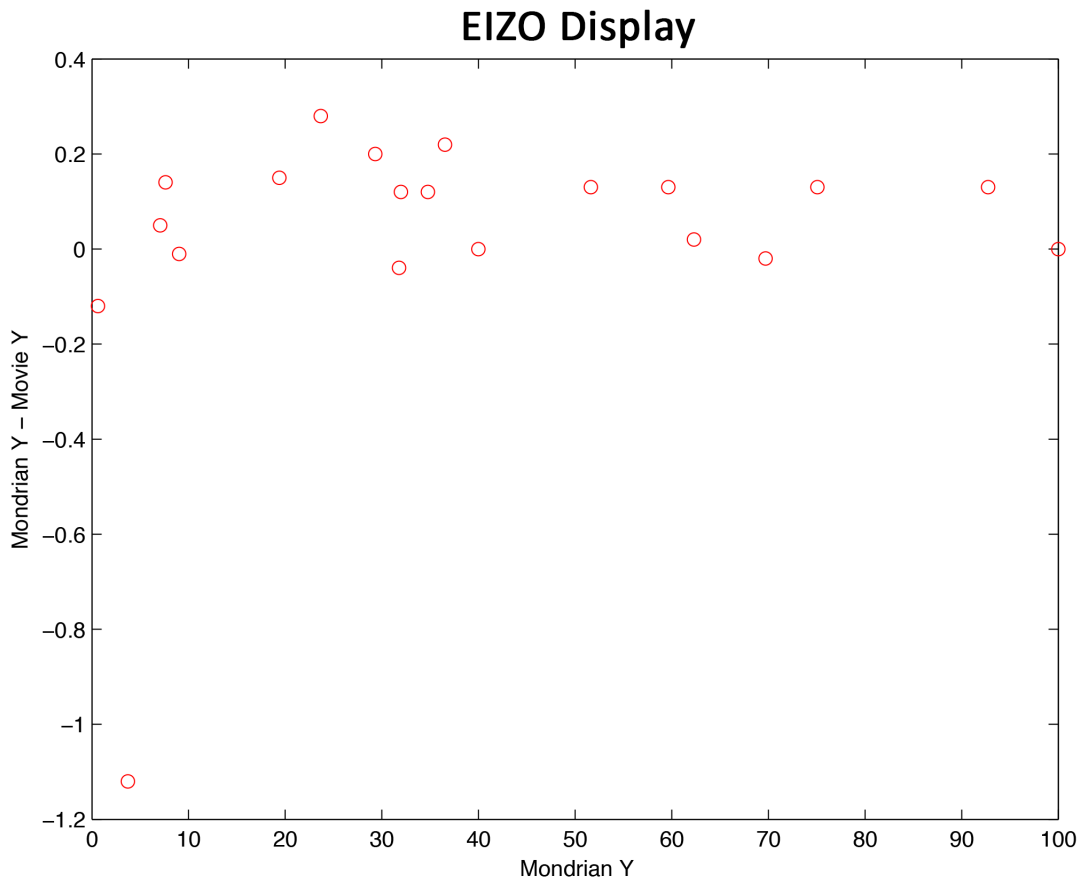


Fig. 8.3 Difference between Mondrian and Movie Y value plotted against Mondrian Y value for each colour stimulus (EIZO display).

A one-sample t-test was carried out to test the hypothesis that the colour difference (0.50) between the two conditions was distinguishable from zero. The result was that the difference was statistically significant ($p < 0.01$). The data were also analysed for the other two displays. In both cases, no effect on chromaticity was observed for the background condition. However, Fig. 8.3 and 8.4 show that the Y values for Mondrian condition were, for both displays, greater than the Y values for the Movie condition. Thus, for all three displays, there seems to be an effect that the Movie condition causes a small reduction in luminance. The colour differences for the EIZO and HP displays were 0.62 ($p < 0.01$) and 0.77 ($p < 0.01$) respectively and both were significantly greater than zero [166].

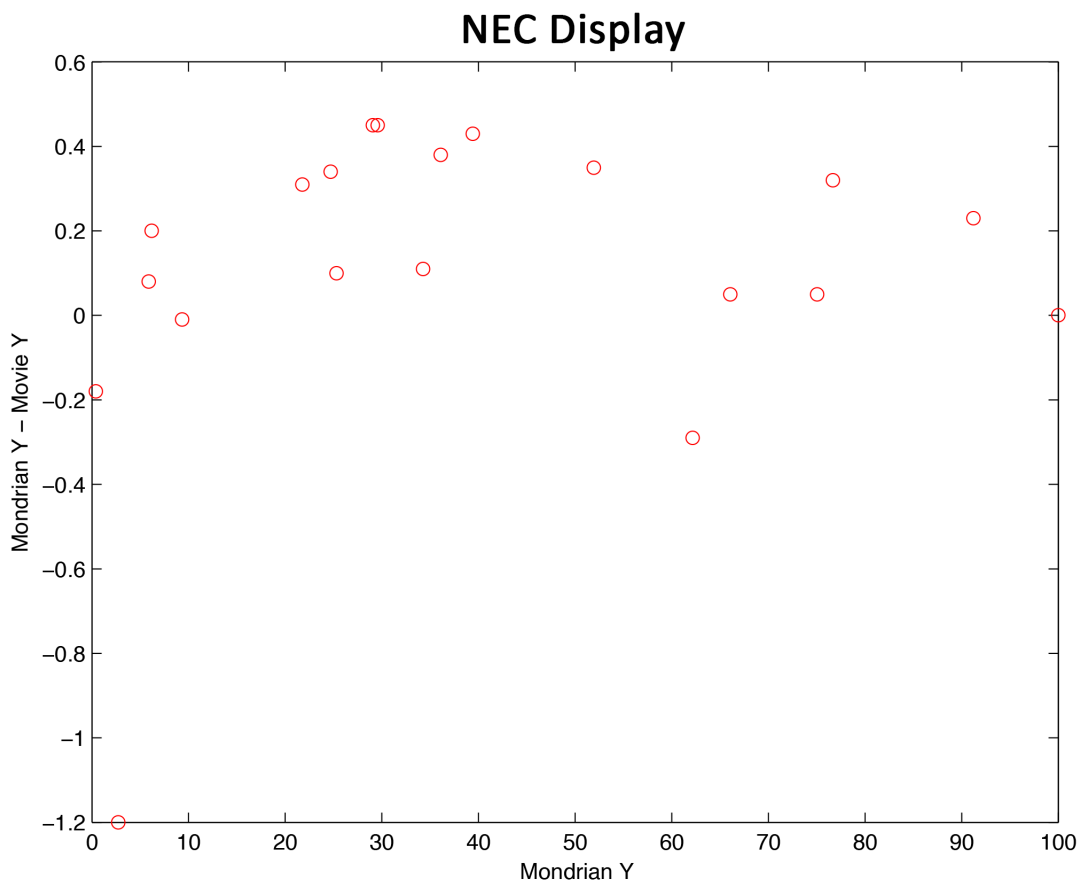


Fig. 8.4 Difference between Mondrian and Movie Y value plotted against Mondrian Y value for each colour stimulus (NEC display).

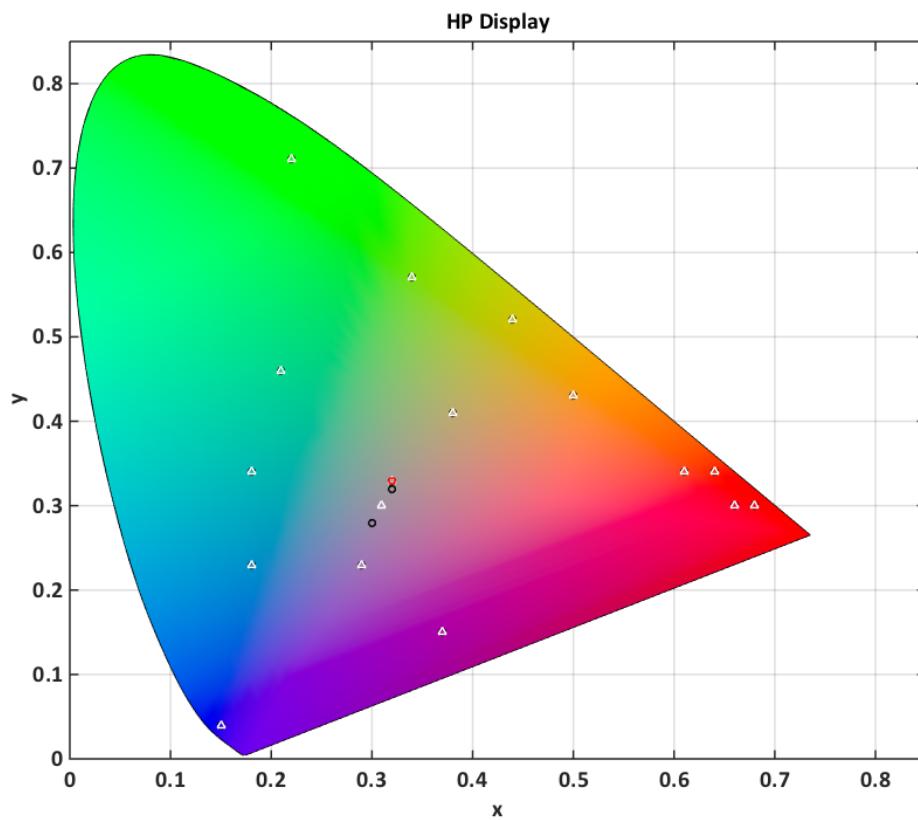


Fig. 8.5 CIE chromaticity coordinates for Mondrian (black circle symbols) and Movie (white triangle symbols) conditions respectively as well as the white point of HP display (red circle).

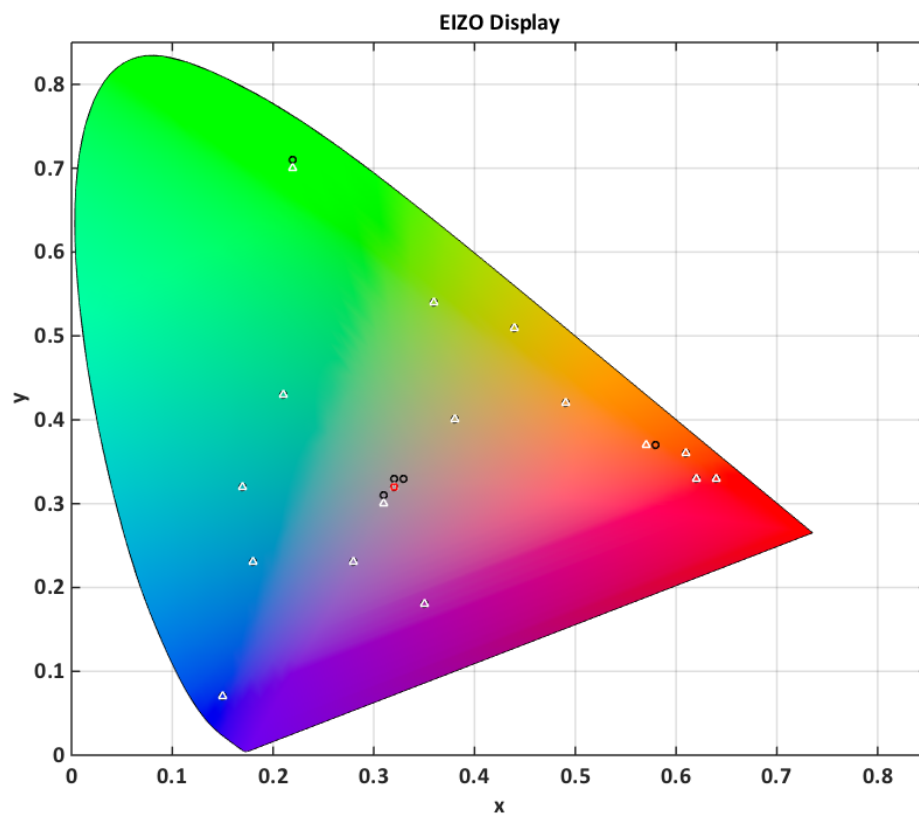


Fig. 8.6 CIE chromaticity coordinates for Mondrian (black circle symbols) and Movie (white triangle symbols) conditions respectively as well as the white point of EIZO display (red circle).

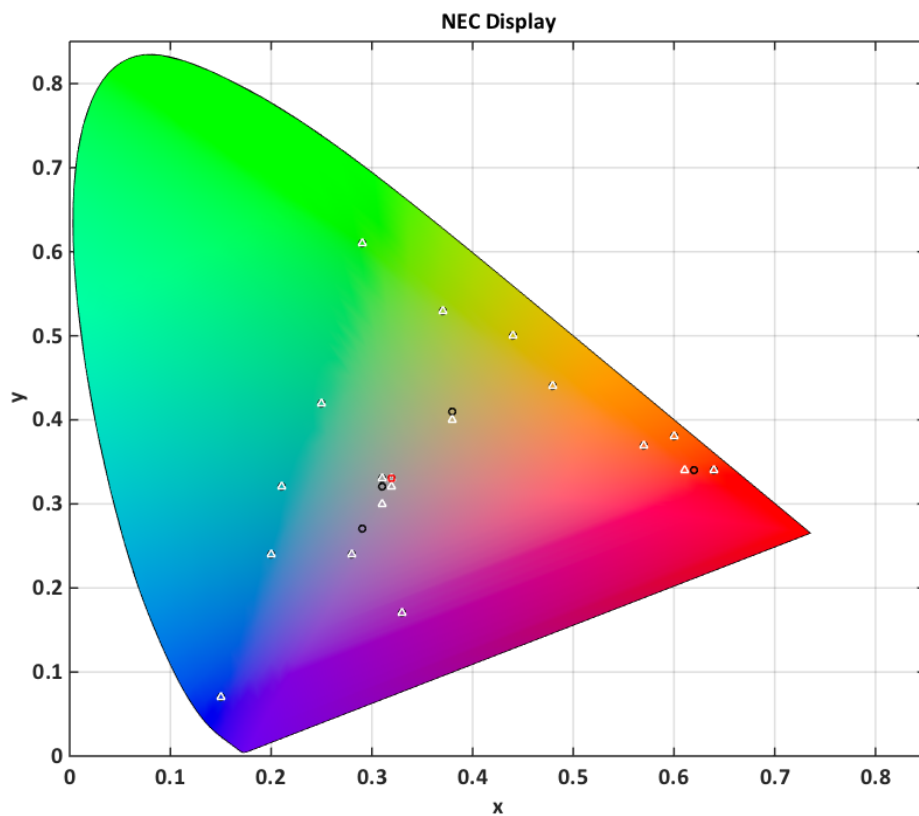


Fig. 8.7 CIE chromaticity coordinates for Mondrian (black circle symbols) and Movie (white triangle symbols) conditions respectively as well as the white point of NEC display (red circle).

8.4 Summary and conclusion

In this chapter, the effect of background colour on the colour of calibration patches has been investigated by comparing the five different backgrounds (grey-background, solid Mondrian-background, moving Mondrian-background, black-background and white-background). The colour difference between the Mondrian-background condition and the grey-background condition was, on average, $0.25 \Delta E_{ab}^*$ units. However, the mean colour difference for the movie-background condition was $0.70 \Delta E_{ab}^*$ and this is statistically different from the Mondrian-background condition ($p < 0.05$). In contrast, the colour differences between the black-background condition and the grey-background condition is an average of $3.50 \Delta E_{ab}^*$ units and the colour differences between the white-background condition and the grey-background condition is an average of $4.01 \Delta E_{ab}^*$ units which is greater than the colour difference of the Mondrian-background no matter it is moving or not. The colour differences obtained using either black or white background condition are greater than using the grey-background condition. Either using black or white background does not make any changes of being statistically different from the grey-background condition as p -value is greater than 0.05. A novel stimulus has been used to show that the colour of a calibration patch depends not just on the colour and lightness of the surround but also on whether the surround is moving. This has implications for the design of stimuli for use when building display characterisation models and suggests that if these models are to be used to process movies then measurements should be taken on a moving background.

Chapter 9

Conclusion and future work

9.1 Conclusion

The experimental work in this thesis is contained in Chapter 5-8 and is concerned with the colorimetric characterisation of displays. Traditionally, the GOG model has been used to characterise CRT displays. However, CRT displays are now seldom used and difficult to obtain; they have been replaced by several technologies including LCD displays. The GOG model assumes that the tone-reproduction curve (TRC) of a display can be modelled by a power function but it has been noted [14] that this model may not be appropriate for modern displays. This work, therefore, compares the performance of the parametric GOG model with an interpolation method known as PLCC. In addition, regardless of whether GOG or PLCC is used, it is possible to base the characterisation on either grey-ramp linearisation samples or on colour-ramp linearisation samples. There is no published data that provides any robust findings on whether grey-ramp or colour-ramps should best be used (although Berns [14] recommended the neutral samples). In this thesis, the effect of these parameters on the characterisation performance is evaluated for 20 different displays. All 256 levels (for both the three primaries and the grey) were measured for all 20 displays. These samples are used for linearisation (explicitly in the case of PLCC and GOG and implicitly in the case of PLVC) but were sub-sampled to allow the effect of the number of linearisation samples on characterisation performance to be explored. Colour characterisation was assessed using statistical measures of colour difference (calculated between actual and predicted XYZ values for sets of

samples) and, as part of this work, several different sets of samples were specified and used for this purpose.

Models such as GOG and PLCC also assume that the chromaticities of the primary channels remain constant. yet there is uncertainty about whether this assumption can be met in practice, especially given the range of new technologies that are becoming common. Therefore, a more recent model (PLVC), which does not assume chromaticity constancy, was also evaluated. A number of research questions were raised at the beginning of this thesis. The questions are listed below and the findings from the thesis are discussed in the context of each of these questions.

- **What are relative merits of the GOG, PLCC and PLVC models for colour characterisation of modern displays and how can they be optimally used?**
In Chapter 6 a meta-analysis of the colour characterisation of 20 displays was described. There is clear evidence from this meta-analysis that the PLCC method is superior to the GOG model and should be preferred. When all of the 256 available samples for linearisation were used, the median ΔE_{ab}^* (averaged across all devices and all samples in the Macbeth colour chart) was 3.40 and 0.96 for the GOG and PLCC methods respectively when using grey-ramp linearisation samples. When using colour-ramps linearisation samples the ΔE_{ab}^* was 3.20 and 1.60 for the GOG and PLCC method respectively. In Chapter 7, the performance of the PLVC model was evaluated. When using all the available linearisation samples the median ΔE_{ab}^* (again, averaged over all devices and all samples in the Macbeth colour chart) was 1.71 using the colour-ramps linearisation samples. Therefore, if all the linearisation samples are available on average the PLCC method gives the best performance; however, for some displays, the GOG or PLVC methods performed best.
- **What is the effect of using different test charts on the evaluation of different characterisation methods?**
The first research question was addressed in terms of the results from the Macbeth colour checker chart. This was done because this chart is widely used in the colour-imaging industries. In Chapters 6 and 7 several other colour charts were used. When using the Chart4 and Matlab60 charts (which were designed to include highly chromatic samples) the PLVC method performed well for some of the displays, suggesting that the choice of method

might depend upon the nature of the samples that are being displayed. Using all linearisation samples the average median ΔE_{ab}^* values using Chart4 was 2.07 (PLVC), $\Delta E_{ab}^*=1.5$ (PLCC using colour-ramps linearisation samples), $\Delta E_{ab}^*=1.10$ (PLCC using grey-ramp linearisation samples) and $\Delta E_{ab}^*=2.22$ (GOG using colour-ramps linearisation samples), $\Delta E_{ab}^*=2.23$ (GOG using grey-ramp linearisation samples) and the average median ΔE_{ab}^* for MATLAB60 was 2.00 (PLVC), $\Delta E_{ab}^*=2.04$ (PLCC using colour-ramps linearisation samples), $\Delta E_{ab}^*=1.13$ (PLCC using grey-ramps linearisation samples) and $\Delta E_{ab}^*=3.99$ (GOG using colour-ramps linearisation samples), $\Delta E_{ab}^*=3.98$ (GOG using grey-ramp linearisation samples).

- **What is the effect of using different sets of linearisation samples?**

There is clear evidence that the grey-ramp linearisation samples produce better performance than the colour-ramps linearisation samples; this was true for all test sets other than the highly chromatic colour-ramps set (even for these samples the grey-ramp linearisation samples performed well). For example, using all of the linearisation samples and the Macbeth colour chart the average median ΔE_{ab}^* using PLCC was 1.86 (using colour-ramps linearisation samples) and 0.73 (using grey-ramp linearisation samples) respectively.

- **How does the number of linearisation samples affect the characterisation performances using the various models?**

The effect of the number of linearisation samples on characterisation performance was interesting and showed that for the PLCC model the error increases as the number of linearisation samples (N) is reduced. The relationship between error and N is not linear, however, and when $N > 25$ there is little further improvement so that an N of 25 is probably a practical compromise. When N is very small the error in PLCC increases markedly and for $N < 10$ sometimes the GOG model gives better performance than PLCC.

- **Known samples are required for the characterisation models and these need to be measured against specific backgrounds; how does the background affect colour measurements (and hence characterisation performance)?**

In Chapter 8 the effect of background colour on the colour of calibration patches was investigated by comparing the different backgrounds (grey-background, solid Mondrian-background, moving Mondrian-background,

black-background and white-background). Characterisation patches are routinely measured on a grey background but then applied to real images where the background may not even be of a single colour. This was the rationale behind using a Mondrian-like background for one of the conditions. The colour difference between the Mondrian-background condition and the grey-background condition was, on average, $0.25 \Delta E_{ab}^*$ units. Either using black or white background does not make any changes of being statistically different from the grey-background condition as p -value is greater than 0.05.

- **Devices are characterised using the measurement of colour patches on a static display; are the models so-derived applicable to moving images?**

Two different Mondrian background conditions (static and moving) were also tested. Furthermore, a moving Mondrian was also used because of characterisation models derived from static patches on the display are increasingly being used to enable colour management of movies. The mean colour difference for the movie-background condition was $0.70 \Delta E_{ab}^*$ and this is statistically different from the Mondrian-background condition ($p < 0.05$). There is a statistically significant effect of motion but it is small in magnitude and further work may be required to ascertain whether it is of practical importance. In contrast, the colour differences between the black-background condition and the grey-background condition is an average of $3.50 \Delta E_{ab}^*$ units and the colour differences between the white-background condition and the grey-background condition is an average of $4.01 \Delta E_{ab}^*$ units which greater than the colourful background no matter it is moving or not. The colour differences obtained using either black or white background condition are greater than using the grey-condition background. A novel stimulus has been used to show that the colour of a calibration patch depends not just on the colour and lightness of the surround but also on whether the surround is moving. This has implications for the design of stimuli for use when building display characterisation models and suggests that if these models are to be used to process movies then measurements should be taken on a moving background.

9.2 Future works

The current research provides the performance evaluation of 20 different displays using the PLVC model and the other two popular models known as GOG and PLCC using the grey-ramp and colour-ramps linearisation samples with different colour patches set of samples. In addition, the effect of using different background conditions on colour calibration patches has been tested. Furthermore, the display characterisation is tested for moving images. Some areas should be extended in future studies, such as the range of display devices and varying display sizes as well as using different settings and resolutions. All the evaluation in current work is based on an LCD display technologies. However, the present results may not hold for different types of displays such as an LED, OLED or any other much newer technologies.

Having the accurate colour display devices is always not just depends on a display colour characterisation models. Lack of channel independence, uniformity, spatial independence have evaluated, but there is still a question of Why our models are not perfect. What are the other display attributes which can effect on the display characterisation results? for example, Is there any noises? Are there any better devices to do the colour measurements?

Developing more effective models than PLCC and PLVC is difficult. However, developing AI or machine learning methods is one possible way in which it may be possible. The investigation of data-based colour characterisation could help as a possible research method. Furthermore, the further work includes performing a more in-depth statistical analysis of the results and testing more types of devices to improve the significance of the experiment. As a straightforward continuation of this work, we think it could be of great interest to utilise a spectral-data to the display characterisation.

References

- [1] ABRARDO, A., CAPPELLINI, V., CAPPELLINI, M., AND MECOCCHI, A. Art-works colour calibration by using the vasari scanner. In *Color and Imaging Conference* (1996), no. 1, Society for Imaging Science and Technology, pp. 94–96.
- [2] ANDERSON, M., MOTTA, R., CHANDRASEKAR, S., AND STOKES, M. Proposal for a standard default color space for the internet- sRGB. In *Color and imaging conference* (1996), no. 1, Society for Imaging Science and Technology, pp. 238–245.
- [3] ANDERSON, M., SRINIVASAN, C., MOTTA, R., AND STOKES, M. A standard default colour space for the internet - sRGB. Tech. rep., International Colour Consortium, (1996).
- [4] AREND, L. E., AND SPEHAR, B. Lightness, brightness, and brightness contrast: 2. reflectance variation. *Perception & Psychophysics* 54, 4 (1993), 457–468.
- [5] Standard terminology of appearance, E284-09, (2009).
- [6] BALA, R., AND BRAUN, K. A camera-based method for calibrating projection color displays. In *Color and Imaging Conference* (2006), no. 1, Society for Imaging Science and Technology, pp. 148–152.
- [7] BALA, R., KLASSEN, R. V., AND BRAUN, K. M. Efficient and simple methods for display tone-response characterization. *Journal of the Society for Information Display* 15, 11 (2007), 947–957.
- [8] BALA, R., AND SHARMA, G. Digital colour imaging handbook. Tech. rep., (2003).
- [9] BALASUBRAMANIAN, R., AND MALTZ, M. S. Refinement of printer transformations using weighted regression. In *Electronic Imaging: Science & Technology* (1996), International Society for Optics and Photonics, pp. 334–340.
- [10] BARTLESON, C. J. *Factors affecting color appearance and measurement by psychophysical methods*. PhD thesis, City University London, 1977.
- [11] BERNS, R. S. Methods for characterizing CRT displays. *Displays* 16, 4 (1996), 173–182.

- [12] BERNS, R. S., FERNANDEZ, S. R., AND TAPLIN, L. Estimating black-level emissions of computer-controlled displays. *Colour Research & Application* 28, 5 (2003), 379–383.
- [13] BERNS, R. S., GORZYNSKI, M. E., AND MOTTA, R. J. CRT colorimetry. part ii: Metrology. *Color Research & Application* 18, 5 (1993), 315–325.
- [14] BERNS, R. S., AND KATOH, N. Methods for characterising displays. John Wiley & Sons New York, NY, USA, pp. 143–164.
- [15] BERNS, R. S., MOTTA, R. J., AND GORZYNSKI, M. E. CRT colorimetry. part i: Theory and practice. *Color Research & Application* 18, 5 (1993), 299–314.
- [16] BERNS, R. S., AND REIMAN, D. M. Color managing the third edition of billmeyer and saltzman’s principles of color technology. *Color Research & Application* 27, 5 (2002), 360–373.
- [17] BLONDÉ, L., STAUDER, J., AND LEE, B. Inverse display characterization: A two-step parametric model for digital displays. *Journal of the Society for Information Display* 17, 1 (2009), 13–21.
- [18] BRAINARD, D. H. Calibration of a computer controlled color monitor. *Color Research & Application* 14, 1 (1989), 23–34.
- [19] BRAINARD, D. H., PELLI, D. G., AND ROBSON, T. Display characterization. *Encyclopedia of imaging science and technology* (2002).
- [20] BRETTEL, H., VIÉNOT, F., AND MOLLON, J. D. Computerized simulation of colour appearance for dichromats. *JOSA A* 14, 10 (1997), 2647–2655.
- [21] BRODY, T., ASARS, J. A., AND DIXON, G. D. A 6× 6 inch 20 lines-per-inch liquid-crystal display panel. *Electron Devices, IEEE Transactions on* 20, 11 (1973), 995–1001.
- [22] BROWN, S. W., SANTANA, C., AND EPELDAUER, G. P. Development of a tunable LED-based colorimetric source. *Journal of research of the National Institute of Standards and Technology* 107, 4 (2002), 363.
- [23] BUNTING, F., MURPHY, C., AND FRASER, B. Real world colour management. *Second Edition 2005* (2005).
- [24] CHEUNG, V., AND WESTLAND, S. Methods for optimal colour selection. *Journal of Imaging Science and Technology* 50, 5 (2006), 481–488.
- [25] CIE, C., AND PUB, C. CIE standard colorimetric observers, no. s2. *Bureau Central de la CIE, Vienna, Austria* (1986a).
- [26] CIE1931 and CIE1964 observer comparison. <http://www.gravurexchange.com/gravurezine/0704-ezine/graphics/sole7.gif> (visited: 2012-01-18).
- [27] CIE1931 chromaticity diagram. http://www.ledke.com/up_files/file200908240137279104.jpg (visited: 2011-06-21).

- [28] Colorimetry, CIE publication number 15.2, second edition.
- [29] Parametric effect in colour-difference evaluation. *Commission Internationale de l'Eclairage (CIE)*, 101 (1993).
- [30] Colorimetry, CIE vienna, (2004a).
- [31] A colour appearance for colour management system, CIECAM02, (2004b).
- [32] CIE1976 Chromaticity diagram. <http://wlc.enterprises/what-we-do/> (visited: 2016-04-22).
- [33] CIELAB diagram. <http://www.coatsindustrial.com/en/information-hub/apparel-expertise/colour-by-numbers> (visited: 2016-04-22).
- [34] CLARKE, F., McDONALD, R., AND RIGG, B. Modification to the jpc79 colour-difference formula. *Journal of society of dyers and colourists* 100, 4 (1984), 128–132.
- [35] COLANTONI, P., AND THOMAS, J.-B. A color management process for real time color reconstruction of multispectral images. In *Scandinavian Conference on Image Analysis* (2009), Springer, pp. 128–137.
- [36] COLLINGS, P. J., AND HIRD, M. *Introduction to liquid crystals: chemistry and physics*. CRC Press, (1997).
- [37] COMMISSION, I. E., ET AL. Multimedia systems and equipment—colour measurement and management—part 2-1: Colour management—default rgb colour space—srgb. Tech. rep., IEC 61966-2-1, 1999.
- [38] CONSORTIUM, I. C. The role of ICC profiles in a colour reproduction system, 2004.
- [39] CONSORTIUM, I. C., ET AL. Image technology colour management architecture, profile format, and data structure. *Specification 201*, 1 (2004), 2004–10.
- [40] COWAN, W. B. An inexpensive scheme for calibration of a colour monitor in terms of cie standard coordinates. *ACM SIGGRAPH Computer Graphics* 17, 3 (1983), 315–321.
- [41] COWAN, W. B., AND ROWELL, N. On the gun independence and phosphor constancy of colour video monitors, (1986).
- [42] Structure of CRT display. <http://www.ustudy.in/node/9490> (visited: 2014-07-21).
- [43] DAY, E. Colorimetric characterisation of a computer- controlled liquid crystal display. *Colour research and application* 29 (2004), 365–373.
- [44] DEN BOER, W. *Active matrix liquid crystal displays: fundamentals and applications*. Elsevier, (2011).

- [45] DONALD, D. Spectral power distribution wang moreno. <http://white.stanford.edu/teach/index.php/WangMoreno> (visited: 2016-02-20).
- [46] FAIRCHILD, M. *Refinement of the RLAB colour space*. Wiley InterScience: Colour Research & Application, (1998).
- [47] FAIRCHILD, M. D. Visual evaluation and evolution of the RLAB colour space. In *Colour and Imaging Conference ((1994))*, vol. 1994, pp. 9–13.
- [48] FAIRCHILD, M. D. A revision of CIECAM97s for practical applications. *Colour research and application* 26, 6 (2001), 418–427.
- [49] FAIRCHILD, M. D. Human colour vision. Wiley Online Library, pp. 1–37.
- [50] FARLEY, W. W., AND GUTMANN, J. C. Digital image processing systems and an approach to the display of colors of specified chrominance. Tech. rep., Virginia Polytechnic institute and state University black sburg human Factors Lab, 1980.
- [51] FENG, X.-F., PAN, H., AND DALY, S. Comparisons of motion-blur assessment strategies for newly emergent LCD and backlight driving technologies. *Journal of the Society for Information Display* 16, 10 (2008), 981–988.
- [52] FLEMING, P. D., AND SHARMA, A. Colour management and ICC profiles; can't live without it so learn to live with it! *Gravure Magazine* 56 (2002).
- [53] GARCIA-SUAREZ, L., AND RUPPERTSBERG, A. I. Why higher resolution graphics cards are needed in colour vision research. *Colour Research & Application* 36, 2 (2011), 118–126.
- [54] GIBSON, J. E., AND FAIRCHILD, M. D. Colorimetric characterization of three computer displays (LCD and CRT). *Munsell color science laboratory technical report* 40 (2000).
- [55] GIORGIANNI, E. J., MADDEN, T. E., AND SPAULDING, K. E. Colour management for digital imaging systems. *Digital colour imaging handbook* (2003), 239–268.
- [56] GOLDMARK, P. C. Brightness and contrast in television. *Electrical Engineering* 68, 3 (1949), 237–242.
- [57] GREEN, P. *Understanding digital colour*. GATF Press, (1999).
- [58] GREEN, P. *Overview of characterization methods*. John Wiley & Sons, (2002).
- [59] GREEN, P., AND MACDONALD, L. *Colour engineering: achieving device independent colour*, vol. 30. John Wiley & Sons, (2011).
- [60] GUAN, S.-S., AND LUO, M. R. Investigation of parametric effects using small colour differences. *Color Research & Application* 24, 5 (1999), 331–343.
- [61] GUILD, J. The colorimetric properties of the spectrum. vol. 230, JSTOR, pp. 149–187.

- [62] GUTH, S. L. Atd model for colour vision i: background and discussion. In *IS&T/SPIE 1994 International Symposium on Electronic Imaging: Science and Technology* (1994), pp. 149–152.
- [63] GUTH, S. L. Atd model for colour vision ii: applications. In *IS&T/SPIE 1994 International Symposium on Electronic Imaging: Science and Technology* (1994), pp. 153–162.
- [64] HAR-NOY, S., AND NGUYEN, T. Q. LCD motion blur reduction: A signal processing approach. *Image Processing, IEEE Transactions on* 17, 2 (2008), 117–125.
- [65] HARDEBERG, J. Y. *Acquisition and reproduction of color images: colorimetric and multispectral approaches*. Universal-Publishers, 2001.
- [66] HARDEBERG, J. Y., SEIME, L., AND SKOGSTAD, T. Colorimetric characterization of projection displays using a digital colorimetric camera. In *Electronic Imaging 2003* (2003), International Society for Optics and Photonics, pp. 51–61.
- [67] HOLST, G. C. *CCD arrays, cameras, and displays*, vol. 38. Citeseer, (1998).
- [68] HUNT, C. C. The effect of stretch receptors from muscle on the discharge of motoneurons. *The Journal of physiology* 117, 3 (1952), 359.
- [69] HUNT, R. The specification of colour appearance. i. concepts and terms. *Color Research & Application* 2, 2 (1977), 55–68.
- [70] HUNT, R. Revised colour-appearance model for related and unrelated colours. *Colour Research & Application* 16, 3 (1991), 146–165.
- [71] HUNT, R. *Measuring colour*. (1998), Kingsley-Upon-Thames, vol. 15. England: Fountain press, (1998).
- [72] HUNT, R., LI, C., JUAN, L., AND LUO, M. Further improvements to CIECAM97s. *Color Research & Application* 27, 3 (2002), 164–170.
- [73] HUNT, R. W. G. *The reproduction of colour*. John Wiley & Sons, (2005).
- [74] HUNT, R. W. G., AND POINTER, M. R. *Measuring colour*. John Wiley & Sons, (2011).
- [75] IN GREEN, P., AND W., M. L. Method for characterising colour scanners and digital cameras. *Colour engineering* (2002), 165–178.
- [76] INGLIS, A. F., AND LUTHER, A. C. *Video engineering*. McGraw-Hill, Inc., (1996).
- [77] Graphic technology and photography-colour characterisation of digital still cameras-part 1: Stimuli, metrology and test procedures. technical report ISO:17321-1, (2006).
- [78] JACK, K. *Video demystified: a handbook for the digital engineer*. Elsevier, 2011.

- [79] JIMÉNEZ BARCO, L. D., DÍAZ, J., JIMÉNEZ, J., AND RUBINO, M. Considerations on the calibration of colour displays assuming constant channel chromaticity. *Colour Research & Application* 20, 6 (1995), 377–387.
- [80] JOHNSON, T. Methods for characterising colour scanners and digital cameras. *Displays* 16, 4 (1996), 183–191.
- [81] JUDD, D. B., MACADAM, D. L., WYSZECKI, G., BUDDE, H., CONDIT, H., HENDERSON, S., AND SIMONDS, J. Spectral distribution of typical daylight as a function of correlated colour temperature. *Josa* 54, 8 (1964), 1031–1040.
- [82] KANG, H. R. *Color technology for electronic imaging devices*. SPIE press, 1997.
- [83] KANG, H. R. *Computational colour technology*. Spie Press Bellingham, (2006).
- [84] KATOH, N., DEGUCHI, T., AND BERNS, R. S. An accurate characterization of CRT monitor (i) verifications of past studies and clarifications of gamma. *Optical Review* 8, 5 (2001), 305–314.
- [85] KATOH, N., DEGUCHI, T., AND BERNS, R. S. An accurate characterization of CRT monitor (ii) proposal for an extension to cie method and its verification. vol. 8, Springer, pp. 397–408.
- [86] KENNEL, G. *Colour and mastering for digital cinema*. CRC Press, (2012).
- [87] KIM, J.-M., KIM, J., CHO, Y., KIM, M., AND LEE, S.-W. Liquid crystal displays with temperature-independent characteristics. *Optical Engineering* 51, 7 (2012), 077402–1.
- [88] KIPPHAN, H. *Handbook of print media: technologies and production methods*. Springer Science & Business Media, (2001).
- [89] KRISS, M., AND GREEN, P. *Colour management: understanding and using ICC profiles*, vol. 17. John Wiley & Sons, 2010.
- [90] KWAK, Y., LI, C., AND MACDONALD, L. Controlling color of liquid-crystal displays. *Journal of the Society for Information Display* 11, 2 (2003), 341–348.
- [91] KWAK, Y., AND MACDONALD, L. Characterisation of a desktop LCD projector. *Displays* 21, 5 (2000), 179–194.
- [92] LAND, E. H., AND MCCANN, J. J. Lightness and retinex theory. *JOSA* 61, 1 (1971), 1–11.
- [93] LAYCOCK, J. Colour contrast calculations for displays viewed in illumination. *Electronic and Radio Engineers, Journal of the Institution of* 56, 3 (1986), 96.
- [94] LCD Structure. http://www.chimei-innolux.com/opencms/export/sites/CMOWebsite/upload/UploadImages/tft_lcd-2.gif (visited: 2012-05-26).
- [95] LEE, H.-C. *Introduction to color imaging science*. Cambridge University Press, 2005.

- [96] Flexible OLED. <http://www.gsmdome.com/xiaomi-will-receive-oled-displays.html> (visited: 2015-12-20).
- [97] LI, C., LUO, M. R., RIGG, B., AND HUNT, R. W. Cmc 2000 chromatic adaptation transform: Cmccat2000. *Colour Research & Application* 27, 1 (2002), 49–58.
- [98] LUO, M., AND RIGG, B. Bfd (l: c) colour-difference formula part 1ndashdevelopment of the formula. *Journal of the Society of Dyers and Colourists* 103, 2 (1987), 86–94.
- [99] LUO, M. R., CUI, G., AND RIGG, B. The development of the CIE 2000 colour-difference formula: CIEDE2000. vol. 26, Wiley Online Library, pp. 340–350.
- [100] LUO, M. R., AND LI, C. CIE colour appearance models and associated colour spaces. pp. 261–294.
- [101] LUO, M. R., LO, M.-C., AND KUO, W.-G. The LLAB (l: c) colour model. vol. 21, Wiley Online Library, pp. 412–429.
- [102] MACADAM, D. L. Visual sensitivities to colour differences in daylight. *JOSA* 32, 5 (1942), 247–274.
- [103] MACDONALD, L. W. Developments in colour management systems. *Displays* 16, 4 (1996), 203–211.
- [104] MACVOY, B. 1964 XYZ colour matching functions. <http://www.handprint.com/HP/WCL/color6.html> (visited: 2016-04-12).
- [105] MACVOY, B. Real colour matching functions. <http://www.handprint.com/HP/WCL/color6.html> (visited: 2016-04-12).
- [106] MAHY, M., EYCKEN, L., AND OOSTERLINCK, A. Evaluation of uniform color spaces developed after the adoption of cielab and cieluv. *Color Research & Application* 19, 2 (1994), 105–121.
- [107] Matching colour with profile. <https://helpx.adobe.com/lightroom/help/color-management.html> (visited: 2014-07-21).
- [108] McCAMY, C. S. Correlated colour temperature as an explicit function of chromaticity coordinates. *Colour Research & Application* 17, 2 (1992), 142–144.
- [109] McCAMY, C. S., MARCUS, H., AND DAVIDSON, J. A colour-rendition chart. *J. App. Photog. Eng* 2, 3 (1976), 95–99.
- [110] MIKALSEN, E. B., HARDEBERG, J. Y., AND THOMAS, J.-B. Verification and extension of a camera-based end-user calibration method for projection displays. In *Conference on Colour in Graphics, Imaging, and Vision* (2008), vol. 2008, Society for Imaging Science and Technology, pp. 575–579.
- [111] MINOLTA, K. *Spectroradiometer CS-2000*. Catalogue,[Referred 10.6. 2008] <http://www.konicaminolta.com>, 2008.

- [112] MORONEY, N., FAIRCHILD, M. D., HUNT, R. W., LI, C., LUO, M. R., AND NEWMAN, T. The CIECAM02 colour appearance model. In *Colour and Imaging Conference* (2002), no. 1, pp. 23–27.
- [113] MOROVIČ, J. *Colour gamut mapping*, vol. 10. John Wiley & Sons, (2008).
- [114] MOROVIC, J., AND LUO, M. R. The fundamentals of gamut mapping: A survey. *Journal of Imaging Science and Technology* 45, 3 (2001), 283–290.
- [115] NATHANS, J., PIANTANIDA, T. P., EDDY, R. L., SHOWS, T. B., AND HOGNESS, D. S. Molecular genetics of inherited variation in human colour vision. *Science* 232, 4747 (1986), 203–210.
- [116] NAYATANI, Y. Revision of the chroma and hue scales of a nonlinear colour-appearance model. *Colour Research & Application* 20, 3 (1995), 143–155.
- [117] NEUMANN, A., ARTUSI, A., ZOTTI, G., NEUMANN, L., AND PURGATHOFER, W. An interactive perception-based model for characterization of display devices. In *Color Imaging IX: Processing, Hardcopy, and Applications* (2003), vol. 5293, International Society for Optics and Photonics, pp. 232–242.
- [118] OHTA, N., AND ROBERTSON, A. R. Light, vision and photometry. *Colorimetry: Fundamentals and Applications* (2005), 1–38.
- [119] OHTA, N., AND ROBERTSON, A. R. CIE standard colorimetric system. *Colorimetry: Fundamentals and Applications* (2006), 63–114.
- [120] OKUMURA, H., AND FUJIWARA, H. A new low-image-lag drive method for large-size LCTVs. *Journal of the Society for Information Display* 1, 3 (1993), 335–339.
- [121] Structure of OLED. <http://electronics.howstuffworks.com/oled4.htm> (visited: 2015-12-20).
- [122] ON ILLUMINATION, I. C. *Colorimetry: Official Recommendations of the International Commission on Illumination (CIE), May, 1970*. Bureau central de la CIE, (1971).
- [123] PARK, S.-H. K., RYU, M., HWANG, C.-S., YANG, S., BYUN, C., LEE, J.-I., SHIN, J., YOON, S. M., CHU, H. Y., CHO, K. I., ET AL. 42.3: Transparent ZnO thin film transistor for the application of high aperture ratio bottom emission AM-OLED display. In *SID Symposium Digest of Technical Papers* (2008), vol. 39, Wiley Online Library, pp. 629–632.
- [124] PASCALE, D. RGB coordinates of the macbeth colourchecker. *The BabelColour Company* (2006), 1–16.
- [125] Structure of plasma display panel. <http://sciencelearn.org.nz/Contexts/Gases-and-Plasmas/Science-Ideas-and-Concepts/Plasmas-explained> (visited: 2014-05-27).
- [126] PELLI, D. G. Pixel independence: Measuring spatial interactions on a CRT display. *Spatial vision* 10, 4 (1997), 443–446.

- [127] PIZARRO BONDIA, C., MARTÍNEZ VERDÚ, F. M., ARASA MARTÍ, J., ET AL. Minimization of the reproduction error of natural objects in calibrated CRT display using the GOG model, *International Colour Association* (2005).
- [128] POINTER, M. Colourfulness: A new concept. *Colour* 77 (1978), 327–330.
- [129] POINTER, M. R. The concept of colourfulness and its use for deriving grids for assessing colour appearance. *Colour Research & Application* 5, 2 (1980), 99–107.
- [130] POINTER, M. R., AND ATTRIDGE, G. The number of discernible colours. *Colour Research & Application* 23, 1 (1998), 52–54.
- [131] POST, D. L., AND CALHOUN, C. S. An evaluation of methods for producing desired colors on CRT monitors. *Color Research & Application* 14, 4 (1989), 172–186.
- [132] POST, D. L., AND CALHOUN, C. S. Further evaluation of methods for producing desired colors on crt monitors. Tech. rep., AIR FORCE RESEARCH LAB WRIGHT-PATTERSON AFB OH VISUAL DISPLAY SYSTEMS, 2000.
- [133] POST, D. L., AND LLOYD, C. J. Colour display gamuts and ambient illumination. *Displays* 15, 1 (1994), 39–43.
- [134] POYNTON, C. Gamma FAQ: Frequently asked questions about gamma. <http://www.poynton.com/PDFS/GammaFAQ.pdf>, (2008 (visited: 2014-12-07)).
- [135] POYNTON, C. A. SMPTE tutorial: gamma and its disguises: The nonlinear mappings of intensity in perception, CRTs, film, and video. *SMPTE journal* 102, 12 (1993), 1099–1108.
- [136] NTSC. <http://www.poynton.com/PDFs/ColorFAQ.pdf> (visited: 2016-02-20 and 2010-08-12).
- [137] PRIDMORE, R. W. Bezold–brücke hue-shift as functions of luminance level, luminance ratio, interstimulus interval and adapting white for aperture and object colors. *Vision research* 39, 23 (1999), 3873–3891.
- [138] PRIDMORE, R. W. Bezold–brücke effect exists in related and unrelated colors and resembles the abney effect. *Color Research & Application* 29, 3 (2004), 241–246.
- [139] R. STEHLING, M. NASCIMENTO, A. F. *Multimedia Mining: A Highway to intelligent Multi-media documents*. Kluwer academic publishers, (2002).
- [140] RAYLEIGH, J. W. S. B. Scientific papers. *Scientific Papers* 1, 1 (1899), 84–86.
- [141] Gamut of Rec 709. <http://avsforum.com/forum/rec-601-smpte-c-rec-709.html> (visited: 2015-05-26).
- [142] RGB colour space. http://www.infovis-wiki.net/index.php?title=Color_Coding/_Color (visited: 2012-11-10).

- [143] RHODES, P. A., AND LUO, M. R. A system for WYSIWYG colour communication. *Displays* 16, 4 (1996), 213–221.
- [144] SASAOKA, T., SEKIYA, M., YUMOTO, A., YAMADA, J., HIRANO, T., IWASE, Y., YAMADA, T., ISHIBASHI, T., MORI, T., ASANO, M., ET AL. 24.4 I: Late-news paper: A 13.0-inch AM-OLED display with top emitting structure and adaptive current mode programmed pixel circuit (TAC). In *SID Symposium Digest of Technical Papers* (2001), vol. 32, Wiley Online Library, pp. 384–387.
- [145] SCHANDA, J. *Colorimetry: understanding the CIE system*. John Wiley & Sons, (2007).
- [146] SCHANDA, J., AND SCHANDA, J. Colour rendering of light sources. *Colorimetry: understanding the CIE system*. Hoboken (NJ): Wiley (2007), 207–217.
- [147] SCHUBERT, E. F., GESSMANN, T., AND KIM, J. K. *Light emitting diodes*. Wiley Online Library, (2005).
- [148] SHARMA, A. *Understanding colour management*. Cengage Learning, (2004).
- [149] SHARMA, A., AND FLEMING, P. D. Measuring the quality of ICC profiles and colour management software. *The Seybold Report* 4, 20 (2005), 10–16.
- [150] SHARMA, G. Colour fundamentals for digital imaging. *Digital colour imaging handbook* 20 (2003).
- [151] SHARMA, G., WU, W., AND DALAL, E. N. The CIEDE2000 colour-difference formula: Implementation notes, supplementary test data, and mathematical observations. *Colour Research & Application* 30, 1 (2005), 21–30.
- [152] SHERMAN, C. *Cathode Ray Tube Displays*. Boca Raton: CRC Press LLC, (2000).
- [153] SHIMA, T., OKUMURA, M., AND HIGUCHI, T. Liquid-crystal display cell model using piecewise approximations. *Electronics and Communications in Japan (Part II: Electronics)* 79, 3 (1996), 73–81.
- [154] SMITH, T., AND GUILD, J. The CIE colorimetric standards and their use. *Transactions of the Optical Society* 33, 3 (1931), 73.
- [155] sRGB Colour space. <http://www.sRGB.com/sRGB64> (visited: 2016-07-25).
- [156] Adobe(1998) RGB. http://www.gballard.net/psd/Chromaticity_Diagram.jpg (visited :2012-05-26).
- [157] sRGB. <https://en.wikipedia.org/wiki/SRGB> (visited: 2012-05-26).
- [158] STEVENS, S. S., AND GUIRAO, M. Subjective scaling of length and area and the matching of length to loudness and brightness. *Journal of Experimental Psychology* 66, 2 (1963), 177.
- [159] STONE, M. C. *Device Independent Colour Reproduction*. IS&T, (1991).

- [160] SÜSSTRUNK, S., BUCKLEY, R., AND SWEN, S. Standard rgb color spaces. In *Color and Imaging Conference* (1999), vol. 1999, Society for Imaging Science and Technology, pp. 127–134.
- [161] TAMURA, N., TSUMURA, N., AND MIYAKE, Y. Masking model for accurate colorimetric characterization of LCD. *Journal of the Society for Information Display* 11, 2 (2003), 333–339.
- [162] THOMAS, J.-B., HARDEBERG, J. Y., FOUCHEROT, I., AND GOUTON, P. Additivity based lc display color characterization. In *Proc. of Gjøvik Color Imaging Symposium* (2007), vol. 4, pp. 50–55.
- [163] THOMAS, J.-B., HARDEBERG, J. Y., FOUCHEROT, I., AND GOUTON, P. The plvc display color characterization model revisited. *Color Research & Application* 33, 6 (2008), 449–460.
- [164] TON, M., FOSTER, S., CALWELL, C., AND CONWAY, K. LED lighting technologies and potential for near-term applications. *ECOS Consulting Report* (2003).
- [165] UTSUMI, Y., KOMURA, S., HIYAMA, I., TSUMURA, M., AND KONDO, K. Improving color tracking in in-plane switching mode liquid-crystal displays. *MRS Bulletin* 27, 11 (2002), 870–873.
- [166] VAZIRIAN, M., CHEUNG, V., AND WESTLAND, S. Display characterization for moving images. In *Color and Imaging Conference* (2013), vol. 2013, Society for Imaging Science and Technology, pp. 167–170.
- [167] VAZIRIAN, M., WESTLAND, S., AND CHEUNG, T. Effect of background colour on monitor characterisation. In *Proceedings of AIC Colour 2013: Twelfth Congress of the International Color Association* (2013), The Colour Group (Great Britain), pp. 1025–1028.
- [168] WALLNER, D. Building ICC profiles—the mechanics and engineering. *Sun Microsystems* (2000).
- [169] WALLNER, D. Colour management and transformation through ICC profiles. *Colour Engineering* (2002), 247–261.
- [170] WEN, S., AND WU, R. Two-primary crosstalk model for characterizing liquid crystal displays. *Color Research & Application* 31, 2 (2006), 102–108.
- [171] WESTLAND, S., AND CHEUNG, V. Rgb systems. In *Handbook of visual display technology*. Springer, (2012), pp. 147–153.
- [172] WESTLAND, S., AND RIPAMONTI, C. Colour toolbox. *Computational Colour Science Using MATLAB* (2004), 189–197.
- [173] WESTLAND, S., RIPAMONTI, C., AND CHEUNG, V. Computational colour science using matlab. Wiley Online Library, pp. 131–141.
- [174] WESTLAND, S., RIPAMONTI, C., AND CHEUNG, V. *Computational colour science using matlab*. John Wiley & Sons, (2012).

- [175] Gamut of Rec 709 with the white point. https://en.wikipedia.org/wiki/White_point (visited: 2014-07-21).
- [176] WIDDEL, H., AND POST, D. L. *Colour in electronic displays*, vol. 3. Springer Science & Business Media, (2013).
- [177] WITT, K. CIE guidelines for coordinated future work on industrial colour-difference evaluation. *Colour Research & Application* 20, 6 (1995), 399–403.
- [178] WRIGHT, W. D. A re-determination of the trichromatic coefficients of the spectral colours. *Transactions of the Optical Society* 30, 4 (1929), 141.
- [179] WU, S.-T., AND WU, C.-S. High-speed liquid-crystal modulators using transient nematic effect. *Journal of applied physics* 65, 2 (1989), 527–532.
- [180] WYSZECKI, G. Proposal for a new colour-difference formula. *J. Opt. Soc. Amer* 53 (1963), 1318–1319.
- [181] WYSZECKI, G. S., AND STILES, W. *WS,(1982), Colour Science: Concepts and Methods, Quantitative Data and Formulae*. New York: John Wiley & Sons, (1982).
- [182] x , y chromaticity coordinates. http://www.pfk.ff.vu.lt/cie/images/cie_full2.png (visited: 2012-10-04).
- [183] YOSHIDA, Y., AND YAMAMOTO, Y. Color calibration of LCDs. In *Color and Imaging Conference* (2002), vol. 2002, Society for Imaging Science and Technology, pp. 305–311.
- [184] YOU, B. H., LEE, J. P., KIM, D. G., PARK, J. H., KIM, Y.-J., BERKELEY, B. H., AND KIM, S. S. 61.3: A novel driving method using 2-dimension spatial averaging for high speed driving of AMLCD. In *SID Symposium Digest of Technical Papers* (2007), vol. 38, Wiley Online Library, pp. 1725–1728.
- [185] ZHANG, J.-Q., CAI, F., LIU, Z., WU, G.-Y., AND ZHU, M. A composite model for accurate colorimetric characterization of liquid crystal displays. *Journal of the Society for Information Display* 24, 10 (2016), 600–610.
- [186] ZHELUDEV, N. The life and times of the LED 100-year history. *Nature Photonics* 1, 4 (2007), 189–192.
- [187] ZWINKELS, J. C. Colour-measuring instruments and their calibration. *Displays* 16, 4 (1996), 163–171.